



Callison, June (2011) *The investigation of a side reaction leading to colour formation in a polyurethane production chain*. PhD thesis.

<http://theses.gla.ac.uk/2498/>

Copyright and moral rights for this thesis are retained by the author

A copy can be downloaded for personal non-commercial research or study, without prior permission or charge

This thesis cannot be reproduced or quoted extensively from without first obtaining permission in writing from the Author

The content must not be changed in any way or sold commercially in any format or medium without the formal permission of the Author

When referring to this work, full bibliographic details including the author, title, awarding institution and date of the thesis must be given

**The Investigation of a Side Reaction Leading
to Colour Formation in a Polyurethane
Production Chain**

June Callison

For the degree of Doctor of Philosophy

Department of Chemistry



**University
of Glasgow**

April 2011

Declaration

The work contained in this thesis, submitted for the degree of Doctor of Philosophy is my own original work, except where due reference is made to other authors and has not been previously submitted for a degree at this or any other university.

June Callison

© June Callison 2011

Abstract

In the industrial synthesis of 4,4'-methylene diphenyl diisocyanate (MDI), an unwanted side reaction between the product and the starting material, 4,4'-methylene dianiline, can lead to the formation of ureas. It has been postulated these ureas undergo further reaction with phosgene to produce a precursor to chlorine radicals, which could then attack the MDI backbone forming conjugated systems that would promote colour in the final products.

To investigate this process model compounds including 4-benzylaniline (4-BA) and 1,3-diphenylurea were used as starting materials. The reactions carried out showed the phosgenation of the urea forms a chloroformamidine-*N*-carbonyl chloride (CCC) which upon heating > 303 K can break down to form an isocyanide dichloride (ID). Conventional synthesis routes were used to gain high yields of *p*-tolyl and phenyl isocyanide dichlorides in order to analyse the compounds. It was found that upon heating to 453 K or irradiating the isocyanide dichlorides in the process solvent (chlorobenzene) coloured solutions were formed; with the presence of MDI and oxygen increasing the intensity of the colouration.

Electron paramagnetic resonance spectroscopy was used to gain information on the use of isocyanide dichlorides as a source of chlorine radicals. Using *N*-*tert*-butyl- α -phenylnitrone (PBN) as a spin trap, an 8 line spectra relating to the chlorine adduct was measured confirming the production of Cl^\bullet .

Throughout the project side reactions involving the formation of carbodiimide from CCC and a secondary route for the phosgenation of the urea to the isocyanate have been investigated and are presented within a global reaction scheme. It was also found the ureas were only partially soluble in the process solvent leading to research into the structure of three different urea molecules and the proposal of a modified reaction scheme.

Acknowledgements

I would like to thank everyone involved in this project and to those that have helped me throughout my years at university.

Special thanks to my supervisor Dr David Lennon for all the support and guidance over the years. Thank you for having faith in me, for all the good advice and for the intriguing conversations in the pub.

To Prof John Winfield, thank you for sharing your immense knowledge and all your help throughout this project. It has been a pleasure working with you.

Thank you to my industrial sponsors Huntsman Polyurethanes for providing an interesting project to work on. To my supervisor Rob Carr and to Archie Eaglesham thanks for the informative meetings and for being approachable when I needed advice.

Thanks to Willem van der Borden, Klaas van der Velde and Kimberly de Cuba for the help in carrying out the experiments at the Huntsman Polyurethanes Process Research and Development Laboratory and for the support and friendship during my short stay in Rozenburg. Also for the wonderful meals, beer and introducing me to Frikandellen.

Thanks to Franziska Betzler and Andrew Farrell, who carried out work associated with this project through undergraduate projects.

From the University of Manchester thanks to Dr Ruth Edge for help in carrying out the EPR measurements. Prof David Collison and Prof Eric McInnes for the advice and expertise and to Dr Joseph McDouall for carrying out the DFT calculations.

Thanks to Alex Burns for the advice on the safety aspects of this work, to Dr Louis Farrugia for helping with the crystallographic studies and to Dr David Adam for help with the NMR work.

To Emma, Neil, Ian, Liam and Andrew thanks for the great times in the lab and in the pub. Especially to Emma for showing me the ropes and putting up with my questions. Plus a special mention to Franziska and Niko for being great hosts on our trip to Oktoberfest. Also to my friends, you know who you are, thank you for being there.

And finally to Mum, Dad and James thank you for all your love, patience, and support throughout the years.

“You are here to learn the subtle science and exact art of potion-making. I don’t expect you will really understand the beauty of the softly simmering cauldron with its shimmering fumes, the delicate power of liquids that creep through human veins, bewitching the mind, ensnaring the senses ... I can teach you how to bottle fame, brew glory, even stopper death.”

– Professor Severus Snape, *Harry Potter and the Philosopher’s Stone*

Contents

1	Introduction.....	2
1.1	Polyurethanes in Industry	2
1.2	Isocyanates	2
1.3	MDI Production.....	3
1.4	Phosgene.....	6
1.4.1	Triphosgene.....	7
1.5	New Methods for MDI Synthesis.....	9
1.6	Colouration Problems.....	10
1.7	Postulated Reaction Scheme.....	11
1.8	Urea Compounds	12
1.8.1	Crystal Structure	13
1.8.2	Tautomerism.....	13
1.9	Analytical Techniques.....	14
1.9.1	Electron Paramagnetic Resonance (EPR) Spectroscopy	14
1.9.2	Infrared Spectroscopy	15
1.9.3	Ultraviolet and Visible Absorption Spectroscopy	16
2	Experimental.....	19
2.1	Chemicals	19
2.2	Apparatus for Synthesis Reactions	20
2.2.1	Phosgenation.....	21
2.2.2	Chlorination.....	26
2.3	Characterisation Techniques	27
2.3.1	Fourier Transform Infrared (FTIR) Spectroscopy	27
2.3.2	Nuclear Magnetic Resonance (NMR) Spectroscopy	27
2.3.3	Elemental Analysis.....	27
2.3.4	Melting Point Determination	28
2.3.5	Thermal Analysis.....	28
2.3.6	Available Chlorine	28
2.3.7	Mass Spectrometry (MS).....	31
2.3.8	Gas Chromatography-Mass Spectrometry (GCMS)	31
2.3.9	Gel Permeation Chromatography (GPC)	31
2.3.10	Yellow Index	31
2.3.11	UV/Vis Spectroscopy.....	32
2.4	Phosgenation of 4-Benzylaniline.....	32
2.4.1	Triphosgene.....	32
2.4.2	Eckert Cartridge	33
2.5	Synthesis of Urea	35
2.5.1	1,3-Di- <i>p</i> -benzylphenylurea (Urea 2).....	35
2.5.2	Oligomeric Urea (Urea 3)	36
2.6	Structure Analysis of Ureas by X-Ray Diffraction (XRD).....	39
2.6.1	Crystal Preparation	39
2.6.2	Diffractionmeter	39

2.6.3	Structure Determination	39
2.7	Solubility Determination of Urea.....	40
2.7.1	Gravimetric Method.....	40
2.7.2	¹ H-NMR Spectroscopy Method.....	40
2.8	Phosgenation of Urea.....	42
2.9	Synthesis of 1,3-Di- <i>p</i> -Tolylchloroformamidine- <i>N</i> -carbonyl Chloride (TCCC)	43
2.10	Synthesis of Isocyanide Dichlorides.....	45
2.11	Characterisation of Isocyanide Dichlorides.....	46
2.11.1	FTIR Spectroscopy	46
2.11.2	NMR Spectroscopy	48
2.11.3	Gas Chromatography-Mass Spectrometry (GCMS)	51
2.11.4	Thermal Analysis.....	51
2.11.5	Available Chlorine	53
2.11.6	Summary	53
2.12	Storage Methods for Unstable Compounds.....	54
2.13	Rozenburg Reactions	55
2.13.1	Heat Treatments of Chloroformamidine- <i>N</i> -carbonyl Chloride (CCC).....	55
2.13.2	Isocyanide Dichloride and Chloroformamidine- <i>N</i> -carbonyl Chloride Compounds as a Source of Colour	57
2.14	Heat Treatments and Photolysis of Isocyanide Dichlorides.....	58
2.14.1	Apparatus	58
2.14.2	Preliminary Reactions	59
2.14.3	Concentration Dependence of Isocyanide Dichlorides	60
2.15	EPR Study of Isocyanide Dichlorides.....	62
2.15.1	Irradiation of Hexachloroplatinate (IV) Hexahydrate.....	63
2.15.2	Simulation of Experimental Spectra.....	64
2.15.3	DFT Calculations of EPR Parameters to Support Radical Identification.....	64
2.15.4	Temperature Study	65
2.15.5	PBN Concentration Study.....	65
2.15.6	Kinetic Analysis.....	65
3	Ureas	68
3.1	Urea Compounds	68
3.2	Phosgenation of Ureas	69
3.2.1	Identification of Products	69
3.2.2	Triphosgene Reactions (1-4)	73
3.2.3	Eckert Cartridge Reactions (5-8)	76
3.2.4	High Temperature Reactions (9-15).....	78
3.2.5	Discussion	82
3.2.6	Alternative Routes to Chloroformamidine- <i>N</i> -carbonyl Chloride (CCC).....	84
3.3	Urea Structure.....	86
3.3.1	Solubility	86
3.3.2	Structure Determination of 1,3-Di- <i>p</i> -benzylphenylurea.....	89
3.3.3	FTIR Study.....	93
3.4	Alternative Reaction Mechanism.....	96
3.5	Summary.....	97

4	Chloroformamidine-<i>N</i>-carbonyl Chloride (CCC)	100
4.1	Heat Treatments of 1,3-Di- <i>p</i> -tolylchloroformamidine- <i>N</i> -carbonyl Chloride (TCCC).....	100
4.1.1	CCC/Carbodiimide Equilibrium	100
4.1.2	Isocyanide Dichloride as a Decomposition Product.....	106
4.1.3	Heat Treatment of Isothiocyanate.....	109
4.2	Summary.....	110
4.3	Modified Reaction Scheme.....	111
5	Electron Paramagnetic Resonance (EPR) Study of Isocyanide Dichlorides	114
5.1	Blank Reactions	115
5.2	Identification of the EPR Active Species	117
5.3	Verification of Benzoyl <i>N</i> - <i>tert</i> -butyl Nitroxide Radical.....	122
5.3.1	DFT Calculations.....	122
5.3.2	Simulations	124
5.4	Low Temperature Study	125
5.5	PBN Concentration Study.....	127
5.6	Reaction Study and Kinetics	129
5.7	Summary.....	136
6	Isocyanide Dichlorides	138
6.1	Reaction of Isocyanide Dichlorides with Isocyanates (Preliminary Reactions).....	138
6.1.1	Heat Treatments (Low Temperature Studies)	138
6.1.2	Photolysis Reaction.....	146
6.1.3	Identification of Products Using Spectroscopic Methods	148
6.1.4	Analysis and Characterisation of Isocyanide Dichlorides.....	150
6.1.5	Heat Treatments (High Temperature Studies)	151
6.2	Source of Colour Formation.....	155
6.2.1	Yellow Index Analysis (Rozenburg)	155
6.2.2	Thermolysis and Photolysis of Isocyanide Dichlorides – Concentration Dependence	157
6.2.3	Nitrogen Purge Experiments (High Temperature)	162
6.2.4	Analysis of Product Mixtures by GCMS	166
6.3	Summary and Discussion	169
6.3.1	Issues Relating to Oxidising Reagents	171
6.3.2	Colour Formation	173
6.3.3	Thermolysis Vs Photolysis.....	174
7	Conclusions	176
7.1	Side Reaction from Ureas to Isocyanide Dichlorides	178
7.2	Radical Chemistry	181
7.3	Formation of Colour.....	181
7.4	MDI Scheme	182
7.5	Future Work	184
8	References	185

List of Figures

Figure 1. Plant process for the synthesis of MDI ²¹	6
Figure 2. Quinone-imide structure derived from oxidation of MDI based polyurethanes	10
Figure 3. <i>N,N</i> bis(4-biphenyl)urea	13
Figure 4. Synthesis apparatus	21
Figure 5. Release of phosgene from Eckert cartridge ⁹⁰	23
Figure 6. Modifications to apparatus for the use of Eckert cartridge	24
Figure 7. Scrubber system for destruction of excess phosgene.....	25
Figure 8. Modifications to apparatus for use in chlorination reactions.....	26
Figure 9. FTIR spectrum of 4-benzylphenyl isocyanate (4-BAI), product from phosgenation of 4-benzylaniline (4-BA) with triphosgene.....	33
Figure 10. FTIR spectra of the starting material, 4-benzylaniline, and the product 4-benzylphenyl isocyanate from reaction involving the Eckert cartridge.....	34
Figure 11. Urea compounds studied within this research project.....	35
Figure 12. FTIR spectrum of 1,3-di- <i>p</i> -benzylphenylurea formed from reaction between 4-benzylaniline and 4-benzylphenyl isocyanate	36
Figure 13. FTIR spectrum of oligomeric urea produced via mono isocyanate and diamine	37
Figure 14. FTIR spectrum of oligomeric urea produced via mono amine and diisocyanate	38
Figure 15. Plot of the integrals of CH ₂ and NH ₂ signals of 4-benzylaniline with respect to concentration	42
Figure 16. FTIR Spectrum of 1,3-di- <i>p</i> -tolylchloroformamidine- <i>N</i> -carbonyl chloride produced from phosgenation of 1,3-di- <i>p</i> -tolylcarbodiimide.....	45
Figure 17. FTIR spectra of phenyl isocyanide dichloride and <i>p</i> -tolyl isocyanide dichloride synthesised from chlorination of the corresponding isothiocyanates.....	46
Figure 18. FTIR spectra of <i>p</i> -tolyl isocyanide dichloride taken 1, 4 and 5 days after synthesis.....	48
Figure 19. Hydrogen labels for the aryl isocyanide dichloride compounds	49
Figure 20. ¹ H-NMR spectra of aryl isocyanide dichlorides	50
Figure 21. ¹ H-NMR spectra of aryl isocyanide dichlorides – aromatic region, * indicates peaks attributed to Cl-TID.....	50
Figure 22. TGA profiles of aryl isocyanide dichlorides.....	52
Figure 23. DSC trace of aryl isocyanide dichlorides	53
Figure 24. Schlenk tube used to store sensitive materials.....	54
Figure 25. Vacuum line	55
Figure 26. Isocyanate compounds in polymeric MDI	61
Figure 27. EPR spectrum of Cl-PBN adduct from irradiation of sodium hexachloroplatinate (IV) hexahydrate in the presence of the spin trap, PBN	64
Figure 28. Urea compounds investigated within this research project.....	68

Figure 29. FTIR spectrum of 4-benzylaniline purchased from Alfa Aesar	71
Figure 30. FTIR spectrum of 4-benzylphenyl isocyanate purchased from Sigma-Aldrich	71
Figure 31. FTIR spectrum of 1,3-diphenylurea purchased from Sigma-Aldrich	71
Figure 32. FTIR spectrum of 1,3-di- <i>p</i> -benzylphenylurea synthesized in-house (Section 2.5.1).....	72
Figure 33. FTIR spectrum of 1,3-di- <i>p</i> -tolylchloroformamidine- <i>N</i> -carbonyl chloride synthesized as described in section 2.9.....	72
Figure 34. FTIR spectrum of 1,3-di- <i>p</i> -tolylcarbodiimide purchased from Sigma-Aldrich	72
Figure 35. FTIR spectra of reactions 1 and 2, * indicates peaks attributed to triphosgene (I), isocyanate (III) and CCC (VI).....	74
Figure 36. FTIR spectra of reactions 3 and 4, * indicates peaks attributed to triphosgene (I), isocyanate (III) and CCC (VI).....	75
Figure 37. FTIR spectra of reactions 5 to 8, * indicates peaks attributed to urea (IV), CCC (VI) and carbodiimide (VII).....	77
Figure 38. FTIR spectra of reactions 9 to 12, * indicates peaks attributed to isocyanate (III), CCC (VI) and carbodiimide (VII).....	79
Figure 39. FTIR Spectra of reactions 10 and 14, * indicates peaks attributed to isocyanate (III), CCC (VI) and carbodiimide (VII).....	81
Figure 40. FTIR Spectra of reactions 11 and 15, * indicates peaks attributed to isocyanate (III), CCC (VI) and carbodiimide (VII).....	81
Figure 41. Reference ¹ H-NMR spectrum of 1,3-di- <i>p</i> -benzylphenylurea in DMSO	87
Figure 42. ¹ H-NMR spectra of 4-BA in MCB and ureas 1, 2 and 3 in MCB before and after heating	88
Figure 43. Molecular structure of 1,3-di- <i>p</i> -benzylphenylurea	91
Figure 44. Hydrogen bonding in 1,3-di- <i>p</i> -benzylphenylurea	91
Figure 45. Unit cell of 1,3-di- <i>p</i> -benzylphenylurea	92
Figure 46. FTIR spectra of ureas 1, 2 and 3.....	94
Figure 47. FTIR spectra of urea 3 before and after recrystallization	95
Figure 48. Structure modification of urea 3	95
Figure 49. GPC traces of a solution of TCCC in chlorobenzene heated to 448 K and 463 K over three hours.....	102
Figure 50. GC chromatograph of a solution of TCCC in chlorobenzene heated to 448 K over three hours	102
Figure 51. GPC traces of a solution of TCCC in chlorobenzene with 5% phosgene heated to 448 K and 463 K over three hours	103
Figure 52. GPC traces of a solution of TCCC in chlorobenzene with 1% phosgene heated to 423 K and 448 K over six hours.....	103
Figure 53. GPC traces of solutions of TCCC in chlorobenzene in open vials for one hour	104
Figure 54. Ratio of carbodiimide/CCC peak area with respect to temperature	105
Figure 55. GC chromatograph of <i>p</i> -tolyl isocyanide dichloride (TID) in chlorobenzene	106

Figure 56. GC chromatograph of reaction 9, TCCC in chlorobenzene with 1 % phosgene at 448 K	108
Figure 57. GC chromatograph of TCCC in chlorobenzene with 1 % phosgene after 2 hours at various temperatures.....	109
Figure 58. GC chromatograph of <i>p</i> -tolyl isothiocyanate in chlorobenzene after heating to 448 K	110
Figure 59. PBN-Cl adduct splitting diagram	115
Figure 60. EPR spectrum of phenyl isocyanide dichloride (PID) in benzene after 47 minutes of constant irradiation.....	116
Figure 61. EPR spectrum of <i>N</i> - <i>tert</i> -butyl- α -phenylnitron (PBN) in benzene after 47 minutes of constant irradiation.....	116
Figure 62. Hydroxybenzyl- <i>N</i> - <i>tert</i> butyl nitroxide (XIII)	117
Figure 63. EPR spectra of PID + PBN in benzene with constant irradiation at 0, 25 and 50 minutes	118
Figure 64. EPR spectra of PID + PBN in benzene after 30 s irradiation.....	119
Figure 65. Postulates for identity of second radical species on irradiation of PID + PBN in benzene	120
Figure 66. EPR spectrum of PID + PBN in benzene without irradiation	122
Figure 67. EPR spectrum of PID + PBN in benzene without irradiation (dark) after 47 minutes ..	122
Figure 68. B3LYP/EPR-III (Cl: IGLO-III) spin densities (isosurface value 0.004 au, <i>t</i> -Bu group shown in wireframe for clarity) for a) benzoyl- <i>N</i> - <i>tert</i> -butyl nitroxide radical (XVII) and b) PBN-PID adduct (XV).....	123
Figure 69. Simulation and experimental spectra of PID + PBN in benzene after 50 mins constant irradiation, parameters from simulation are $a_N = 12.32$ G, $a_{Cl-35} = 6.25$ G, $a_{Cl-37} = 5.20$ G and $a_H = 0.80$ G.....	124
Figure 70. Simulation and experimental spectra of PID + PBN in benzene after 30 s irradiation, parameters from simulation are 0 mins – $a_N = 12.32$ G, $a_{Cl-35} = 6.25$ G, $a_{Cl-37} = 5.20$ G, 50 mins – $a_N = 8.00$ G.....	125
Figure 71. EPR spectra of PID + PBN in toluene after 30 s irradiation at various temperatures ..	126
Figure 72. EPR spectra of PID in benzene with different concentrations of PBN after 30 s irradiation	128
Figure 73. EPR spectra of PID in benzene with different concentrations of PBN with constant irradiation.....	129
Figure 74. Reaction profile of the PBN-Cl adduct at various temperatures	131
Figure 75. Reaction profile of the benzoyl radical at various temperatures	131
Figure 76. Plot of $[A]_0 - [A]$ versus time for benzoyl- <i>N</i> - <i>tert</i> -butyl nitroxide (XVII) > 3500 s at various temperatures.....	133
Figure 77. UV spectra before and after thermolysis of selected isocyanates	139
Figure 78. UV spectra before and after thermolysis of TID – UV region.....	140
Figure 79. UV spectra before and after thermolysis of TID – visible region.....	140
Figure 80. UV spectra of thermolysis of TID + TI in acetonitrile – UV region.....	141
Figure 81. UV spectra of thermolysis of TID + TI in acetonitrile – visible region.....	142

Figure 82. UV spectra of thermolysis of TID + 4-BAI in acetonitrile – UV region	142
Figure 83. Quinone type structure arising from 4-benzylphenyl isocyanate (4-BAI)	143
Figure 84. UV spectra of thermolysis of TID + 4-BAI in acetonitrile at 313 K over 3.5 hours – UV region	143
Figure 85. Plot of absorbance at 273 nm vs time for reaction of TID + 4-BAI at 313 K.....	144
Figure 86. UV spectra of thermolysis of TID + 4-BAI in acetonitrile at 313 K over 5 hours – visible region	144
Figure 87. UV spectra of thermolysis of TID + MDI in acetonitrile – UV region.....	145
Figure 88. UV spectra of thermolysis of TID + MDI in acetonitrile – visible region.....	146
Figure 89. UV spectra of photolysis of TID + 4-BAI in acetonitrile – UV region	147
Figure 90. UV spectra of photolysis of TID + 4-BAI in acetonitrile – visible region	147
Figure 91. FTIR spectra of MDI, TID and mixtures after heating at 373 K and photolysis.....	149
Figure 92. ¹ H-NMR spectra of MDI, TID and mixtures after heating at 373 K and photolysis	150
Figure 93. UV spectra of thermolysis of TID + 4-BAI in chlorobenzene at 403 K.....	152
Figure 94. UV spectra of thermolysis of TID + 4-BAI in <i>o</i> -dichlorobenzene at 453 K.....	152
Figure 95. 1,4-Dibenzylbenzene.....	153
Figure 96. UV spectra of thermolysis of TID + DBB in <i>o</i> -dichlorobenzene at 453 K	154
Figure 97. UV spectra of thermolysis of TID and 4-BAI in <i>o</i> -dichlorobenzene at 453 K.....	155
Figure 98. Graph of yellow index vs concentration for solutions heated at 448 K for 2 hours	157
Figure 99. UV spectra of solutions of PID (at different concentrations indicated) before and after heating at 448 K or photolysis for 2 hours.....	159
Figure 100. UV spectra of solutions of PID (concentrations shown in legend) + 0.05 M MDI before and after heating at 448 K or photolysis for 2hours	160
Figure 101. UV spectra of solutions of PID (concentrations shown) + 0.05 M polymeric MDI before and after heating at 448 K or photolysis for 2 hours	161
Figure 102. UV spectra of PID + 0.05 M MDI in solution before and after heating at 448 K with a N ₂ purge for 2 hours.....	162
Figure 103. UV spectra of PID + 0.05 M PMDI in solution before and after heating at 448 K with a N ₂ purge for 2 hours.....	163
Figure 104. Integrations of the UV spectra from Figure 99 to Figure 101.....	163
Figure 105. UV spectra of PID + PMDI in solution heated to 448 K over time.....	165
Figure 106. UV spectra of PID + PMDI in solution heated to 448 K with N ₂ purge for 120, then purge stopped.....	166
Figure 107. Chlorinated compounds.....	168

List of Tables

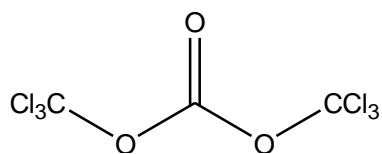
Table 1. Experimental details for the phosgenation of ureas	43
Table 2. Characteristic IR bands for aryl isocyanide dichlorides	47
Table 3. NMR data for aryl isocyanide dichlorides PID ($C_6H_5N=CCl_2$), TID ($4-CH_3C_6H_4N=CCl_2$) and Cl-TID ($4-CH_2ClC_6H_4N=CCl_2$)	49
Table 4. Mass spectra details of aryl isocyanide dichlorides.....	51
Table 5. Experimental details for the heat treatments of 1,3-di- <i>p</i> -tolylchloroformamidine- <i>N</i> -carbonyl chloride (TCCC)	56
Table 6. Details of solutions used for colour experiments.....	57
Table 7. Reaction details for the preliminary thermolysis and photolysis reactions of isocyanide dichlorides.....	60
Table 8. Concentration details of solutions for concentration dependence thermolysis and photolysis reactions.....	61
Table 9. Details of Solutions for use in EPR experiments.....	62
Table 10. Experimental details for EPR experiments	63
Table 11. Infrared assignments of compounds from the postulated reaction scheme	70
Table 12. Product details from the phosgenation of urea reactions	73
Table 13. X-ray details of 1,3-di- <i>p</i> -benzylphenylurea	90
Table 14. Bond distances for 1,3-di- <i>p</i> -benzylphenylurea.....	91
Table 15. Bond angles for 1,3-di- <i>p</i> -benzylphenylurea	92
Table 16. Infrared assignments of ureas 1, 2 and 3	93
Table 17. Details of heat treatment reactions of TCCC	107
Table 18. Hyperfine coupling constants for hydroxybenzyl- <i>N-tert</i> butyl nitroxide radical observed together with literature values.....	117
Table 19. Hyperfine coupling constants for PBN-Cl adduct observed together with literature values, a-c derived from: (a) $PtCl_6^{2-}$, (b) $C_6H_5N=CCl_2$, (c) $4-CH_3C_6H_4N=CCl_2$	118
Table 20. Hyperfine coupling constants for benzoyl- <i>N-tert</i> -butyl nitroxide radical (XVII) observed together with literature values, a-b derived from: (a) $C_6H_5N=CCl_2$, (b) $4-CH_3C_6H_4N=CCl_2$	121
Table 21. Half life values for radicals produced by PID + PBN in solution.....	132
Table 22. Solutions used to measure yellow index.....	156
Table 23. Colour photos of solutions of PID, PID + MDI and PID + PMDI before and after reactions (highest concentration is on the left hand side, decreasing to the right).....	164
Table 24. Table of components found in the GCMS analysis, PID = phenyl isocyanide dichloride, MDI = 4,4'-methylene diphenyl diisocyanate, Poly = Polymeric MDI, + = low peak height, ++ = medium peak height, +++ = high peak height	167

List of Schemes

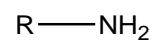
Scheme 1. Formation of a urethane from reaction between an isocyanate and a polyol	2
Scheme 2. Industrial synthesis of 4,4'-methylene diphenyl diisocyanate (MDI) from benzene	4
Scheme 3. Formation of urea from reaction of amine and isocyanate	5
Scheme 4. Breakdown process of triphosgene on reaction with nucleophile	8
Scheme 5. Decomposition mechanism for triphosgene via 4 membered transition state ²⁷	8
Scheme 6. Thermal decomposition mechanism for triphosgene via 6 membered transition state ³¹ .	9
Scheme 7. Postulated reaction scheme – phosgenation of urea to form isocyanide dichloride	11
Scheme 8. Hydrolysis of <i>p</i> -tolyl isocyanide dichloride	47
Scheme 9. Reaction of urea with triphosgene	76
Scheme 10. Reaction of urea with phosgene (Eckert cartridge)	78
Scheme 11. Urea reaction summary.....	82
Scheme 12. Formation of allophanoyl chloride via O-attack.....	83
Scheme 13 Reaction schemes from literature ^{62, 102, 103, 122-125, 128-137} , red arrows indicate reactions seen in the experimental described in this section	85
Scheme 14. Alternative reaction mechanism for phosgenation of urea.....	97
Scheme 15. Postulated equilibrium between 1,3-di- <i>p</i> -tolylchloroformamidine- <i>N</i> -carbonyl chloride and 1,3-di- <i>p</i> -tolylcarbodiimide.....	105
Scheme 16. Postulated reaction of 1,3-di- <i>p</i> -tolylchloroformamidine- <i>N</i> -carbonyl chloride	111
Scheme 17. Modified reaction scheme	112
Scheme 18. Addition of chlorine radical to the spin trap, PBN.....	114
Scheme 19. Formation of benzoyl- <i>N-tert</i> -butyl nitroxide radical through a consecutive reaction .	130
Scheme 20. Postulated scheme 1 for the formation of benzoyl <i>N-tert</i> -butyl nitroxide radical.....	134
Scheme 21. Postulated scheme 2 for the formation of benzoyl <i>N-tert</i> -butyl nitroxide radical.....	135
Scheme 22. Proposed kinetic processes	135
Scheme 23. Hydrolysis of phenyl isocyanide dichloride (PID) leading to phenyl isocyanate	168
Scheme 24. Conjugation of MDI via attack from Cl [•] radicals.....	169
Scheme 25. Conjugation of Polymeric MDI via attack from Cl [•] radicals	170
Scheme 26. Activation of MDI by Cl [•] followed by oxidation and conjugation.....	173
Scheme 27. Full reaction scheme.....	177
Scheme 28. Reaction between isocyanate and amine to form urea	178
Scheme 29. Phosgenation of phosgene – competing reactions	179
Scheme 30. Decomposition of chloroformamidine- <i>N</i> -carbonyl chloride (CCC) to isocyanide dichloride and isocyanate	180
Scheme 31. Reaction of chlorine radicals with 4-BAI to produce colour	182

Scheme 32. Full reaction scheme based on MDI	183
--	-----

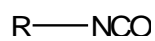
Classification of Compounds



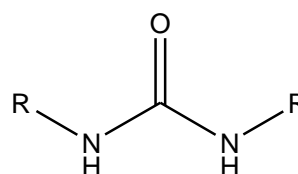
Triphosgene (I)



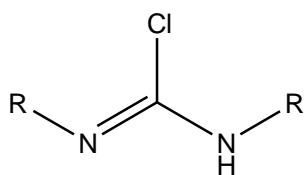
Amine (II)



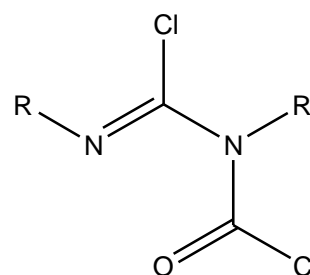
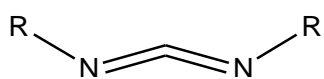
Isocyanate (III)



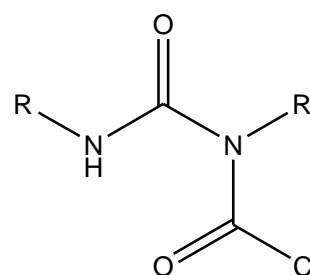
Urea (IV)



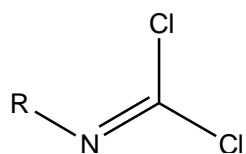
Chloroformamidine (V)

Chloroformamidine-*N*-carbonyl chloride (VI)

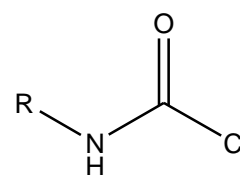
Carbodiimide (VII)



Allophanoyl chloride (VIII)



Isocyanide dichloride (IX)

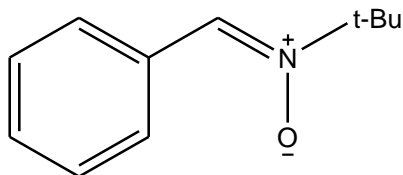


Carbamoyl chloride (X)

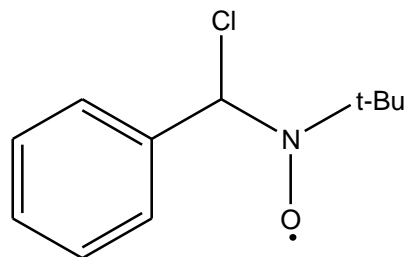
Specific Compounds

	Common Name	Abbreviation	
(IIa)	4-Benzylaniline	4-BA	$R = C_6H_5CH_2C_6H_5$
(IIb)	4,4'-Methylene dianiline	MDA	$R = C_6H_5CH_2C_6H_5NH_2$
(IIIa)	<i>p</i> -Tolyl isocyanate	TI	$R = C_6H_5CH_3$
(IIIb)	4-Benzylphenyl isocyanate	4-BAI	$R = C_6H_5CH_2C_6H_5$
(IIIc)	4,4'-Methylene diphenyl diisocyanate	MDI	$R = C_6H_5CH_2C_6H_5NCO$
(IVa)	1,3-Diphenylurea	Urea 1	$R = C_6H_5$
(IVb)	1,3-Di- <i>p</i> -benzylphenylurea	Urea 2	$R = C_6H_5CH_2C_6H_5$
(IVc)	Oligomeric urea	Urea 3	$R_1 = C_6H_5CH_2C_6H_5, R_2 = C_6H_5CH_2C_6H_5NHONHC_6H_5CH_2C_6H_5$
(VIa)	1,3-Di- <i>p</i> -tolylchloroformamidine- <i>N</i> -carbonyl chloride	TCCC	$R = C_6H_5CH_3$
(VIIa)	1,3-Di- <i>p</i> -tolylcarbodiimide	TCD	$R = C_6H_5CH_3$
(IXa)	Phenyl isocyanide dichloride	PID	$R = C_6H_5$
(IXb)	<i>p</i> -Tolyl isocyanide dichloride	TID	$R = C_6H_5CH_3$
(IXc)	4-Fluoromethylphenyl isocyanide dichloride	4-FPID	$R = C_6H_5F$

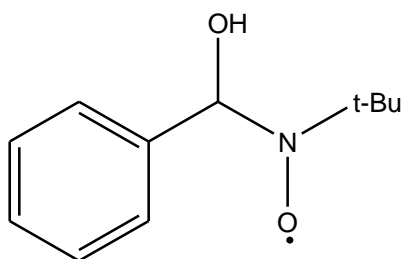
EPR Compounds



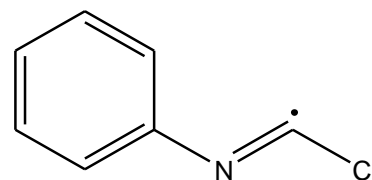
N-tert-Butyl- α -phenylnitronium (PBN) (XI)



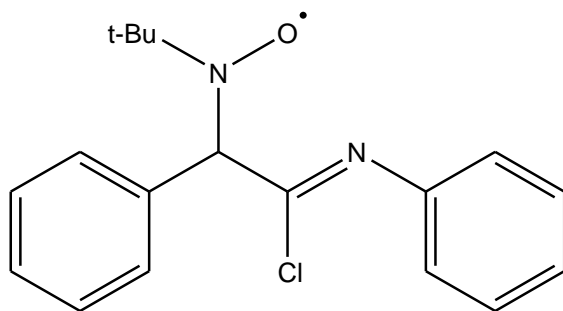
PBN-Cl adduct (XII)



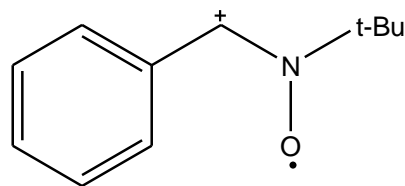
Hydroxybenzyl-*N*-tert butyl nitroxide (XIII)



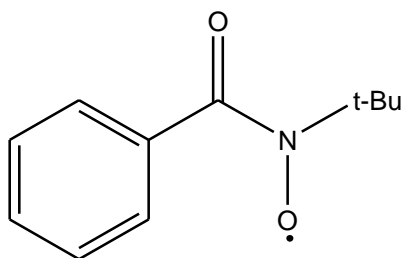
PID radical (XIV)



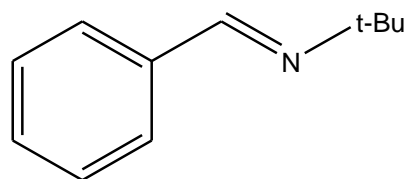
PBN-PID adduct (XV)



PBN cation radical (PBN^{*+}) (XVI)



Benzoyl-*N*-tert-butyl nitroxide (XVII)



N-tert-Butylbenzylimine (XVIII)

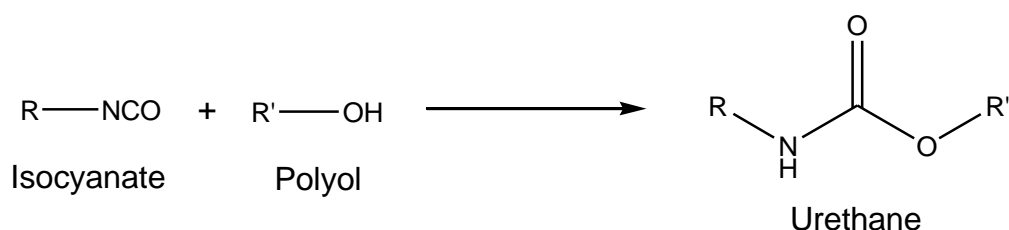
Chapter 1

Introduction

1 Introduction

1.1 Polyurethanes in Industry

Polyurethanes are highly important polymeric materials used in everyday life. They are formed from the reaction between diisocyanate and polyol compounds, forming a urethane linkage¹ (Scheme 1). This reaction was first established in 1937 by Otto Bayer,^{2, 3} pioneering work which acted as a catalyst for the initiation and growth of the polyurethanes industry. The first polyurethanes were produced from the reaction of 1,4-butylene glycol and 1,6-hexamethylene diisocyanate, utilizing a reaction discovered by Wurtz in 1848 whereby urethane could be produced from a mono functional isocyanate and a monofunctional or monohydric alcohol. These first polyurethanes were sold in Germany under the trade names of Igamid U plastics and Perlon U synthetic fibers and bristles.⁴ The production of polyurethanes then moved to the USA, where industrialists were particularly interested in the manufacture of polyurethane foams, almost two billion pounds of which were produced in 1973.⁴ Today polyurethanes are manufactured by companies such as Huntsman Polyurethanes for use in products such as adhesives, footwear, mattresses, car bumpers and refrigerators.⁵

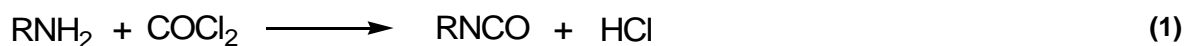


Scheme 1. Formation of a urethane from reaction between an isocyanate and a polyol

1.2 Isocyanates

The practical applications of using isocyanates in industry were realized in the 1940's after Bayer's discovery of polyurethanes. Interest in these compounds grew rapidly particularly in Germany among industrialists⁶ using them as raw materials to make fibres, plastics, foams, adhesives and for polymer modification.⁷ Isocyanates were first produced in 1849 by Wurtz, formed from the reaction between organic sulphates and cyanates.⁸ Over the years many different methods for synthesizing isocyanates have been documented

including the oxidation of isocyanides and the pyrolysis of an amide.⁹ However the method widely used today is the phosgenation of amines, Equation (1), a reaction discovered by Hentschel¹⁰ in 1884 and modified later by Gettermann and Schmidt.¹¹ Both aliphatic and aromatic diisocyanates are used as raw materials, with the most significant being 4,4'-methylene diphenyl diisocyanate (MDI) and toluene diisocyanate (TDI). In 2000 MDI made up 61.3% of the total global isocyanate market, equivalent to 2.7 million tonnes, while TDI had a share of 34.1%, indicating the dominance of these two materials.⁵

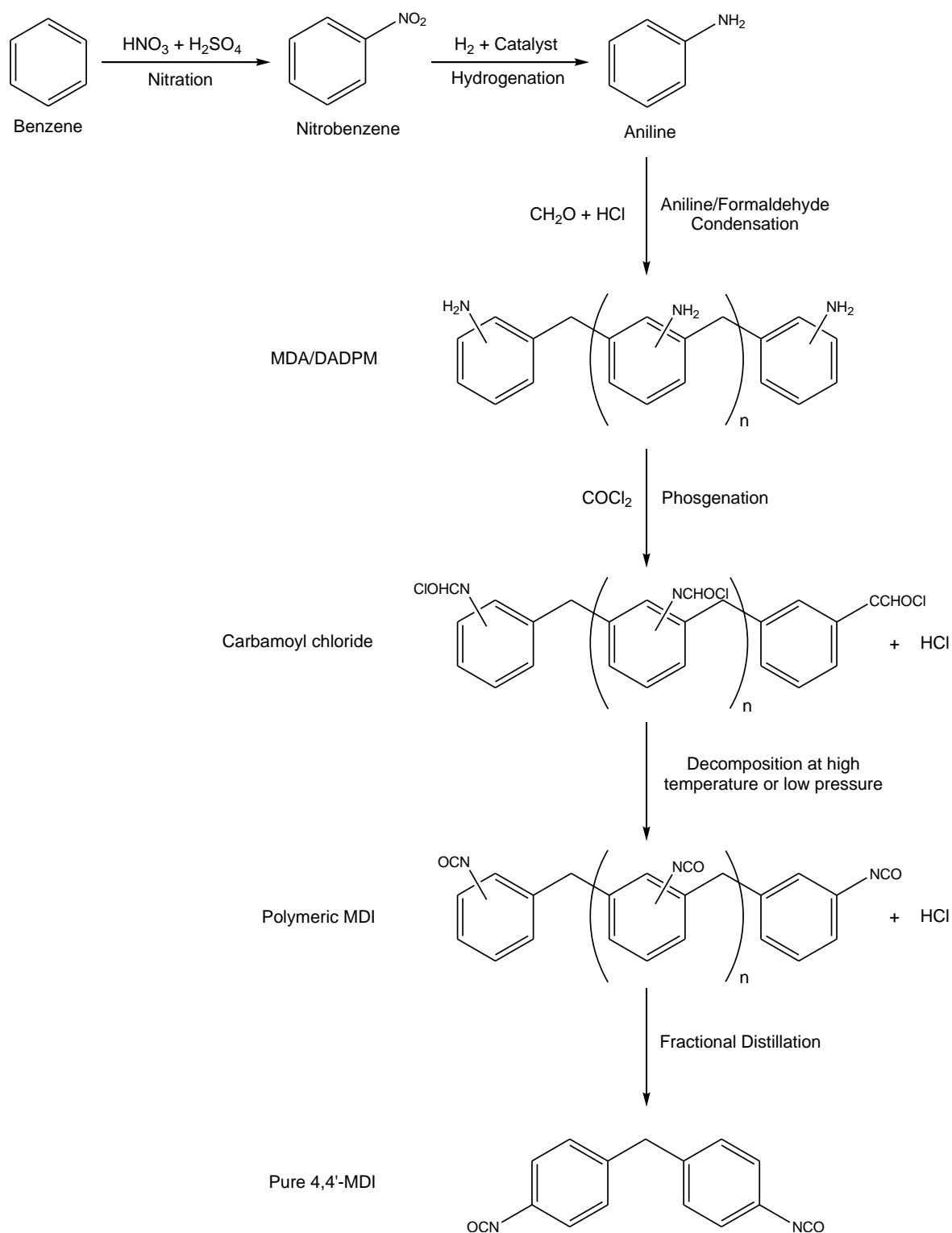


1.3 MDI Production

Scheme 2 shows the industrial route for the production of 4,4'-methylene diphenyl diisocyanate (MDI). The starting material for the synthesis is benzene, which is nitrated to nitrobenzene using a mixture of nitric and sulphuric acids. The nitro group is inserted into the aromatic ring via a nitronium ion, formed from an acid-base reaction between the two acids.¹ This reaction is carried out as an adiabatic process in which the heat produced from the reaction is recycled and used to remove water from the reaction mixture.¹² The nitrobenzene product, formed with 99.7% purity, is then catalytically hydrogenated to aniline.⁵ This process is normally carried out in the gas phase over solid catalysts but liquid phase processes can also be used. Bayer and Allied use fixed bed reactors with nickel sulphide catalysts giving a selectivity of >99%.¹³ Other catalysts involving metals such as Cu, Mn and Fe are employed by Lonza and ICI. Companies such as BASF use fluidized bed reactors with catalysts such as Cu, Cr, Ba and Zn oxides on a SiO₂ support. This produces a selectivity of 99.5%.¹³ Alternative routes to form aniline involve the ammonolysis of chlorobenzene or phenol and the reaction between benzene and ammonia. Interest in improving the efficiency of these processes is due to the importance of aniline in aromatic chemistry, by 1996 around 80% of aniline produced in the USA, Western Europe and Japan was used to make MDI.¹³

Before the phosgenation step to create the isocyanate, aniline undergoes a condensation reaction with formaldehyde. This is the 'functionality building' step in the production of MDI.⁵ The formaldehyde is added to mixtures of hydrochloric acid and aniline and acts as an acid catalyst to form methylene dianiline (MDA). The product mixture contains 50-80% MDA along with oligomeric compounds such as tri, tetra and pentamines. The ratios of

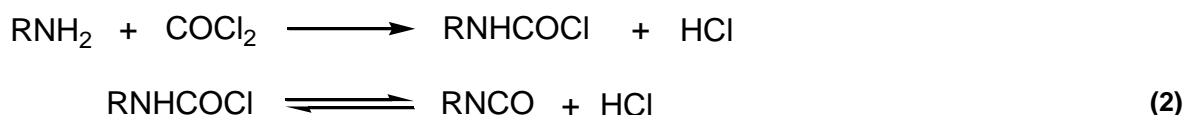
these compounds can be altered by changing the reaction conditions.⁵ Many isomeric forms of these compounds exist, MDA has three different isomers, 4,4' MDA, 2,4' MDA and 2,2' MDA.



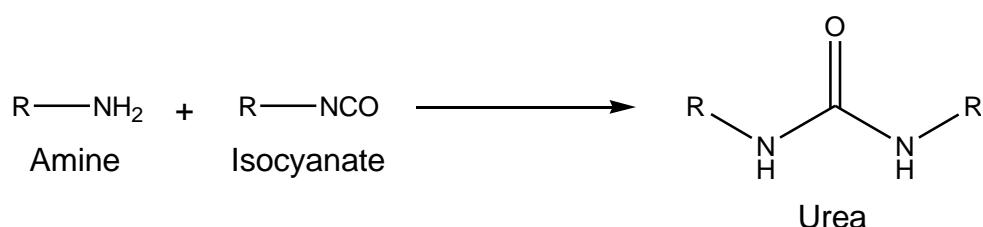
Scheme 2. Industrial synthesis of 4,4'-methylene diphenyl diisocyanate (MDI) from benzene

Research into the use of solid acid catalysts to replace hydrochloric acid has created interest since the 1970's and is still valuable to industrialists in order to reduce the costs involved and to avoid acid consumption.¹⁴ The most interesting developments thus far has been with the use of zeolites, although studies are still far away from industrial application.¹²

Once the desired amine mixture has been produced the final chemical stage in the production of MDI is carried out. This involves the introduction of phosgene, a highly reactive chemical species that will react with amines to form an isocyanate group via a carbamoyl chloride (2). During this reaction two exothermic side reactions create unwanted by-products. The first involves the addition of HCl to the amine starting material to form highly insoluble amine hydrochlorides. Research by Gibson into the structure and stability of these compounds has lead to a kinetic model for the recovery of the amine.¹⁵⁻¹⁷



The second reaction involves the formation of urea via reaction between the isocyanate and the amine (Scheme 3).^{18, 19} This reaction is well known and occurs via nucleophilic addition with the isocyanate behaving as an electrophilic reagent.²⁰ This reaction can be curtailed in the industrial process by using excess phosgene.⁵



Scheme 3. Formation of urea from reaction of amine and isocyanate

Once excess phosgene, solvent and hydrogen chloride have been removed, the crude isocyanate product can be purified by fractional distillation. Figure 1 shows a diagram representing this part of the plant process. The final MDI product consists of a mixture of isomers and oligomers, sold as polymeric MDI. This can be further fractionated to produce a 'pure' MDI product consisting only of the 4,4'-MDI isomer.⁵

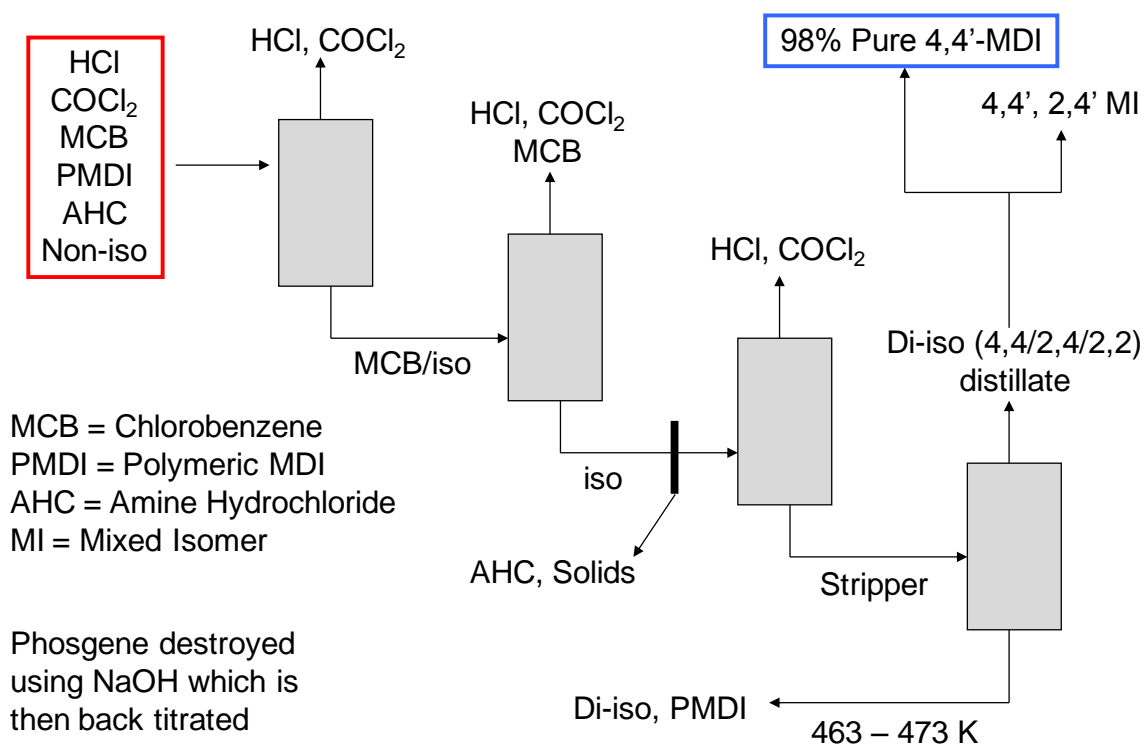


Figure 1. Plant process for the synthesis of MDI²¹

1.4 Phosgene

Phosgene is a highly toxic gas discovered by John Davy in 1812 after research into the reaction between dichlorine and carbon monoxide.²² Phosgene was first used in the late 1800's for the preparation of crystal violet and the dye precursor, Michler's ketone. German companies Friedrich Bayer & Co and BASF went on to utilize phosgene for the manufacture of synthetic dyes. During World War I, phosgene was used as a chemical weapon, ~18,000 tons of the gas was produced in Germany for this reason, with around the same amount produced by the Allies combined.²³ Nowadays phosgene is widely used in the chemical industry, utilized in the production of ureas, carbamates, chloroformates, polycarbomates and isocyanates as described in section 1.3. This leads to a range of products including plastics, solvents, perfumes, pesticides, dyestuffs and pharmaceuticals.²³ In the early years of the 21st century, 5-6 million tons y⁻¹ of phosgene was produced.²⁴ It is produced commercially by the chlorination of carbon monoxide using chlorine gas, by a process developed in the 1920's.

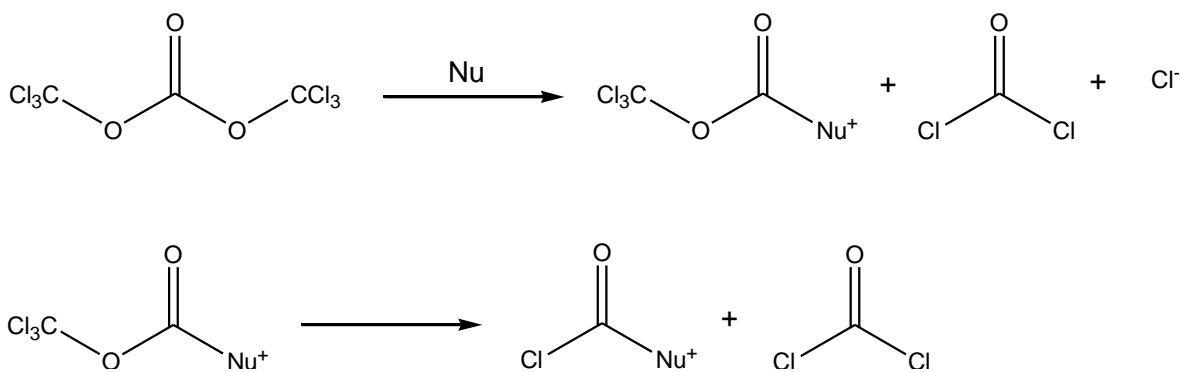
Due to the toxicity of phosgene, the vast majority of the gas is used at the site of production, and special expertise is needed in working with the compound. This has led to

the use of other compounds as phosgene substitutes. Compounds such as catechol phosphorus trichloride, oxalyl chloride and chloroformates have all shown to be successful in replacing phosgene in certain reactions.²⁴ Trichloromethyl chloroformate (diphosgene) and bis-(trichloromethyl) carbonate (triphosgene) can be used as sources of phosgene with the advantage of being easier to handle and transport.²⁵⁻²⁸ Diphosgene was also used as a warfare agent²⁹ and can be decomposed via a first order reaction to form phosgene above 573 K.²⁶ Phosgene is also formed after reaction with activated charcoal, however at room temperature metallic chlorides such as aluminium chloride can be used to breakdown diphosgene to CO₂ and CCl₄.³⁰

1.4.1 Triphosgene

Bis(trichloromethyl) carbonate, also known as triphosgene can act as a source or a substitute for phosgene, with its uses in organic synthesis rising considerably in the early 90's.^{31,32} It was first prepared by Counciler in 1880 by exhaustive chlorination of dimethyl carbonate.³³ The name triphosgene is actually a misnomer as it is not formed from carbonyl chloride.²⁷

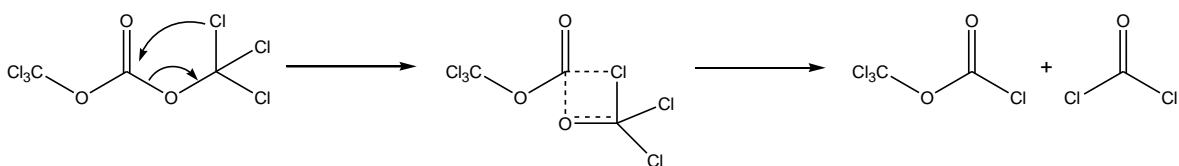
Triphosgene will produce phosgene upon heating or reaction with a nucleophile. Even at ambient temperature triphosgene has shown slow decomposition to phosgene.²³ It therefore is described as having the same toxicity of phosgene,³⁴ but it does have advantages over the gas. The compound is a stable solid at room temperature (mp 354-356 K, bp 476-479 K³⁵) making it easy to store, transport and safer to handle. As it will not diffuse as easily as the gaseous phosgene will, it does not need to be used in several fold excess. It has been used as a phosgene source in the phosgenation of amines, alcohols, ureas and phenols, reacting under mild conditions to give high yields.³⁶⁻³⁸ Triphosgene has previously been looked at as a replacement for phosgene in the synthesis of isocyanates,³⁹ this reaction is self-catalyzing with the amine starting material acting as a nucleophile to break down the triphosgene (Scheme 4).²⁸ Oxygen can also act as a nucleophile in compounds containing carboxylic acid and alcohol functional groups.



Scheme 4. Breakdown process of triphosgene on reaction with nucleophile

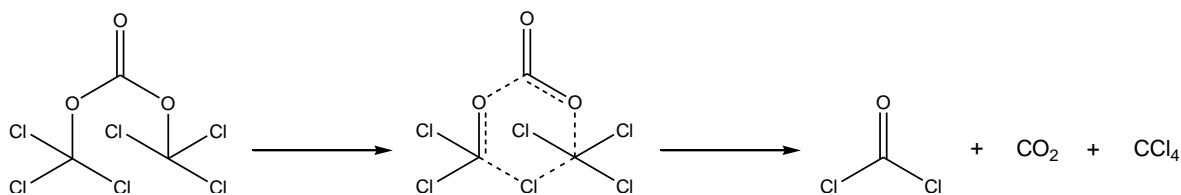
Nucleophiles such as triethylamine (TEA) and pyridine can be used as a base to promote the generation of phosgene; however these can complicate the work up of the product.³⁹ Iron oxide and activated charcoals can also be used as catalysts in order to breakdown the triphosgene to 3 equivalent moles of phosgene, while deactivated amine and imine functionality can also be used to control the decomposition.³⁵ A commercially available catalyst produced by Dr Eckert GmbH has been used in reactions with triphosgene to generate phosgene for downstream reactions. The catalyst activates the production of phosgene when the triphosgene reaches its melting point, thus producing a stream of phosgene that can be carried in an inert gas into the reaction mixture.²⁴

Without a nucleophile or catalyst present, triphosgene undergoes several decomposition pathways. Hood noted that under distillation conditions the compound decomposed to phosgene and diphosgene.²⁹ The mechanism for this reaction is postulated to involve a cyclic dissociation pathway (Scheme 5), this stems from electrostatic attraction between a negative chlorine and the positive carbonyl carbon atom.²⁷ This mechanism is favourable due to the conformation of triphosgene in the crystal structure, where each molecule consists of a planar chain, Cl-C-O-CO-O-C-Cl, with the remaining chlorine atoms almost symmetrically placed above and below.³¹



Scheme 5. Decomposition mechanism for triphosgene via 4 membered transition state²⁷

The thermal decomposition of triphosgene occurs at 403 K, producing phosgene, CO₂ and CCl₄. In this case the reaction is thought to proceed via a six-membered transition state (Scheme 6).³¹ Above 523 K, triphosgene can decompose directly into three molar equivalents of phosgene.²³ It is important to understand the conditions in which phosgene is released by triphosgene in order to introduce the safe use of the compound in organic synthesis. It has been shown to be a useful reagent in place of phosgene for small scale reactions and in research laboratories.



Scheme 6. Thermal decomposition mechanism for triphosgene via 6 membered transition state³¹

1.5 New Methods for MDI Synthesis

Currently in the chemical industry research is being undertaken in order to make processes more efficient and environmentally friendly (green chemistry).⁴⁰ As the synthesis of MDI involves the highly toxic phosgene as a reagent and also delivers HCl as a by-product, new methods for synthesizing MDI are currently being researched. Corma et al have had recent success with the use of gold to catalyse the *N*-carbamoylation of 2,4-diaminotoluene with organic carbonates.⁴¹ The production of a carbamate as a precursor to the isocyanate is a useful reaction as alcohol is formed as the by-product which is easily recycled. Various articles⁴⁰⁻⁴⁴ on this subject have appeared in the last decade, however due to high costs any new process is far from being implemented in industry. It is also noted that although the use of gold catalysts convey high selectivity, the reaction rates are rather slow (full conversion after ~ 5 hours⁴¹). This additional barrier prevents the application of this technology at present.

1.6 Colouration Problems

Various unwanted by-products and problems can occur in the industrial synthesis of MDI. One such problem is the issue of colouration. Strong red and brown colours are often seen in the final product which is undesirable to the customer.⁴⁵ For some applications colour can be an important factor in the acceptability of the product, for instance in the manufacture of footwear. A recognized feature of aromatic isocyanates is that the polyurethanes produced from them rapidly yellow on exposure to light or heat, whereas aliphatic isocyanates produce more stable products.^{5, 46} In fact polyurethanes produced from MDI are the most unstable.⁴⁷ The cause of this colouration has been investigated and is thought to occur through a radical mechanism where the urethanes will oxidise to produce the conjugated quinone-imide (Figure 2), a yellow chromophore.⁵ Other postulates for the colouration are the formation of azo ester compounds⁴⁸, the formation of polycarbodiimides and polypseudo urea compounds⁴⁹ and the oxidation of free amine groups in the mixtures.⁴⁶

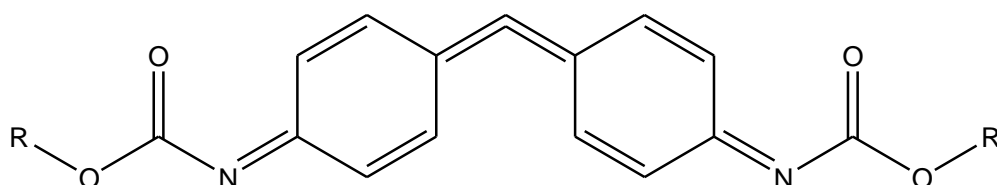
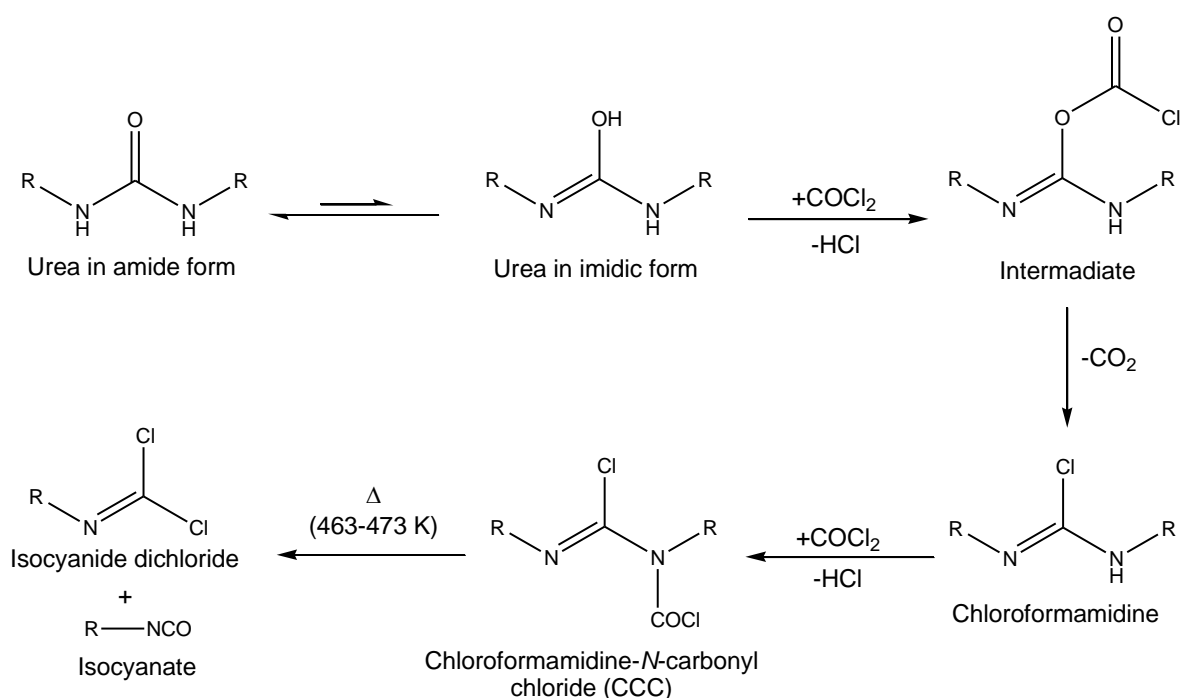


Figure 2. Quinone-imide structure derived from oxidation of MDI based polyurethanes

Investigations undertaken with toluene diisocyanate (TDI) have shown that in the presence of light or heat a yellowing can occur to the compound.⁴⁹ The mechanism for this reaction however is not fully understood. The research undertaken in the literature to date focuses on the yellowing of the polymeric material, providing mechanistic insight and treatments to this problem. However limited research is found on the colouration problem within the production of the isocyanate material. One such study was reported by Twitchett,⁵⁰ in which a reaction scheme centred on the urea side reaction described in section 1.3 is postulated. Significant aspects of Twitchett's article correspond to studies not accessible in the open literature. The work in this project aims to thoroughly investigate the claims made by Twitchett and the link to the colouration of MDI.

1.7 Postulated Reaction Scheme

The reaction scheme proposed by Twitchett⁵⁰ involves the urea compounds, produced via reaction of the product isocyanate with the starting amine, undergoing further reaction to produce precursors to the colouration seen in the final MDI product. The first step in the process is the tautomerism of urea to the imidic form. This then undergoes phosgenation to form a chloroformamidine (Scheme 7). The carbonyl group of the phosgene reacts with the oxygen on the urea to form the intermediate shown and releasing HCl. Release of CO₂ then occurs to give the chloroformamidine, which then reacts further with phosgene at the nitrogen position to form a chloroformamidine-*N*-carbonyl chloride molecule (CCC).⁵⁰ The CCC formed from the urea is then postulated to break down to an isocyanate and an isocyanide dichloride,⁵⁰ of which the latter is suggested to act as a source of chlorine radicals.⁵¹ This reaction occurs in the industrial process when the product mixture containing polymeric MDI goes through a heat treatment in a stripper (Figure 1) up to 453 K in order to get rid of the excess phosgene.¹⁸



Scheme 7. Postulated reaction scheme – phosgenation of urea to form isocyanide dichloride

A perception within the polyurethane manufacturing industry is that the chlorine radicals produced will initiate a reaction leading to the colouration of the MDI. However no scheme is described within the literature. The research carried out within the industrial

sector is also incomplete, with no clear evidence found linking the isocyanide dichloride to the production of colour.⁵¹

As suggested previously, colour can be a highly important factor in the purity of the final product, therefore providing an understanding of the reaction chemistry involved with a view to limiting the colouration would be useful information for operators of the process.

1.8 Urea Compounds

As discussed earlier, urea compounds are well known side products in the production of MDI. Urea was discovered in 1773 by Hilaire Rouelle, who isolated it from human urine. The compound was first synthesized in 1828 by Friedrich Wöhler by the reaction of silver cyanate with ammonium chloride, and was one of the most important discoveries in chemistry, marking the beginning of organic synthesis.^{52, 53} Substituted ureas have various applications in the chemical industry, particularly in agriculture as plant growth regulators, pesticides and herbicides. There are various methods of synthesizing substituted urea compounds such as the reaction of amines with alkyl halides or metal cyanates and catalytic or oxidative carbonylation of amines.⁵⁴ The most popular method however is the reaction between an isocyanate and an amine (Scheme 3), most widely used for asymmetric ureas.⁵⁴ The mechanism of this reaction is debatable. It is believed to occur via a two-step process, the first step involving the formation of an activated complex, followed by reaction with the amine.⁵⁵ However thermodynamic studies carried out showed the possibility of a four-centre activated intermediate complex.⁵⁴

1,3-Diphenylurea is a commercially available compound that is relevant to the work carried out in this project as it provides a model to the more complex ureas formed in the industrial process. The compound was first synthesized by Hoffman by passing phosgene through a saturated aqueous solution of aniline.⁵⁶ The mechanism for this reaction is complicated involving several processes with carbamoyl chloride and amine hydrochlorides formed as intermediates or by-products.⁵⁷

1.8.1 Crystal Structure

The structure of urea ($\text{CO}(\text{NH}_2)_2$) was one of the earliest crystal structures to be solved by X-ray crystallographic methods. It was found to have a unit cell containing two molecules and the packing is largely based on hydrogen bonding.^{58, 59} Deshapande produced a study on the crystal structure of several disubstituted aromatic ureas, including 1,3-diphenylurea, which was found to have a space group of $P2_1cn$ in an orthorhombic crystal system. The unit cell consisted of 3.90 molecules.⁶⁰ The findings indicated that the $\text{C}=\text{O}$ bond would be aligned with the c axis and molecular chains would be formed through hydrogen bonding between the amide hydrogens and the oxygen on the next molecule. This structure is typical of symmetrical disubstituted ureas and was also seen in the longer chain N,N' bis(4-biphenyl)urea (Figure 3).⁶¹

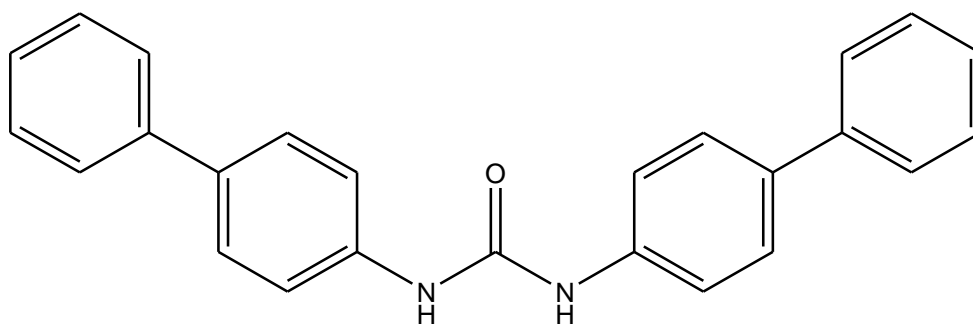


Figure 3. N,N' bis(4-biphenyl)urea

1.8.2 Tautomerism

The postulated reaction mechanism for the phosgenation of the urea leads with the conversion of the urea from its amide form to the imidic form (Scheme 7). This mechanism is proposed by both Twitchett⁵⁰ and Ulrich et al,⁶² with the oxygen lone pair attacking the carbonyl of the phosgene to create an intermediate which, through the loss of CO_2 , forms the chloroformamidine. However urea compounds are almost exclusively found in the amide form, with evidence for the imidic form lacking and controversial, as well as being found to be thermodynamically unstable.⁶³⁻⁶⁵ A number of authors have proposed a zwitterionic structure, although this is also contentious.⁶⁴ Piasek and Urbanski studied the infrared spectra of urea dissolved in polar solvents, finding that a band occurs for the vibration of $\text{C}=\text{N}$ in the imidol form. This was backed up by reaction with diazomethane to give O-methyl-iso-urea, leading to the statement that ‘experimental fact gives final

evidence of the tautomerism of urea'.⁶⁶ However a more recent study using mass spectrometry suggests that although disubstituted thioureas proved to undergo tautomerism, imidolization was not seen in the case of 1,3-diphenylurea.⁶⁴

1.9 Analytical Techniques

1.9.1 Electron Paramagnetic Resonance (EPR) Spectroscopy

Electron paramagnetic resonance (EPR) spectroscopy is a technique that can be used to identify free radicals by using a concept analogous to NMR. The first successful measurement of an EPR spectrum was by Zavoisky in 1945. In the case of EPR, the interaction between electromagnetic radiation and magnetic moments arising from electrons are studied.⁶⁷ EPR spectroscopy is limited to systems which have electronic angular momentum arising from contributions from both the intrinsic spin and the orbital motion of electrons. Therefore EPR is normally only observed in systems containing unpaired electrons, such as radical species.⁶⁸ Spectra are recorded by passing a beam of electromagnetic radiation through the sample material and measuring the attenuation versus frequency.⁶⁷

1.9.1.1 Spin Trapping

In many occasions the direct detection of radical intermediates is still impossible. Reasons for this are that the concentration of the species is too low to be measured by the spectrometer, the radicals are too short lived or the radicals give broad, undetectable features (eg. alkoxy radicals).⁶⁹ Spin trapping is a procedure that was developed in order to capture and measure these types of radicals, by transforming them into a more stable paramagnetic species in order that the concentration can be increased to the level required for detection.^{70, 71}



The general reaction scheme for a spin trap is shown in Equation (3). In this case R-ST[•] is known as the 'spin adduct'. The most common compounds used as spin traps are nitrones and C-nitroso compounds. *N-tert-Butyl- α -phenylnitron*e (PBN) is one such nitron

is a popular choice of spin trap due to its longevity and high reactivity.⁷² The spin adduct in this case is a stable nitroso radical.⁷³

1.9.1.2 Chlorine Radicals

The role of the chlorine radical in mechanistic studies has been well reported due to the importance of chlorocarbons and chlorohydrocarbons.⁷⁴ For example, Cl^\bullet has been implicated as a catalyst in the dehydrochlorination of simple hydrochlorocarbons.^{75, 76} The lifetime of Cl^\bullet is short, at room temperature and low pressure its mean lifetime is a few ms.⁷⁷ This makes the direct recording of EPR spectra for these species problematic. Although the EPR spectrum has been recorded in the gas phase,⁷⁸ the radicals are not detectable in solution.⁷⁹ A number of studies using the spin trapping method with *N-tert-Butyl- α -phenylnitron* (PBN) to record chlorine adducts has been successful.^{80, 81} Therefore this technique is utilized within this project

1.9.2 Infrared Spectroscopy

Infrared spectroscopy is an important technique used to measure molecular vibrations. The infrared region of the electromagnetic spectrum is sub-divided into 3 ranges, the near infrared (1 – 2.5 μm), the mid infrared (2.5 – 50 μm), and the far infrared (beyond 25 μm).⁸² The most useful vibrations within an organic compound occur in the range of 2.5 – 1.6 μm ⁸³ with an infrared spectrometer normally recording in the range 4000 – 625 cm^{-1} .⁸³ Each functional group will vibrate at a specific frequency, providing a method of identification. The frequency at which a group vibrates is determined by interatomic distances, bond angles and force constants within the molecule.⁸⁴ The simplicity, accuracy and versatility of IR spectroscopy makes it one of the most popular techniques for identification of organic compounds.⁸⁵

The development of Fourier transform infrared (FTIR) spectroscopy in the 1960's has increased the ease at which infrared spectra can be recorded. This technique utilizes a Michelson interferometer, an optical device developed in 1880 by Albert Abraham Michelson and a minicomputer running the Cooley-Tukey algorithm.⁸⁶ FTIR is a single beam technique in which the radiation from the source is split into two. One beam is transmitted to a movable mirror with the other reflected to a fixed mirror. The two beams

then recombine to interact with the sample and then strikes the detector. The signal adsorbed from the mirrors can then be transformed into the desired result using a Fourier transform algorithm.^{87, 88}

1.9.2.1 Attenuated Total Reflectance (ATR)

Within this project the method of attenuated total reflectance was used to measure the infrared spectra of any compounds studied. This is a simple method for measuring solids and oily substances with little or no sample preparation.⁸² Spectra are obtained by reflection rather than transmission. An accessory containing a material of high refractive index known as an internal reflection element (IRE), is placed in the spectrometer. The sample is placed so that it is in close contact with the IRE, which is typically ZnSe or Ge.^{86, 88} Infrared light is then internally reflected multiple times, affected by the presence of the sample material.

1.9.3 Ultraviolet and Visible Absorption Spectroscopy

Ultraviolet-visible (UV/Vis) spectroscopy is concerned with measuring electronic transitions in organic compounds in the region between 180 and 1100 nm. The region is split into three sections, near UV (185 – 400 nm), visible (400 – 700 nm) and very near infrared (700 – 1100 nm).⁸² It is difficult to distinguish between different functional groups in UV/Vis spectroscopy. However this technique is very useful for quantitative measurements. This type of spectroscopy is based on two laws; Beer's law states that absorption is proportional to the number of absorbing molecules, Lambert's law states that the fraction of the incident light adsorbed is independent of the intensity of the source.⁸³ These laws are combined to give the equation (4) below⁶⁸:

$$\text{Absorbance} = \log_{10} \frac{I_0}{I} = \epsilon c l \quad (4)$$

Where:

- I_0 = incident monochromatic light intensity
- I = transmitted monochromatic light intensity
- ϵ = molar extinction coefficient
- c = concentration (M L⁻¹)
- l = path length (cm)

In order to measure the absorbance of a compound it is dissolved in a solvent until the solution is dilute, a sample is then added to a transparent cell in which a beam of light is passed through. A second beam of light is passed through a cell containing the pure solvent acting as a reference solution. The difference in transmission is used to create the absorbance spectrum.

1.9.3.1 Transitions

A number of transitions are measured in UV/Vis spectrometry. These include $\sigma \rightarrow \sigma^*$, $n \rightarrow \sigma^*$, $n \rightarrow \pi^*$, $\pi \rightarrow \pi^*$ and $d \rightarrow d$ transitions. These transitions occur at different wavelengths with different intensities. Therefore it is useful to look at different regions of the spectrum with different concentrations of the sample solution.⁸²

1.9.3.2 Factors Affecting Absorption

Conjugated systems in particular give rise to informative spectra. The number of double bonds in a molecule has an effect on the absorption of that molecule. As the conjugation increases, the wavelength of the maximum absorption will increase, moving into the visible range. Polyene compounds are examples of simple conjugated materials showing this phenomenon.⁸³

Substituted benzene rings also produce a shift in wavelength and a change in intensity depending on the substituent. A shift to higher wavelength ('red shift') is known as a bathochromic effect.⁸² Again this occurs when more conjugation is added to the benzene ring or the presence of an auxochrome. The shape of the spectra do not show any major changes as the conjugation is increased in these cases.⁸³ The type of transitions seen in aromatic compounds like benzene are $\pi \rightarrow \pi^*$ transitions. These are concerned with alternating double and single bonds and arise from overlap of the π -orbital. This reduces the energy separation between the ground and excited states resulting in absorbance at longer wavelengths and produces an intense band referred to as the *K*-band.⁶⁸

Chapter 2

Experimental

2 Experimental

2.1 Chemicals

1,3-Diphenylurea (Urea 1)	Sigma-Aldrich, 98%
1,3-Di- <i>p</i> -tolylcarbodiimide	Sigma-Aldrich, 96%
1,4-Dibenzylbenzene	Sigma-Aldrich
2-Butanone	Sigma-Aldrich, $\geq 99\%$
4,4'-Methylene dianiline (MDA)	Sigma-Aldrich, $\geq 97\%$
4,4'-Methylene diphenyl diisocyanate (MDI)	Huntsman Polyurethanes
4-Benzylaniline (4-BA)	Alfa Aesar, 98%
4-Benzylphenyl isocyanate (4-BAI)	Sigma-Aldrich, 97%,
Acetone	VWR Prolabo, 99.5%
Acetone AR	Fisher Scientific, 99.8%
Acetone- d_6	Cambridge Isotopes Limited, 99.9%
Acetonitrile	Fisher Scientific, 99.9%
Ammonium iron (III) sulphate dodecahydrate	Sigma-Aldrich, $\geq 99\%$
Benzene	Sigma-Aldrich, $\geq 99\%$
Benzene- d_6	Cambridge Isotopes Limited, 99.6%
Chlorobenzene	Sigma-Aldrich, 99.8%, anhydrous
Chloroform	Fisher Scientific, 99.8%
Chloroform- d	Cambridge Isotopes Limited, 99.8%
Cyclohexane	Fisher Scientific, 99%
Dichlorine	Linde 99%
Dichloromethane	Fisher Scientific, 99.8%
Dimethyl sulfoxide	Fisher Scientific, $>99\%$
Dimethyl sulfoxide- d_6	Cambridge Isotopes Limited, 99.9%
Eckert cartridge for phosgene generation	Sigma-Aldrich
Ethanol	Sigma-Aldrich, absolute $\geq 99.5\%$
Methanol	VWR Prolabo, 99.8%
Methyl orange	Fluka, indicator
Nitric acid	Fisher Scientific, 69.7%, 1.42 S.G.
Nitrogen gas	BOC
<i>n</i> -Propanol AR	Fisher Scientific, 99%

<i>N-tert</i> -butyl- α -phenyl nitron (PBN)	Sigma-Aldrich, $\geq 98\%$
<i>o</i> -Dichlorobenzene (ODCB)	Sigma-Aldrich, 99%, anhydrous
Phenyl isothiocyanate	Sigma-Aldrich, 99%
Polymeric MDI (PMDI)	Huntsman Polyurethanes
Potassium thiocyanate	Sigma-Aldrich, $\geq 99\%$
Propan-2-ol - AR	VWR Prolabo, $\geq 99.7\%$
<i>p</i> -Tolyl isothiocyanate	Sigma-Aldrich, 97%
Silicone oil (Rhodorsil [®] Fluid)	Bentley Chemicals, 47V100
Silver nitrate	Fisher Scientific, 0.02 N
Sodium hexachloroplatinate (IV) hexahydrate	Sigma-Aldrich, 98%
Sodium Hydroxide	Riedel-de Haën, 99%
Sulphuric acid	Alfa Aesar, 3 mol dm ⁻³
Terephthaloyl chloride	Fluka, 99%
Tetrahydrofuran	Fisher Scientific, 99.9%
Toluene	Fisher Scientific, 99.9%
Triphosgene	Fluka, $\geq 99\%$
Water (deionised)	Elga, Reservoir, 75 L

Potassium thiocyanate solution (0.02 N): Solid potassium thiocyanate (0.49 g, 5.0 mmol) was dissolved in distilled water (250 cm³).

Ferric ammonium sulfate solution (saturated): Ammonium iron (III) sulphate dodecahydrate (8.05 g, 16.7 mmol) was dissolved in distilled water (20 cm³) and a few drops of concentrated nitric acid added.

2.2 Apparatus for Synthesis Reactions

The synthesis reactions were carried out in a four-neck Pyrex, round bottomed flask reactor that could be modified to suit the specific reactions (Figure 4). A condenser was fitted to the top of the flask with the output connected first to an expansion vessel, in order to create space in the case that a large volume of gas was expelled from the reactor, then to a scrubber system. The temperature of the solution was measured using a thermocouple inserted into a glass sleeve in one of the necks, making direct contact with the solution. N₂ was flowed into the reactor passing through a series of taps, variable flow meter, trap, oil

bubbler containing silicone oil and glass sparge. The fourth neck was blocked with a SubaSeal rubber septum through which the reagents could be added by means of a syringe. An IKA stirrer hotplate with an oil bath (silicone) was used to heat the solutions, using a contact thermometer to control the temperature of the oil. Magnetic stirrer bars were placed in both the four-neck flask and the oil bath. The solution could also be cooled by swapping the oil bath for a cooling bath. Different mixtures of solvent, ice or solid CO_2 were used to produce the desired temperature for each reaction.

Several different reactions were carried out using this apparatus. Sections 2.2.1 to 2.2.2 describe the different classes of reactions and any modifications made. Sections 2.4 to 2.10 go on to describe the procedure for the individual reactions carried out.

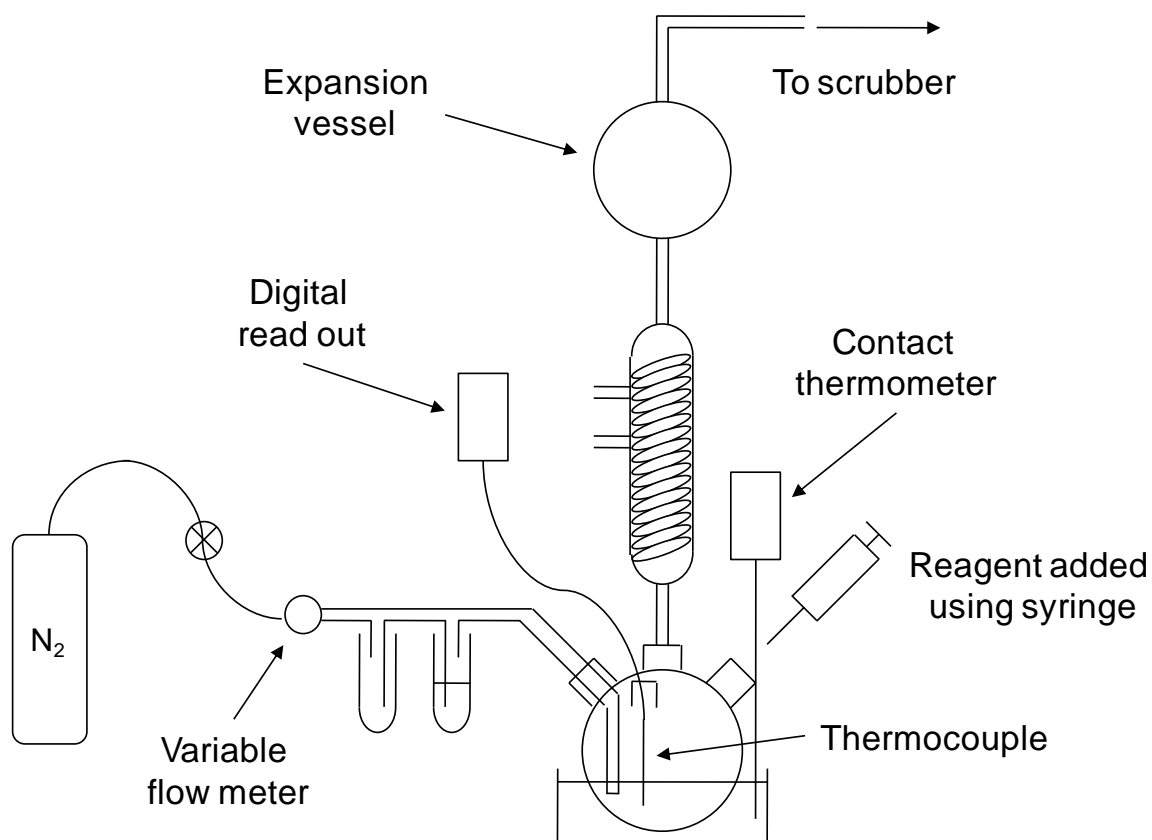


Figure 4. Synthesis apparatus

2.2.1 Phosgenation

Two different phosgenation reactions were carried out as detailed in sections 2.4 and 2.8. Due to the toxicity of phosgene, it was decided not to use neat phosgene in the laboratory as a safety precaution. This led to the use of triphosgene, a solid compound which can be

used as an alternative to phosgene, as outlined in section 1.4. However problems, which are discussed later, arose in the use of this molecule as a source of phosgene. Therefore a second method involving an Eckert cartridge was used and found to be successful.

2.2.1.1 Triphosgene

Reactions involving triphosgene as one of the reactants were carried out by first dissolving the triphosgene in the solvent, chlorobenzene (MCB), and adding this directly to the reactor via a funnel. The solution was purged for 5 min with N₂ and a cyclohexane/CO₂ bath was used to keep the solution below 283 K whilst the starting material was added using a syringe. The reaction could then be set to the desired temperature and left for a period of time. After the reaction had finished the solution was transferred to a single-necked round bottom flask and the solvent is evaporated using a rotary evaporator. This also ensures no phosgene is left in the product.

2.2.1.2 Eckert Cartridge

For the second method of producing phosgene, cartridges for safe generation of phosgene designed by Eckert⁸⁹ were purchased from Sigma-Aldrich. These cartridges consist of a capped plastic test tube containing triphosgene and a deactivated amine or imine based catalyst, used to stimulate the decomposition of the triphosgene into three moles of phosgene. The reaction is activated at the temperature which the triphosgene begins to melt (~353 K) and proceeds cleanly up to 383 K.²⁴ The rate of reaction increases with temperature therefore the release of phosgene can be controlled. Figure 5⁹⁰ shows the rate of phosgene produced over time at different temperatures. This figure, provided by the suppliers can therefore be used as an aid to deciding on the reaction parameters.

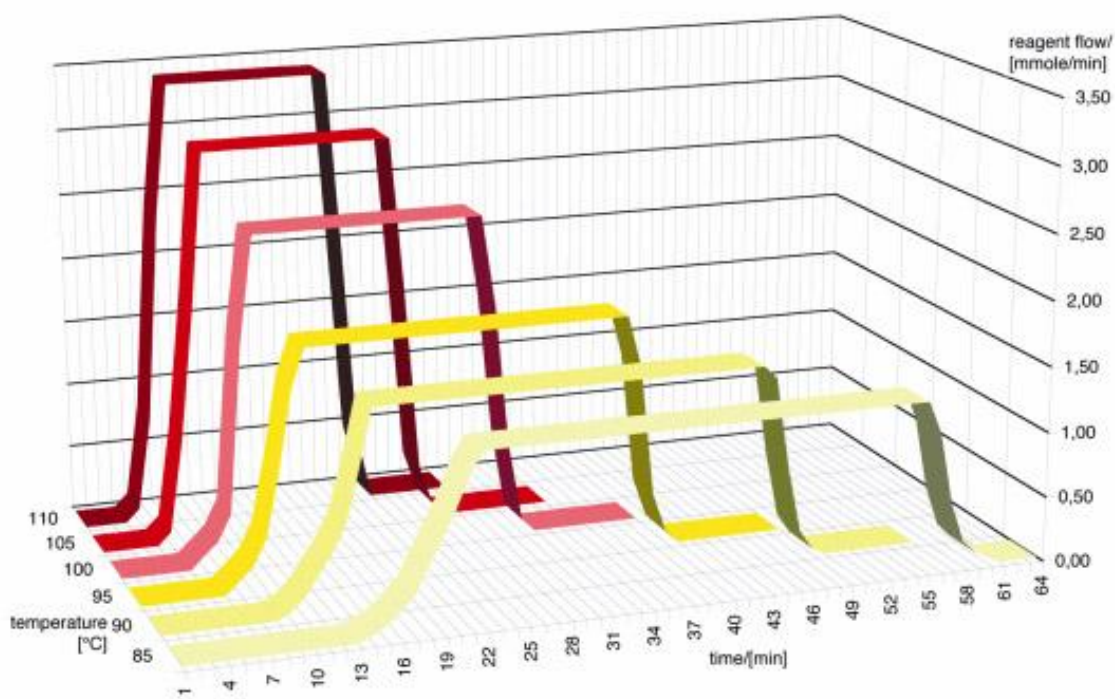


Figure 5. Release of phosgene from Eckert cartridge⁹⁰

Modifications to the apparatus for use of this cartridge are shown in Figure 6. Rubber tubing and a L2 Young's tap are used to connect the test tube to the gas flow going into the reactor. The starting material is dissolved in the solvent and added to the reactor with a cyclohexane/ CO_2 bath to keep the solution below 283 K. The solution is purged with N_2 for 5 min then the Eckert cartridge is heated to between 363 K and 383 K for the length of time required to react all of the triphosgene. This then creates a flow of phosgene into the reactor. The N_2 purge is kept on to allow the gas to flow through the solution and into the scrubber. The Eckert cartridge is then disconnected and made safe using methanol.⁹⁰ The solution in the reactor could then be heated and left to react under a nitrogen purge. As with the triphosgene reactions, the solution is then transferred to a single-necked round bottom flask and the solvent is evaporated using a rotary evaporator. As this method uses phosgene as the reactant, a fourfold molar excess is needed to ensure all the starting material is used up.²⁸

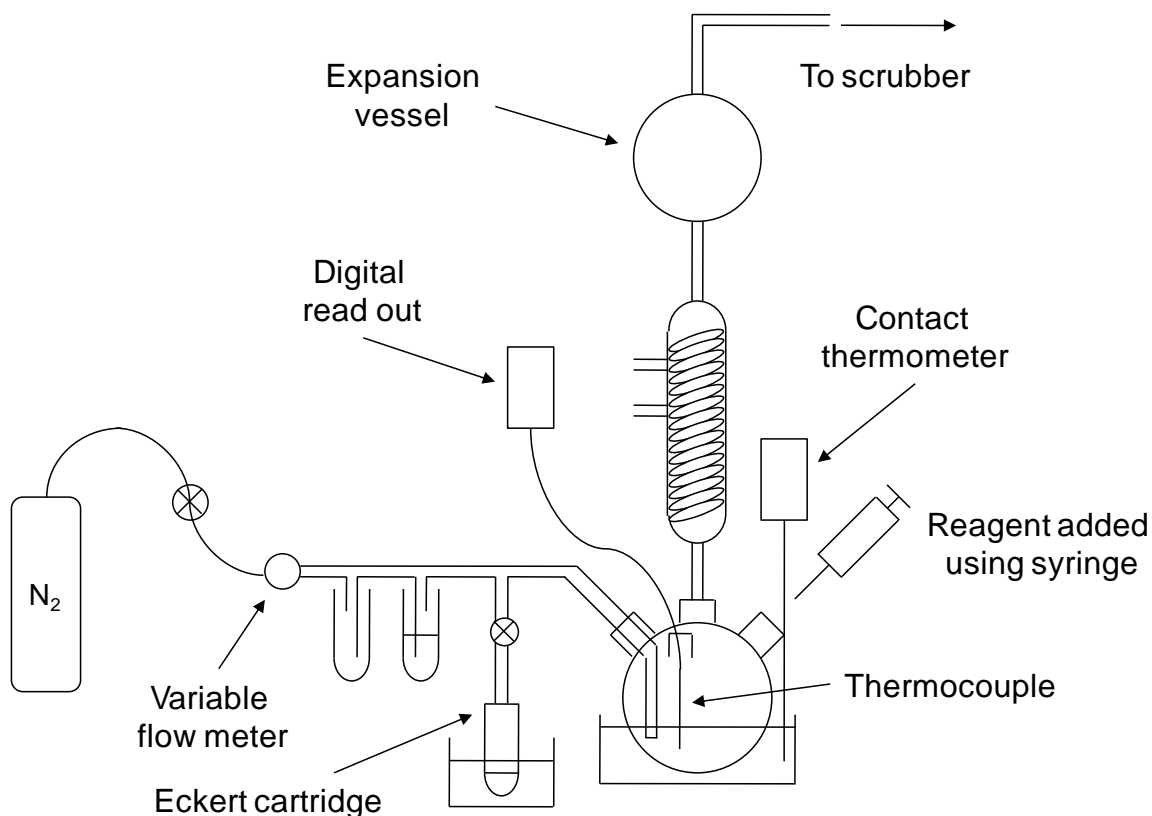
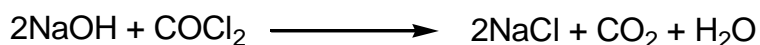
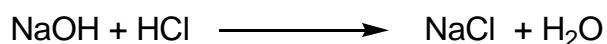
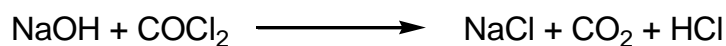


Figure 6. Modifications to apparatus for the use of Eckert cartridge

2.2.1.3 Scrubber System

A scrubber system was put in place at the back end of the reactor to neutralise any excess phosgene gas or HCl produced in the reaction. Equation (5) describes the reaction process. A peristaltic pump is used to force a 10% solution of NaOH through a column containing raschig rings where it meets the gas from the reactor (Figure 7). A condenser is also built into the system in order to stop the solution overheating and a thermocouple is inserted into the reservoir of NaOH to measure any change in temperature.



(5)

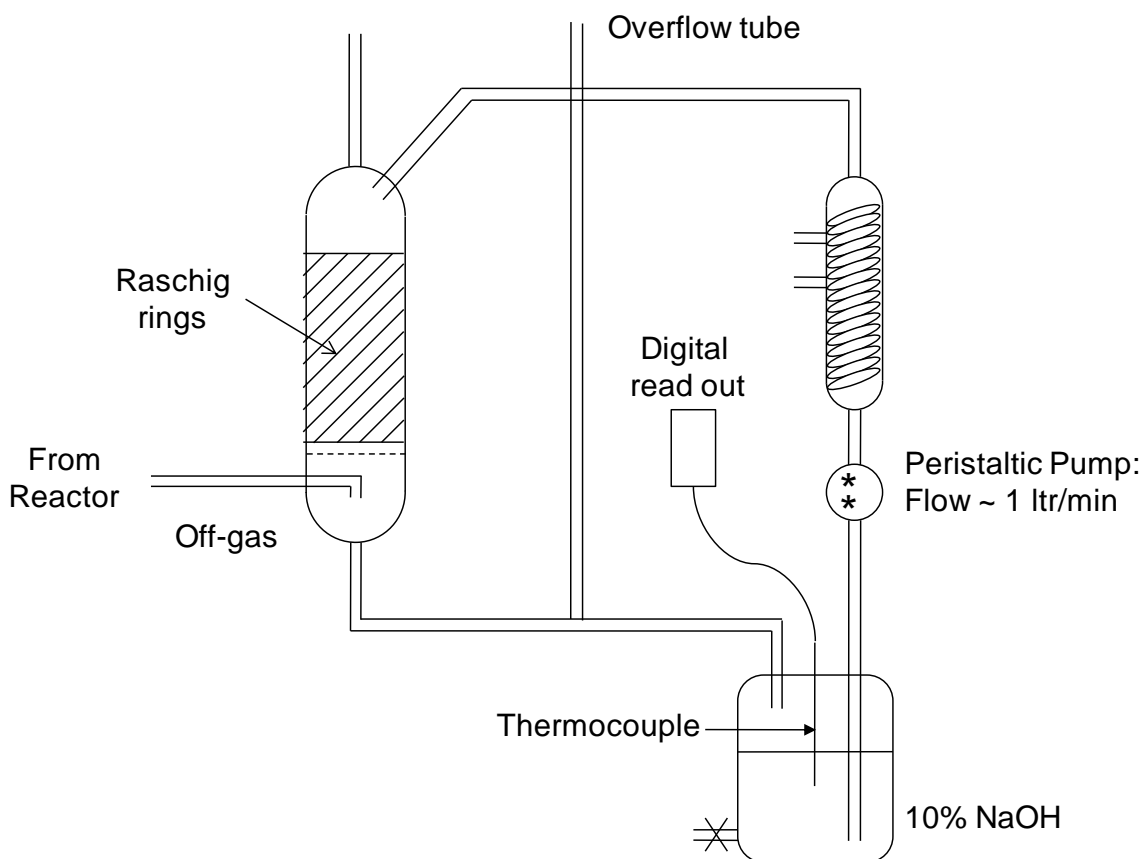


Figure 7. Scrubber system for destruction of excess phosgene

2.2.1.4 Detection Methods

Another safety measure put in place was a fixed detection unit for phosgene gas (Compur Statox 501). The unit comprised of a controller and a sensor head with a measuring range of 0 – 0.3 ppm. An alarm was set to go off when the detector registered 0.02 ppm. This value is the occupational exposure limit (OEL) for phosgene in the EU over an 8 hour period. Phosgene dosimeter badges (Compur) were also used by any personnel entering the laboratory where the phosgenations were being carried out. The badges consisted of two types of paper, diffusion and indicator, which changes from yellow to brick red on exposure to phosgene. A colour comparator chart could then be used to accurately evaluate the phosgene dose that the person had been exposed to. Up to 150 ppm min^{-1} can be measured in this way.

Indicator paper acquired from Honeywell Analytics was also used to determine whether samples contained any phosgene. This paper turned from cream to red on exposure to phosgene gas; therefore it could be used to detect any toxicity in the samples and also in the reaction apparatus. This paper is more sensitive than other methods used and can

measure phosgene in the ppb range, making it a highly useful tool in maintaining the safety of the laboratory procedure.

2.2.2 Chlorination

Another modification was made to the reactor in order to carry out chlorination reactions. The front end of the reactor was modified so that both Cl_2 and N_2 were able to flow into the reactor together or separately (Figure 8). An extra trap was also inserted after the oil bubbler. A round bottom flask containing H_2O and methyl orange as an indicator is placed after the expansion vessel in the outlet line. This allows any excess Cl_2 to be neutralised before entering the scrubber system. Cl_2 gas is provided by a lecture bottle. A N_2 flow is used at all times to ensure the gases flow into the reactor and out into the scrubber.

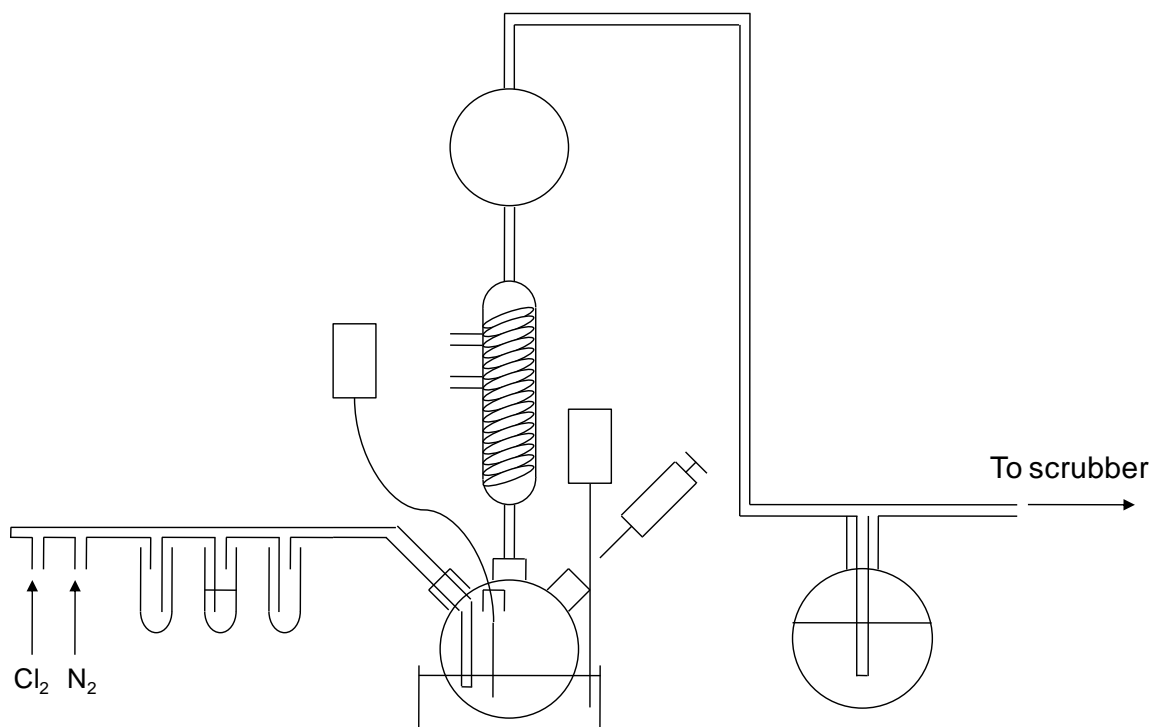


Figure 8. Modifications to apparatus for use in chlorination reactions

2.3 Characterisation Techniques

2.3.1 Fourier Transform Infrared (FTIR) Spectroscopy

Infrared analyses were carried out on a Nicolet Avatar 360 FTIR spectrometer. A Pike MIRacle ATR accessory with a diamond/ZnSe element was used for all samples as this provided a straightforward way of measuring a range of substances including solids, liquids and oils. Solid samples were measured using the high pressure clamp with a flat tip. For liquids and oils, a trough insert was used forming a shallow well to allow close contact with the crystal. The accessory was continually purged with dry air, from which the carbon dioxide had been removed (Donaldson Ultrapac MSD 0025 M). All spectra were recorded in absorbance with a resolution of 2 cm^{-1} , giving a data spacing of 0.964 cm^{-1} . 256 scans were run in the region of $400 - 4000\text{ cm}^{-1}$.

2.3.2 Nuclear Magnetic Resonance (NMR) Spectroscopy

^1H -NMR and ^{13}C -NMR spectra were recorded on a Bruker Avance spectrometer fitted with a Quattro nucleus probe (QNP) at 400 MHz for ^1H and 100 MHz for ^{13}C . A few mg of the sample to be measured was dissolved in a deuterated solvent. Chloroform-d (CDCl_3) was used where possible and dimethyl sulfoxide- d_6 (DMSO) was used for the urea compounds as they would not dissolve in other solvents. The solution was added to an NMR tube to a 4 cm depth, which was then capped. This was added to an auto sampler connected to the spectrometer. For samples measured without removal of the reaction solvent, chlorobenzene, a Wilmad NMR capillary tube allowed a deuterated solvent (in this case benzene- d_6) to be added to the NMR tube with the sample solution. This allowed analysis of the product out with the aromatic NMR region where peaks for chlorobenzene would appear.

2.3.3 Elemental Analysis

Elemental analysis for C, H and N were carried out using an Exeter Analytical C440 Elemental Analyser. Samples were weighed using a Mettler ultra micro balance.

2.3.4 Melting Point Determination

The melting point determination was carried out on solid materials using a Stuart Scientific SMP1 manual melting point reader, consisting of an electrically powered heating block, a magnifying eyepiece and a mercury-in-glass thermometer. A few mg of the sample to be analysed is placed in a capillary tube sealed at one end using a Bunsen burner, making sure the depth of the sample was ~ 1 cm. The tube is placed in the heating block where it is heated with a ramp rate of 10 K min^{-1} to determine a rough melting point for the sample. A fresh tube with more sample material added is then placed in the heating block after it has cooled. This sample is heated at the same rate until it reaches $\sim 75\%$ of the expected melting point. The ramp is then slowed to $\sim 2 \text{ K Min}^{-1}$ in order to evaluate a more precise result. The sample is watched throughout and the melting point recorded at the point the sample turns to a liquid. This procedure was repeated several times in order to gain an accurate result.

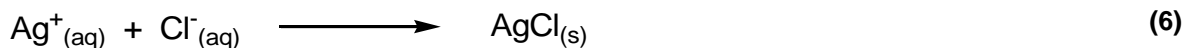
2.3.5 Thermal Analysis

Thermal gravimetric analysis was carried out on a Q500 Thermogravimetric Analyser (TA Instruments) between the temperature range of 295 K to 503 K. A Q100 Differential Scanning Calorimeter (TA Instruments) was used to carry out differential scanning calorimetry analysis between the temperature range of 303 K to 503 K.

2.3.6 Available Chlorine

Available (or ionisable) chlorine is defined as the % weight of chlorine as determined after reaction with an alcohol^{5, 91}. The loss of chlorine under these conditions is believed to occur by a polar mechanism, as alcohol has an ionizing capability similar to that of polyols. This method is used in industry to determine free chlorine content or chlorine containing impurities.⁹² It can therefore be used as a measure of the effect of these impurities within isocyanate mixtures on its reactivity in polyurethane formulations. After reaction with alcohol, the available chlorine can be determined by argentometry.⁹³ For example, the Volhard method^{94, 95} for the determination of chloride ions uses a back titration with potassium thiocyanate to determine the concentration of chlorine in a solution. First, a known volume of a silver nitrate is added to the solution, whereby the

silver ions will react with the chlorine forming a precipitate of silver chloride (6). Using an excess amount ensures all the chloride ions will react. The solution is then titrated with potassium thiocyanate solution as the thiocyanate will react with any excess silver to produce silver thiocyanate (7). Fe^{3+} (ferric ion) is added to the solution as an indicator as the slightest excess of thiocyanate reacts with Fe^{3+} to form a dark red complex⁹⁶ (8). This method is used when the solution is acidic as this prevents hydrolysis of the Fe^{3+} ion.



Two methods of chloride analysis were used to determine the available chlorine as described below.

2.3.6.1 Volhard Method

A sample (~0.1 g) of the compound to be analysed was weighed into a dry conical flask, dissolved in acetone (5 cm³, AR) and *n*-propanol (10 cm³, AR) was added. The solution was stirred for 10 minutes before adding sulphuric acid (3 mol dm⁻³, 1cm³) to acidify the solution. The solution was then split into 3 equal portions and analysed for chloride content using the Volhard method. Silver nitrate (20 cm⁻³, 0.02 N) was added to the solution to form AgCl. A few drops of ferric ammonium sulphate were added as an indicator and the solution titrated with potassium thiocyanate (0.02 N) to find the number of moles of excess Ag^+ ions. The end point in the titration was taken when the solution turns orange. The procedure was repeated to test the accuracy of the experiment. The ionisable chlorine content is found from equations (9) and (10).

$$\begin{aligned} &= \text{Moles of silver} - \text{moles of thiocyanate} \\ \text{Moles of chlorine} &= ([\text{Ag}^+] \times V(\text{AgNO}_3)) - ([\text{SCN}^-] \times V(\text{KSCN})) \\ &= 0.012 - (0.02 \times \text{titre (L)}) \end{aligned} \quad (9)$$

$$\text{Ionisable chlorine} = \frac{\text{Moles of chlorine} \times 35.5}{\text{Sample weight of chlorine (g)}} \quad (10)$$

2.3.6.2 Chloride Analyser

A sample (~0.01 g) of the compound to be analysed was weighed into a dry conical flask, dissolved in acetone (5 cm³, AR) and *n*-propanol (10 cm³, AR) was added. The solution was stirred for 10 minutes before adding sulfuric acid (3 mol dm⁻³, 1cm³) to acidify the solution. A Sherwood chlorine analyser was used to quantify the amount of free chlorine in the solution using the argentometry method. An aliquot (0.5 cm³) of the sample solution is added to an acid buffer and titrated against Ag⁺, generated electrochemically using silver electrodes. The readout on the instrument gives the chloride concentration in mg L⁻¹. The range for the analyser is 0 - 200 mgL⁻¹. The solution was analysed by the instrument 3 times and the average result taken. The percentage of chlorine available from the sample can then be calculated using equations (11) and (12), giving the final result in % w/wCl.

$$\text{Mass of chlorine} = \frac{\text{Mass of Sample} \times \text{gfm Cl in compound}}{\text{gfm of compound}} \quad (11)$$

$$\text{Ionisable chlorine} = \frac{\text{Concentration of Cl} \times \text{Total volume of solution}}{\text{Sample weight of chlorine}} \times 100 \quad (12)$$

2.3.6.3 Standard Reaction

In order to test the two methods for measuring the available chlorine, a test reaction was carried out using terephthaloyl chloride and analysed using both the Volhard titration method and the chloride analyser. This compound is an acyl chloride which readily reacts with alcohol to liberate HCl. The Volhard method gave an average result of 96.2 % w/w Cl. The titration was carried out three times in order to provide a more accurate result. The analyser method gave an average result of 98.0 % after being carried out four times. As the expected result would be 100 %, these figures show that both methods are not exact, but can be considered to be a satisfactory determination of the chlorine content. The analyser method performed best most likely due to human error in carrying out the titration as the end point is hard to see.

2.3.7 Mass Spectrometry (MS)

Mass spectra were measured using JMS-700 by JEOL with fast atom bombardment as the ionisation technique. The matrix used was 3-nitrobenzyl alcohol.

2.3.8 Gas Chromatography-Mass Spectrometry (GCMS)

Mass spectra were also recorded at Huntsman Polyurethanes Research and Development Laboratories in Rozenburg using GCMS. A Varian CP-3800 gas chromatograph (Varian FactorFour VF-5ms column) integrated with a Saturn 2200 mass spectrometer was used. Solutions were analysed neat, by adding $\sim 2 \text{ cm}^3$ to a vial with a crimp top and placed in an autosampler.

2.3.9 Gel Permeation Chromatography (GPC)

Gel Permeation Chromatography was also carried out in Rozenburg on a Hewlett Packard HP1550 with a Polymerlab PLgel column, $5 \mu\text{m}$, 100\AA , $300 \times 7.5 \text{ mm}$. The UV detector used was a spectroflow 757. Dichloromethane (DCM) was used as an eluent with a flow rate of 0.75 ml min^{-1} for 40 minutes. A 10% dilution of the solutions to be analysed was carried out, 1g of product mixture was made up to 10g with DCM. Peak positions were determined using standard solutions; however the instrument was not calibrated.

2.3.10 Yellow Index

The yellow index is a colour measurement carried out at the industrial centre (ASTM D1925). This analysis was carried out in Rozenburg on a HunterLab UltraScan PRO. This instrument is a high-performance colour measurement spectrophotometer which measures transmittance between the range of 350 nm to 1050 nm. The yellow index is then calculated by the computer. Solutions to be tested were analysed before and after the reaction was carried out in screw top vials. When reporting results, the initial yellow index result was subtracted from the result after the reaction had finished. This gave us an indication to how much colour was produced during the reaction and not by the individual starting materials.

2.3.11 UV/Vis Spectroscopy

UV/Vis spectroscopy was carried out using a Perkin Elmer Lambda 850 spectrometer. This is a double beam, double monochromatic spectrometer with a photomultiplier R6872 detector. The spectrometer utilises pre-aligned tungsten-halogen and deuterium lamps to record spectra in the range 175 nm to 900 nm with a resolution of ≤ 0.05 nm. A sample of the solution to be analysed was added to a rectangular quartz cell (Apollo Scientific) with a path length of 10 nm. A second cell containing the solvent is used as a reference.

2.4 Phosgenation of 4-Benzylaniline

4-Benzylaniline (4-BA) is used as a model compound to investigate the synthesis of the isocyanate and the side reaction producing urea and the dichloride molecule. This molecule was chosen as it is the mono functional version of the diamine starting material used in the industrial process. Therefore this simple molecule will be less likely to form polymeric chains and other side products during the reactions. In order to test out the reaction apparatus the phosgenation of 4-BA to 4-benzylphenyl isocyanate (4-BAI) was carried out. Both methods of phosgenation were tested; the procedures and product analyses are given below.

2.4.1 Triphosgene

Triphosgene (0.09 g, 3.3 mmol) was added to the reactor with chlorobenzene (15 cm³). The resulting solution was cooled to 281 K using a cyclohexane/dry ice cooling bath. At this stage the nitrogen purge was turned on then 4-benzylaniline (4-BA) (0.45 g, 2.5 mmol) dissolved in chlorobenzene (15 cm³) was added dropwise to the solution via syringe. At this point the solution is cloudy and yellow in colour. The reaction mixture is then heated to 383 K and refluxed for 1 hour. At $\sim 83^{\circ}\text{C}$ the solution turns from cloudy to clear with a hint of brown colour. The solution was allowed to cool and a sample taken for analysis (without evaporation of the solvent).

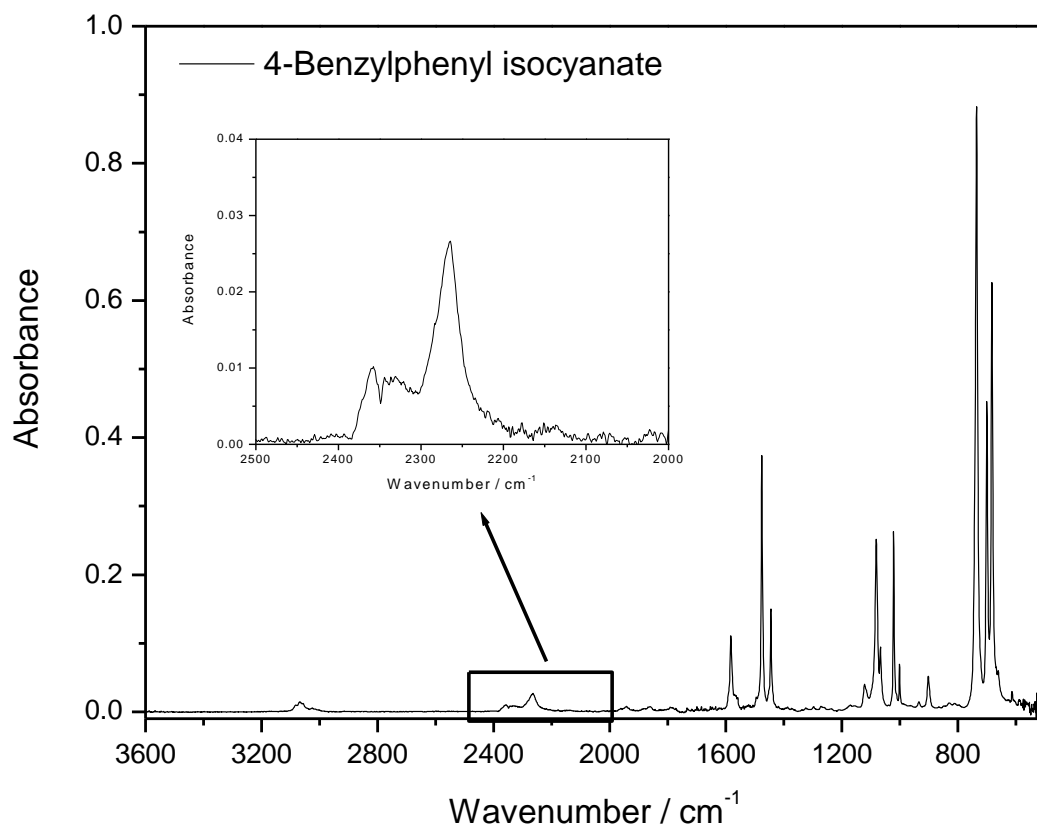


Figure 9. FTIR spectrum of 4-benzylphenyl isocyanate (4-BAI), product from phosgenation of 4-benzylaniline (4-BA) with triphosgene

The product solution was analysed using infrared and NMR spectroscopy as detailed in sections 2.3. The IR spectrum (Figure 9) shows a peak at 2265 cm^{-1} corresponding to the isocyanate out-of-phase stretching mode.⁹⁷ The three bands at 1583 cm^{-1} , 1476 cm^{-1} and 1445 cm^{-1} correspond to the C-H deformations in the solvent chlorobenzene. ^1H and ^{13}C NMR were carried out using an insert with benzene- d_6 as a reference as the product was still in solution. This made it hard to distinguish between the atoms in the aromatic region of the spectra; however the proton NMR did show the disappearance of the NH_2 peak at $\sim 3.17\text{ ppm}$. The analysis therefore indicates that the isocyanate was formed with no evidence of the starting material.

2.4.2 Eckert Cartridge

A solution of 4-benzylaniline (4-BA) (0.91 g, 5.0 mmol) in chlorobenzene (30 cm^3) was added to the reactor with a cyclohexane/dry ice cooling bath keeping the temperature below 283 K. The N_2 purge was turned on and the flow set to $\sim 20\text{ ml min}^{-1}$. An Eckert

cartridge (20 mmol) was connected to the reactor as described in section 2.2.1.2 and heated to 378 K. The tap is opened to allow the phosgene produced to flow into the reactor alongside the nitrogen. After 10 mins the solution changed from clear brown to cloudy. After a further 20 mins the heat was removed from the Eckert cartridge and the reactor was heated to 363 K. As the temperature reached 355 K the solution turned clear. The N₂ purge was increased to ~50 ml min⁻¹ and the reaction left for 3 hours. After the reaction has finished, the solution is left to cool and the solvent is evaporated using rotary evaporation at 318 K leaving a brown oil. The resulting product is tested for any residual phosgene using phosgene indicator paper.

The IR spectrum of the product shows a broad peak at 2261 cm⁻¹ corresponding to the isocyanate (Figure 10), with no evidence of the NH₂ stretching frequencies ($\nu_{\text{asym}}(\text{N-H}) = 3459 \text{ cm}^{-1}$ and $\nu_{\text{sym}}(\text{N-H}) = 3371 \text{ cm}^{-1}$). The ¹H-NMR and ¹³C-NMR spectra confirm that the product is 4-benzylphenyl isocyanate again with no evidence of the amine. The spectra was compared to that of 4-BAI purchased from Sigma-Aldrich and the starting material. Therefore it has been proven that the use of the Eckert cartridge can provide a source of phosgene and using a four-fold excess will see the reaction to completion.

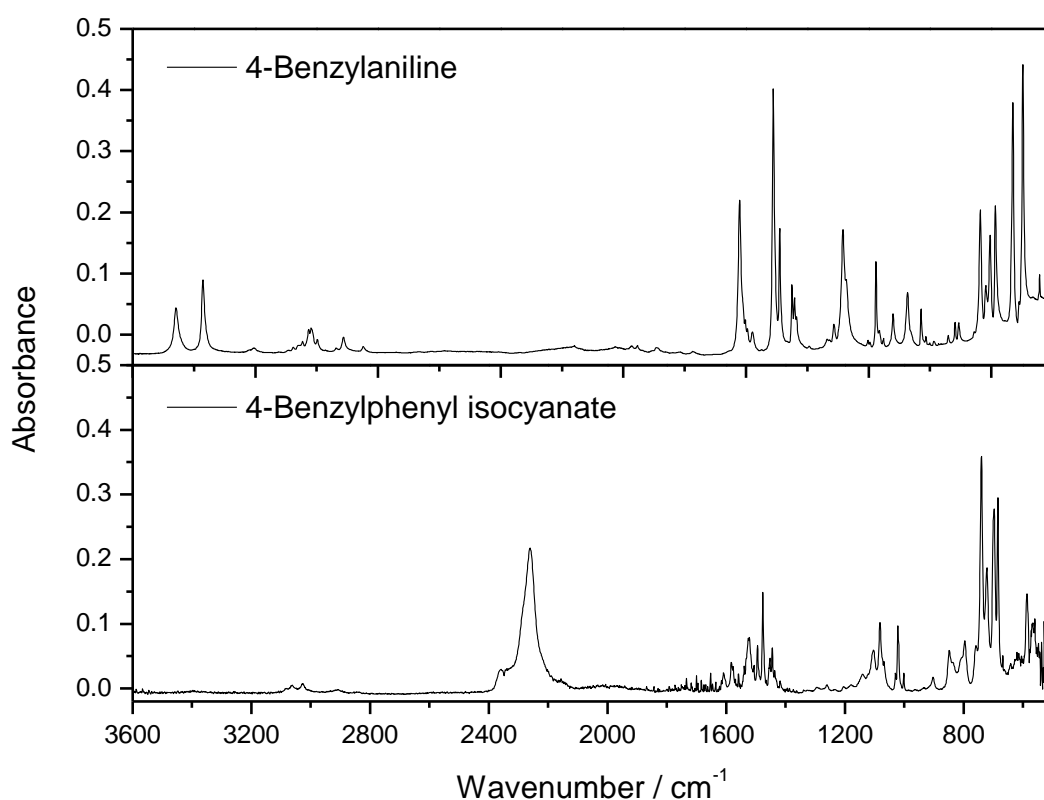
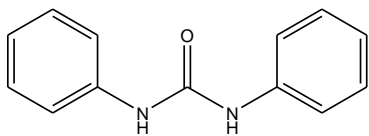


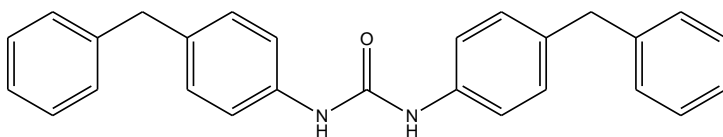
Figure 10. FTIR spectra of the starting material, 4-benzylaniline, and the product 4-benzylphenyl isocyanate from reaction involving the Eckert cartridge

2.5 Synthesis of Urea

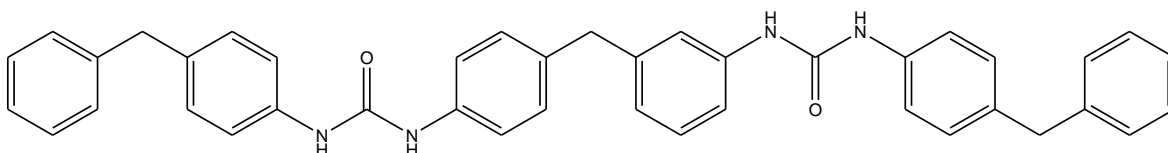
Three different urea compounds were used within this project (Figure 11). Urea 1 was acquired from Sigma-Aldrich. Ureas 2 and 3 were synthesized in-house as described below.



1,3-Diphenylurea (urea 1)



1,3-Di-*p*-benzylphenylurea (urea 2)



Oligomeric urea (urea 3)

Figure 11. Urea compounds studied within this research project

2.5.1 1,3-Di-*p*-benzylphenylurea (Urea 2)

A solution of 4-benzylaniline (0.55 g, 3.0 mmol) in chlorobenzene (15 cm³) was added to the reactor described earlier. A solution of 4-benzylphenyl isocyanate (0.52 g, 2.5 mmol) in chlorobenzene (15 cm³) was added drop wise to the solution using a syringe. The reaction was carried out under nitrogen with an ice bath to stop a fast reaction taking place ensuring all the material would react. On addition of the isocyanate the solution turns from clear to cloudy. After 2 hours the product was recovered by vacuum filtration using a Buchner flask to remove any trace of the starting material, leaving behind a white powder. Analysis of the compound shows the product to be di-*p*-benzylphenyl urea with no starting material present. Figure 12 presents the FTIR spectrum of the product, showing no starting material is present.

IR: $\tilde{\nu}$ / cm^{-1} (intensity): 3301 (vs), 3023 (w), 1636 (m), 1588 (m), 1543 (m), 1511 (w), 1414 (w), 1303 (m), 1231 (m), 848 (w), 793 (m), 772 (m), 741 (m), 725 (m), 694 (m), 650 (m), 612 (m).

$^1\text{H-NMR}$: (400 MHz, DMSO-d_6) δ / ppm: 3.91 (2H, s, CH_2), 7.17 (4H, d, arom. CH), 7.27 (10H, m, arom. CH), 7.39 (4H, d, arom. CH), 8.60 (2H, s, NH).

$^{13}\text{C}\{^1\text{H}\}$ -NMR: (100.5 MHz, DMSO-d_6) δ / ppm: 40.47 (CH_2), 118.35 (aromat. CH), 124.88 (aromat. CH), 128.41 (aromat. CH), 128.61 (aromat. CH), 129.01 (aromat. CH), 134.63 (aromat. C_q), 137.71 (aromat. C_q), 141.67 (aromat. C_q), 152.56 (NHC_qONH).

Elemental analysis: $\text{C}_{27}\text{H}_{24}\text{N}_2\text{O}$ result (theory): C 82.04% (82.65%), H 6.12% (6.12%), N 7.09% (7.14%).

MS: (FAB+) m/z : 184 ($[\text{C}_6\text{H}_5\text{CH}_2\text{C}_6\text{H}_4\text{NH}]^+$), 392 ($[\text{M}]^+$), 393 ($[\text{M}+\text{H}]^+$).

Melting Point: 521 K.

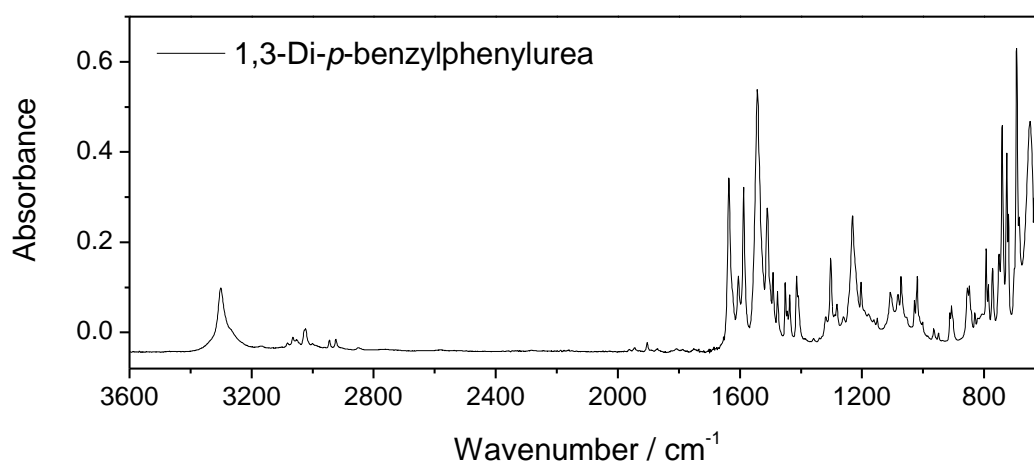


Figure 12. FTIR spectrum of 1,3-di-*p*-benzylphenylurea formed from reaction between 4-benzylaniline and 4-benzylphenyl isocyanate

2.5.2 Oligomeric Urea (Urea 3)

1,1'-(4,4'-methylenebis(4,1-phenylene))bis(3-(4-benzylphenyl)urea), shortened to oligomeric urea for ease, can be synthesised in two separate ways. Reaction of a mono isocyanate with a diamine or reaction of a mono amine with a diisocyanate will each produce an oligomeric compound with two urea groups. Both methods were utilised using the process described in section 2.5.1, the details are given below.

2.5.2.1 Mono Isocyanate

4,4'-Methylene dianiline (MDA, 0.55 g, 2.8 mmol) in chlorobenzene (25 cm³) was reacted with a solution of 4-benzylphenyl isocyanate (4-BAI, 2.26 g, 10.8 mmol, 25 cm³). The product was a white powder identified as the oligomeric urea with a yield of 76.0 %. A large excess of the mono isocyanate ensured that all of the amine groups on the MDA would react. The analysis carried out on the product is detailed below and the FTIR spectrum shown in Figure 13.

IR: $\tilde{\nu}$ / cm⁻¹ (intensity): 3309 (m), 3026 (w), 2899 (w), 2360 (w), 1640 (s), 1590 (s), 1550 (s), 1511 (s), 1493 (m), 1452 (w), 1427 (w), 1412 (m), 1302 (m), 1239 (m), 1176 (w), 1108 (w), 1074 (w), 1017 (w), 908 (w), 859 (m), 809 (m), 750 (w), 731 (s), 697 (m), 639 (s).

¹H-NMR: (400 MHz, DMSO-d₆) δ / ppm: 3.77 (6H, m, CH₂), 7.14 (26H, m, aromat. CH), 8.55 (4H, s, NHCCH).

¹³C{¹H}-NMR: (100.6 MHz, DMSO-d₆) δ / ppm: 40.42 (CH₂), 118.28 (aromat. CH), 118.31 (aromat. CH), 125.81 (aromat. CH), 128.33 (aromat. CH), 128.55 (aromat. CH), 128.85 (aromat. CH), 128.94 (aromat. CH), 134.54 (aromat. C_q), 134.91 (aromat. C_q), 137.59 (aromat. C_q), 137.69 (aromat. C_q), 141.60 (aromat. C_q), 152.51 (NHC_qONH).

Elemental analysis: C₄₁H₃₆N₄O₂ result (theory): C 79.43% (79.87%), H 5.87% (5.84%), N 8.91% (9.09%).

MS: (FAB+) m/z: 77 ([C₆H₅]⁺), 182 ([C₆H₅CH₂C₆H₄NH]⁺), 329 ([HN-C₆H₄-CH₂-C₆H₄-NHCONH-C₆H₄-CH₂]⁺⁺), 618 ([M+H]⁺).

Melting point: 571 K

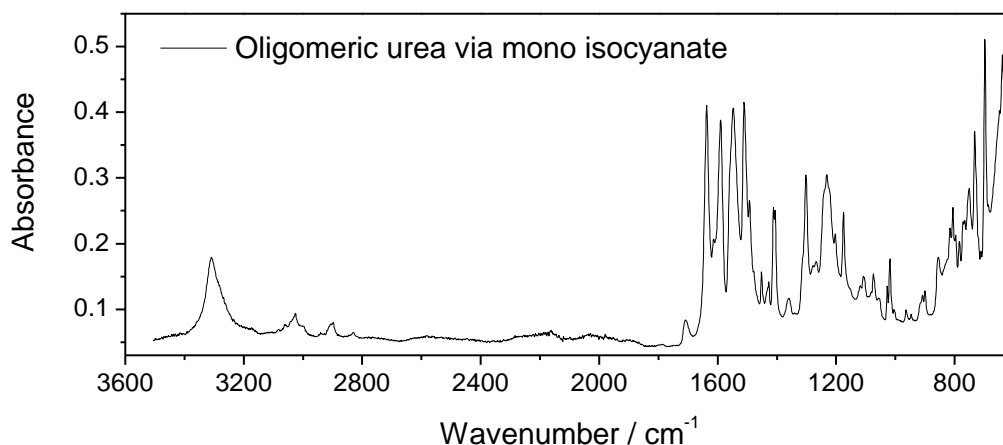


Figure 13. FTIR spectrum of oligomeric urea produced via mono isocyanate and diamine

2.5.2.2 Mono Amine

4-Benzylaniline (4-BA, 1.05 g, 5.7 mmol) in chlorobenzene (20 cm³) was reacted with a solution of 4,4'-methylene diphenyl diisocyanate (MDI, 0.70 g, 2.8 mmol, 15 cm³). The product was a white powder identified as the oligomeric urea with a yield of 94.1 %. Figure 14 shows the FTIR spectra and the characterisation details are shown below. On comparison with Figure 13, both spectra show the same product is formed, with the other analytical data providing evidence that in both cases the oligomeric urea is created.

IR: $\tilde{\nu}$ / cm⁻¹ (intensity): 3307 (m), 3026 (w), 2898 (w), 1640 (s), 1590 (s), 1550 (s), 1511 (s), 1493 (m), 1452 (w), 1427 (w), 1412 (m), 1302 (m), 1239 (m), 1176 (w), 1108 (w), 1074 (w), 1018 (w), 908 (w), 859 (m), 809 (m), 750 (w), 731 (s), 697 (m), 639 (s).

¹H-NMR: (400 MHz, DMSO-d₆) δ / ppm: 3.77 (6H, m, CH₂), 7.16 (26H, m, arom. CH), 8.54 (4H, s, NHCCH).

¹³C{¹H}-NMR: (100.6 MHz, DMSO-d₆) δ / ppm: 40.43 (CH₂), 118.28 (aromat. CH), 125.83 (aromat. CH), 128.35 (aromat. CH), 128.57 (aromat. CH), 128.87 (aromat. CH), 128.96 (aromat. CH), 130.29 (aromat. CH), 134.55 (aromat. C_q), 134.92 (aromat. C_q), 137.61 (aromat. C_q), 137.70 (aromat. C_q), 141.63 (aromat. C_q), 152.51 (NHC_qONH).

Elemental analysis: C₄₁H₃₆N₄O₂ result (theory): C 79.23% (79.87%), H 5.83% (5.84%), N 9.08% (9.09%).

MS: (FAB+) m/z: 617 ([M]⁺), 618 ([M+H]⁺).

Melting point: 571 K.

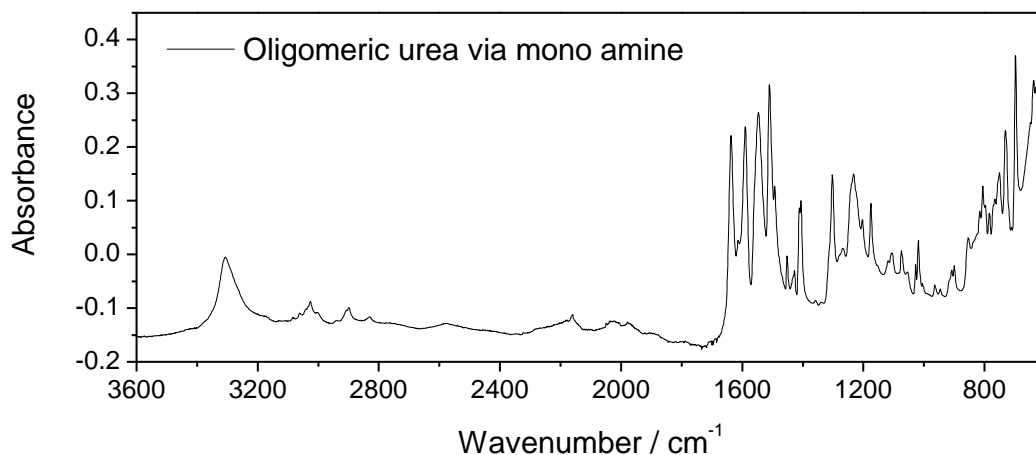


Figure 14. FTIR spectrum of oligomeric urea produced via mono amine and diisocyanate

2.6 Structure Analysis of Ureas by X-Ray Diffraction (XRD)

2.6.1 Crystal Preparation

A few mg of 1,3-di-*p*-benzylphenyl urea was recrystallized with dimethyl sulfoxide (7 cm³). Some of the solvent was evaporated off at 462 K, the boiling point of dimethyl sulfoxide, leaving a concentrated solution. This was left for 48 hours at room temperature until crystals had been formed. The crystals were filtered using vacuum filtration and dried with acetone.

The same procedure was carried out on the oligomeric urea in order to crystallise the material. Unfortunately the compound was found to be too insoluble and attempts at using different solvents or methods were unsuccessful.⁹⁸

2.6.2 Diffractometer

The crystallographic measurements were determined using a Bruker-Nonius APEX-II diffractometer with a Mo-K_α radiation, $\lambda = 0.71073 \text{ \AA}$ at 100 K. A list of reflections with positions and intensities formed the output from the diffractometer, this data can then be used to determine the crystal structure.

2.6.3 Structure Determination

Determination of the crystal structure was carried out using WinGX software.⁹⁹ This is a suite that incorporates various programs such as SHELX97, SIR97, PLATON and ORTEPIII.⁹⁹ SHELXL97 is used to refine the structure of the urea.¹⁰⁰ The PLATON software was then used for validation by checking the crystallographic information file (CIF) and issuing a set of alerts. Tests implemented by the software include checking bond angles and lengths against standard averages, checking the symmetry is of the highest order and checking intermolecular contacts and atom positions are accurate.¹⁰¹ The PLATON software also produced a list of atom coordinates, bond lengths, bond angles, intermolecular interactions and checks on the planarity of aromatic rings.¹⁰¹ For the visualisation of the crystal structure the program ORTEPIII was used.

2.7 Solubility Determination of Urea

Two different procedures were carried out in order to test the solubility of the urea compounds. In both methods a sample of the urea compound to be measured was heated in solution to 363 K. The solubility was then determined by weight measurements or using $^1\text{H-NMR}$ spectroscopy.

2.7.1 Gravimetric Method

1,3-Diphenylurea (0.49g, 2.31 mmol) was added to a round bottom flask with chlorobenzene (20 cm³). The solution was heated to 363 K for and stirred for 60 mins. This temperature was chosen to represent the temperature at which the phosgenation of 4,4'-methylene dianiline (MDA) is carried out at in the industrial process. While still warm, the solution was immediately filtered using a Buchner flask to leave a white solid. This was dried in an oven at 373 K and the leftover urea weighed. The weight difference in this case was 0.0656 g, giving a solubility of 15 mmol L⁻¹. The procedure was repeated with no heating and gave a solubility of 13 mmol L⁻¹.

2.7.2 $^1\text{H-NMR}$ Spectroscopy Method

This heat treatment described in section 2.7.1 was repeated with 1,3-diphenylurea (0.048 molL⁻¹), 1,3-di-*p*-benzylphenylurea (0.026 molL⁻¹) and oligomeric urea (0.016 molL⁻¹) where samples were taken before and after heating for $^1\text{H-NMR}$ analysis. The samples were filtered with 0.2 μm Whatman syringe filters before the spectra were measured. No weights were recorded for these reactions as the samples taken would affect the resultant calculations. The results are discussed in section 3.3.1.

2.7.2.1 Quantitative $^1\text{H-NMR}$ Spectroscopy

As the solvent used in the heat treatments of the ureas is not deuterated, a Wilmad NMR capillary tube containing benzene-d₆ was inserted into the main NMR tube in order to provide the NMR spectrometer with an external lock. This set up allowed the deuterated

solvent to remain separated from the solution to be analysed. The spectra obtained in this way however were still dominated by the chlorobenzene (MCB) solvent peaks. Therefore in order to increase sensitivity a solvent-suppression pulse sequence was used. This method minimises the peaks in the region that the solvent peaks appear, in this case $\sim 7 - 9$ ppm. Reference spectra were prepared by recording spectra of the urea compounds dissolved in DMSO, a solvent in which the ureas are soluble. This allowed identification of the region in which to expect the signals relevant to the urea compounds to appear.

2.7.2.2 Solvent –Suppression Pulse Sequence

The solvent suppression method carried out was developed by Gibson¹⁵ to determine the solubility of amine hydrochloride salts in MCB. The pulse program used was lc1pnf2 which was taken from the standard Bruker library supplied with the spectrometer. This program allowed the chlorobenzene protons to be selectively pre-saturated. A ¹H-NMR spectrum was first recorded in the normal way to measure the range at which the MCB protons occur. These were in the aromatic region therefore should not interfere with the CH₂ or NH signals expected from the ureas.

2.7.2.3 Calibration of 4-BA as a Reference for Urea

In order to use ¹H-NMR methods quantitatively, an internal reference was used. A known concentration of dichloromethane (DCM) was added to the insert containing the deuterated solvent. The signal appearing for DCM could then be compared to the signal intensity of the species to be investigated in order to calculate concentration. This method ensured the reference species would not interact with the solution to be analysed.

4-Benzylaniline (4-BA) was used as a model species for urea as this compound is soluble in chlorobenzene and has a CH₂ peak for the methylene bridge in the NMR similar to urea 2. Six solutions of 4-BA in chlorobenzene were made up and the ¹H-NMR recorded using the solvent suppression method. The concentration of these solutions ranged from 5.0 mmol L⁻¹ to 1.0 mol L⁻¹. An insert with the DCM reference was added to the NMR tube. The integrals of the peaks referring to CH₂ (3.71 ppm) and NH₂ (3.15 ppm) were calculated and plotted with respect to concentration of 4-BA (Figure 15). This gave a calibration curve in which the CH₂ peak of the urea could be compared to and the

concentration calculated. The gradient of the linear regression was 217.364 ± 2.607 a.u. $(\text{mol L}^{-1})^{-1}$. Therefore the urea concentration can be calculated by dividing the integral of the CH_2 peak by 217.364.

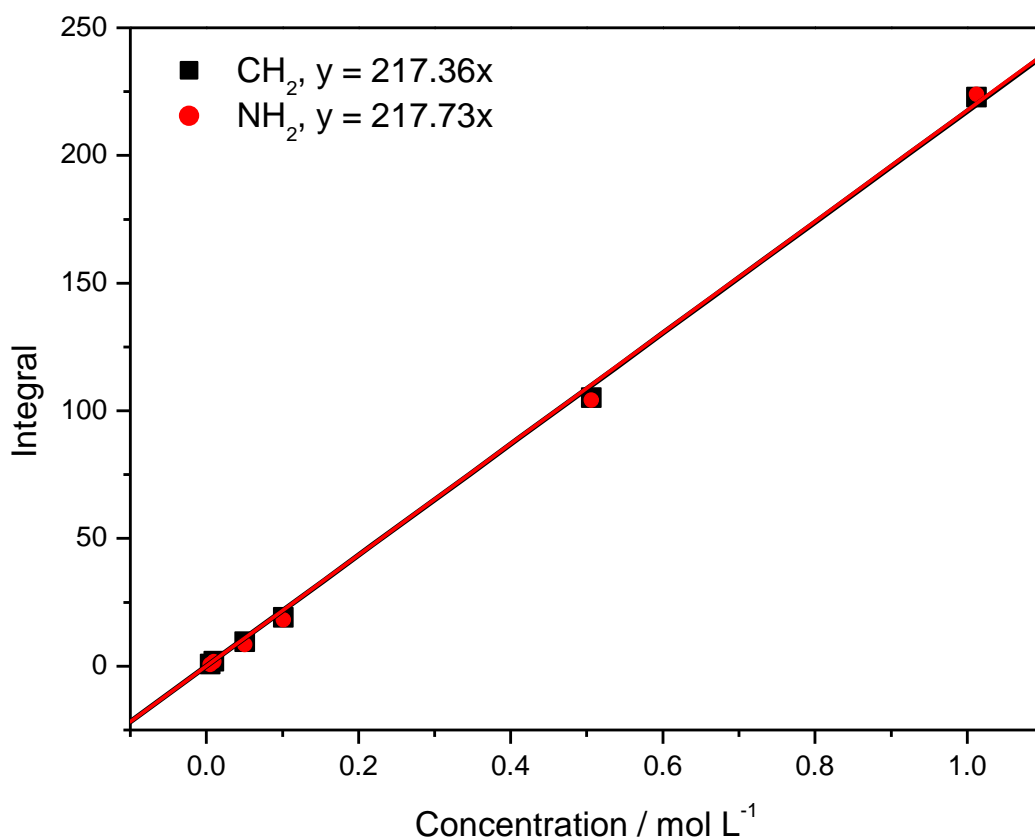


Figure 15. Plot of the integrals of CH_2 and NH_2 signals of 4-benzylaniline with respect to concentration

2.8 Phosgenation of Urea

Two different urea compounds were used, 1,3-di-*p*-benzylphenylurea (prepared as described in section 2.5.1) and 1,3-diphenylurea. Phosgenations were carried out in the same way as described for 4-BA, section 2.4, utilising both methods for introducing phosgene. However the temperature and quantities of the reactants were altered between reactions. Table 1 describes the reactions carried out detailing the particulars. At the end of each reaction the solvent was removed by rotary evaporation and analysis carried out on the product using FTIR. The products in each case were a combination of several compounds and are discussed in section 3.2

Reaction	Urea Compound	Moles of Starting Material / mmol	Phosgene Method	Moles of Phosgene / mmol	Temperature / K	Time / mins
1	1,3-di- <i>p</i> -benzylphenylurea		Triphosgene	10	363	60
2	1,3-di- <i>p</i> -benzylphenylurea		Triphosgene	10	323	150
3	1,3-diphenylurea	2.5	Triphosgene	10	323 353	240 60
4	1,3-diphenylurea	2.5	Triphosgene	10	363	120
5	1,3-diphenylurea	5	Eckert	20	333	300
6	1,3-diphenylurea	5	Eckert	20	353	120
7	1,3-diphenylurea	1.25	Eckert	20	333	180
8	1,3-diphenylurea	1.25	Eckert	20	363	210
9*	1,3-diphenylurea	2.5	Eckert	20	388	300
10 [#]	1,3-diphenylurea	5	Eckert	20 20	383 383	180 240
11	1,3-di- <i>p</i> -benzylphenylurea	0.5	Eckert	20	383	120
12 [#]	1,3-di- <i>p</i> -benzylphenylurea	2.24	Eckert	30 48	373 368	210 300
13*	Product from reaction 9		Eckert	20	299	240
14	Product from reaction 10		Eckert	20	295	180
15	Product from reaction 11		Eckert	20	297	180

*Carried out in ODCB, [#]Two step reaction, more phosgene added to convert all urea present

Table 1. Experimental details for the phosgenation of ureas

2.9 Synthesis of 1,3-Di-*p*-Tolylchloroformamide-*N*-carbonyl Chloride (TCCC)

1,3-Di-*p*-tolylchloroformamide-*N*-carbonyl chloride (TCCC) was produced by the phosgenation of 1,3-di-*p*-tolylcarbodiimide^{102, 103} for use as a model compound. The Eckert method described in section 2.2.1.2 was used to produce phosgene for the reaction. A

solution of 1,3-di-*p*-tolylcarbodiimide (1.0431 g, 4.7 mmol) in chlorobenzene (25 cm³) was added to the reactor and the temperature set to 298 K. Nitrogen was flowed through the reactor at ~50 ml/min. The Eckert cartridge was heated to 373 K and left for 3 hours to let the phosgene mix with the solution. The cartridge is then removed and the reaction left for a further hour with the N₂ flow turned up to 250 ml min⁻¹. The solvent was stripped using a rotary evaporator at 313 K leaving behind the product as a yellow oil. The product was analysed as shown below. The FT-IR showed strong bands for the carbonyl chloride stretch at 1753 cm⁻¹ and the ν(C=N) at 1662 cm⁻¹. The main bands in the IR spectra are similar to that seen in the literature^{102, 103} therefore we can assume the product is 1,3-di-*p*-tolylchloroformamidine-*N*-carbonyl chloride (TCCC). NMR analysis carried out supports this statement with two separate peaks seen for the methyl groups in the compound. In the starting material both methyl groups are seen in the same position as the compound is symmetrical. The aromatic region is also split and the ¹³C-NMR shows an extra carbon peak for the carbonyl chloride group. Mass spectra of the compound showed the mass of the compound to be 321 g mol⁻¹ which corresponds to [M+H]⁺. Peaks at 323 and 325 were also present due to the chlorine isotope (³⁷Cl).

After a few days, the airspace in the vial containing a sample of TCCC tested positive for phosgene. This was a possible indication that the TCCC was releasing phosgene to form the carbodiimide. This will be discussed in detail later (Chapter 4.1.1).

IR: $\tilde{\nu}$ / cm⁻¹ (intensity): 2922 (w), 1753 (s), 1662 (s), 1505 (m), 1476 (w), 1189 (m), 1100 (w), 1022 (w), 815 (w), 740 (s), 700 (w).

¹H-NMR: (400 MHz, CDCl₃) δ/ ppm: 2.29 (3H, s, CH₃), 2.34 (3H, s, CH₃), 6.86 (2H, d, aromat. CH), 7.13 (2H, d, aromat. CH), 7.25 (2H, m, aromat. CH), 7.30 (2H, m, aromat. CH).

¹³C{¹H}-NMR: (100.6 MHz, CDCl₃) δ/ ppm: 21.05 (CH₃), 21.27 (CH₃), 120.36 (aromat. CH), 127.51 (aromat. CH), 128.61 (aromat. CH), 129.62 (aromat. CH), 129.71 (aromat. CH), 130.43 (aromat. CH), 136.21 (N=C_qClN), 139.94 (NC_q=OCl).

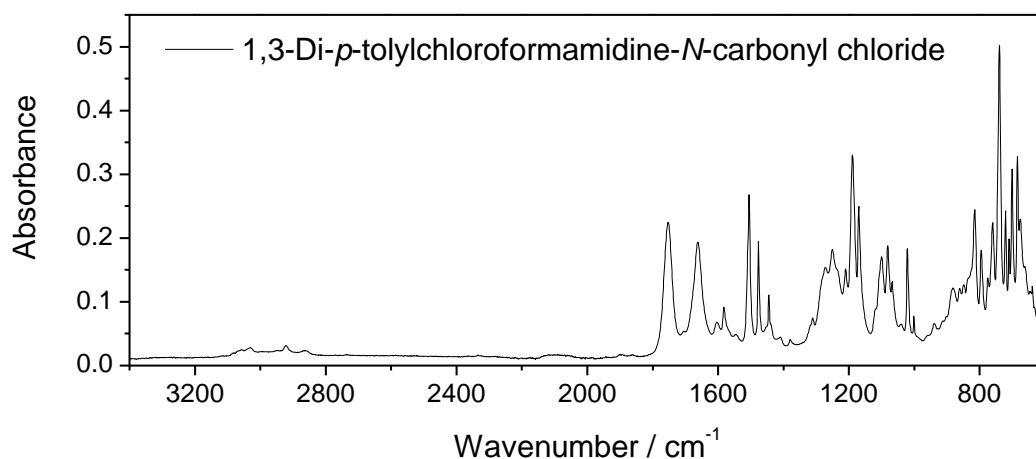


Figure 16. FTIR Spectrum of 1,3-di-*p*-tolylchloroformamidine-*N*-carbonyl chloride produced from phosgenation of 1,3-di-*p*-tolylcarbodiimide

2.10 Synthesis of Isocyanide Dichlorides

Phenyl isocyanide dichloride (PID) was synthesized by conventional methods from phenyl isothiocyanate and dichlorine.¹⁰⁴⁻¹⁰⁶ A solution of phenyl isothiocyanate (1.41 g, 10.4 mmol) in chloroform (25 cm³) was added to the reactor described in section 2.2.2. An ice bath was used to cool the reaction keeping the temperature below 276 K and a N₂ purge used to maintain an inert atmosphere. Dichlorine gas was flowed at 30 cm³ min⁻¹ for 30 min ensuring an excess amount of chlorine entered the system in order to push the reaction to completion (a 2:1 Cl₂: C₆H₅NCS mol ratio is required). During this time the solution became saturated with chlorine and turned a dark yellow/orange colour. The mixture was stirred under N₂ for 2 h after which the solvent and sulfur dichloride were removed by rotary evaporation at 308 K to leave a yellow oil identified from its properties as moisture sensitive, phenyl isocyanide dichloride (yield 75-85 %). The reaction timings were chosen to balance consumption of C₆H₅NCS with minimisation of ring chlorination.^{105, 106}

Similarly prepared was *p*-tolyl isocyanide dichloride (TID) from *p*-tolyl isothiocyanate (0.89 g, 5.96 mmol). The product after removal of solvent and SCl₂ was also isolated as a yellow oil.

4-Fluoromethylphenyl isocyanide dichloride (4F-PID) was provided by Huntsman, after being prepared from 4-fluoromethylphenyl isothiocyanate.

2.11 Characterisation of Isocyanide Dichlorides

Samples of both phenyl and *p*-tolyl isocyanide dichloride compounds were investigated by several methods to achieve identification and to determine sample integrity.

2.11.1 FTIR Spectroscopy

The aryl isocyanide dichloride compounds were characterised in their ATR IR spectra by a strong $\nu(\text{C}=\text{N})$ band ($1654 - 1647 \text{ cm}^{-1}$) and $\nu(\text{C}-\text{Cl})$ features ($907 - 859 \text{ cm}^{-1}$, $846 - 808 \text{ cm}^{-1}$). The positions of the strong characteristic peaks were generally in good agreement with corresponding data reported previously.¹⁰⁵⁻¹⁰⁸ There was no evidence in the spectra for isothiocyanate starting materials, since the intense band of the $-\text{NCS}$ group *ca.* 2050 cm^{-1} was not observed.¹⁰⁹ Figure 17 and Table 2 show the spectra and the assignments form the main peaks attributed to both isocyanide dichlorides.

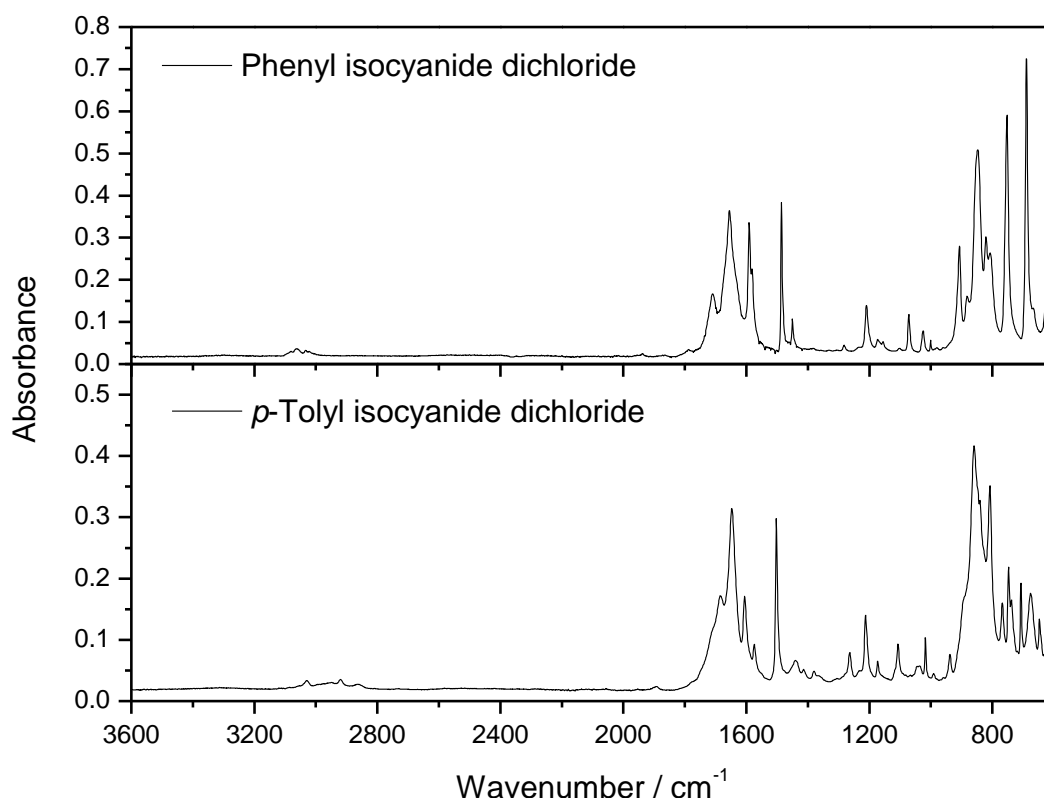
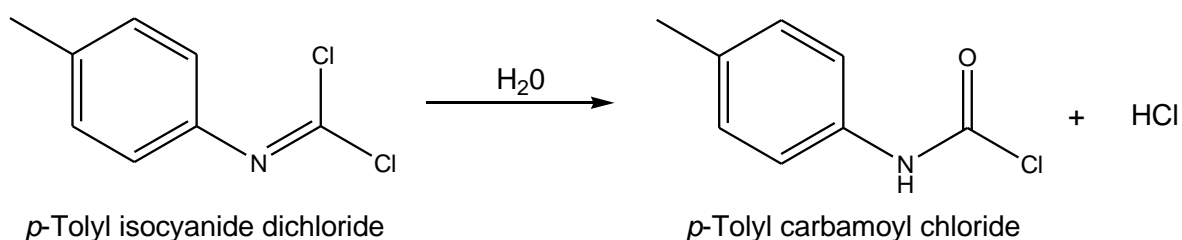


Figure 17. FTIR spectra of phenyl isocyanide dichloride and *p*-tolyl isocyanide dichloride synthesised from chlorination of the corresponding isothiocyanates

$\nu_{max} / \text{cm}^{-1}$				Assignment
Phenyl isocyanide dichloride (PID)		<i>p</i> -Tolyl isocyanide dichloride (TID)		
Present work	Reference ¹⁰⁵	Reference ¹⁰⁷	Present work	
3062	3067	-	-	aromatic $\nu(\text{CH})$
-	-	-	2920	aliphatic $\nu(\text{CH})$
1654	1650	1650	1647	$\nu(\text{C}=\text{N})$
1486	1481	1480	1502	aromatic $\nu(\text{C}=\text{C})$
907	913	907	859	$\nu_{asym}(\text{C}-\text{Cl})$
846	845	875	808	$\nu_{sym}(\text{C}-\text{Cl})$

Table 2. Characteristic IR bands for aryl isocyanide dichlorides

After a few days storage in a sealed vessel, the produced *p*-tolyl isocyanide dichloride (TID) had physically changed from a liquid to an oily substance. Repeating the IR over several days showed the $\nu(\text{C}=\text{N})$ band intensity had decreased and a new band was observed at *ca.* 1751 cm^{-1} (Figure 18). This was attributed to the $\text{C}=\text{O}$ bond of a carbamoyl chloride. A band at 1538 cm^{-1} also appeared, this was assigned to an amide II bend. These peaks indicate hydrolysis is taking place¹⁰⁵ to the product, *p*-tolyl carbamoyl chloride (Scheme 8), spontaneous loss of HCl from this compound would lead to *p*-tolyl isocyanate.¹¹⁰



Scheme 8. Hydrolysis of *p*-tolyl isocyanide dichloride

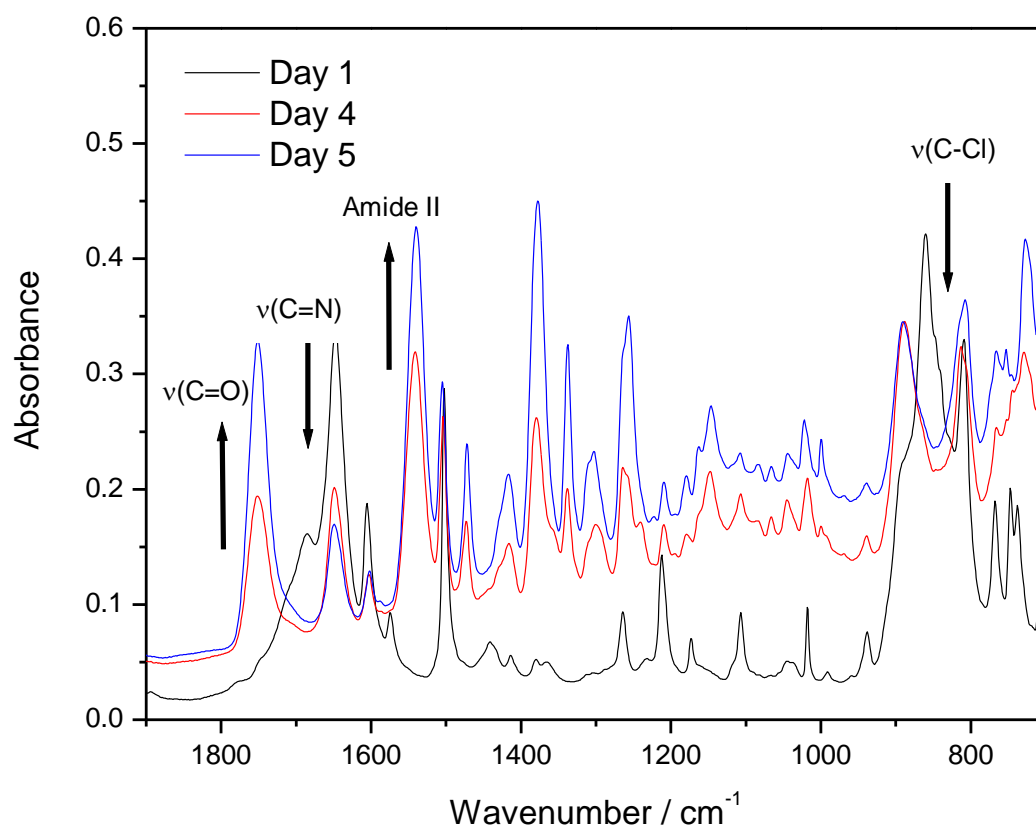


Figure 18. FTIR spectra of *p*-tolyl isocyanide dichloride taken 1, 4 and 5 days after synthesis

2.11.2 NMR Spectroscopy

NMR data for both aryl isocyanide dichlorides are given in Table 3, chemical shifts being reported using δ_{H} and δ_{C} scales. The proton labelling is shown in Figure 19 and the spectra for both compounds are presented in Figure 20. The ^1H -NMR spectrum for phenyl isocyanide dichloride is previously reported.¹¹¹ Its $^{13}\text{C}\{^1\text{H}\}$ spectrum contained additional, very weak features arising from a hydrolysis product described above. The ^1H -NMR spectrum from the *p*-tolyl isocyanide dichloride sample showed it to be a 2:1 mixture of 4- $\text{CH}_3\text{C}_6\text{H}_4\text{N}=\text{CCl}_2$ (TID) and 4- $\text{CH}_2\text{ClC}_6\text{H}_4\text{N}=\text{CCl}_2$ (Cl-TID), formed from chlorination of the methyl group during synthesis. A DEPT ^{13}C spectrum was recorded and found to be in agreement with this conclusion as the spectra showed the signal at 4.63ppm was attributed to a secondary carbon atom, indicating the methyl group has been chlorinated. After repeat runs of the synthesis reaction it was found that limiting the flow of Cl_2 would limit the chlorination of the methyl group. Therefore the reaction must proceed by first chlorinating the isothiocyanate group fully then the methyl group. No evidence for chlorination of the phenyl rings was observed for any compound.

The aromatic region of the spectra is shown in Figure 21. The PID spectrum was characteristic of an AA'BB'C spin system for a monosubstituted benzene, whereas TID was represented an AA'BB' system.¹¹² Extra peaks are seen due to the CI-TID.

NMR parameter	PID	TID	CI-TID
¹H-NMR			
$\delta_{\text{H}}(\text{CH}_3)$		2.39	
$\delta_{\text{H}}(\text{CH}_2\text{Cl})$			4.63
AA'BB' (AB) spin system; signal centred at δ_{H}		7.09	7.23
AA'BB'C spin system; signals centred at δ_{H}	7.08(o), 7.27(p), 7.43(m)		
¹³C{¹H}-NMR			
$\delta_{\text{C}}(\text{CH}_{\text{Ar}})$	121.21, 126.01, 129.13	121.23, 129.68	121.55, 129.48
$\delta_{\text{C}}(\text{C}_{\text{Ar}})$	135.79	135.17, 135.90	134.78, 136.16
$\delta_{\text{C}}(\text{Cl}_2\text{CN})$	144.82	142.11	144.80
$\delta_{\text{C}}(\text{CH}_3)$		21.08	
$\delta_{\text{C}}(\text{CH}_2\text{Cl})$			45.83

Table 3. NMR data for aryl isocyanide dichlorides PID ($\text{C}_6\text{H}_5\text{N}=\text{CCl}_2$), TID ($4\text{-CH}_3\text{C}_6\text{H}_4\text{N}=\text{CCl}_2$) and CI-TID ($4\text{-CH}_2\text{ClC}_6\text{H}_4\text{N}=\text{CCl}_2$)

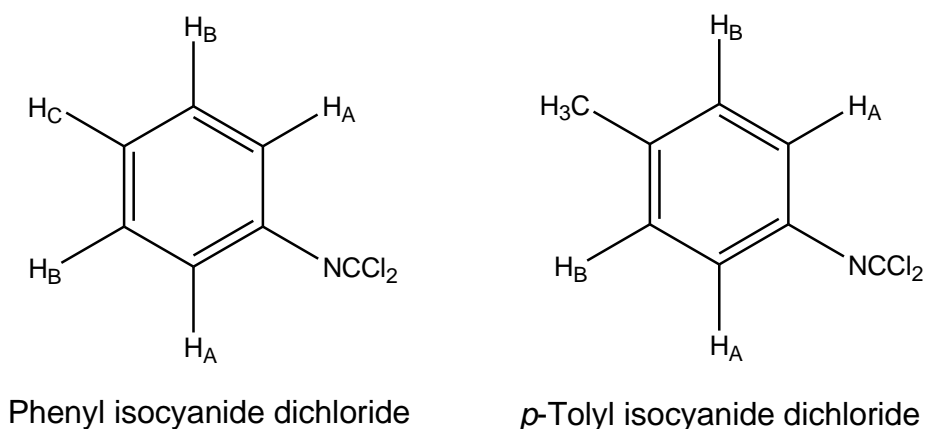


Figure 19. Hydrogen labels for the aryl isocyanide dichloride compounds

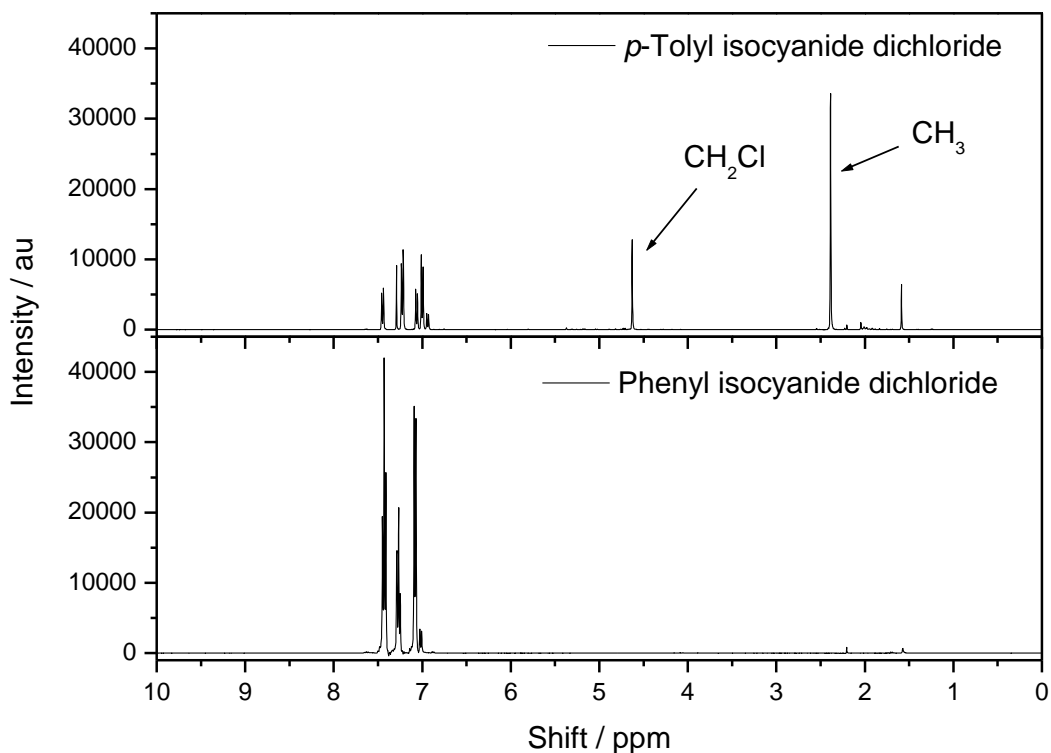


Figure 20. $^1\text{H-NMR}$ spectra of aryl isocyanide dichlorides

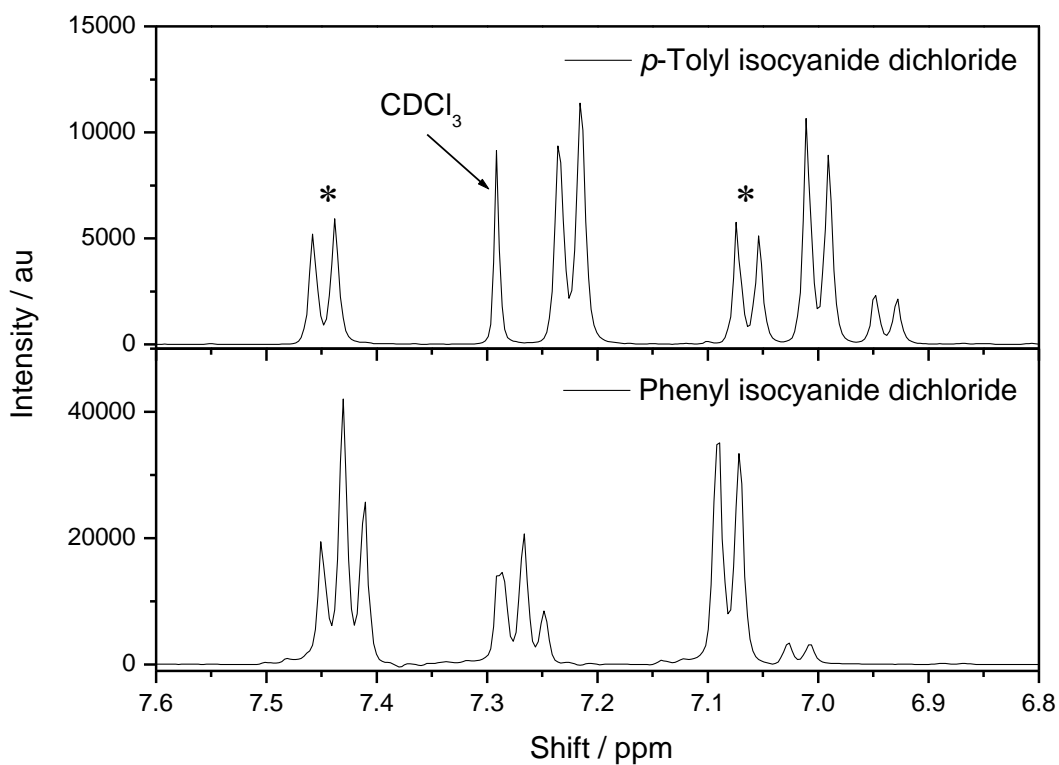


Figure 21. $^1\text{H-NMR}$ spectra of aryl isocyanide dichlorides – aromatic region, * indicates peaks attributed to Cl-TID

2.11.3 Gas Chromatography-Mass Spectrometry (GCMS)

GC-MS analysis additionally confirmed the existence of the aryl isocyanide dichlorides. PID showed two main peaks at 173 and 138 m/z. The compound can be identified as PID due to the chlorine isotope pattern in the mass spectrum. For a molecule with two chlorines 3 lines will appear due to the presence of the chlorine isotope ^{37}Cl . This isotope exists as 24% with the ^{35}Cl being 76%. Statistically there is a 24% chance that a Cl atom in a molecule will have a mass of 37. Therefore we can determine that in a molecule with two chlorine atoms, there is a 57% chance both will have a mass of 35, a 37% chance both the isotopes exist and a 6% chance they will both be ^{37}Cl . These numbers give a ratio to which the mass spectrum pattern will follow. For a molecule with one chlorine attached, the mass spectrum will show 2 lines, with 76% a ^{37}Cl and 24% a ^{35}Cl . For PID, the experimental ratios are 56%, 39% and 5% for 173, 175 and 177 respectively. The peak at 138 m/z shows a loss of chlorine in the analysis.

Table 4 gives the molecular ion peaks, ratios and characteristic mass fragments. The GC-MS traces of both compounds indicated the presence of isothiocyanate starting materials. GC-MS also showed that traces of ring- and/or CH_3 -group chlorinated species were present.

Compound	<i>m/z</i>	Fragment
Phenyl isocyanide dichloride (PID)	173 (56%), 175 (39%), 177 (5%)	$\text{C}_6\text{H}_5\text{NCCl}_2$
	138 (75%), 140 (25%)	$\text{C}_6\text{H}_5\text{NCCl}$
	77	C_6H_5
<i>p</i> -Tolyl isocyanide dichloride (TID)	187 (59%), 189 (35%), 191(6%)	$\text{CH}_3\text{C}_6\text{H}_4\text{NCCl}_2$
	152 (74%), 154 (26%)	$\text{CH}_3\text{C}_6\text{H}_4\text{NCCl}$
	91	$\text{CH}_3\text{C}_6\text{H}_4$

Table 4. Mass spectra details of aryl isocyanide dichlorides

2.11.4 Thermal Analysis

Thermo gravimetric analysis (TGA) and differential scanning calorimetry (DSC) were carried out on both isocyanide dichlorides synthesized to investigate the stability of both compounds.

2.11.4.1 Thermal Gravimetric Analysis (TGA)

Figure 22 shows that decomposition commenced at a temperature of 338 K with large decreases in mass observed at 393-413 K. In total 69.8% of the sample weight of phenyl isocyanide dichloride had been lost, with a 48.0% weight loss for 4-methylphenyl isocyanide dichloride. This weight loss corresponds to 121.39g in PID and 90.3g in TID, a considerable part of the compound.

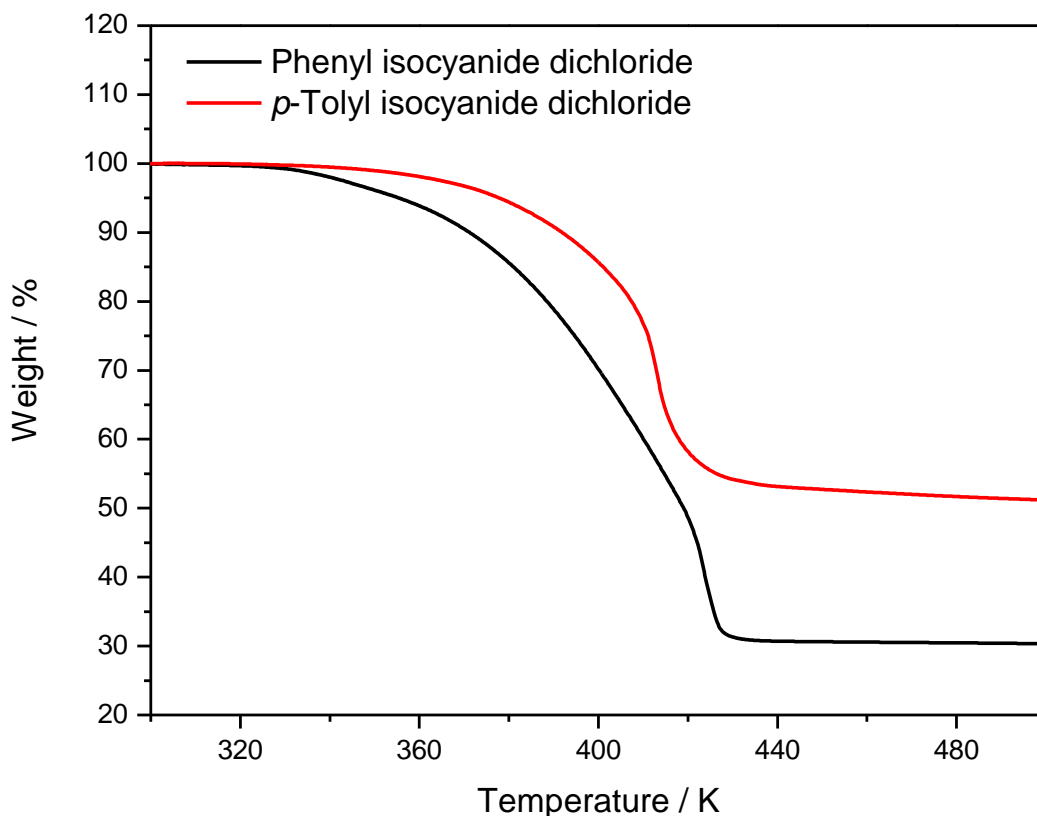


Figure 22. TGA profiles of aryl isocyanide dichlorides

2.11.4.2 Differential Scanning Calorimetry (DSC)

From Figure 23 shown below, both aryl isocyanide dichlorides have two peaks with maxima of 406 and 432 K for PID and at 416 and 427 K for TID. These indicated the occurrence of exothermic processes at temperatures significantly in excess of 353 K; on this basis it was concluded that a temperature of *ca.* 430 K would be needed to decompose thermally the aryl isocyanide dichlorides.

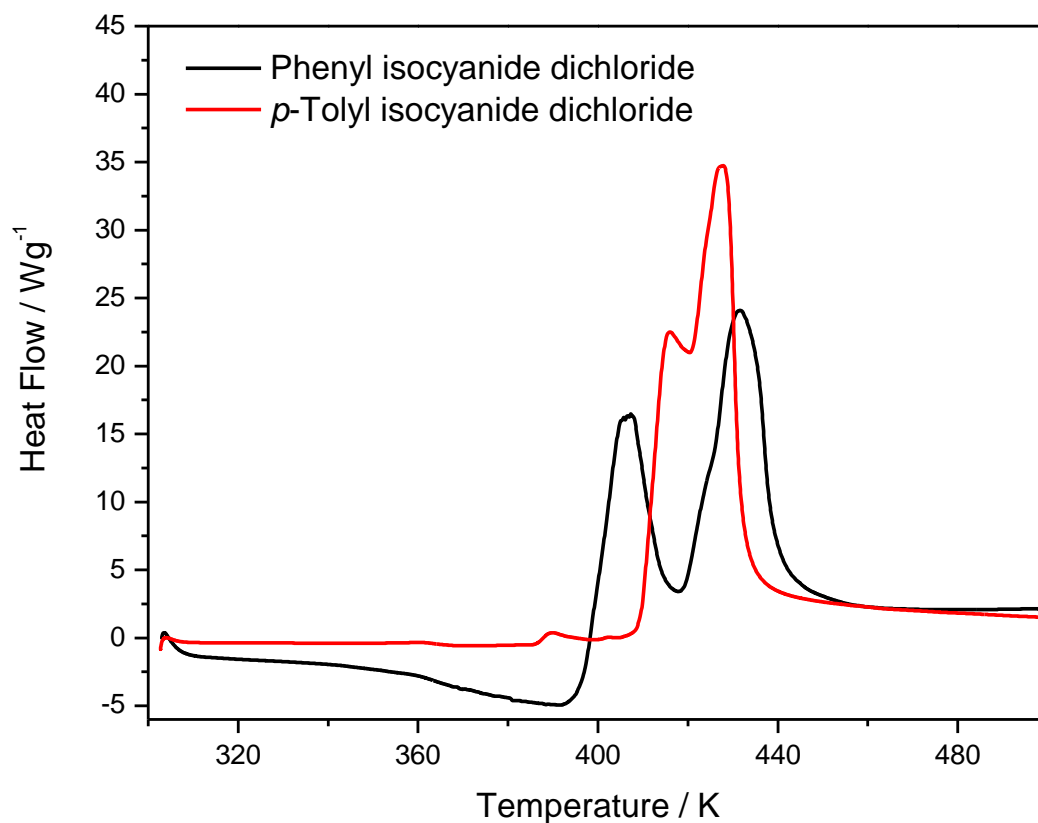


Figure 23. DSC trace of aryl isocyanide dichlorides

2.11.5 Available Chlorine

The available chlorine content of both aryl isocyanide dichlorides were measured using the technique described in section 2.3.6.2. For PID, the result was 53% w/w Cl whilst TID gave a result of 88% w/w Cl. Therefore the release of Cl for either compound was not quantitative, although it was substantial in each case. These measurements indicate that although release of chlorine was readily achieved, under these conditions it corresponded to release of greater than one but less than two Cl atoms per molecule.

2.11.6 Summary

From the spectroscopic analysis of the isocyanide dichloride compounds it is fair to say that the materials have been synthesized in high purity, however trace starting materials remain, as detected by the very sensitive technique of GCMS.

The thermal analysis carried out on the compounds indicate them to be thermally stable up to 338 K, with a drastic change in the composition of the molecule at ~393 – 445 K. This indicates a molecular decomposition path is occurring at this temperature. The available chlorine analysis on both compounds shows that at least one chlorine atom is readily released from the molecule; therefore it is proposed that the thermal degradation will begin with the loss of chlorine.

2.12 Storage Methods for Unstable Compounds

As both isocyanide dichlorides and 1,3-di-*p*-tolylchloroformamidine-*N*-carbonyl chloride (TCCC) were found to be unstable compounds in atmospheric conditions, a method of storing the compounds without further reaction had to be used. Initially the samples were kept in crimped top vials in a fridge. This proved to be sufficient for TCCC but not for the isocyanide dichlorides as evidenced by changes in the infrared spectra. They were then moved to a desiccator, with the vials first flushed with nitrogen. This proved successful for 2-4 days, however after this time signs of hydrolysis were seen. Therefore a more rigorous set up was developed in order to store the compounds for longer. The modified Schlenk tube in Figure 24 was prepared for use as a storage vessel. This vessel containing the compound to be stored was attached to a vacuum line (Figure 25) via Quickfit joints sealed with silicon grease and attached with a Keck clip. The vessel was then evacuated and backfilled with nitrogen. As the pressure reached atmospheric (760 Torr), the young's tap on the vessel was closed, sealing the compound in an inert atmosphere. This method proved successful in storing the isocyanide dichlorides until they were required.

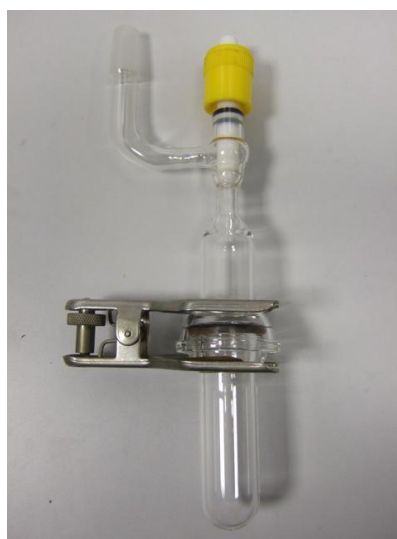


Figure 24. Schlenk tube used to store sensitive materials

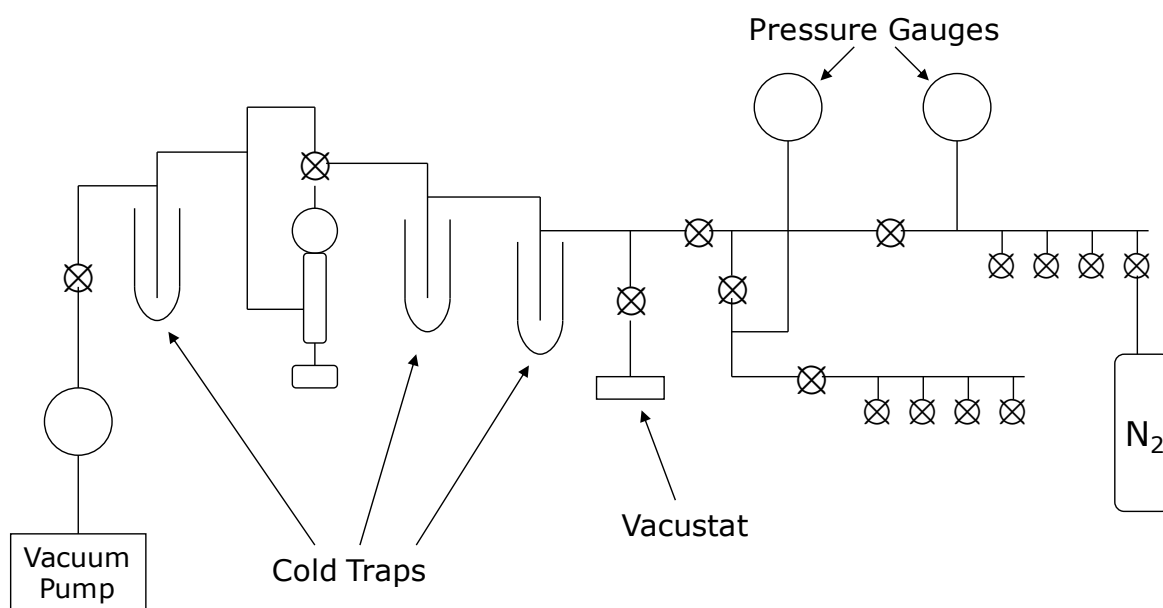


Figure 25. Vacuum line

2.13 Rozenburg Reactions

The following reactions were carried out at Huntsman Polyurethanes Process Research and Development Laboratory in Rozenburg. All experiments were carried out using a Stuart block heater (SBH200D/3) with an aluminium block (ESTSHT1/0) with drilled holes to accommodate glass vials. This provided a temperature range of 271 K to 473 K.

2.13.1 Heat Treatments of Chloroformamidine-*N*-carbonyl Chloride (CCC)

Experiments were carried out on 1,3-di-*p*-tolylchloroformamidine-*N*-carbonyl chloride (TCCC) to determine whether the isocyanide dichloride was a decomposition product. In order to evaluate this a series of heat treatments were carried out on different solutions of TCCC. It was also important to test solutions where an excess of phosgene was present in order to mimic the industrial process. In order to do this phosgene was added to the solvent, chlorobenzene. Two different concentrations were used, 1% w/w and 5% w/w.

2.13.1.1 Closed Experiments

Solutions of TCCC in chlorobenzene (MCB) or phosgenated chlorobenzene were made up at different concentrations. $\sim 7 \text{ cm}^3$ of the chosen solution was added to a number of vials and sealed with a screw cap. These vials were then added to the heat block set at the desired temperature. After a period of time, one vial was removed, crash cooled with air and the solution analysed by GPC and CG-MS. Table 5 shows the details of all the reactions carried out.

Reaction	TCCC Concentration / mmol L^{-1}	Solvent	Temperature / K	Sample Time / min
1	6	MCB	403	0, 120, 300
2	20	MCB	403	0, 120, 300
3	6	MCB	448	0, 60, 120, 180
4	$<13^{\#}$	MCB	463	0, 15, 60, 120, 180
5	6	MCB	463	0, 120, 300
6	20	MCB	463	0, 120, 300
7	36	1% Phosgene/MCB	403	0, 120, 300
8	36	1% Phosgene/MCB	423	0, 60, 120, 240, 360
9	36	1% Phosgene/MCB	448	0, 60, 120, 240, 360
10	36	1% Phosgene/MCB	463	0, 120, 300
11	6	5% Phosgene/MCB	448	0, 60, 120, 180
12	6	5% Phosgene/MCB	463	0, 60, 120, 180

- Filtered to get rid of solid particles therefore unknown concentration

Table 5. Experimental details for the heat treatments of 1,3-di-*p*-tolylchloroformamidine-*N*-carbonyl chloride (TCCC)

2.13.1.2 Open Experiments

Experiments were carried out with open vials to let any gas produced escape from the reaction. These were carried out in order to test if the carbodiimide would be produced from the loss of phosgene in the reaction. A 0.1 M stock solution of TCCC (1.6084 g, 5.0 mmol) in chlorobenzene (50 cm^3) was made up. A portion (20 cm^3) was diluted in more chlorobenzene (100 cm^3) to give a 0.02 M solution. 10 cm^3 of this solution was then added to 6 separate glass vials with no caps. The vials were then placed in different temperature environments to study the decomposition of TCCC. The temperatures studied were 273, 293, 313, 333, 353 and 373 K. An ice bath was used for the vial at 273 K, one vial was left standing at room temperature (293 K) while the others were placed in the heat block set to the desired temperature. After an hour a sample of the solution was taken and analysed by GPC and GC-MS.

2.13.2 Isocyanide Dichloride and Chloroformamidine-*N*-carbonyl Chloride Compounds as a Source of Colour

It was important to establish if colour is produced from isocyanide dichloride or chloroformamidine-*N*-carbonyl chloride compounds and the extent at which the colour is produced. A series of experiments were designed to test different concentrations of 4-fluoromethylphenyl isocyanide dichloride (4F-PID) and 1,3-di-*p*-tolylchloroformamidine-*N*-carbonyl chloride (TCCC) with or without the presence of 4,4'-methylene diphenyl diisocyanate (MDI).

A number of solutions were made up as described in Table 6. For each solution different concentrations of the main reactants (4F-PID or TCCC) were tested, the concentration of MDI was kept constant giving different ratios of 4F-PID:MDI or TCCC:MDI. An aliquot (~16 cm³) of each solution was added to a glass vial sealed with a screw cap. A test vial with a solution of MDI in chlorobenzene (MCB) was made up in order to ensure the vials were able to retain fluid and if any colour would be produced without the addition of the isocyanide dichloride compound. These were placed in a heat block for 2 hours at 448 K. The solutions were tested for colour using the yellow index indicator before and after the reaction. The highest concentrated solutions were also analysed by GC-MS after the reaction.

From the reactions carried out in sections 2.13.1 and 2.13.2 a selection of vials were weighed before and after the experiments in order to see if any gas had escaped through the screw top. The findings were that between 0.08 – 1.19 % weight was lost, with the average being 0.36 %.

Experiment	Concentration of Reactants / mmol			Solvent
	4F-PID	TCCC	MDI	
1	-	-	50	MCB
2	50, 25, 12.5, 5, 1, 0.5	-	-	MCB
3	50, 25, 12.5, 5, 1	-	50	MCB
4	-	50, 25, 12.5, 5, 1, 0.5	50	MCB
5	-	20, 10, 5, 2.5, 1	-	1% Phosgene/MCB
6	-	20, 10, 5, 2.5, 1	50	1% Phosgene/MCB

Table 6. Details of solutions used for colour experiments

2.14 Heat Treatments and Photolysis of Isocyanide Dichlorides

Reactions were carried out to look at the effect of thermolysis and photolysis on the isocyanide dichloride molecules. UV/Vis and GCMS were used as analytical techniques in an attempt to understand the mechanisms of colour formation.

2.14.1 Apparatus

2.14.1.1 Flask Reactor

Thermolysis reactions were carried out using either a three-neck or a one-neck round bottom flask connected to a refluxer and heated using an IKA stirrer hotplate and an oil bath. A contact thermometer was used to control the temperature. 20 cm³ of the solution to be reacted was added to the reactor and heated for a set length of time at the desired temperature. Using a three-neck flask allowed a nitrogen purge to be added to one neck of the reactor and this was used when necessary. In this case a rubber septum was used to block the third neck of the flask. Using this set up allowed reactions to be followed over time, whereby an aliquot of the solution could be removed by a syringe through the rubber septum.

2.14.1.2 Radley's Reactor

A Radley's carousel 6 place reaction station was also utilised for the thermolysis reactions. This allowed 6 reactions to be carried out simultaneously. The reactor contained a water cooled aluminium reflux head and was placed on an IKA hotplate stirrer with a Fuzzy Logic digital temperature controller used to monitor the temperature. The reaction vessels were 25cm³ glass round bottom reaction flasks connected to the reactor via gas tight threaded PTFE caps with a PTFE valve. These contained a stainless steel gas outlet which was connected to a vent and an opening for sampling which was capped with a Suba-Seal septum. 15cm³ of the solution to be heated was added to a reaction flask and attached to the carousel. One flask was set up as a blank with only the solvent added. A thermocouple linked to a digital readout was pushed through the rubber septum to measure the

temperature inside the flask as a control. Solutions were then heated to 448 K for 2 hours, cooled and samples taken for analysis.

2.14.1.3 Photoreactor

20cm³ of the solution to be irradiated was added to a 5-neck flask reactor in which a mercury lamp was placed in the middle of the flask (Photochemical reactors, mercury lamp, model number 3010, 125 W, housed in a quartz immersion well). A cooling jacket was used to keep the lamp and the solution cool. The radiation produced by the lamp was predominantly at 365-366 nm, with smaller amounts in the ultraviolet region at 254, 265, 270, 289, 297, 302, 313 and 334 nm. Also significant amounts of radiation are produced in the visible region at 405-408, 436, 546 and 577-579 nm. The reaction was left for 2 hours before the solution was removed for analysis.

2.14.2 Preliminary Reactions

Reactions involving a combination of *p*-tolyl isocyanide dichloride (TID) with different isocyanates (*p*-tolyl isocyanate (TI), 4-benzylphenyl isocyanate (4-BAI), 4,4'-methylene diphenyl diisocyanate (MDI)) were carried out under different conditions in order to gain some initial understanding of the colouration produced. Table 7 outlines the details of the reactions carried out. The solutions were first analysed by UV/Vis separately before mixing occurred. An aliquot of each were then added together and analysed again by UV/Vis, the concentration of the reactants in these circumstances are halved. The solutions then underwent thermolysis or photolysis in the apparatus outlined above, after which further analysis was carried out. Direct analysis of the solutions afforded spectra in the visible range, dilutions were then carried out to measure the absorbance in the UV range if required.

TID Conc. / mol L ⁻¹	Reactant	Conc. / mol L ⁻¹	Solvent	Temperature / K	Time / mins
-	TI	4.1 x 10 ⁻⁵	Acetonitrile	353	60
-	4-BAI	4.3 x 10 ⁻⁵	Acetonitrile	353	60
-	MDI	3.7 x 10 ⁻⁵	Acetonitrile	353	60
3.5 x 10 ⁻²	-	-	Acetonitrile	353	60
4.4 x 10 ⁻²	TI	5.0 x 10 ⁻²	Acetonitrile	353	60
4.0 x 10 ⁻²	4-BAI	4.9 x 10 ⁻²	Acetonitrile	353	60
3.0 x 10 ⁻⁵	4-BAI	3.2 x 10 ⁻⁵	Acetonitrile	313	210
3.0 x 10 ⁻²	4-BAI	3.0 x 10 ⁻²	Acetonitrile	313	300
3.9 x 10 ⁻²	MDI	4.0 x 10 ⁻²	Acetonitrile	353	60
2.4 x 10 ⁻⁵	4-BAI	4.0 x 10 ⁻⁵	Acetonitrile	Irradiation	90
2.4 x 10 ⁻²	4-BAI	4.0 x 10 ⁻²	Acetonitrile	Irradiation	180
1.2 x 10 ⁻³	MDI	1.4 x 10 ⁻³	-	373 K	60
5.2 x 10 ⁻²	MDI	4.4 x 10 ⁻²	Acetonitrile	Irradiation	180
5.2 x 10 ⁻²	4-BAI	5.0 x 10 ⁻²	Chlorobenzene	403	120
4.2 x 10 ⁻²	4-BAI	4.7 x 10 ⁻²	<i>o</i> -Dichlorobenzene	453	180
1.6 x 10 ⁻²	DBB	1.5 x 10 ⁻²	<i>o</i> -Dichlorobenzene	453	180
4.1 x 10 ⁻²	-	-	<i>o</i> -Dichlorobenzene	453	180
-	4-BAI	4.1 x 10 ⁻²	<i>o</i> -Dichlorobenzene	453	180

DBB = 1,4-Dibenzylbenzene

Table 7. Reaction details for the preliminary thermolysis and photolysis reactions of isocyanide dichlorides

2.14.3 Concentration Dependence of Isocyanide Dichlorides

It was important to look at whether colour was formed from isocyanide dichloride at different concentrations. Mixtures of phenyl isocyanide dichloride (PID) with 4,4'-methylene diphenyl diisocyanate (MDI) and polymeric MDI (PMDI) were looked at in order to replicate the environment at the industrial centre. The polymeric MDI used in the reactions was supplied by Huntsman Polyurethanes. This is a mixture which consists of isocyanates with a varying amount of aromatic rings. In general this mixture will contain 50% 4,4'-methylene diphenyl diisocyanate, 5% 2,4'-methylene diphenyl diisocyanate, 25% tri-isocyanates, 12% tetra-isocyanates and 8% higher methylene-bridged polyphenylene polyisocyanates. Figure 26 shows examples of the compounds described. The commercial product mixture of polymeric MDI contains an average of 2.8 NCO groups.⁵⁰

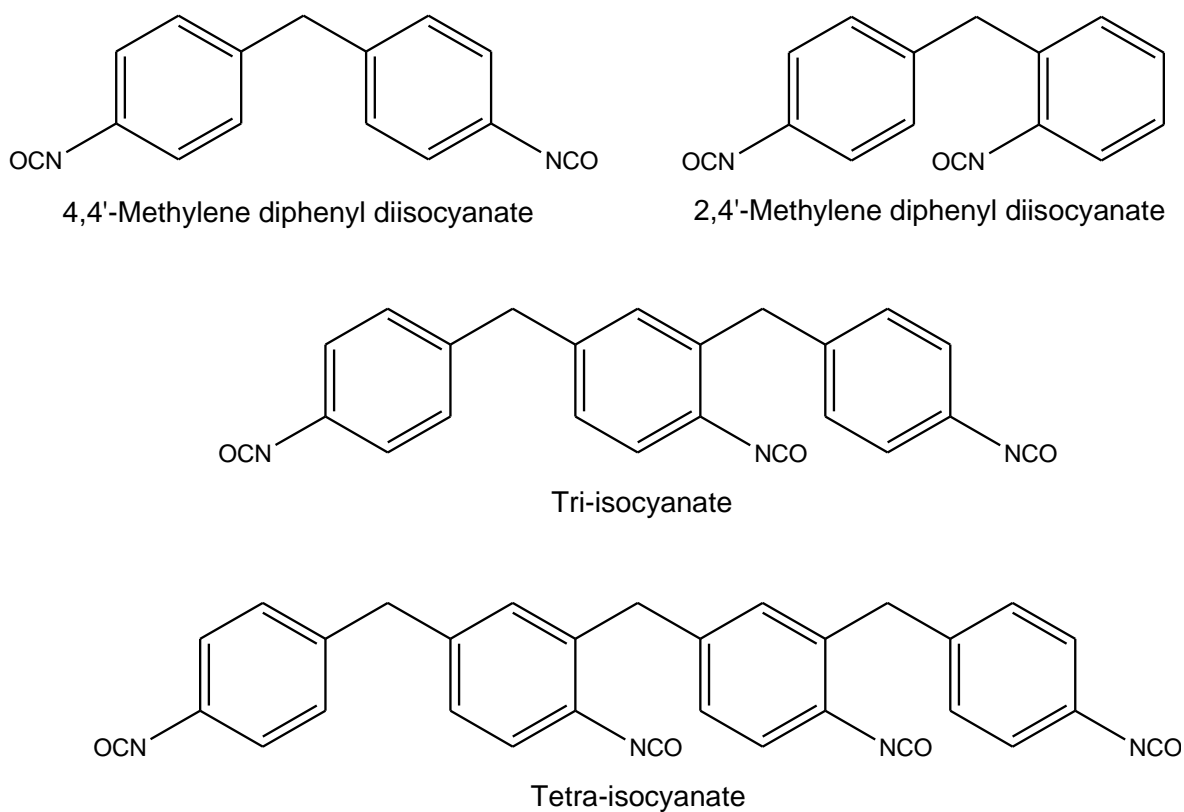


Figure 26. Isocyanate compounds in polymeric MDI

Solution	Concentration / M		
	PID	MDI	Polymeric MDI
PID (a)	0.0504	-	-
PID (b)	0.0252	-	-
PID (b)	0.0126	-	-
PID (d)	0.0050	-	-
PID (e)	0.0005	-	-
PID + MDI (a)	0.0505	0.0515	-
PID + MDI (b)	0.0253	0.0515	-
PID + MDI (c)	0.0126	0.0515	-
PID + MDI (d)	0.0050	0.0515	-
PID + MDI (e)	0.0005	0.0515	-
PID + Polymeric MDI (a)	0.0505	-	0.0502
PID + Polymeric MDI (b)	0.0253	-	0.0502
PID + Polymeric MDI (c)	0.0125	-	0.0502
PID + Polymeric MDI (d)	0.0050	-	0.0502
PID + Polymeric MDI (e)	0.0005	-	0.0502

Table 8. Concentration details of solutions for concentration dependence thermolysis and photolysis reactions

2.15 EPR Study of Isocyanide Dichlorides

EPR spectroscopic measurements were carried out at the University of Manchester using a Bruker EMX Micro X-band spectrometer equipped with a digital temperature control system. Reactions were carried out *in situ* where the cavity could be set to the desired temperature using the integrated heater for higher temperatures or cooled to lower temperatures using liquid nitrogen. The compound *N-tert-butyl- α -phenyl nitron*e (PBN)⁸⁰ was used as a spin trap to identify the formation of Cl[•].

Solutions containing phenyl isocyanide dichloride or *p*-tolyl isocyanide dichloride (0.1 mol dm⁻³) with the spin trap PBN (0.01 – 0.1 mol dm⁻³) in benzene or toluene were flushed with nitrogen before a sample was added to an EPR tube, which was then placed in the spectrometer cavity. For blank reactions, solutions of separate components in benzene were examined. A xenon arc lamp was used to photolyse the solutions *in situ* with a quartz filter to cut off the radiation with a wavelength below 310 nm (i.e. irradiation at $\lambda > 310$ nm). For all reactions a scan was run before irradiation commenced to check that no radicals were present initially. For some of the runs such as the blank reactions or for solutions with a low concentration, several scans were run and added together in order to see if any radicals were present. Two different procedures were set up to follow the reactions over time. The timer program was either set to record one scan every 30 seconds, or to scan constantly (one scan taking 14 seconds to complete). Recording of the spectra was carried out for up to 2 hours. Irradiation of the samples was either carried out constantly whilst scanning took place, or the sample would be irradiated for 30 seconds then the scanning was started immediately. Table 9 shows the details for the solutions that were used in the EPR experiments and Table 10 shows all the procedures that were carried out.

Solution	Reactant	Reactant Concentration / mol dm ⁻³	Spin Trap Concentration / mol dm ⁻³	Solvent
A	-	-	0.051	Benzene
B	PID	0.100	-	Benzene
C	TID	0.108	-	Benzene
D	PID	0.105	0.051	Benzene
E	PID	0.110	0.103	Benzene
F	PID	0.110	0.026	Benzene
G	PID	0.100	0.026	Benzene
H	PID	0.118	0.050	Toluene
I	TID	0.108	0.051	Benzene

Table 9. Details of Solutions for use in EPR experiments

Reaction	Spectrum File	Temperature / K	Irradiation	No. Of Scans	Time per Scan
A1	2980x1	295	None	500	14
A2	2818x2	292	30s	100	30
A3	2980x2	288	Constant/None	200/211	14
B1	2979x1	288	None	200	14
B2	2979x2	288	Constant/None	250/50	14
C1	3815x3	290	None	100*	14
C2	3815x4	290	10s	100	14
D1	2816x4	289	None	100*	14
D2	2978x1	290	None	250	14
D3	2816x5	289	30s	200	30
D4	2816x6	291	Constant	200	30
E1	2816x11	290	30s	100	30
E2	2816x12	292	Constant	100	30
F1	2816x8	290	30s	50	30
F2	2816x9	290	Constant	100	30
G1	2978x5	288	Constant/None	200/200	14
G2	2978x7	298	Constant/None	200/200	14
G3	2978x9	308	Constant/None	200/200	14
H1	2819x4	193	30s	200	30
H2	2819x6	223	30s	200	30
H3	2819x8	253	30s	200	30
H4	2819x10	283	30s	200	30
H5	2819x2	293	30s	100	30
H6	2819x12	313	30s	100	30
I1	2814x3	286	30s	100	30
I2	2814x4	288	Constant	100	30

* Scans were added to each other rather than ran separately

Table 10. Experimental details for EPR experiments

2.15.1 Irradiation of Hexachloroplatinate (IV) Hexahydrate

The literature on the use of spin traps to trap Cl radicals is sparse and understanding of the production, decay and side reactions of the process is limited. The irradiation of sodium hexachloroplatinate (IV) hexahydrate in the presence of the spin trap PBN was carried out, as described by Rehorek et al⁸⁰ in order to validate the experimental protocols. Photoaquation and photoreduction to Pt^{III} both occur and the accompanying Cl[•] is trapped using PBN. Sodium hexachloroplatinate (IV) hexahydrate (few mg) and PBN (*ca* 0.05 mol dm⁻³) were dissolved in DMSO as this solvent was successful in dissolving both the hexachloroplatinate salt and the PBN. When the solution was irradiated constantly,

scanning showed an eight line spectrum (Figure 27) previously seen in the literature, clearly showing that the PBN-Cl adduct is formed. The hyperfine values $a_{\text{Cl-35}} = 6.28 \text{ G}$ are similar to that reported by Rehorek⁸⁰. This outcome confirms the experimental procedure can detect the presence of Cl^\bullet .

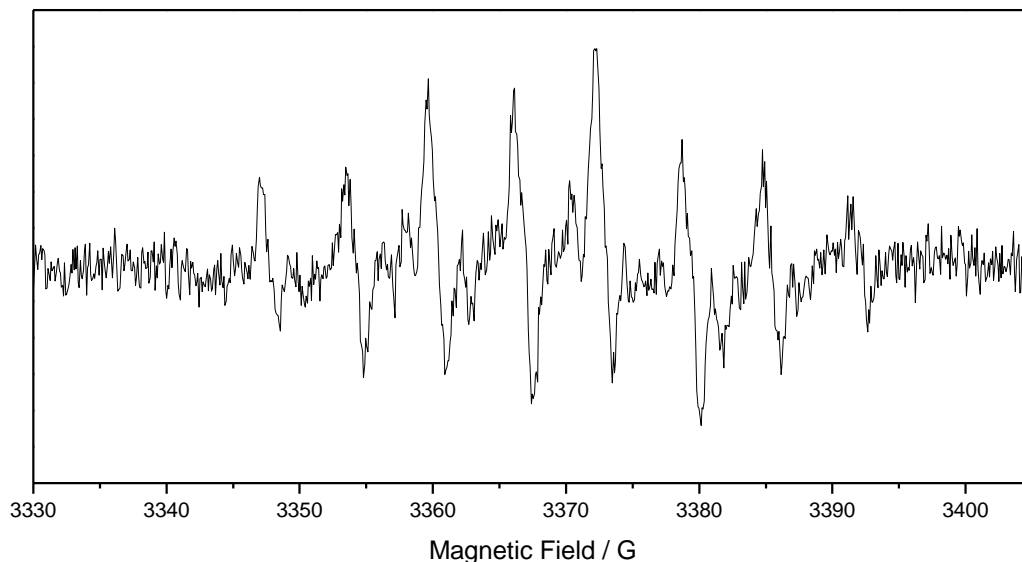


Figure 27. EPR spectrum of Cl-PBN adduct from irradiation of sodium hexachloroplatinate (IV) hexahydrate in the presence of the spin trap, PBN

2.15.2 Simulation of Experimental Spectra

Simulation work on selected recorded spectra was carried out using Bruker SimFonia software package (version 1.25).

2.15.3 DFT Calculations of EPR Parameters to Support Radical Identification

Density functional calculations were carried out at Manchester using the Gaussian03 suite of programs.¹¹³ Geometries for the structures examined were fully optimized using the B3LYP functional¹¹⁴ and the 6-311G(d,p)¹¹⁵⁻¹¹⁷ basis. All structures were confirmed as minima through vibrational analysis. Isotropic Fermi contact coupling constants were calculated at these optimized geometries. For the evaluation of hyperfine couplings the large EPR-III¹¹⁸ basis set was employed for all atoms except Cl. For Cl (since the EPR-III basis is not defined for this atom) the IGLO-III¹¹⁹ basis was employed.

2.15.4 Temperature Study

Experiments were carried out at low temperatures to investigate the behaviour of the radicals produced (H1-H6). Toluene was used as a solvent as its melting point (180 K) allowed us to use lower temperatures than benzene (melting point = 279 K). It was thought the cooling of the reaction would slow down the formation of the radicals providing clearer spectra. Six different temperatures were investigated, 193 K, 223 K, 253 K, 283 K, 293 K, 313 K. For each temperature the sample was irradiated for 30 seconds and stopped. Scanning was started immediately with 1 scan collected every 30 seconds. This was done for up to 200 scans, or 100 minutes.

2.15.5 PBN Concentration Study

It was also important to study whether concentration had an effect on the radicals produced. To investigate this separate solutions of PID with PBN were made up, each contained different concentrations of PBN, however the concentration of PID was kept constant. Three different concentrations of the spin trap were used, 0.1M, 0.05M and 0.026M (Solutions D, E and F). Reactions were carried out both where the sample was irradiated for 30 s and where constant irradiation took place.

2.15.6 Kinetic Analysis

Reactions were also carried out to study temporal effects (G1-G3). For these the solutions were irradiated for 45 minutes while constant scanning took place, the lamp was then switched off and scanning was continued for a further 45 minutes. This procedure was carried out at 3 different temperatures: 288 K, 298 K and 308 K. From the reactions carried out the amount of each radical present was calculated and plotted against time to produce a reaction profile. The second chlorine peak (centred at 3345.8 G) and the first nitrogen peak (centred at 3354.2 G) were selected to calculate the radical quantities as they were uniquely representative of the 2 spectral features observed (discussed later), with no overlap of adjacent bands.

In order to produce an accurate reaction profile the peak width has to be taken into consideration when analysing the EPR spectra. Equation (13) outlines the calculation which can be used to calculate the intensity of the radical.¹²⁰ This calculation can be made

more precise by taking into account the lineshape.¹²⁰ The equation is modified by replacing the line width with the width of the line across one lobe of the derivative curve at a height of 1/10 of the amplitude measured between the baseline and the peak maximum. The reason for this is that this value is approximately equal for both Gaussian and Lorentzian lines at one tenth height. Therefore the modified equation can be applied to all recorded EPR spectra. Within the experiments carried out it was found the line width or line shape did not change over time, therefore the peak height was used as an indication of the radical quantities.

$$\text{Intensity of Radical} = w^2 a \quad (13)$$

Where w = line width, a = amplitude

Chapter 3

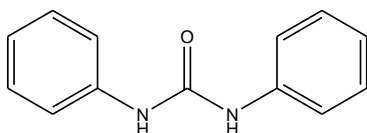
Ureas

3 Ureas

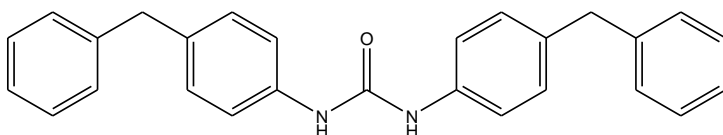
Urea compounds are a common by-product in the industrial synthesis of polyurethanes⁵. They arise from the reaction between the amine starting material and the isocyanate product. Research was undertaken to investigate the postulated side reaction described in section 1.7. This chapter outlines studies carried out specifically on the urea compounds.

3.1 Urea Compounds

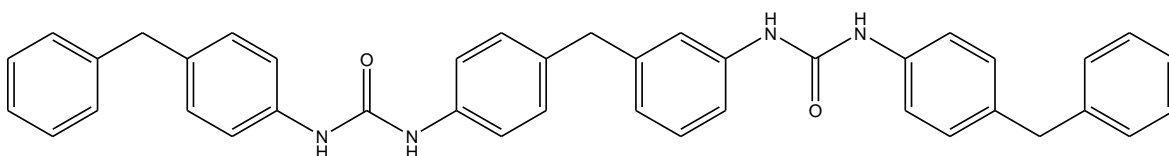
Three urea compounds were utilized in this project as described in section 2.5 and presented in Figure 28. These molecules are model compounds relevant to the ureas that would be produced in the industrial process. 1,3-Diphenylurea (IVa) (urea 1) was the simplest urea used in this research. As it can be acquired in pure form from a supplier it was convenient for looking into different reaction conditions. 1,3-Di-*p*-benzylphenylurea (IVb) (urea 2) was synthesized in-house from a mono-amine and a mono-isocyanate and also used in phosgenation reactions. Changing either the amine or the isocyanate to a di-functional compound produced the oligomeric urea (IVc) (urea 3). This compound was the closest in structure to that formed in the industrial environment (polymeric ureas) and was used as a comparison to urea 2 in order to examine the structure of the molecules.



1,3-Diphenylurea (urea 1)



1,3-Di-*p*-benzylphenylurea (urea 2)



Oligomeric urea (urea 3)

Figure 28. Urea compounds investigated within this research project

3.2 Phosgenation of Ureas

It has been postulated that the ureas produced in the industrial synthesis of MDI will undergo phosgenation to form chloroformamidine-*N*-carbonyl chloride compounds (VI) (CCC).⁵⁰ The process is described in section 1.7. In order to verify this reaction, phosgenation reactions were carried out on diphenyl urea (IVa) and 1,3-di-*p*-benzylphenylurea (IVb). Reactions were carried out as detailed in section 2.8, both triphosgene and the Eckert cartridge methods were used.

3.2.1 Identification of Products

The FTIR carried out on the products from the phosgenations of the ureas show a mixture of compounds including the starting materials. The products were identified by comparison to the compounds listed in Table 11. 4-benzylaniline, 4-benzylphenyl isocyanate, 1,3-diphenylurea and 1,3-di-*p*-tolylcarbodiimide were all purchased from a supplier and the FTIR spectra recorded on the pure compound. 1,3-Di-*p*-benzylphenylurea and 1,3-di-*p*-tolylchloroformamidine-*N*-carbonyl chloride (TCCC) were produced as described in sections 2.5.1 and 2.9 respectively. These compounds are therefore not analytically pure but the spectra are backed up by other reference compounds and from the characterisation we can assume ~90 % purity. The spectra for the compounds so far are shown in Figure 29 to Figure 34. The other compounds listed were taken from literature infrared assignments. The infrared data for the allophanoyl chlorides in the literature is ambiguous. It is our understanding that both carbonyls should be seen as separate peaks in the region of 1700 – 1800 cm⁻¹.¹²¹ Some references have stated 2 peaks in that region for both carbonyls,^{122, 123} however others seem to suggest only one peak is seen alluding to one carbonyl.^{62, 124, 125} This was taken into account when looking at the infrared spectra.

The amount of each compound found in the product mixtures varies from one reaction to the next. Table 12 outlines the compounds identified from the FTIR with the relative size of the product peaks (s = small, m = medium, l = large). The magnitudes of the compounds were not quantitative and estimated by comparing the reference spectra and from one reaction to the next.

Classification	Reference Material	Wavenumber / cm ⁻¹
Triphosgene (I)	Triphosgene ²⁷	1832 ($\nu(\text{C}=\text{O})$), 1178, 967, 945
Amine (II)	4-Benzylaniline (Figure 29)	3459 ($\nu_{\text{asym}}(\text{N-H})$), 3371 ($\nu_{\text{sym}}(\text{N-H})$), 1621, 1511, 1284, 1176, 730, 698
Isocyanate (III)	4-Benzylphenyl isocyanate (Figure 30)	2257 ($\nu(\text{N}=\text{C}=\text{O})$), 1524, 1494, 1453
Urea (IV)	1,3-Diphenylurea (Figure 31)	3280 ($\nu(\text{N-H})$), 1645 ($\nu(\text{C}=\text{O})$), 1592, 1548, 1497, 1447
	1,3-Di- <i>p</i> -benzylphenylurea (Figure 32)	3301 ($\nu(\text{N-H})$), 1636 ($\nu(\text{C}=\text{O})$), 1588, 1543, 1510
Chloroformamidine (V)	N-(2-cyanophenyl)-2-hydroxyanilino)methanimidoyl chloride ¹²⁶	3305 ($\nu(\text{N-H})$), 1650 ($\nu(\text{C}=\text{N})$), 770 ($\nu(\text{C-Cl})$)
CCC (VI)	1,3-Di- <i>p</i> -tolylchloroformamidine- <i>N</i> -carbonyl chloride (Figure 33)	1753 ($\nu(\text{C}=\text{O})$), 1661 ($\nu(\text{C}=\text{N})$)
	1,3-Diphenylchloroformamidine- <i>N</i> -carbonyl chloride	1755 ($\nu(\text{C}=\text{O})$), 1660 ($\nu(\text{C}=\text{N})$), 1590, 1487
Carbodiimide (VII)	1,3-Di- <i>p</i> -tolylcarbodiimide (Figure 34)	3024, 2920, 2101 ($\nu(\text{N}=\text{C}=\text{N})$), 1658, 1503, 1203, 813
	1,3-Diphenylcarbodiimide ¹²⁷	2936, 2139 ($\nu(\text{N}=\text{C}=\text{N})$), 2105, 1588, 1487, 1202, 757
Allophanoyl chloride (VIII)	2,4-Dimethylallophanoyl chloride ¹²⁴	3450 ($\nu(\text{N-H})$), 3020, 1740 ($\nu(\text{C}=\text{O})$), 1560, 1300, 1240, 1060
	2,4-Di- <i>tert</i> -butylallophanoyl chloride ¹²²	3400 ($\nu(\text{N-H})$), 1755 ($\nu(\text{C}=\text{O})$), 1720 ($\nu(\text{C}=\text{O})$), 1490, 1455, 1365

Table 11. Infrared assignments of compounds from the postulated reaction scheme

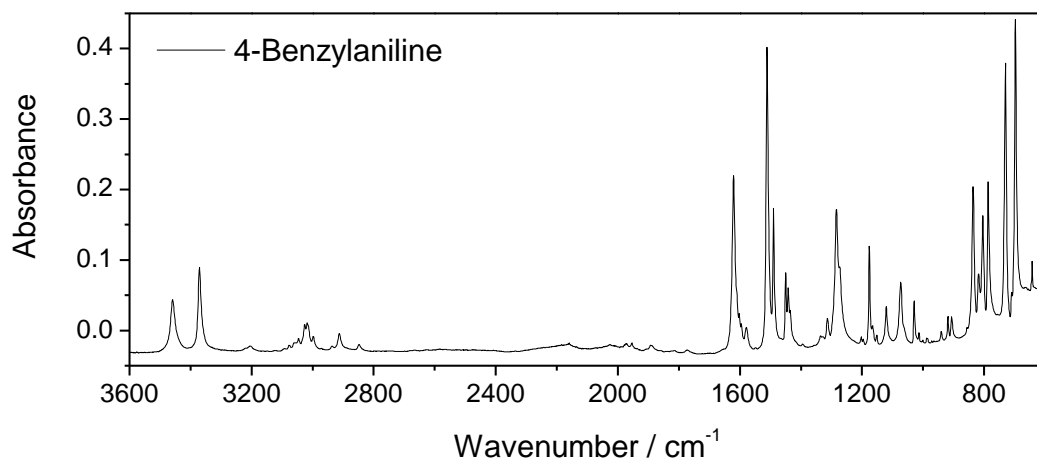


Figure 29. FTIR spectrum of 4-benzylaniline purchased from Alfa Aesar

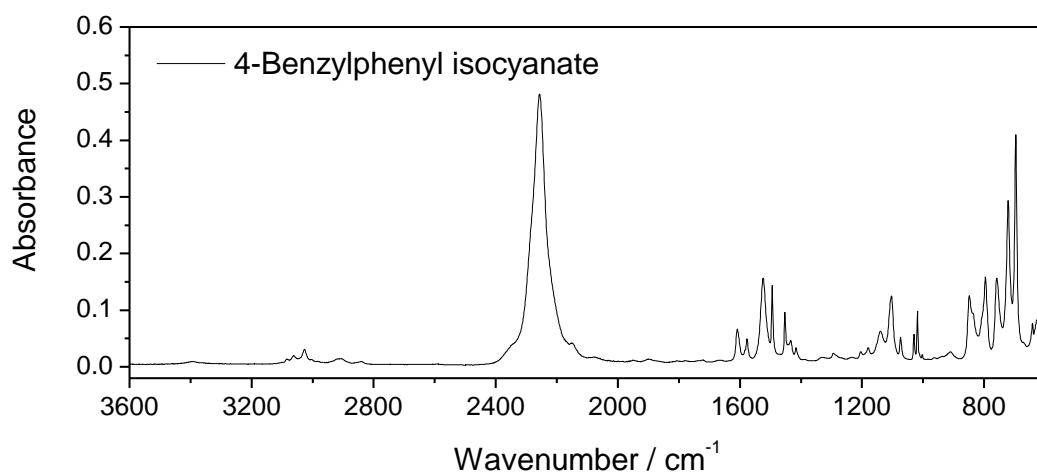


Figure 30. FTIR spectrum of 4-benzylphenyl isocyanate purchased from Sigma-Aldrich

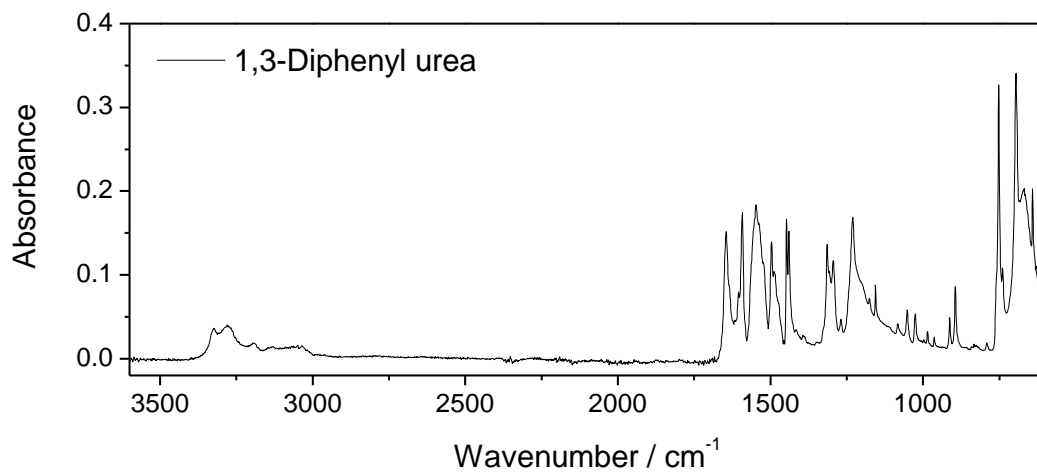


Figure 31. FTIR spectrum of 1,3-diphenylurea purchased from Sigma-Aldrich

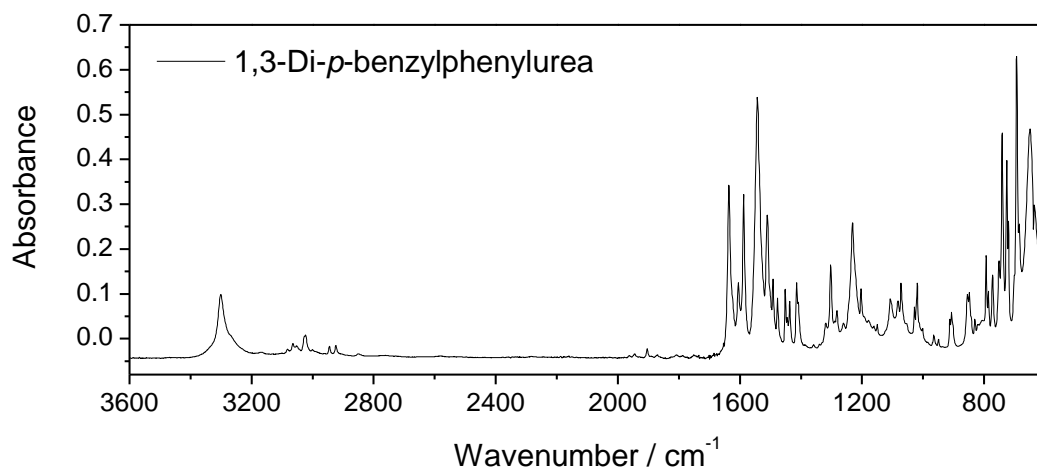


Figure 32. FTIR spectrum of 1,3-di-*p*-benzylphenylurea synthesized in-house (Section 2.5.1)

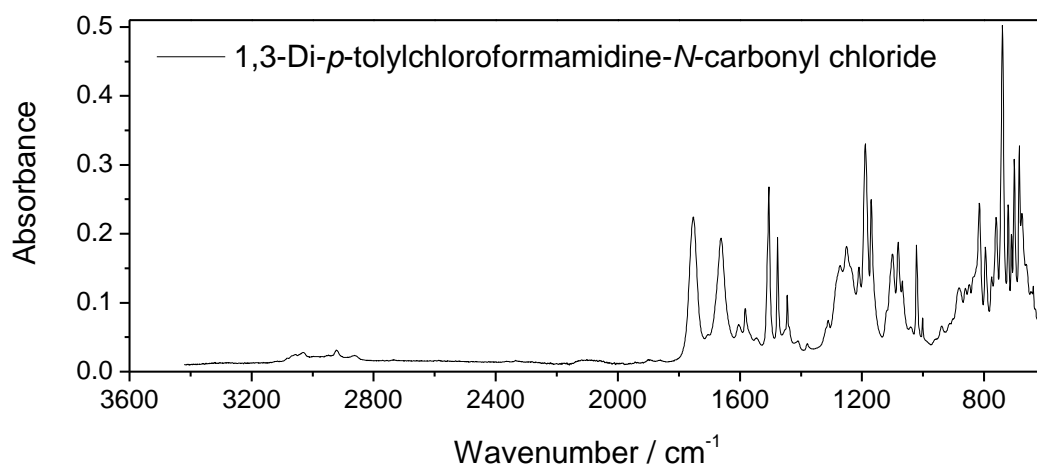


Figure 33. FTIR spectrum of 1,3-di-*p*-tolylchloroformamide-*N*-carbonyl chloride synthesized as described in section 2.9

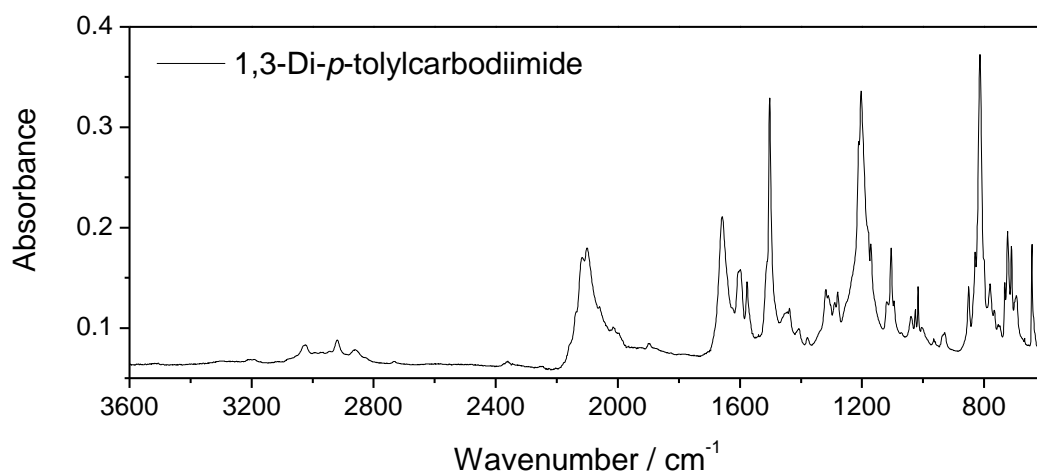


Figure 34. FTIR spectrum of 1,3-di-*p*-tolylcarbodiimide purchased from Sigma-Aldrich

Reaction	Urea Compound	Phosgene Method	Temperature / K	Product (from FTIR)								
				I	II	III	IV	VI	VII	IX	U	
1	4-benzylphenyl urea	Triphosgene	363	M		L		L				
2	4-benzylphenyl urea	Triphosgene	323	L		L						
3	1,3-diphenyl urea	Triphosgene	323 353	L		S						S
4	1,3-diphenyl urea	Triphosgene	363			L		L				
5	1,3-diphenyl urea	Phosgene	333				L	S				
6	1,3-diphenyl urea	Phosgene	353				L	S	S			
7	1,3-diphenyl urea	Phosgene	333				L	S	S			
8	1,3-diphenyl urea	Phosgene	363				S	M	M			
9	1,3-diphenyl urea	Phosgene	388						M			M
10 [#]	1,3-diphenyl urea	Phosgene	383			S		M	L			M
11	4-benzylphenyl urea	Phosgene	383			M		M	M			
12 [#]	4-benzylphenyl urea	Phosgene	373 368			M		L			S*	
13	Product from reaction 9	Phosgene	299		S*			M				M
14	Product from reaction 10	Phosgene	295		S*	S		L				M
15	Product from reaction 11	Phosgene	297			M		L				

Two step reaction, more phosgene added to convert all urea present

*Indicated from mass spectra

s = small, m = medium, l = large

I – IX = indicate products detailed in Table 11, U = unknown peak

Table 12. Product details from the phosgenation of urea reactions

3.2.2 Triphosgene Reactions (1-4)

Reactions 1 to 4 were carried out using the method of adding triphosgene directly to the reactor. Figure 35 and Figure 36 shows the FTIR spectra from the product mixtures of the four reactions. The two reactions carried out below 363 K show large amounts of triphosgene starting material leftover in the product mixture ($\nu(\text{C}=\text{O}) = \sim 1830 \text{ cm}^{-1}$). For

the reactions carried out at 363 K, triphosgene is seen in lower amounts in reaction 1, whereas it has disappeared in reaction 4, which is carried out over a longer period of time. However in the four reactions all of the urea starting material is consumed ($\nu(\text{C}=\text{O}) = \sim 1645 \text{ cm}^{-1}$). This is not surprising as the amount of triphosgene added was measured to provide a four times molar excess of phosgene to the urea. These results back up the statement by Eckert²⁸ that although the use of gaseous phosgene requires this excess to react all of the starting material, this is not the case with the trimer, which can be used in equal amounts to the reactant whilst still producing high yields.

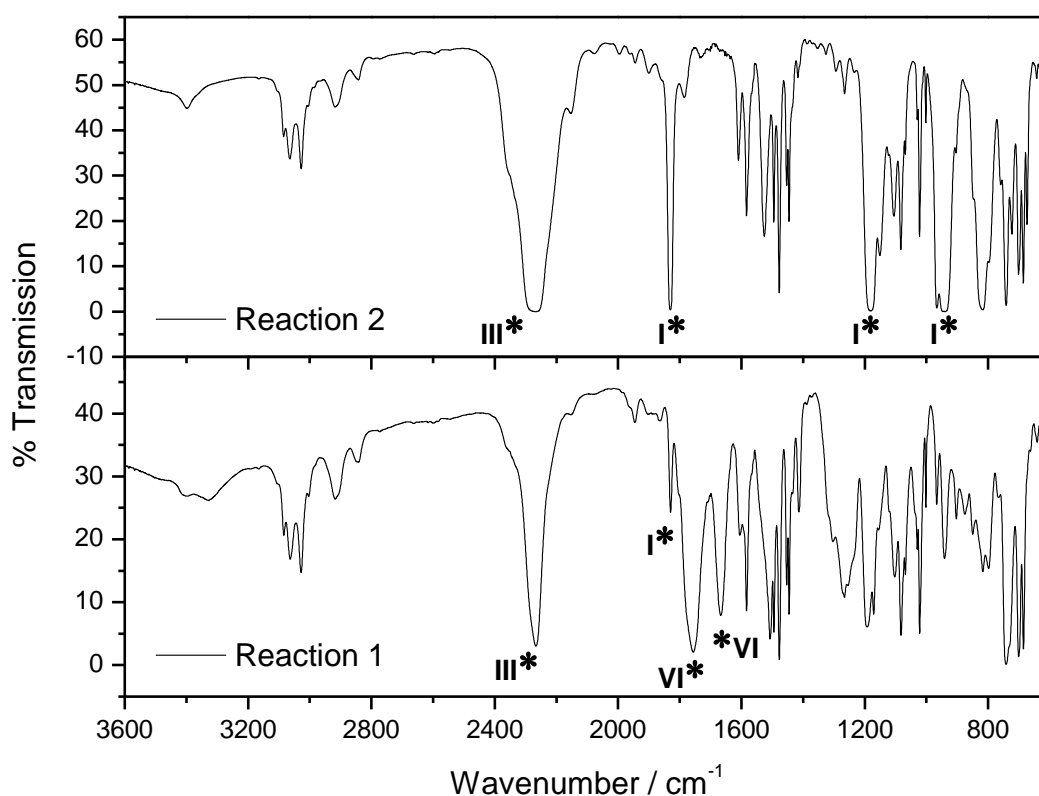


Figure 35. FTIR spectra of reactions 1 and 2, * indicates peaks attributed to triphosgene (I), isocyanate (III) and CCC (VI)

All four reactions (1-4) produce the corresponding isocyanate relative to the urea starting material ($\nu(\text{N}=\text{C}=\text{O}) = \sim 2264 \text{ cm}^{-1}$). Ulrich and Sayigh¹²⁵ reported the formation of isocyanate from di-substituted ureas and phosgene. In this case the nitrogen of the urea will attack the carbonyl group of the triphosgene to form an allophanoyl chloride (VIII), which decomposes to the isocyanate and HCl over time¹²⁸. However Ulrich has only researched dialkyl ureas stating that diphenyl urea only reacts with phosgene above 423 K, proposing a dissociation pathway to an amine plus the isocyanate.^{125, 129} No evidence of the allophanoyl chloride or the amine is seen in the spectra; however at the temperatures and

concentrations used, these compounds may be converted immediately to the isocyanate. Any amine present will also react with the triphosgene and aid its breakdown to phosgene gas. Therefore it is unclear at this stage what reaction mechanism is taking place, although it is possible that the solid triphosgene is reacting differently to phosgene gas as the results seen here are different to those in the literature when aromatic ureas are reacted with phosgene.^{125, 129}

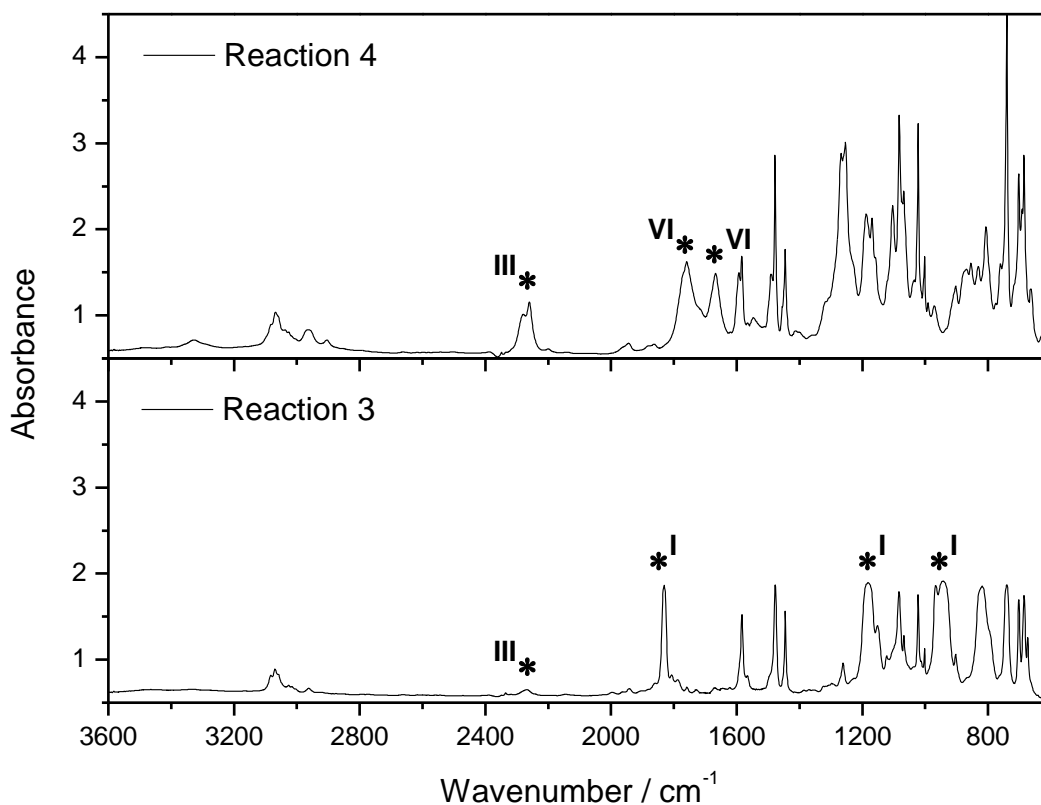
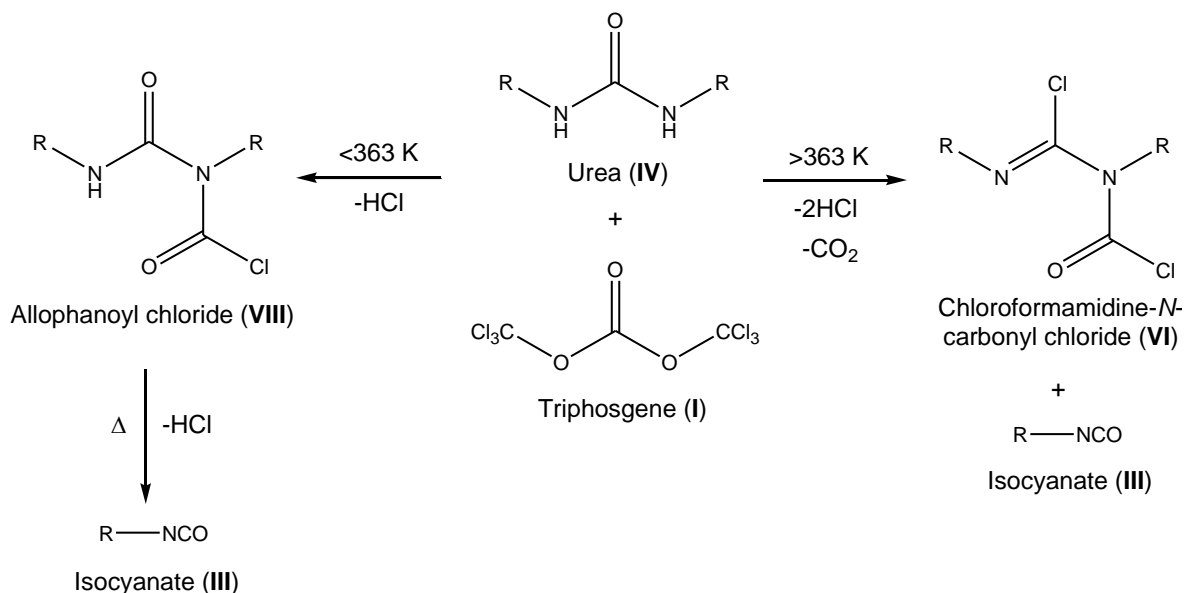


Figure 36. FTIR spectra of reactions 3 and 4, * indicates peaks attributed to triphosgene (I), isocyanate (III) and CCC (VI)

Reactions 1 and 4, which are heated up to at least 363 K both show the chloroformamidine-*N*-carbonyl chloride (CCC) as a product ($\nu(\text{C}=\text{O}) = 1757\text{cm}^{-1}$, $\nu(\text{C}=\text{N}) = 1667\text{cm}^{-1}$), with the longer reaction producing it in a larger amount. From these results, it is noted that below 363 K only the isocyanate is produced and large amounts of the triphosgene are left-over. As the temperature is increased up to 363 K, CCC is produced where heat and a longer reaction time aids the breakdown of excess triphosgene (Scheme 9).

It has been shown that triphosgene will thermally decompose at 403 K³¹, although phosgene has been found in ambient conditions in small quantities. From the results we

have seen thus far, it is possible that two reaction pathways are occurring, below 363 K, urea is reacting with the triphosgene to produce isocyanate via the allophanoyl chloride, whereas above 363 K, the urea is reacting with phosgene (produced via decomposition of the triphosgene) producing both CCC and isocyanate. These results show that the phosgenation of urea is not a simple reaction with a series of pathways available.



Scheme 9. Reaction of urea with triphosgene

3.2.3 Eckert Cartridge Reactions (5-8)

Reactions were then carried out with the second method of phosgenation. For this an Eckert cartridge was used to produce phosgene out with the reactor, which was then flowed into the reaction aided by a nitrogen purge. These reactions were designed to mimic the temperatures used in the first four reactions. The products produced from these reactions differ dramatically from the triphosgene reactions. Firstly, all four reactions with temperatures ranging from 333 K to 363 K produce chloroformamidine-*N*-carbonyl chloride (CCC) ($\nu(\text{C}=\text{O}) = 1749\text{cm}^{-1}$) (Figure 37). Also no isocyanate is observed in any of the product mixtures. This is contradictory to what is seen in the triphosgene experiments; therefore we can conclude that CCC is produced from reaction with phosgene at temperatures up to 363 K. Within this temperature range, isocyanate is only produced when triphosgene is present, again implicating a separate reaction mechanism.

For all four reactions, not all of the urea has reacted, again, confirming different mechanisms between phosgene and triphosgene. Only in reaction 8 do we see a

considerable amount of the urea used up. This reaction differs from the others as it combines the higher temperature of 363 K with a higher excess of phosgene (16 times). During the course of these reactions it has also been noted that the urea is not fully soluble at low temperatures, this is important and will be discussed later.

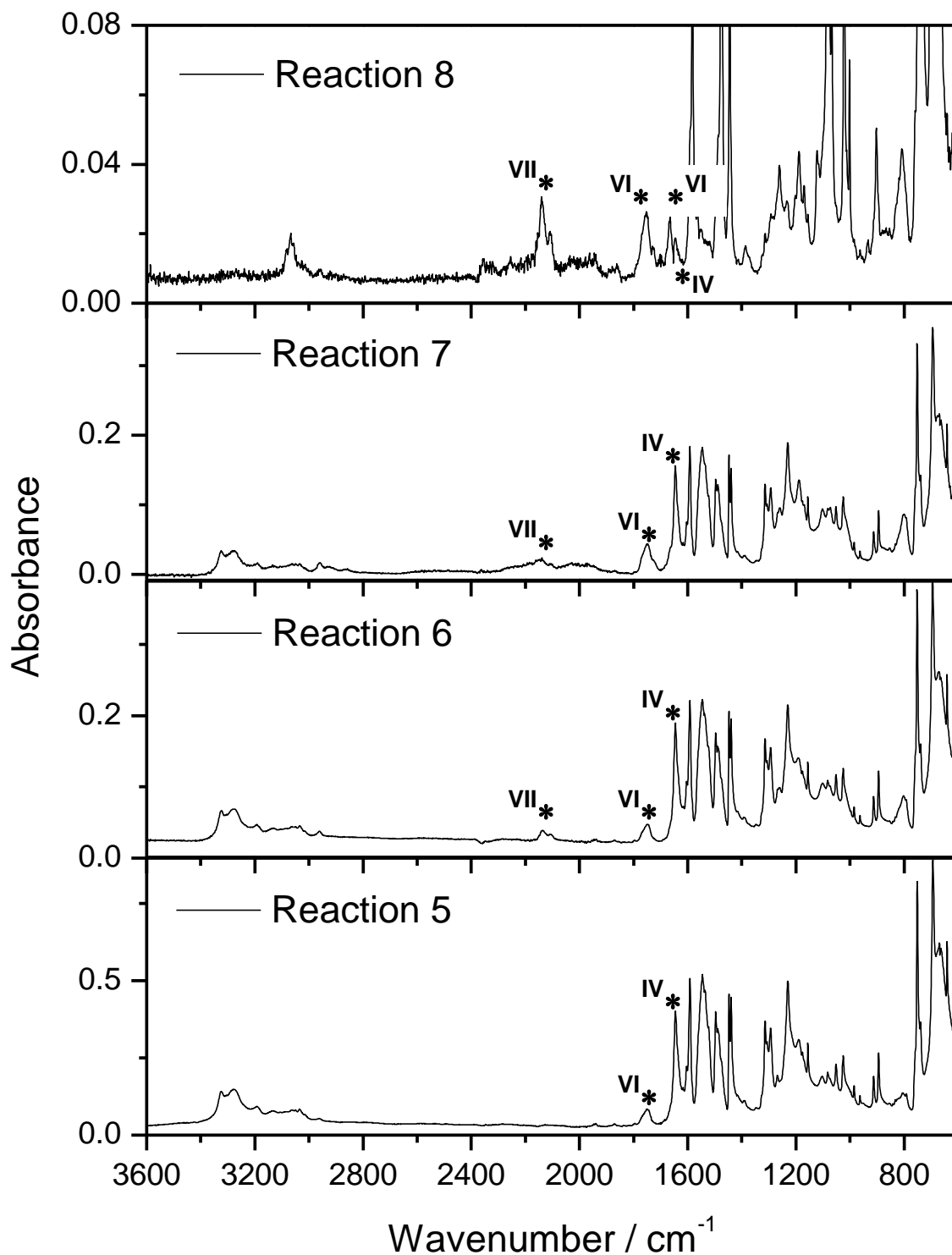
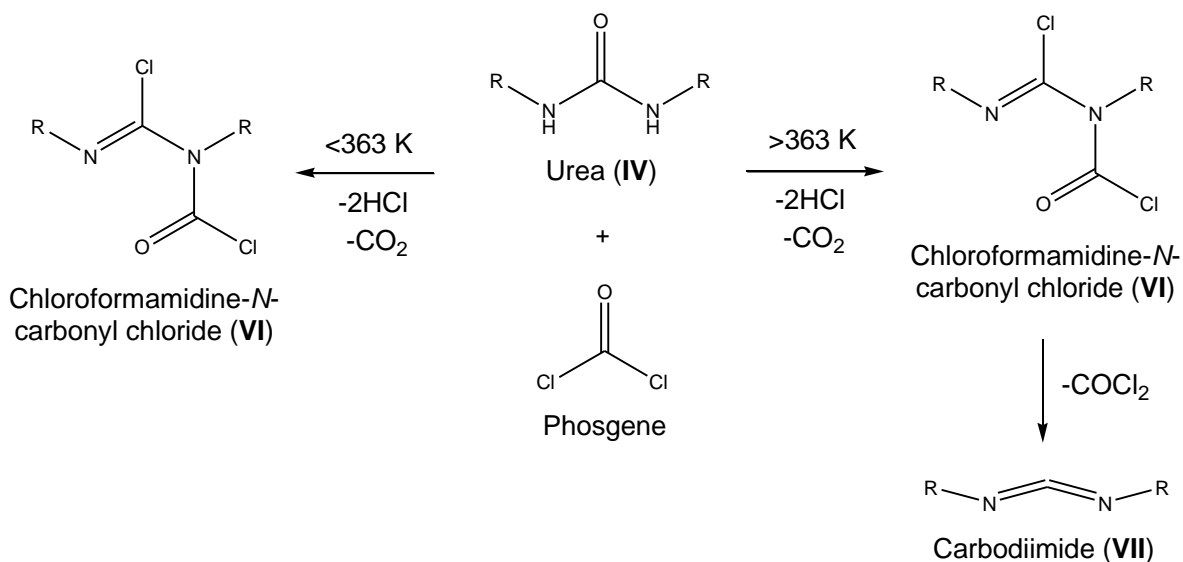


Figure 37. FTIR spectra of reactions 5 to 8, * indicates peaks attributed to urea (IV), CCC (VI) and carbodiimide (VII)

A product first seen in these reactions is carbodiimide ($\nu(\text{N}=\text{C}=\text{N}) = 2138 \text{ cm}^{-1}$), which appears when the reaction temperature is increased to 363 K, although a small amount can be seen in reactions 6 and 7. The carbodiimide is formed from decomposition of the CCC releasing phosgene in the process. This provides an interesting result as although a higher temperature is needed to aid the reaction of the urea, this will lead to breakdown of the desired product, CCC. These results are summed up in Scheme 10.



Scheme 10. Reaction of urea with phosgene (Eckert cartridge)

3.2.4 High Temperature Reactions (9-15)

It has been reported elsewhere¹⁰² that carbodiimide can undergo phosgenation at room temperature to produce chloroformamidine-*N*-carbonyl chloride (CCC). Therefore a two-step reaction was devised whereby higher temperatures would be used to react the urea to the CCC, followed by decomposition to the carbodiimide; more phosgene would then be added at room temperature to convert the carbodiimide back to the CCC.

Reactions 9-12 in Table 12 show experiments that were carried out between 368 and 388 K. In each reaction all the urea starting material is fully reacted (Figure 38). Carbodiimide is produced in significant quantities at 383 – 388 K (as evidenced by $\nu(\text{N}=\text{C}=\text{N})$ at $\sim 2135 \text{ cm}^{-1}$). Experiment 9 uses *o*-dichlorobenzene (ODCB) as the solvent instead of chlorobenzene (MCB) as originally it was thought temperatures higher than 403 K (boiling point of MCB) would be needed to convert all of the urea. The use of ODCB created problems in that after rotary evaporation at 333 K not all of the solvent had been

evaporated, as leftover solvent can be seen in the analysis carried out (the boiling point of ODCB is 453 K). The high temperature needed to remove the solvent also compromises the product. Therefore this result may not be accurate and further reactions were carried out using MCB.

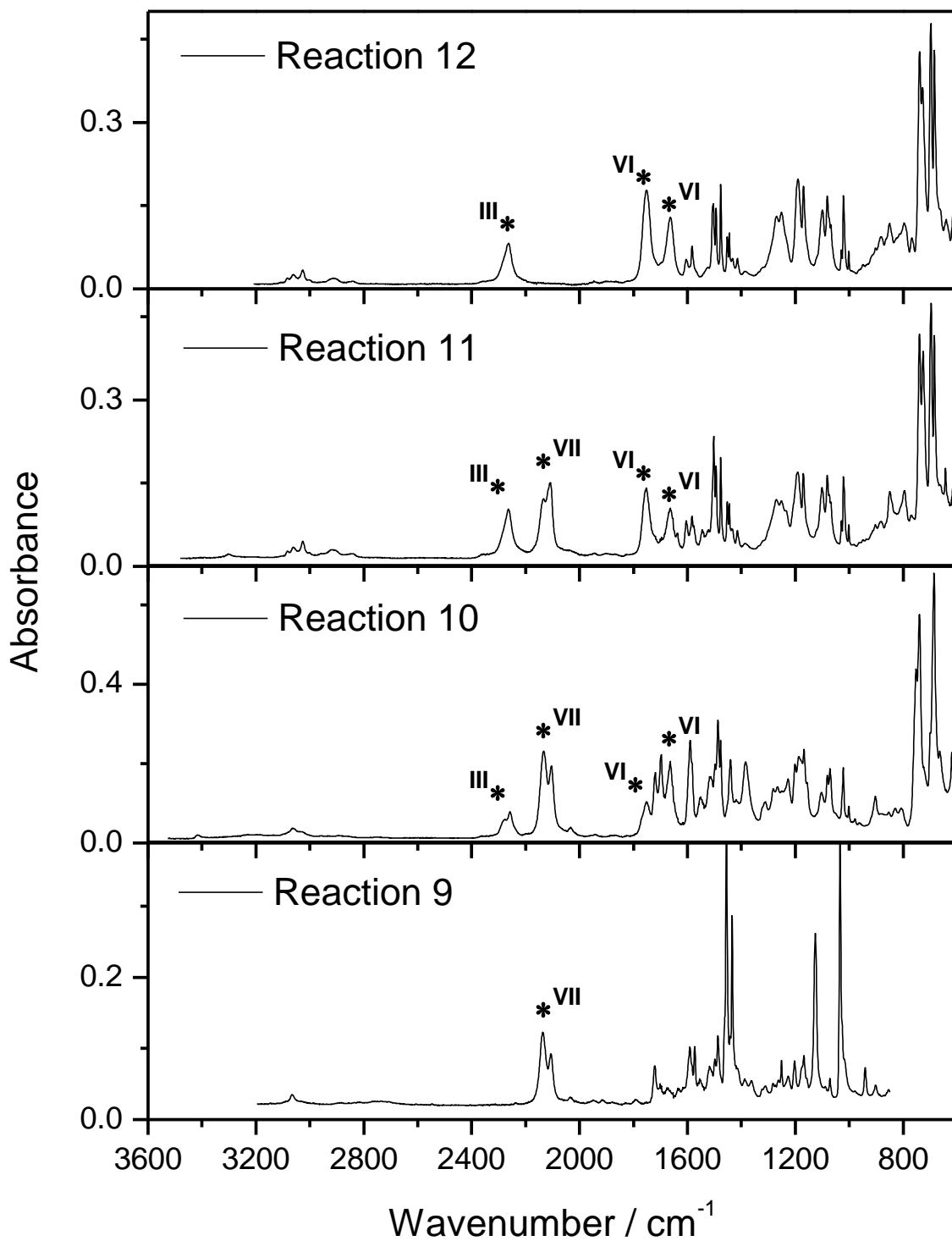


Figure 38. FTIR spectra of reactions 9 to 12, * indicates peaks attributed to isocyanate (III), CCC (VI) and carbodiimide (VII)

Reactions 10 – 12 produced the isocyanate ($\nu(\text{N}=\text{C}=\text{O}) = 2260\text{cm}^{-1}$), increasing as the phosgene excess is increased. This result shows that phosgene can also react with ureas to give isocyanate, but only at temperatures above 363 K. It is possible however that the urea is starting to decompose at the higher temperature to isocyanate and amine, with the amine being phosgenated to isocyanate. The product CCC is seen in reactions 10, 11 and 12 but not in reaction 9. This is due to decomposition of CCC at the temperatures used to evaporate the solvent (ODCB) as previously discussed. The product mixtures from 10 and 11 show a considerable amount of the carbodiimide is produced, however in reaction 12, carried out at a lower temperature, no carbodiimide and a larger amount of CCC is produced. This leads us to believe an equilibrium must be present between the CCC and the carbodiimide and is dependent on temperature and the amount of phosgene in the system. This will be discussed later (section 4.1.1).

The product mixtures from reactions 9-11, in which carbodiimide was produced were phosgenated at temperatures ~ 298 K. The results from these reactions show that the carbodiimide in the solution is converted back to CCC. The $\text{N}=\text{C}=\text{N}$ stretch for the carbodiimide ($\sim 2135\text{ cm}^{-1}$) decreases whilst the $\text{C}=\text{O}$ ($\sim 1753\text{ cm}^{-1}$) and $\text{C}=\text{N}$ ($\sim 1661\text{ cm}^{-1}$) stretches corresponding to the CCC increase (Figure 39 and Figure 40). The isocyanates seen in the mixtures are not largely affected in this reaction. Mass spectroscopy was carried out on the products from reactions 12-15, where the CCC was present in higher quantities. The spectra confirmed the identities of the compounds identified in the FTIR, and also established that no allophanoyl chloride or chloroformamidine was present. A small amount of isocyanide dichloride is seen in the mass spectra of reaction 12. This reaction was carried out with the highest excess of phosgene (40:1) and showed no carbodiimide in the product. It is therefore possible that the decomposition pathway of CCC to the isocyanate and isocyanide dichloride is occurring in this case. The mass spectra recorded for the diphenyl urea phosgenations (reactions 13 and 14) showed a small amount of what appears to be the amine. This could be proof that in these reactions the urea is producing isocyanate via a decomposition route of the urea, not via the allophanoyl chloride.

In reactions 3, 9, 10, 13 and 14 a peak in the infrared spectrum appears at $\sim 1721\text{ cm}^{-1}$. This is an unknown peak and could not be attributed to a specific compound. Possibilities for the identity could be a product of trimerisation of the isocyanate, biuret or urethane. These are all by-products produced in the reactions involving isocyanates.¹⁸

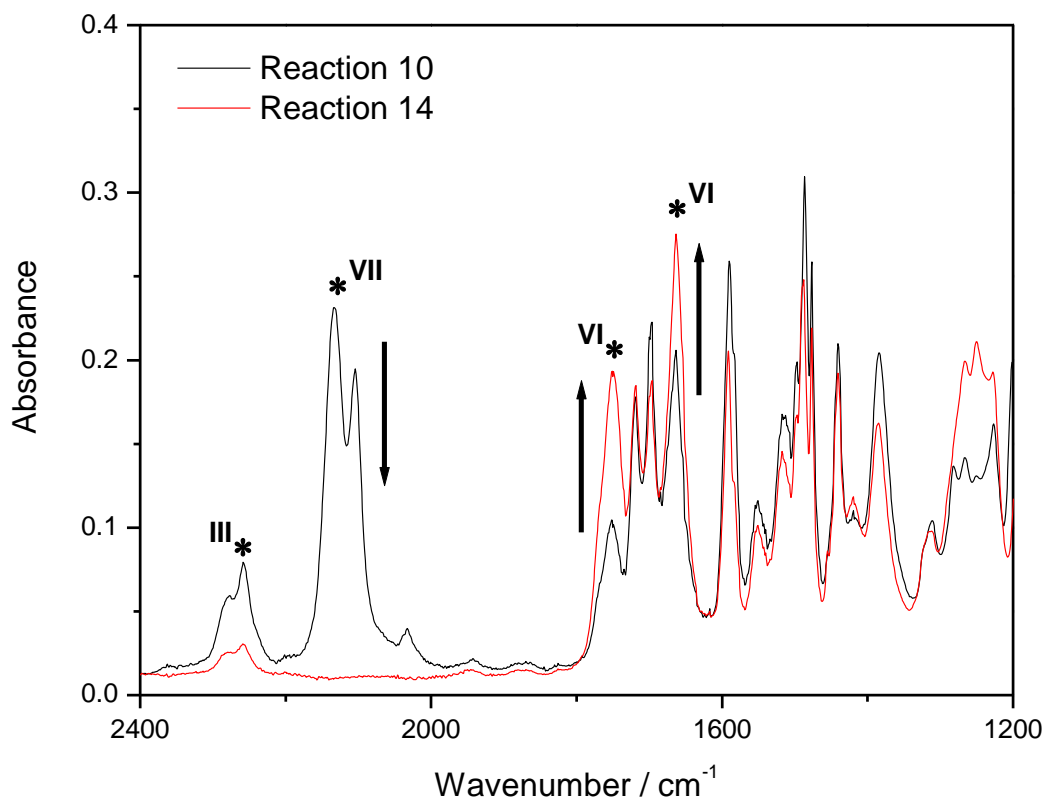


Figure 39. FTIR Spectra of reactions 10 and 14, * indicates peaks attributed to isocyanate (III), CCC (VI) and carbodiimide (VII)

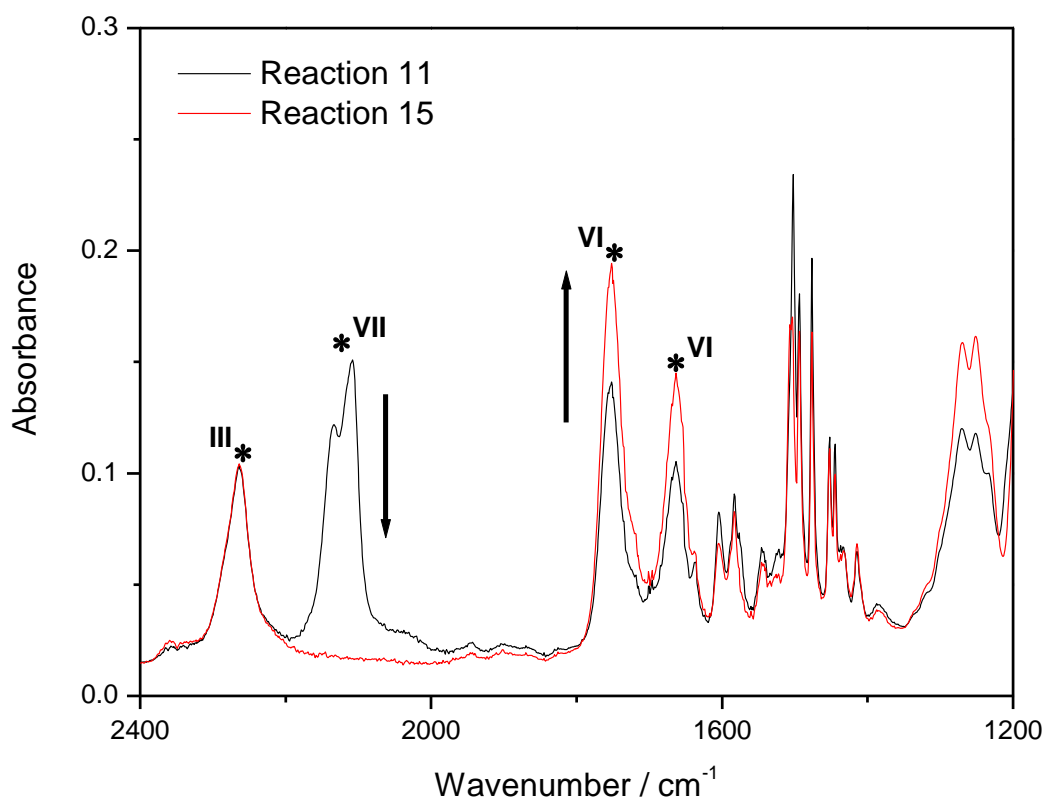
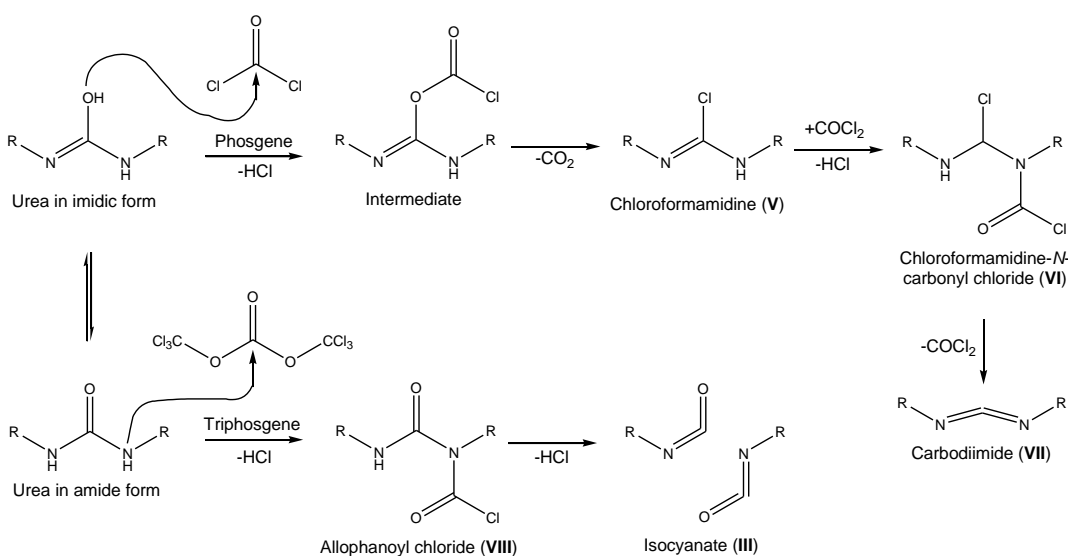


Figure 40. FTIR Spectra of reactions 11 and 15, * indicates peaks attributed to isocyanate (III), CCC (VI) and carbodiimide (VII)

3.2.5 Discussion

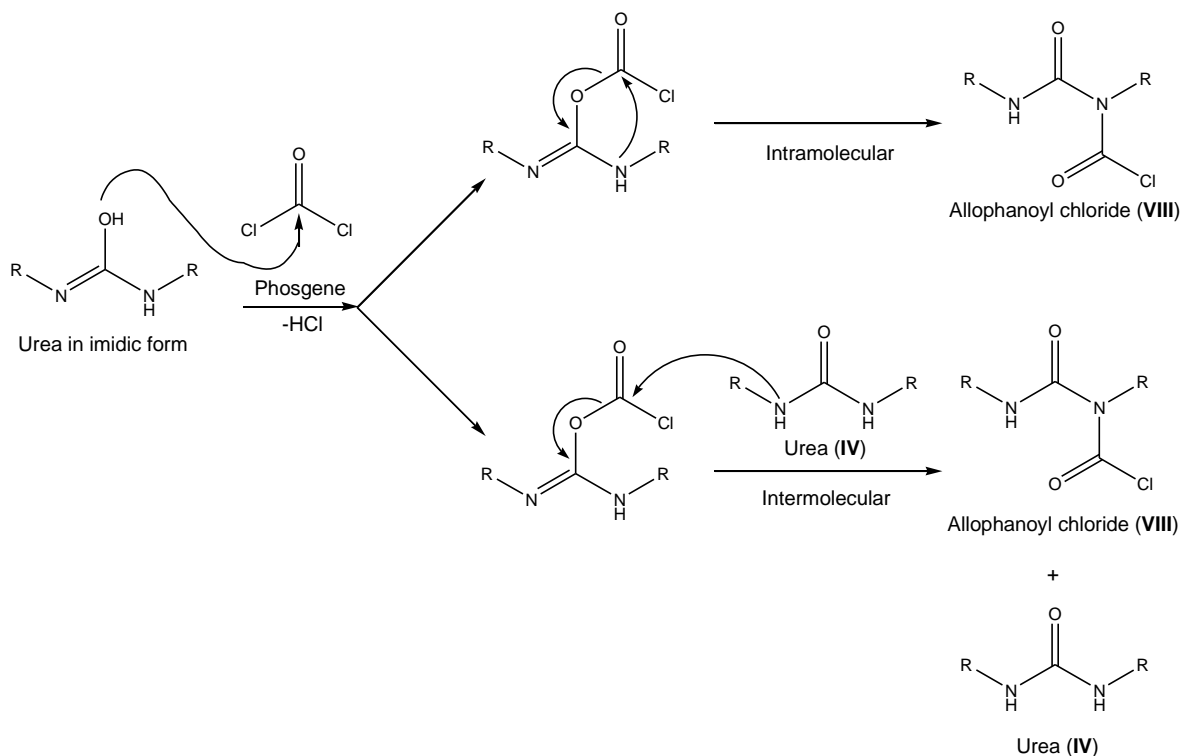
The experiments carried out on the phosgenation of urea compounds have produced varying results when temperature, method of phosgenation and amount of phosgene used are altered. The different products produced in the reactions show there are several reaction pathways occurring. References in the literature which link urea compounds to chloroformamidine-*N*-carbonyl chloride (CCC), carbodiimides and chloroformamidines mostly relate to alkyl substituted ureas or cyclic compounds. The only reference to an aromatic urea, diphenyl urea, states that it reacts with phosgene over 423 K to give isocyanate as the only product via the decomposition to the amine and the isocyanate.¹²⁵

Scheme 11 outlines the reactions that are taking place in the experiments explored in the sections above. It is proposed that two different mechanisms are taking place; in one the nitrogen of the urea is attacked to form the allophanoyl chloride, while the other reaction takes place at the oxygen, releasing CO₂ to form the chloroformamidine leading to the CCC. This is similar to what is seen in the reaction of dialkyl ureas with phosgene, where the ratio of allophanoyl chloride to chloroformamidine is dependent on the substituent.^{125, 128} It is suggested here that triphosgene is reacting with the nitrogen on the urea, whereas above 363 K, it breaks down to phosgene which will then react preferably with the oxygen. In these cases, the allophanoyl chloride is breaking down to produce the isocyanate seen in the product mixtures and the chloroformamidine is being further phosgenated to CCC. It is also possible that the allophanoyl chloride could be formed via hydrolysis of the CCC,^{122, 130} however this is unlikely.



Scheme 11. Urea reaction summary

There are three possible mechanisms for the formation of the allophanoyl chloride from urea and phosgene discussed in the literature. Along with the N-attack from phosgene, the intermediate formed from O-attack can undergo either intramolecular displacement to form the allophanoyl chloride or further reaction with a molecule of urea (Scheme 12).⁶² Hence there are ambiguities over the reaction mechanisms occurring.



Scheme 12. Formation of allophanoyl chloride via O-attack

We can ascertain that the chloroformamidine-*N*-carbonyl chloride (CCC) molecule forms as a product from the combination of phosgene and urea at temperatures above 333 K. However temperatures above 363 K are needed to solvate all of the urea, which can lead to formation of isocyanate and carbodiimide. The formation of the isocyanate in this way could be due to dissociation of the urea to an amine and isocyanate¹²⁹. There is only evidence for a small amount of the amine present in the reactions with diphenyl urea, this is due to further reaction with phosgene to the isocyanate. The addition of aromatic rings to the urea starting material has little effect on the reaction. The reactions using the triphosgene have shown the urea to fully react at lower temperatures; consistent with the hypothesis that a separate reaction mechanism is involved.

The solid triphosgene was initially used in these reactions as it was thought to provide a direct source of phosgene, however this is not necessarily the case and triphosgene has

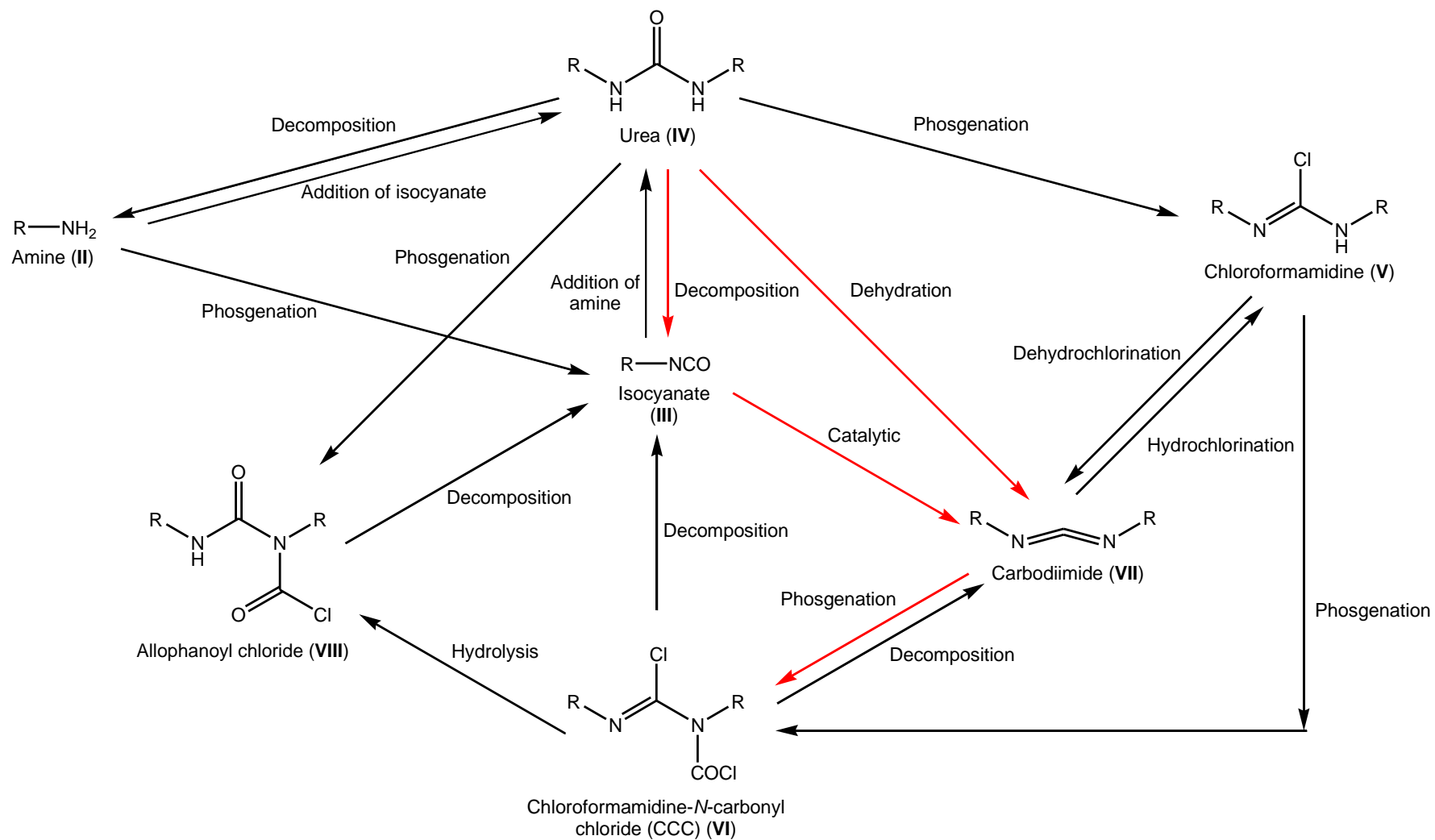
been found to react individually and distinctly. It was therefore established that the Eckert cartridge offered a better source of phosgene and has a considerable advantage in that all traces of phosgene can be removed from the product.

In summary there are several pathways that can occur when phosgene is reacted with aromatic ureas, however it can be concluded that CCC will be produced from the phosgenation of urea at temperatures above 333 K with a high concentration of phosgene present.

3.2.6 Alternative Routes to Chloroformamidine-*N*-carbonyl Chloride (CCC)

In all the reactions carried out no evidence for the allophanoyl chloride or chloroformamidine is seen. This is surprising as both compounds have been identified previously by infrared studies.⁶² It is possible these compounds are either reacting immediately, or alternative mechanisms are occurring. There are numerous references in the literature which link urea compounds to CCC, isocyanates, allophanoyl chlorides, carbodiimides and chloroformamidines.^{62, 102, 103, 122-125, 128-137} Scheme 13 shows the various reactions that have been discussed in the literature. The routes shown in red only involve the compounds that have been identified in the reactions carried out in this project. Ulrich states that urea can be dehydrated to carbodiimides with excess phosgene.¹⁸ If this reaction was occurring, the carbodiimide would be expected in the product mixture. It is seen in the reactions with phosgene but not triphosgene. An explanation for this could be that the CCC is immediately being formed as the triphosgene provides a larger excess of phosgene in solution than the phosgene gas. This could therefore explain the absence of the chloroformamidine.

Another reaction that could occur is the formation of carbodiimide via two molecules of isocyanate reacting together.¹³² However this reaction occurs above 423 K over a long period of time therefore it is unlikely this reaction is occurring in our experimental arrangement.



Scheme 13 Reaction schemes from literature^{62, 102, 103, 122-125, 128-137}, red arrows indicate reactions seen in the experimental described in this section

3.3 Urea Structure

Twitchett⁵⁰ and Ulrich et al⁶² postulated that phosgene would react with the urea via the imidic form (Scheme 11). However no concrete evidence for the tautomerism of the urea can be found in the literature. Thus in order to understand the mechanisms involved in the reaction it was important to gain information about the structure of the urea compounds looked at in this study.

3.3.1 Solubility

Reactions were carried out in an attempt to quantify the solubility of the ureas in the process solvent, chlorobenzene (MCB). This is an important property of the compound as it can provide insight into the reaction mechanisms. The degree of solubility in the solvent may indicate the extent at which tautomerisation to the imidic form takes place. Both weight measurements and ¹H-NMR spectroscopy were used to try and quantify the amount of urea in solution before and after heating at 363 K. The solvent suppression method outlined in section 2.7 was used to record the spectra as this would suppress the solvent peaks in order to lower the limit of the concentration that could be measured.

From the heating of 1,3-diphenylurea (urea 1) in MCB at 363 K, a solubility of 15 mmol L⁻¹ was calculated from weight measurements, with a reaction at room temperature affording a solubility of 13 mmol L⁻¹. This initially indicates that the solubility of 1,3-diphenylurea in MCB is very low, whilst heating the solution increases the value slightly. However this method is not the most accurate, due to human error and possible fluctuations in the weighing device. Therefore quantitative ¹H-NMR measurements were used to see if this could provide more accurate results.

As described in section 2.7.2.3, 4-benzylaniline (4-BA) was used to create a calibration curve for the number of protons in the molecule. Reference spectra of the ureas in DMSO showed the NH signal for the ureas appears at ~8.6 ppm and the CH₂ signal for both ureas 1 and 2 at ~3.85 ppm (Figure 41). Although these signals will change in different solvents, it provides an indication of the region that the signals will appear.

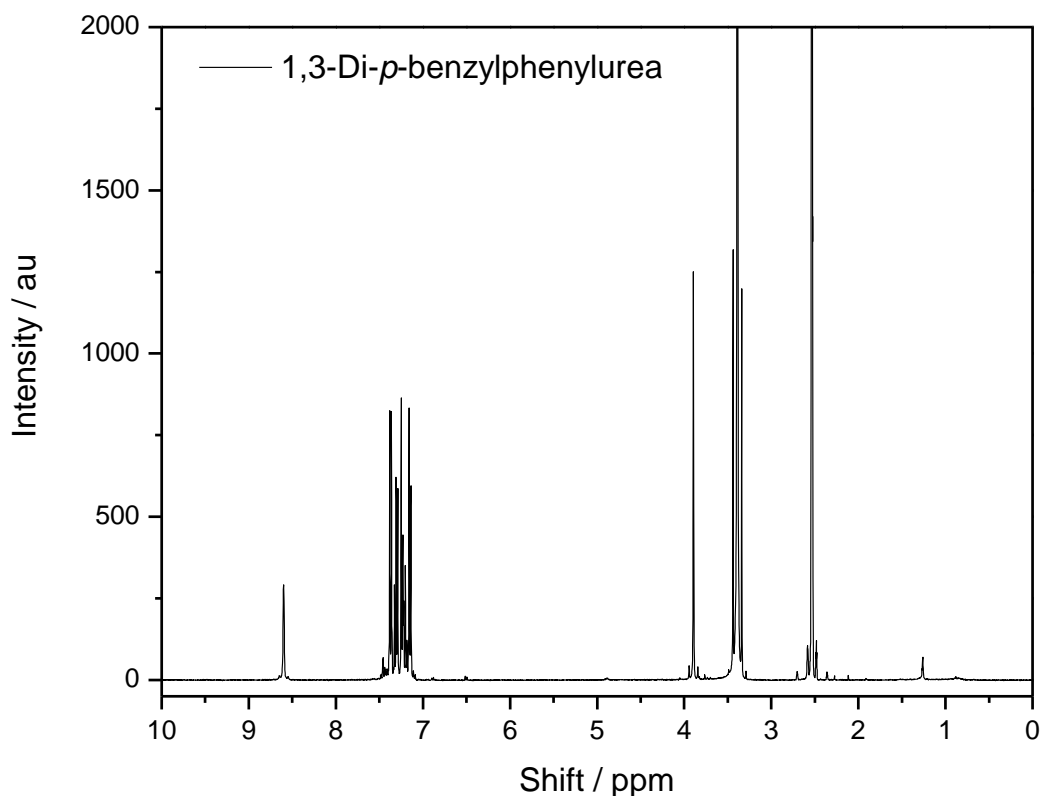


Figure 41. Reference $^1\text{H-NMR}$ spectrum of 1,3-di-*p*-benzylphenylurea in DMSO

Figure 42 presents the spectra of all three ureas in MCB before and after heating at 363 K for 1 hour along with a sample of 4-BA in MCB. The signal at ~ 4.4 ppm refers to the DCM reference in the sample. In each of the spectra there is a broad peak ~ 3.5 ppm. This is likely to be from leftover amine starting material from the synthesis of the ureas. However in the case of ureas 2 and 3 the signal increases after heating. It is possible this is due to the decomposition of urea to the amine and the isocyanate, however the CH_2 peak for the methylene bridge only occurs in the solution of urea 2 after heating. No peaks are seen in any of the spectra in the region where the NH signal of the urea should be. These results indicate that at this level of sensitivity no urea is seen in the $^1\text{H-NMR}$. However as it is possible the spectra is misleading, the concentration of the compound providing the peak at ~ 3.5 ppm was calculated. This was 9.99 mmol L^{-1} for urea 1, 13.5 mmol L^{-1} for urea 2 and 55.9 mmol L^{-1} for urea 3. These values are also consistent with the solubility calculated for 1,3-diphenyl urea by weight measurement. However if the peak is attributed to the urea compound, this would indicate the solubility as Urea 1 < Urea 2 < Urea 3. This is unexpected and contradictory to the observations noted when trying to dissolve the three ureas in various solvents, including MCB. Therefore it is more likely that this peak is due to unreacted amine from the synthesis of the ureas although the results are unfortunately

inconclusive. These values however do provide a maximum limit for the solubility of the ureas of 55.9 mmol L^{-1} , as the peak used to calculate this value was the one with the largest integral in all of the spectra. This work is not as complete as one would have liked, however the spectra recorded does confirm the low solubility of ureas in the process solvent, MCB.

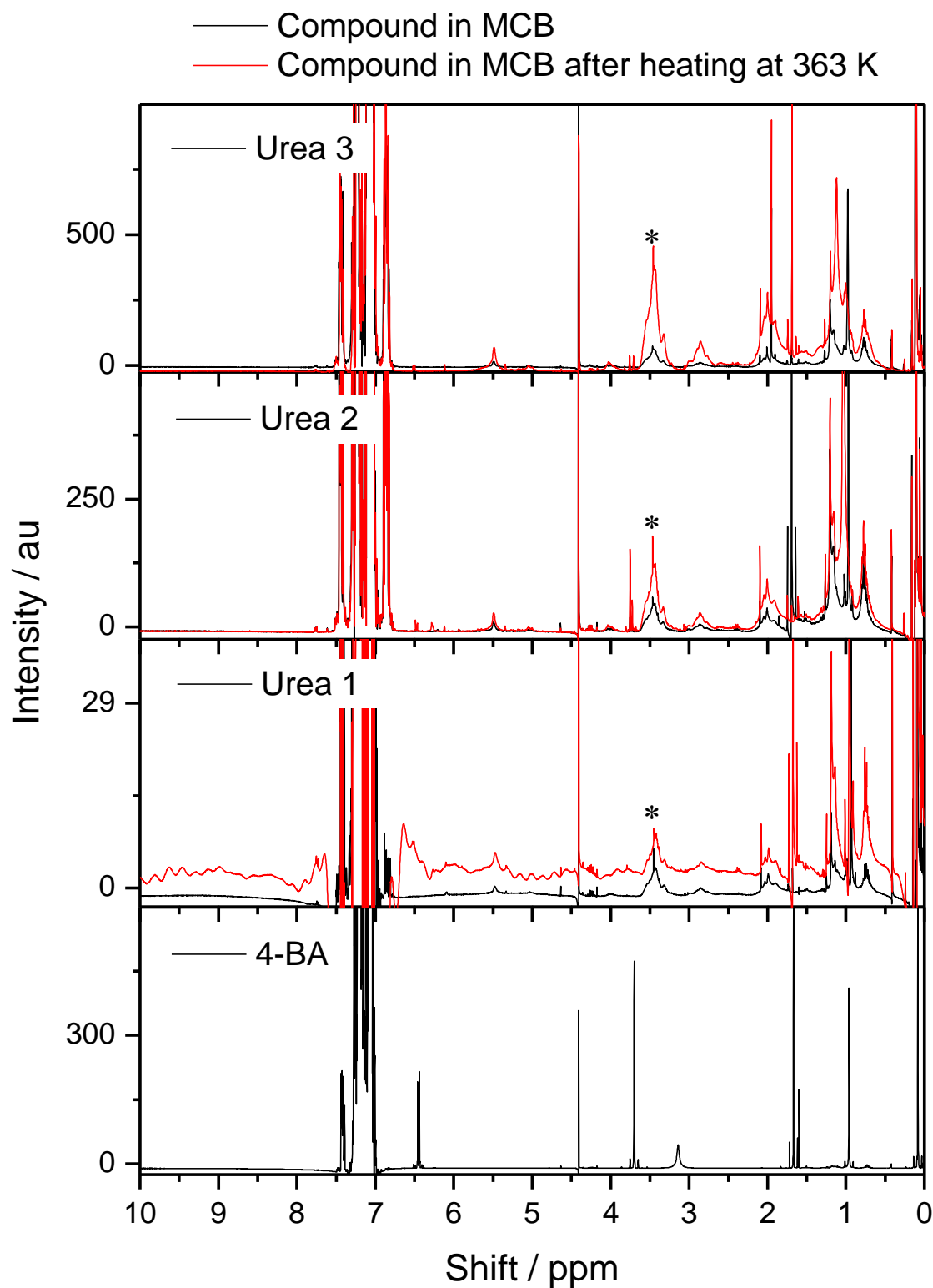


Figure 42. $^1\text{H-NMR}$ spectra of 4-BA in MCB and ureas 1, 2 and 3 in MCB before and after heating

3.3.2 Structure Determination of 1,3-Di-*p*-benzylphenylurea

Further investigation into the reaction mechanism was undertaken using crystallographic studies. 1,3-Di-*p*-benzylphenylurea was recrystallized with DMSO and single crystal X-ray diffraction carried out to gain information about the crystal structure of the molecule. The experimental details are found in section 2.6. The X-ray details and information about the crystal structure are shown in Table 13. The crystals formed are in the orthorhombic system within the polar space group Fdd2. Figure 43 shows the structure of the urea with the numbering system for the atoms. Molecules are stacked together by hydrogen bonding between the *anti* NH donors and the carbonyl O atom acceptors of the next molecule (Figure 44) and by π -stacking. The carbonyl group is parallel to the *c* axis therefore the molecular chains are formed in the *c* direction. Cleavage would consequently be parallel to the *c*-axis. This structure is similar to the crystal structure of 1,3-diphenylurea (urea 1) which had previously been reported by Deshapande⁶⁰ and Bis(4-biphenyl)urea.⁶¹ In general the structures of the disubstituted aromatic ureas already reported all show hydrogen bonding between the amide hydrogens and the oxygen on the next molecule. In di-*p*-benzylphenyl urea the phenyl rings C and A are twisted with respect to each other by 30.7°. The same is seen for the rings B and D. Rings A and B are tilted with respect to the urea plane by 79.3°. The distances and angles are presented in Table 14 and Table 15.

It was also the intention to measure the crystal structure of the oligomeric urea (urea 3), however within the time period of this project attempts to crystallise the material were unsuccessful. The powder form of the compound was used to try and gain some structural information using x-ray powder diffraction; however this technique did not offer any information on the crystal structure.

The intermolecular forces seen in 1,3-di-*p*-benzylphenylurea and the 1,3-diphenylurea studied by Deshapande⁶⁰ give a tightly packed structure. This structure coincides with the low dissolution of urea at low temperatures in the process solvent. In this investigation it was found that DMSO was the best solvent for dissolving the ureas at room temperature, even then all three ureas would only partially dissolve. The favourable solvation power of the DMSO is linked to its high dielectric constant ($\epsilon = \sim 46.5$)^{138, 139} and that it is a highly polar aprotic solvent.¹³⁸ It is also a Lewis base which will coordinate to the carbon atoms,¹⁴⁰ weakening the hydrogen bonding in the urea therefore helping to solubilise the compound. This is more difficult in the longer chain oligomeric ureas as the longer chains will increase hydrophobicity in the compound.

Identification code	1,3-Di- <i>p</i> -benzylphenylurea
Empirical formula	C ₂₇ H ₂₄ N ₂ O
Formula weight	392.49
Temperature / K	100 (2)
Crystal colour	colourless
Crystal description	needle
Crystal size / mm	0.40 x 0.10 x 0.05
Crystal system	orthorhombic
Space group	Fdd2 (No. 43)
<i>a</i> / Å	18.6632 (12)
<i>b</i> / Å	46.730 (3)
<i>c</i> / Å	4.6397 (3)
α / °	90
β / °	90
γ / °	90
<i>V</i> / Å ³	4046.4 (5)
<i>Z</i>	8
ρ (calc) / g cm ⁻³	1.289
μ / mm ⁻¹	0.079
F(000)	1664
λ / Å (Mo-K α)	0.71073
θ range / °	1.74 \leq θ \leq 23
Index ranges	-21 \leq <i>h</i> \leq 23 -58 \leq <i>k</i> \leq 56 -5 \leq <i>l</i> \leq 5
No measured	0
No unique, Rint	1229, 0.000
No observed [<i>I</i> > 2 σ (<i>I</i>)]	105
Tmax, Tmin	0.8969, 0.9914
Data / Parameters	1229 / 142
Goodness-of-fit on F ²	1.143
R1, wR2 [<i>I</i> > 2 σ (<i>I</i>)]	0.0294, 0.0641
R1, wR2 (all data)	0.0347, 0.0665
$\Delta\rho$ (max), $\Delta\rho$ (min) / e Å ⁻³	0.175, -0.178

Table 13. X-ray details of 1,3-di-*p*-benzylphenylurea

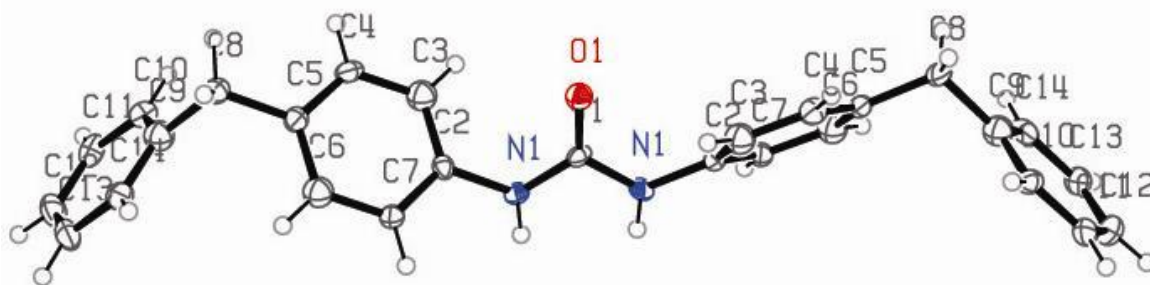


Figure 43. Molecular structure of 1,3-di-*p*-benzylphenylurea

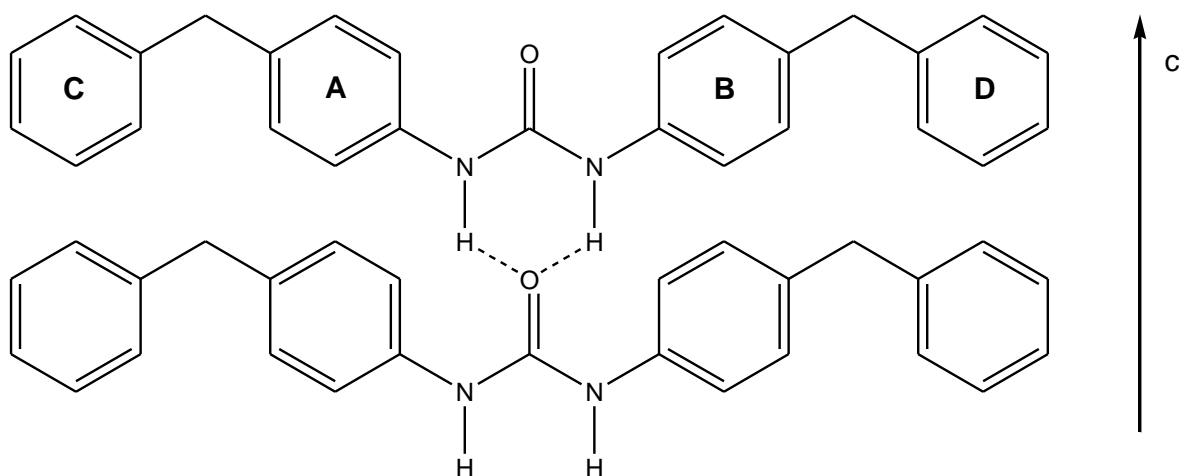


Figure 44. Hydrogen bonding in 1,3-di-*p*-benzylphenylurea

Bond	Distance / Å	Bond	Distance / Å	Bond	Distance / Å
C1–O1	1.223	C4–C5	1.396	C9–C10	1.408
C1–N1	1.352	C5–C6	1.392	C10–C11	1.385
C2–C3	1.387	C5–C8	1.521	C11–C12	1.407
C2–C7	1.400	C6–C7	1.396	C12–C13	1.398
C2–N1	1.441	C8–C9	1.530	C13–C14	1.391
C3–C4	1.393	C9–C14	1.384		

Table 14. Bond distances for 1,3-di-*p*-benzylphenylurea

Bond	Angle / °	Bond	Angle / °	Bond	Angle / °
O1-C1-N1	123.18	C6-C5-C8	121.56	C10-C9-C8	119.89
N1-C1-N1	113.64	C4-C5-C8	119.90	C11-C10-C9	121.53
C3-C2-C7	120.03	C5-C6-C7	121.62,	C10-C11-C12	118.89
C3-C2-N1	121.44	C6-C7-C2	118.94	C13-C12-C11	120.06
C7-C2-N1	118.51	C5-C8-C9	111.76	C14-C13-C12	119.84
C2-C3-C4	120.32	C14-C9-C10	118.57	C9-C14-C13	121.07
C3-C4-C5	120.60	C14-C9-C8	121.47	C1-N1-C2	123.02
C6-C5-C4	118.48				

Table 15. Bond angles for 1,3-di-*p*-benzylphenylurea

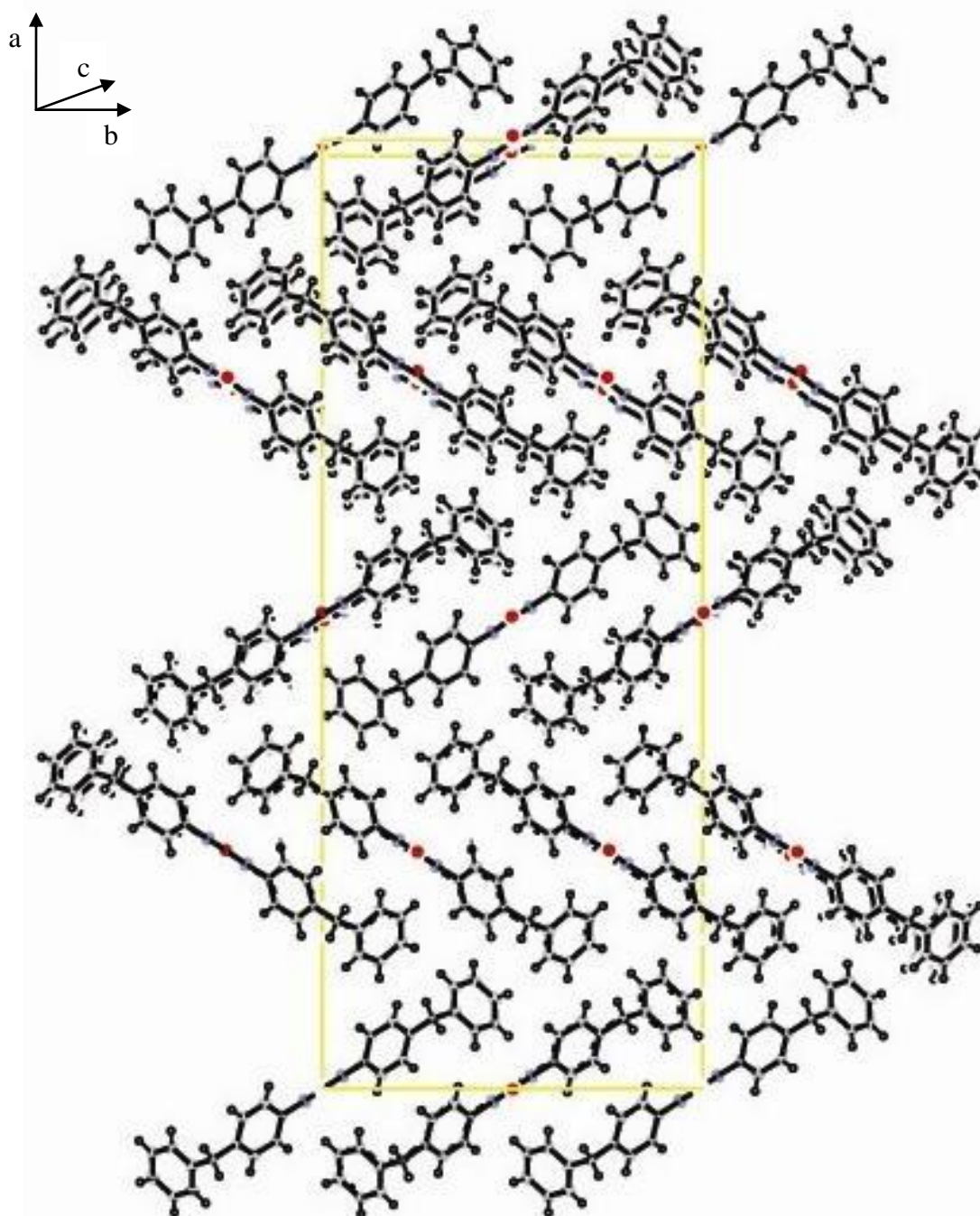


Figure 45. Unit cell of 1,3-di-*p*-benzylphenylurea

3.3.3 FTIR Study

Infrared spectra of the ureas were recorded using ATR FTIR, Figure 46 shows the spectra of 1,3-diphenylurea (Urea 1), 1,3-di-*p*-benzylphenylurea (urea 2) and oligomeric urea (urea 3). The spectra for ureas 2 and 3 were obtained after the crude material was recrystallized in DMSO. The main bands and their assignments are presented in Table 16, the bands were compared to those seen for ureas in the literature.^{121, 141-143} The stretching mode of the N-H vibration is seen at 3280 cm⁻¹ for urea 1 and at ~3305 cm⁻¹ for the two longer chain ureas. All three compounds show a band at ~1640 cm⁻¹ for the carbonyl stretching mode (C=O). This is characteristic for a bidentate urea (ordered H-bonded), with monodentate urea producing a band ~1700 – 1650 cm⁻¹ and a band at ~1715 – 1690 cm⁻¹ would be indicative of free urea.^{143, 144} This is consistent with a study by Hocker, who found that in solution the carbonyl stretching frequency of diphenyl urea can shift from 1640 cm⁻¹ to 1705 cm⁻¹.¹⁴²

Research using density functional theory (DFT) calculations was carried out on these molecules by Farrell and co-workers.¹⁴⁵ The bands seen in the experimental spectra were consistent with calculations based on the crystal structure of ureas 1 and 2, where the molecules are tightly packed via hydrogen bonding. No evidence of an O-H stretch (3600 cm⁻¹) or a C-O-H bend (1410 - 1310 cm⁻¹) representing the imidic form of the urea is seen in any of the spectra recorded for ureas 1, 2 and 3. The C=N stretch is ambiguous as it will be in the same region as the aromatic C=C bonds, making it difficult to identify.¹²¹

Wavenumber / cm ⁻¹			Assignment
Urea 1	Urea 2	Urea 3	
3327	-	-	v(N-H)
3280	3301	3306	v(N-H)
3145 – 3035	3083 – 2924	3085 – 2829	Aromatic v(C-H)
-	-	1709	v(C=O) (non H-bonded)
1645	1636	1640	v(C=O) (H-bonded)
1592	1588	1590	C-H bend (aromatic)
1548	1543	1552	NH deformation (amide II)
1497	1510	1510	v(C-C) skeletal or v(C-N)
1440	1415	1412	v(C-N)
1314	1303	1302	amide III
1230	1231	1239	amide III

Table 16. Infrared assignments of ureas 1, 2 and 3

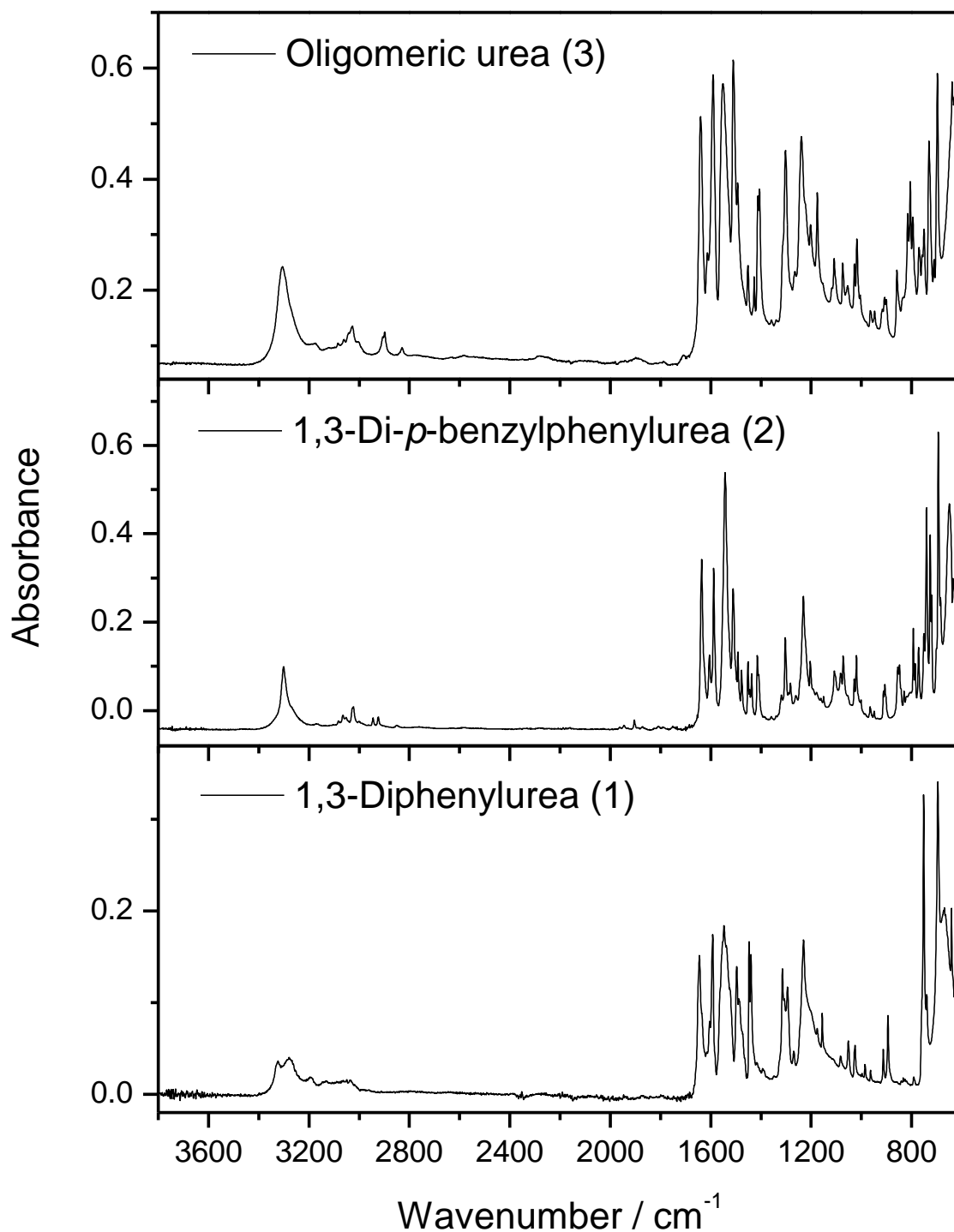


Figure 46. FTIR spectra of ureas 1, 2 and 3

In the spectrum obtained from a crude sample of urea 3 shows a small band at 1709 cm^{-1} , which is reduced after recrystallization (Figure 47). The most plausible explanation for this band is due to less ordered or ‘free’ urea. This could arise from rotation of the dihedral angle leading to an imperfection in the molecular chain (Figure 48). Hence the compound would contain a small percentage of non H-bonded urea linkages, giving rise to the band at

1709 cm^{-1} . This may help to explain the unsuccessful attempts to form crystals from the material. This is more prominent in the longer chain urea due to an increase in the number of linkages leading to an increase in the possibility of defects – conformal options that ultimately work against attainment of a crystalline structure.

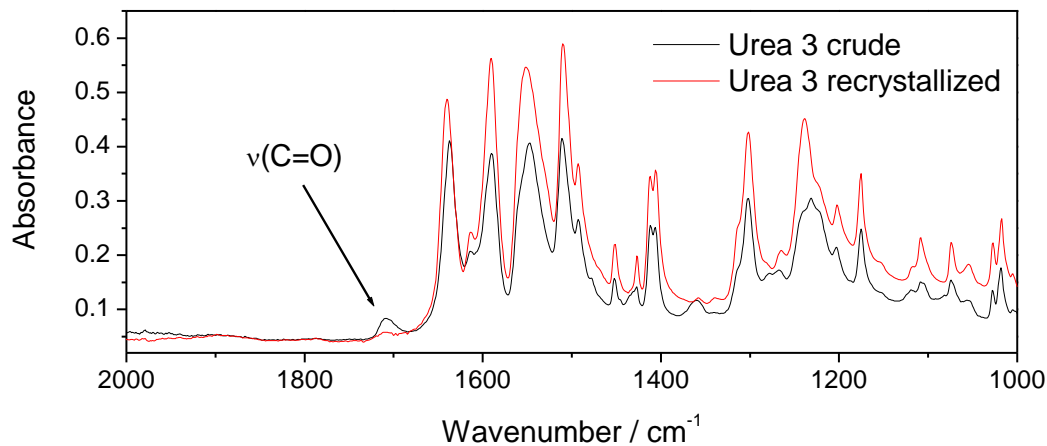


Figure 47. FTIR spectra of urea 3 before and after recrystallization

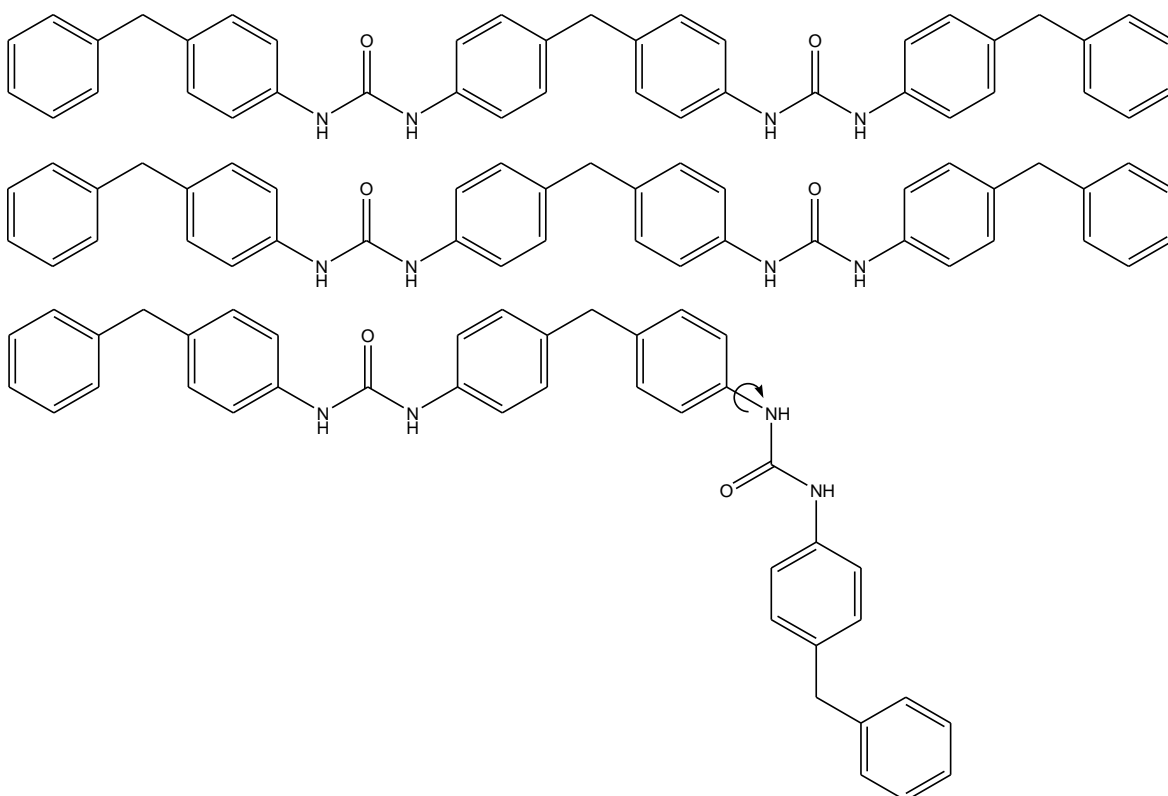


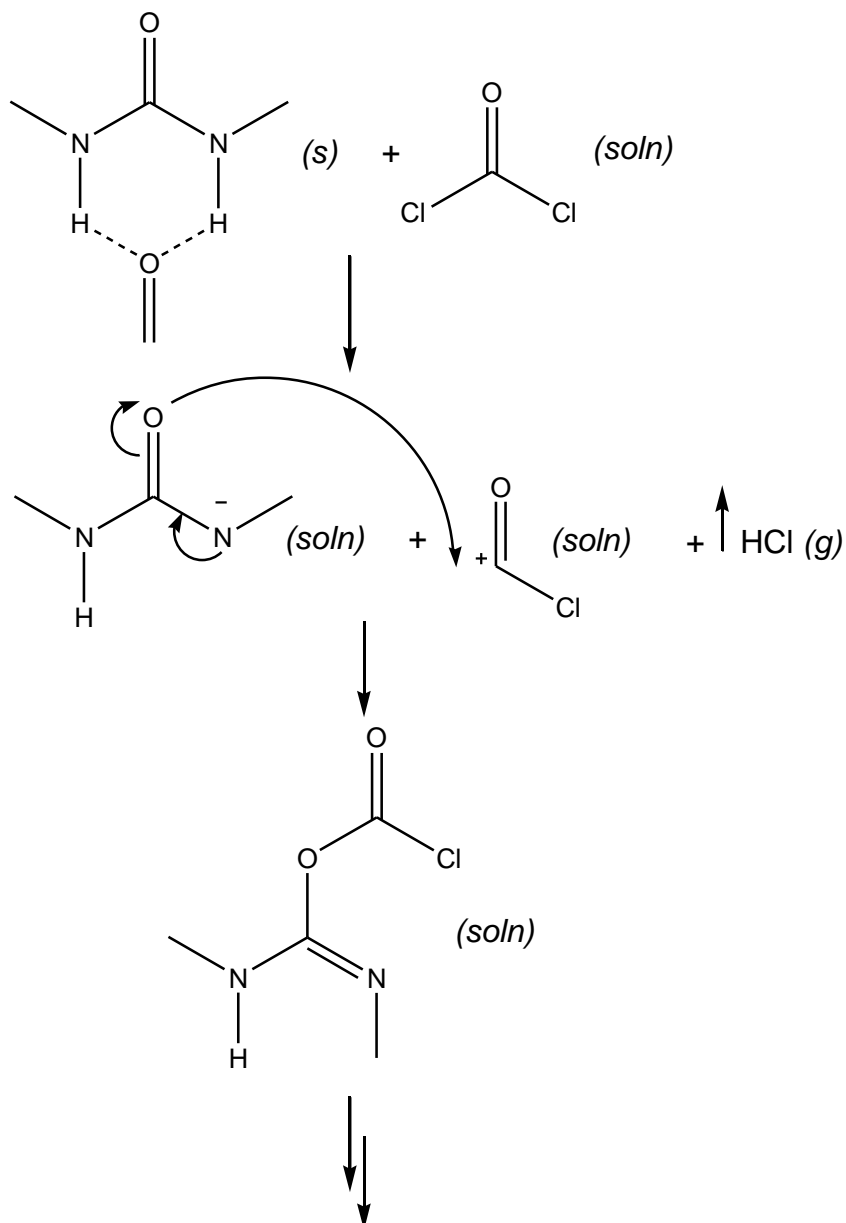
Figure 48. Structure modification of urea 3

3.4 Alternative Reaction Mechanism

From the studies carried out in this body of work, the infrared spectrum of 1,3-di-*p*-benzylphenylurea in the solid state shows no evidence for a tautomeric form. The C=O stretching vibration is seen at 1636 cm^{-1} , indicating the urea is bidentate with H-bonding in an ordered fashion.¹⁴⁴ The compound has also proved to be very insoluble in many solvents, including chlorobenzene, water, tetrahydrofuran, dichloromethane, isopropanol, butanol, ethanol and acetonitrile, only DMSO was found to dissolve the solid, poor solubility is a known issue for aromatic substituted ureas.¹⁴² Also the crystal structure determined for 1,3-di-*p*-benzylphenylurea shows a tightly packed unit cell, therefore the conversion into the imidic form will be hindered. Thus it seems unlikely the urea will undergo tautomerisation unless fully solvated. In the process solvent this may be possible at high temperatures $> 373\text{ K}$. However we have seen urea reacting with phosgene via attack on the oxygen to produce chloroformamidine-*N*-carbonyl chloride (CCC) at a temperature of 333 K . These results have therefore put the mechanism postulated by Twitchett⁵⁰ into doubt as it is difficult to understand how the urea would be soluble enough in the industrial process to form the imide.

We therefore propose an alternative mechanism to the tautomerisation which is shown in Scheme 14. Step one in this reaction would involve interaction between the solid urea and solvated phosgene with elimination of HCl. From the X-ray structure, cleavage of the crystal is likely to occur parallel to the crystal *c* axis. This will expose the N-H---O bifurcated H-bonding motifs that run through the solid along the *c* direction. These can be described reasonably as a (Brønsted) acid-base interaction in which the H of a ArN-H group is transferred partially to the keto oxygen. Addition of OCCl_2 into the system sets up a competition for H between O and Cl (of OCCl_2). The reaction is visualised as requiring two steps, since the geometries of the reactants appear to be incompatible with a four-centred transition state. Only the first (elimination of HCl) is heterogeneous; the second step and all subsequent reactions could occur in solution.

The lack of imidic form for the urea would also help to explain why the triphosgene reacts at the nitrogen rather than the oxygen. Triphosgene reacts primarily with nucleophilic reagents. Both nitrogen and oxygen based nucleophiles can react, however with compounds including an amide carbonyl group triphosgene will react with the enol form of the compound (R-C(=NR')OH).³¹ If the urea does not exist in the enol form at the temperatures investigated, it can be assumed that reaction at the nitrogen is preferred.



Scheme 14. Alternative reaction mechanism for phosgenation of urea

3.5 Summary

The work carried out in this chapter has sought to provide an understanding of the reaction between urea and phosgene relevant to the industrial synthesis of MDI. A number of reactions were carried out on both 1,3-diphenylurea and 1,3-di-*p*-benzylphenylurea using either triphosgene or an Eckert cartridge as the phosgene source. The results showed that several pathways are occurring, with triphosgene and phosgene reacting with the urea differently. The trimer prefers N-attack on the urea to produce the allophanoyl chloride

leading to the isocyanate. Phosgene however prefers O-attack leading to the CCC. Isocyanate can also be formed via decomposition of the urea or the CCC.

The crystal structure of 1,3-di-*p*-benzylphenylurea has been solved and found to contain hydrogen bonding between the oxygen of the carbonyl group and the amide hydrogens, with π -stacking between the aromatic rings. This creates a very stable structure and accounts for the low solubility of the compound. 1,3-Diphenylurea has a similar structure and has also proven to be insoluble in many solvents.⁶⁰ Thus it is unlikely the urea will react via a tautomeric form as postulated by Twitchett.⁵⁰ An alternative mechanism is therefore suggested, whereby the solvated phosgene will react with the solid urea at the oxygen position to form the CCC.

Chapter 4

Chloroformamidine-*N*-carbonyl Chloride (CCC)

4 Chloroformamidine-*N*-carbonyl Chloride (CCC)

The previous chapter outlined the reaction of a diaryl urea with phosgene proving that at temperatures above 333 K the chloroformamidine-*N*-carbonyl chloride (CCC) (VI) compound is produced. However this reaction is not a simple one, with a possible equilibrium between the CCC and the carbodiimide (VII) occurring. It was also unclear as to what the decomposition products of the CCC are. It was therefore important to investigate the CCC compound in a purer form to establish whether the molecule would break down to give the isocyanide dichloride as a product. This chapter describes the experiments carried out on 1,3-di-*p*-tolylchloroformamidine-*N*-carbonyl chloride (TCCC) (VIa).

4.1 Heat Treatments of 1,3-Di-*p*-tolylchloroformamidine-*N*-carbonyl Chloride (TCCC)

It is postulated that the chloroformamidine-*N*-carbonyl chloride (CCC) moiety will break down to form the isocyanide dichloride compound and an isocyanate in the presence of HCl at a temperature of 353 K.^{50, 102} This is suggested by an internal report,⁵¹ although a second pathway to the carbodiimide also exists. A series of heat treatments under closed conditions were performed at Huntsman Polyurethanes Process Research and Development Laboratory in Rozenburg. The reaction details are described in section 2.13. Several solutions of 1,3-di-*p*-tolylchloroformamidine-*N*-carbonyl chloride (TCCC) in chlorobenzene were heated to various temperatures and the products analysed by GC-MS and GPC. Phosgene was added to some of the solutions to recreate the reaction conditions involved at the industrial centre.

4.1.1 CCC/Carbodiimide Equilibrium

Due to limited standards being available, only two compounds were picked out in the GPC traces, these were the starting material, 1,3-di-*p*-tolylchloroformamidine-*N*-carbonyl chloride (TCCC), and 1,3-di-*p*-tolylcarbodiimide (TCD). These compounds appeared as the two major peaks in the traces, with only small peaks indicating other compounds were

present. This did, however, provide a useful tool in examining the formation of carbodiimide from the TCCC under different conditions.

4.1.1.1 Closed Reactions

Solutions of 1,3-di-*p*-tolylchloroformamidine-*N*-carbonyl chloride (TCCC) in chlorobenzene without phosgene were heated at 2 separate temperatures, 448 K and 463 K, for 3 hours. The reactions were carried out in separate closed vials, each analysed by GPC (Figure 49) after a certain length of time. Both reactions show similar results, the TCCC peak (~29.5 mins) appears in the starting solutions, decreasing after the first hour of the reaction. The peak at ~31 mins, attributed to the 1,3-di-*p*-tolylcarbodiimide (TCD), is missing at the start of the reaction but then increases to a maximum. This result shows that all of the TCCC is being converted to the carbodiimide at both temperatures. The trace at 120 mins for 463 K does show a small amount of TCCC, however it is important to note that each solution analysed had come from a separate vial, therefore there may be some discrepancies as all vials may not be under exactly the same conditions. For instance the outer vials on the heat block may be at a slightly different temperature than the inner ones, or some caps may not be sealed properly, leading to the leakage of any gases formed. The drift in the peaks seen in the reaction at 463 K is due to changes in the mobile phase of the instrument that can occur over time. The result is confirmed in the GCMS trace for the reaction at 448 K (Figure 50). The peak at 72.8 mins shows the carbodiimide, which increases with time, whereas the TCCC peak (106.4 mins) decreases.

The reaction was repeated with solutions of TCCC in chlorobenzene containing 5% phosgene. The results are shown in Figure 51, clearly indicating throughout the reaction, no TCCC is lost and no carbodiimide is formed. Similar results are seen when a solution of 1% phosgene was used instead of the 5%. After 4 hours at 448 K one solution showed the carbodiimide had been produced (Figure 52), however this was presumed to be due to phosgene leaking out of the vial, as the solution analysed after 6 hours did not show any carbodiimide. At 423 K the solution at 6 hours showed the carbodiimide had been produced. These results point towards an equilibrium between the CCC moiety and the carbodiimide. In order to look at this further a set of reactions were carried out with open vials.

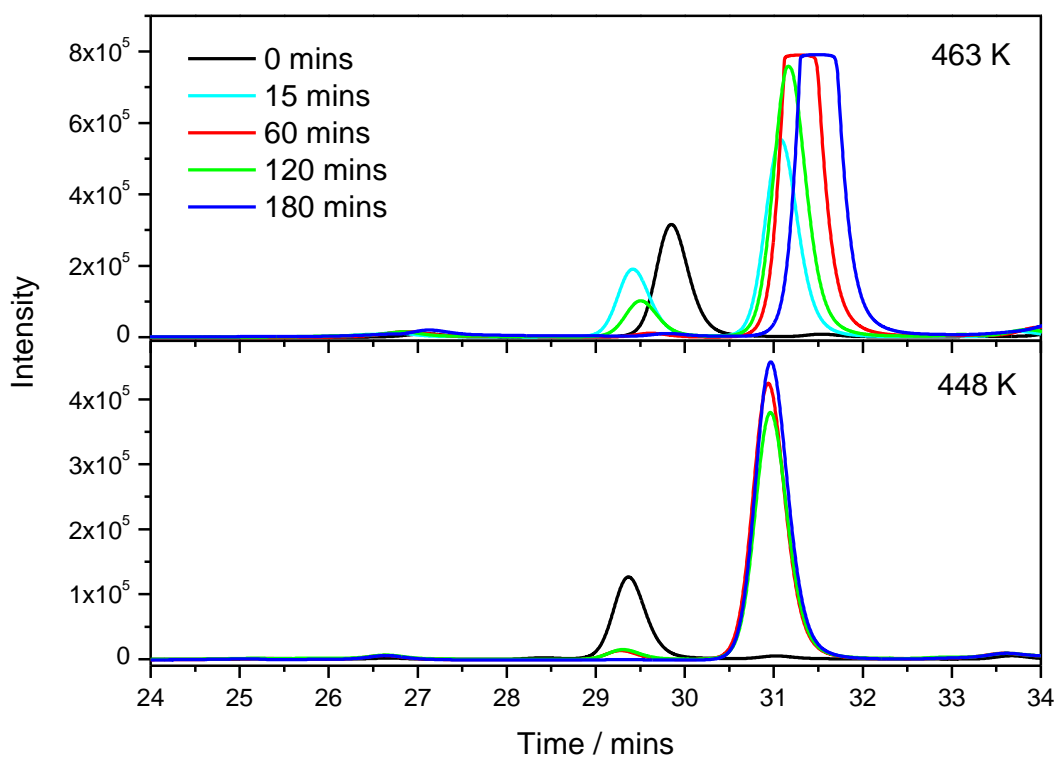


Figure 49. GPC traces of a solution of TCCC in chlorobenzene heated to 448 K and 463 K over three hours

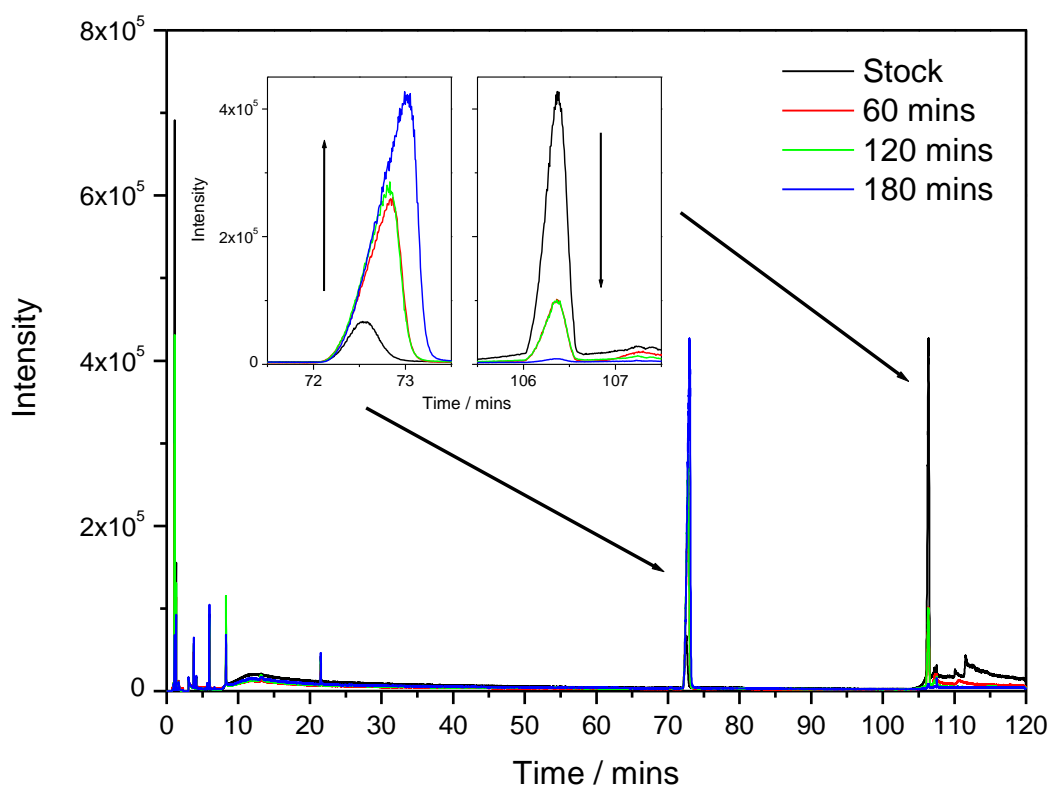


Figure 50. GC chromatogram of a solution of TCCC in chlorobenzene heated to 448 K over three hours

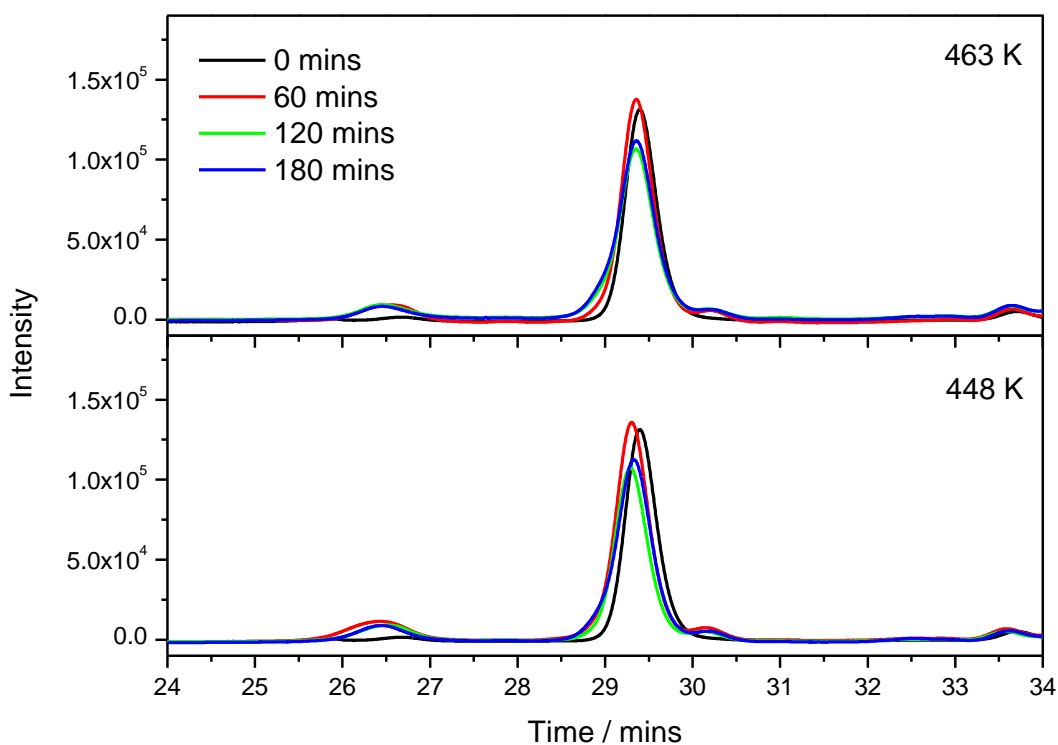


Figure 51. GPC traces of a solution of TCCC in chlorobenzene with 5% phosgene heated to 448 K and 463 K over three hours

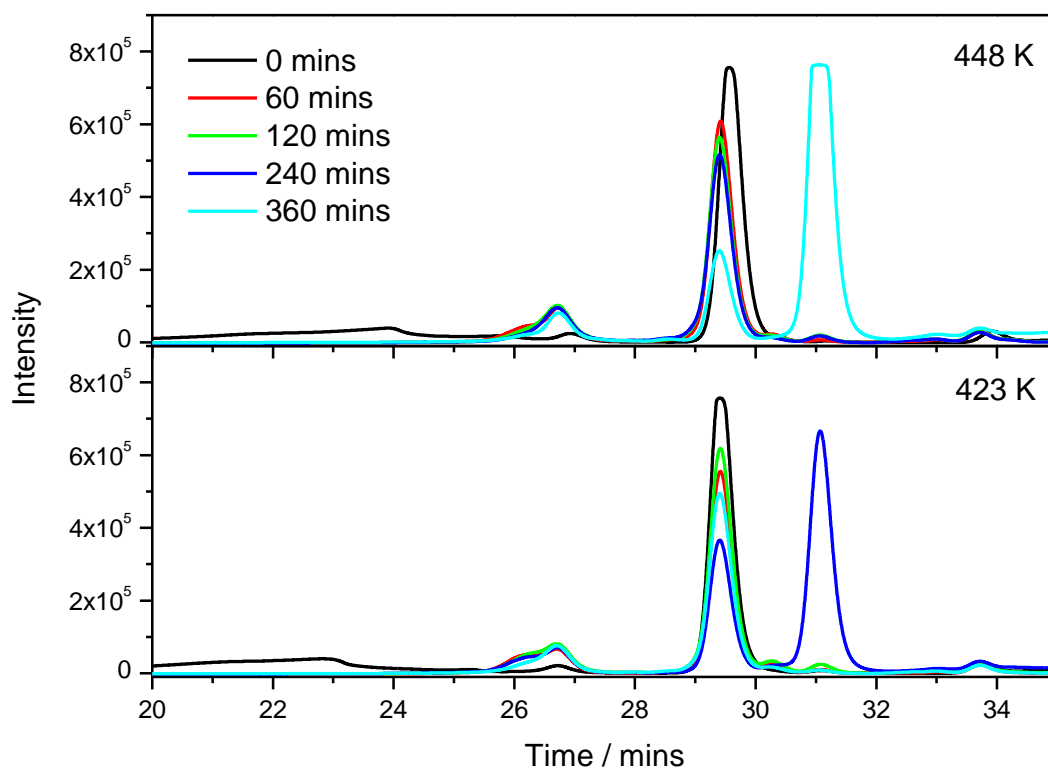


Figure 52. GPC traces of a solution of TCCC in chlorobenzene with 1% phosgene heated to 423 K and 448 K over six hours

4.1.1.2 Open Reactions

Solutions of TCCC in chlorobenzene were placed in vials at different temperatures ranging from 273 K to 373 K. These vials were left open to air for one hour to let any gases escape from the reaction, after which the solutions were analysed by GPC (Figure 53). It is clear from the results that below 313 K only a small amount of 1,3-di-*p*-tolylcarbodiimide (TCD) is produced, however above that temperature, the amount of carbodiimide produced increases significantly. However the peaks pertaining to TCCC do not show an obvious decrease, this is again likely due to the different solutions being analysed. Therefore although the peaks cannot be accurately compared between solutions, the ratio of TCD:TCCC at each temperature indicates the production of carbodiimide increases with increasing temperature. This is presented in Figure 54, which plots the ratio against temperature. The ratio was calculated by dividing the peak area of the carbodiimide by the TCCC peak area. The graph clearly shows the ratio increases with temperature.

We have seen that an excess of phosgene will force the equilibrium to produce CCC even at temperatures of 463 K (Figure 51). Therefore the position of the equilibrium will depend on temperature and the concentration of phosgene in the reaction environment.

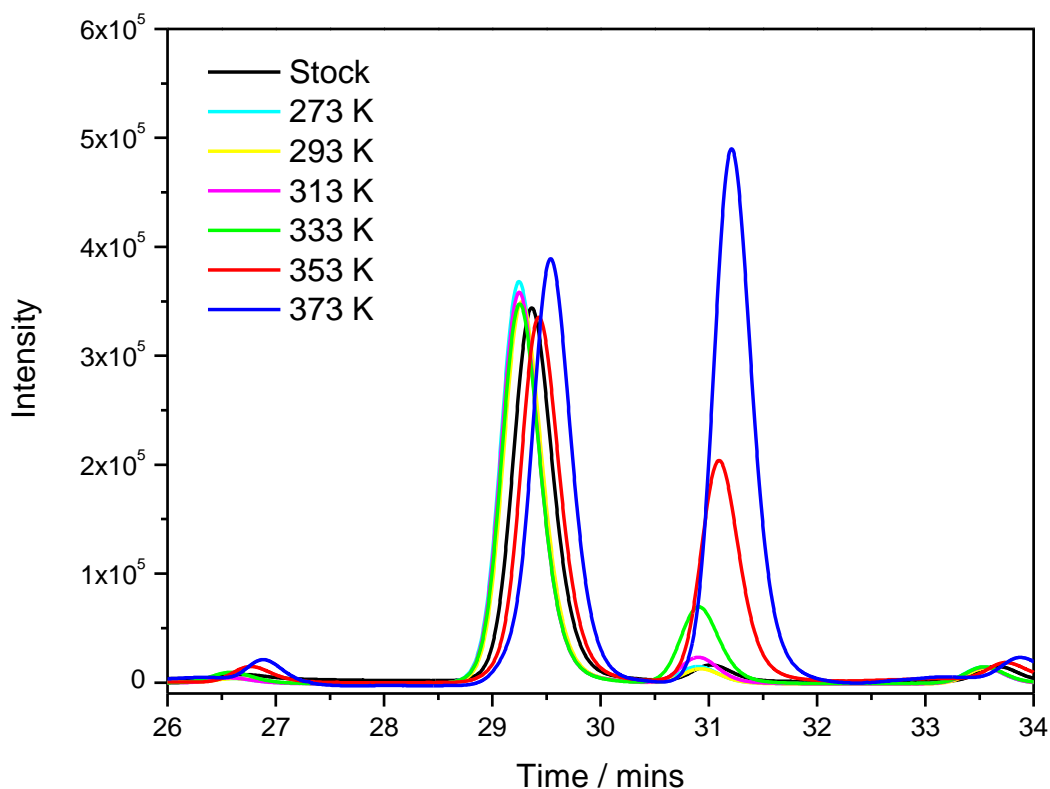


Figure 53. GPC traces of solutions of TCCC in chlorobenzene in open vials for one hour

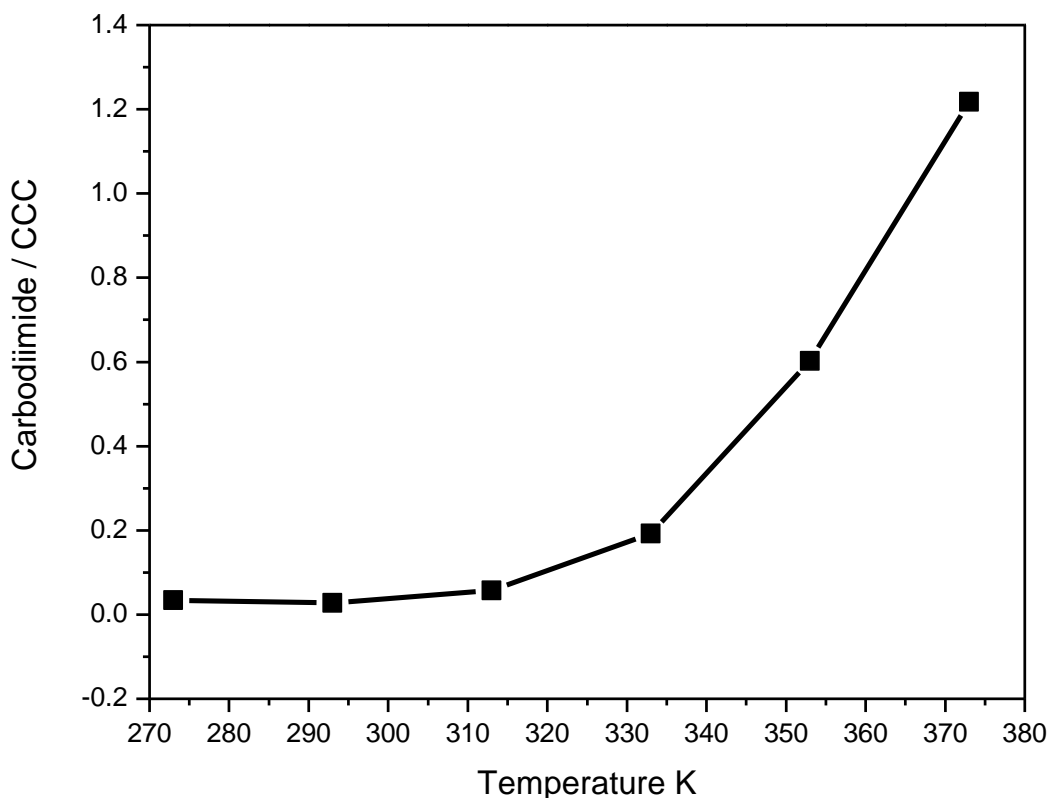
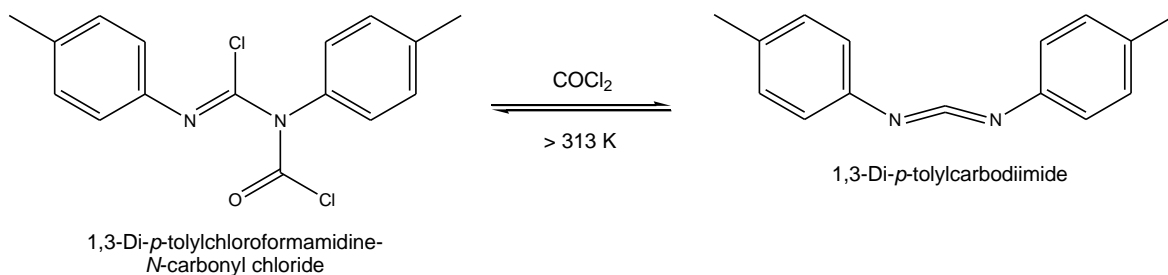


Figure 54. Ratio of carbodiimide/CCC peak area with respect to temperature

4.1.1.3 Equilibrium Involving Chloroformamide-*N*-carbonyl Chloride

The reactions discussed so far have therefore shown that an equilibrium exists between the chloroformamide-*N*-carbonyl chloride (CCC) and the carbodiimide compounds (Scheme 15). This reaction will have an effect on the phosgenation of urea as if the CCC is produced under an atmosphere with no excess phosgene, above 313 K the carbodiimide will be formed. However if an atmosphere of phosgene is used, the formation of the carbodiimide will be impeded and the CCC will be the major product produced.



Scheme 15. Postulated equilibrium between 1,3-di-*p*-tolylchloroformamide-*N*-carbonyl chloride and 1,3-di-*p*-tolylcarbodiimide

4.1.2 Isocyanide Dichloride as a Decomposition Product

GC-MS analysis was a useful tool in determining the trace compounds in the reaction mixtures. It could therefore be used to determine whether or not any isocyanide dichloride compounds had been produced. A solution of *p*-tolyl isocyanide dichloride (TID) in chlorobenzene (MCB) was used as a standard. The GC-MS plot (Figure 55) shows a peak at 20.4 minutes with a mass of 187 corresponding to TID. Smaller peaks are seen at 21.4 minutes and 30.2 minutes, these are due to *p*-tolyl isothiocyanate and 4-chloromethylphenyl isocyanide dichloride respectively. The presence of these species is described in section 2.11.

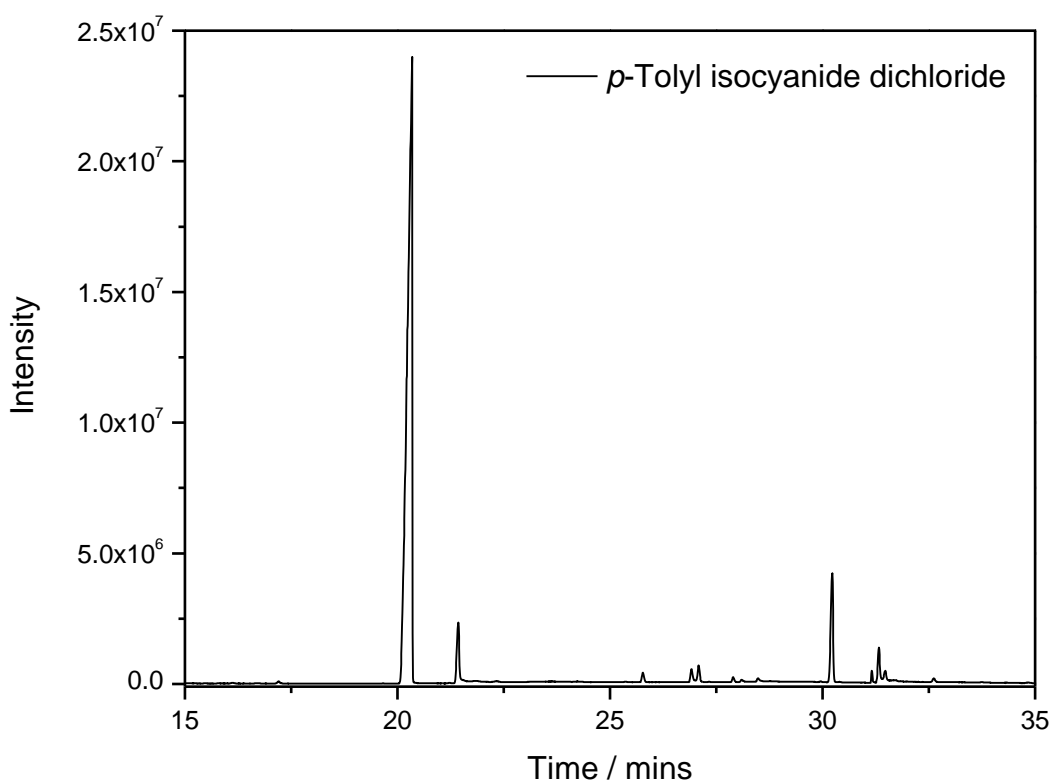


Figure 55. GC chromatograph of *p*-tolyl isocyanide dichloride (TID) in chlorobenzene

All of the closed heat treatments described in section 2.13.1.1 were analysed by GCMS, looking at a range of temperatures, concentration of TCCC and concentration of phosgene. Table 17 shows the reaction details taken from the experimental section along with information about the main products produced. In order to show a rough distribution of the three compounds relevant to this work, the height of the peaks attributed to 1,3-di-*p*-tolylchloroformamidine-*N*-carbonyl chloride (TCCC), 1,3-di-*p*-tolylcarbodiimide (TCD) and *p*-tolyl isocyanide dichloride (TID) were measured and the percentage of each

compound calculated relative to each other. As this did not take into account any side products this did not give an accurate measure of the amount of each product however was deemed a satisfactory method in order to discuss the breakdown of TCCC into TID.

Reaction	TCCC Concentration / mmol L ⁻¹	Phosgene Concentration / %	Temperature / K	Product distribution after 120 mins / %		
				TCCC	TCD	TID
1	6	0	403	66.0	34.0	0.0
2	20	0	403	61.3	37.7	0.9
3	6	0	448	26.3	73.7	0.0
4	<13	0	463	0.0	100.0	0.0
5	6	0	463	2.0	98.0	0.0
6	20	0	463	29.3	70.7	0.0
7	36	1	403	95.2	4.2	0.6
8	36	1	423	95.9	3.5	0.7
9	36	1	448	96.2	3.2	0.6
10	36	1	463	90.6	8.2	1.1
11	6	5	448	98.2	1.6	0.2
12	6	5	463	96.9	2.6	0.5

Table 17. Details of heat treatment reactions of TCCC

No evidence for TID is seen in any of the starting solutions and in all cases where TID is evident; it appears after the first time period. In all of the solutions containing phosgene, a very small amount of carbodiimide is seen compared to the TCCC. The solutions without phosgene show a large amount of carbodiimide, backing up the results from the GPC analysis that in an atmosphere of phosgene the TCCC will be favoured.

For the reactions without phosgene, only one solution of TCCC showed evidence for the TID. This was at the highest concentration of TCCC without phosgene (20 mmol L⁻¹) and at the lowest temperature considered (403 K). In the GC-MS traces for this reaction, a high amount of TCCC was still present in the solutions, whereas the other reactions carried out at higher temperatures in MCB without phosgene showed that although TCCC still existed; the majority of the concentration had been converted into the carbodiimide.

When 5% phosgene solutions were used, a small amount of TID was seen at a TCCC concentration of 6 mmol L⁻¹ for both 448 K and 463 K. For these reactions very little carbodiimide is present. The solutions with 1% phosgene all showed peaks for the isocyanide dichloride, these solutions all had a higher concentration of TCCC of 36 mmol

L^{-1} and were heated to a range of temperatures from 403 to 463 K. Figure 56 shows the GCMS trace of reaction 9 (Table 17), where a 36 mmol L^{-1} solution of TCCC in 1% phosgene/MCB was heated to 448 K for 6 hours. The peaks at 73.3 mins and 106.4 mins correspond to 1,3-di-*p*-tolylcarbodiimide (TCD) and TCCC respectively. A peak relating to the TID can be seen at 20.3 mins, this generally increases as the reaction proceeds and is not in the starting material. A peak is also formed at 21.6 mins showing a mass of 131.9 g mol^{-1} . This is identified as *p*-tolyl isocyanate and shows similar amounts are produced compared to TID. From the GPC results from the same solutions (Figure 52) we see that at 360 minutes the TCCC is converted to the carbodiimide, this can also be seen in the GCMS. Therefore the decrease in the TID peak in that time is due to less TCCC in the solution. The mass spectrum for this peak is identical to that seen in the standard solution of TID, as explained in section 2.11.3. Figure 57 shows the GCMS traces of the four solutions of TCCC in 1% phosgene/chlorobenzene after 2 hours at different temperatures (reactions 7-10). The results show that the amount of TCCC and carbodiimide in the solutions are comparable and that for the TID peak the only considerable difference is at the highest temperature of 463 K, where the peak is larger.

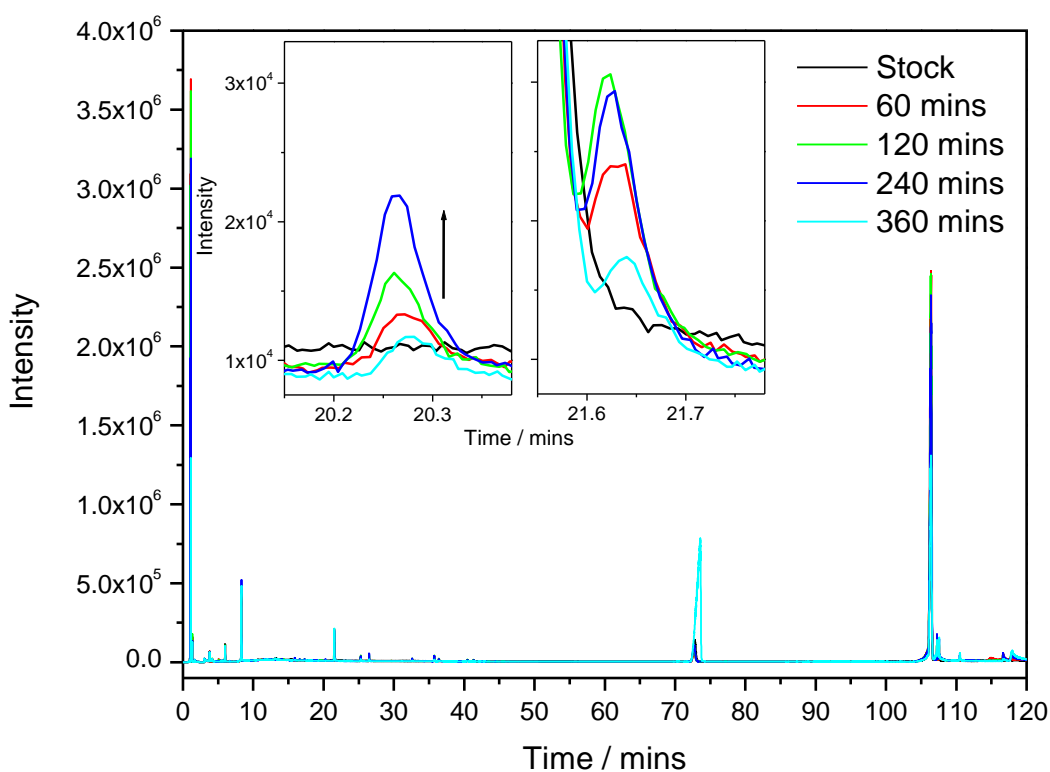


Figure 56. GC chromatograph of reaction 9, TCCC in chlorobenzene with 1 % phosgene at 448 K

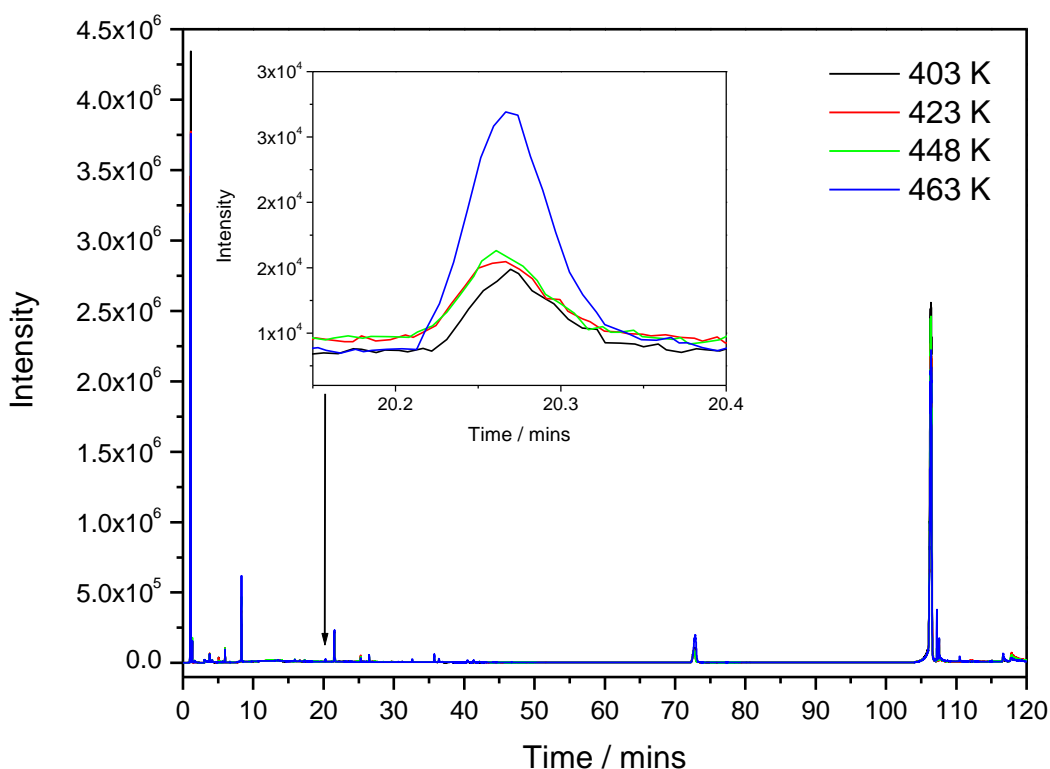


Figure 57. GC chromatograph of TCCC in chlorobenzene with 1 % phosgene after 2 hours at various temperatures

4.1.3 Heat Treatment of Isothiocyanate

In all the GCMS traces a peak at 21.5 mins can be seen for the *p*-tolyl isothiocyanate. This is found to be a trace product in the 1,3-di-*p*-tolylcarbodiimide bought as a starting material for the 1,3-di-*p*-tolylchloroformamidine-*N*-carbonyl chloride (TCCC). GCMS analysis of a solution of 1,3-di-*p*-tolylcarbodiimide in chlorobenzene confirmed this. As an isocyanide dichloride can be produced from reaction of the isothiocyanate with Cl₂, it was important to rule out if it could be produced from isothiocyanate and phosgene. Therefore heat treatments were carried out on *p*-tolyl isothiocyanate (TITC). Reactions 3 and 9 from Table 17 were repeated with TITC in chlorobenzene as the starting material, the results are shown in Figure 58. Both reactions show similar results. The large peak at 21.7 mins corresponds to the starting material. A small peak appears at 20.3 mins, where the TID would be expected, however the mass spectra of this compound was 148.8 g mol⁻¹ and is identified as an isomer of the starting material. The other small peaks between 19 mins and 21 mins are also confirmed to be isomers of TITC. This result confirms that the isocyanide dichloride seen in the heat treatments of TCCC is most likely a breakdown product of the TCCC.

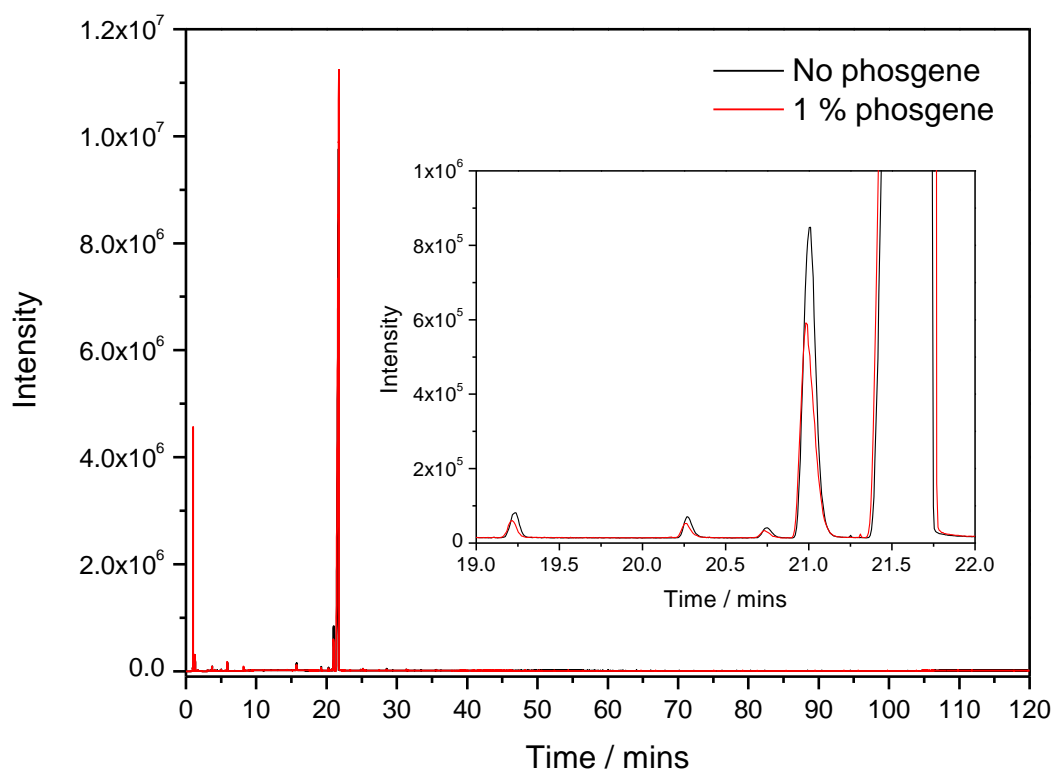
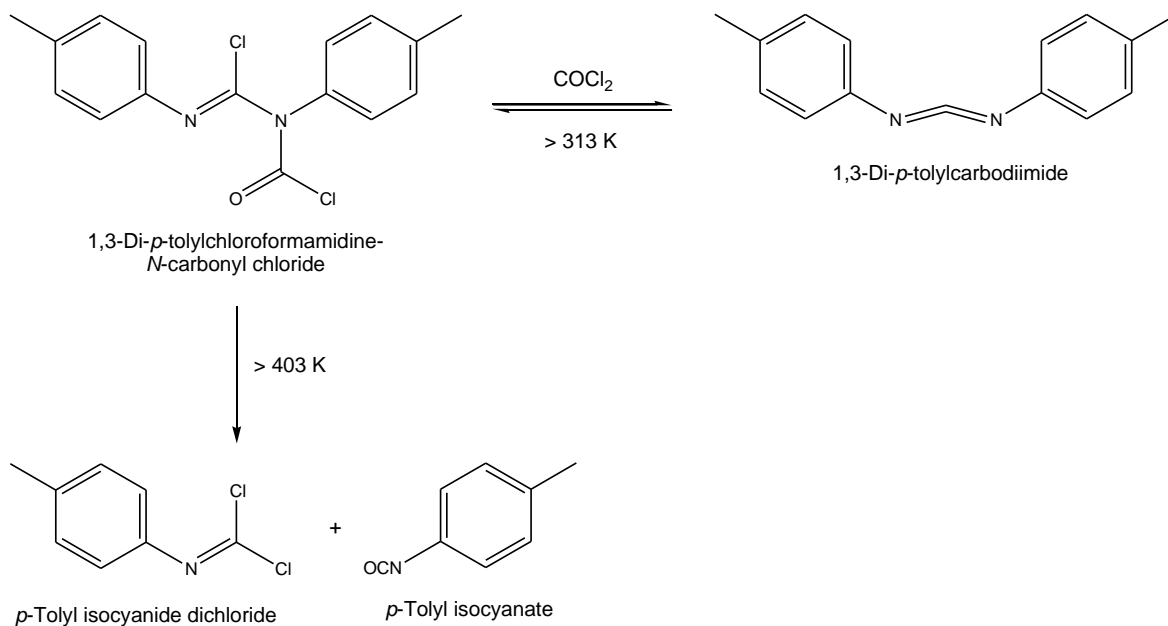


Figure 58. GC chromatograph of *p*-tolyl isothiocyanate in chlorobenzene after heating to 448 K

4.2 Summary

From the reactions discussed above, it can be concluded that 1,3-di-*p*-tolylchloroformamidine-*N*-carbonyl chloride (TCCC) can be broken down to *p*-tolyl isocyanide dichloride (TID) and isocyanate using temperatures above 403 K, with more TID being produced at higher concentrations of TCCC or at a higher temperature of 463 K (Scheme 16). This result correlates what is suggested in the literature⁵⁰. An atmosphere of phosgene is required to stop the TCCC decomposing to the carbodiimide, 1,3-di-*p*-tolylcarbodiimide (TCD). It is postulated from the results seen in section 4.1.1 that an equilibrium exists between TCCC and TCD. This result confirms that if a carbodiimide-*N*-carbonyl chloride compound is produced in the industrial process, it will break down to form an isocyanide dichloride at temperatures above 403 K and with excess phosgene.



Scheme 16. Postulated reaction of 1,3-di-*p*-tolylchloroformamidine-*N*-carbonyl chloride

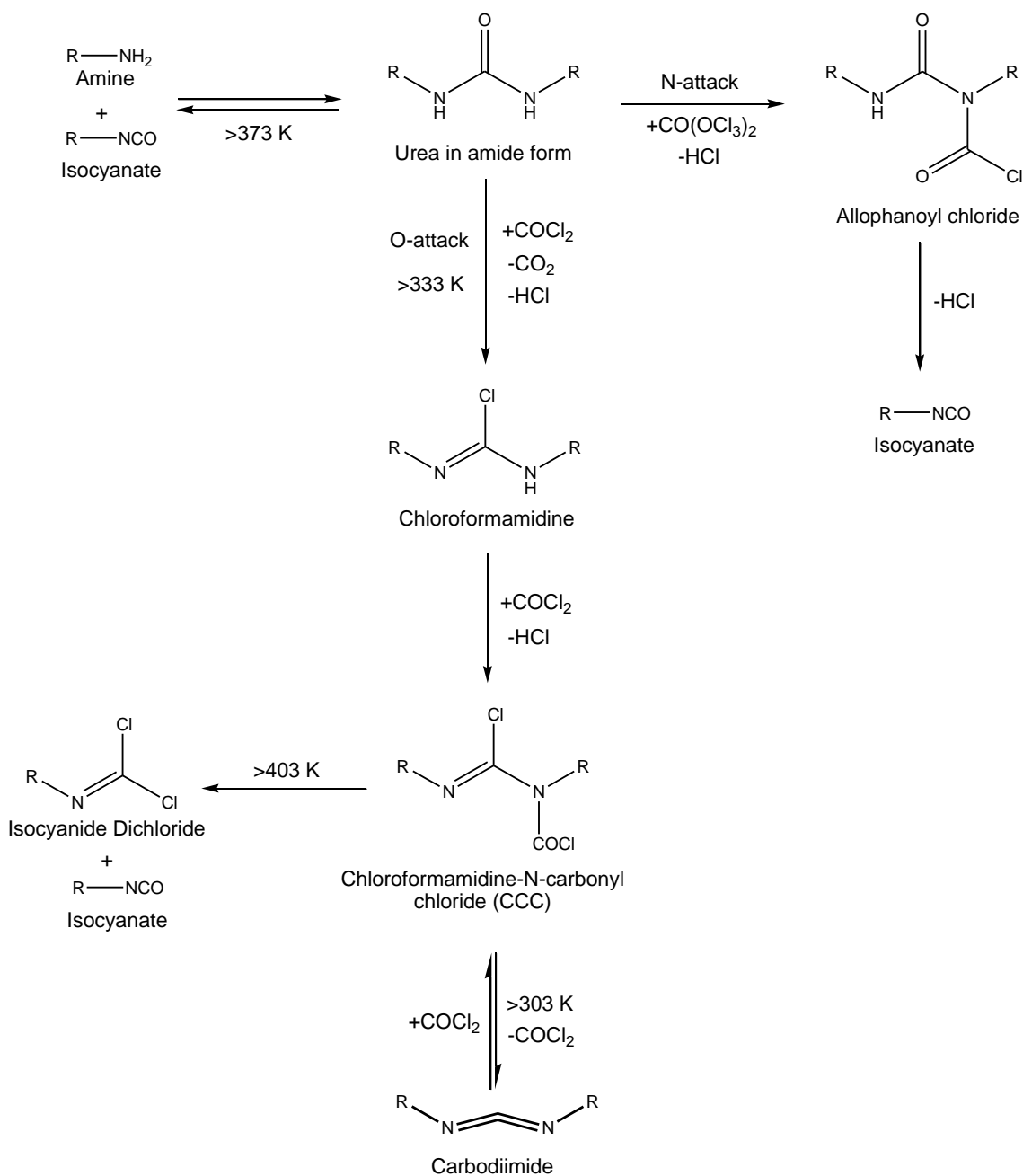
4.3 Modified Reaction Scheme

The work carried out in this project so far has been successful in confirming the postulate that an isocyanide dichloride can be formed in the industrial process to produce MDI.⁵⁰ Scheme 17 shows the reaction scheme proposed from the experiments carried out on model compounds relevant to the more complex materials used at the industrial centre. It was found that the urea compounds produced by reaction between an amine and an isocyanate, a side reaction in the industrial procedure, can be phosgenated to produce a chloroformamidine-*N*-carbonyl chloride (CCC). This reaction occurs at temperatures above 333 K however a separate pathway can occur which forms an allophanoyl chloride, which then decomposes to an isocyanate. Both pathways can occur as the carbonyl of the phosgene can react with either the nitrogen or the oxygen on the urea. It is suggested that the urea doesn't react via tautomerism as proposed⁵⁰ but that solvated phosgene will react with the solid urea compound. This is indicated by the low solubility of urea compounds in a number of solvents.

The chloroformamidine-*N*-carbonyl chloride (CCC) will break down on heating above 403 K to an isocyanide dichloride and an isocyanate. This process however is hindered by equilibrium between the CCC and the carbodiimide compound. The carbodiimide is favoured at temperatures above 303 K where no atmosphere of phosgene is present. Since

there is a large presence of phosgene in the industrial synthesis, the reaction conditions would therefore lead to the formation of the isocyanide dichloride.

The next stage was to discover if this molecule had a role to play in the formation of colour in the MDI product stream. A postulated reaction mechanism involves the release of chlorine radicals which can attack the methylene bridge in MDI.⁴⁵ The subsequent two chapters describe firstly how electron paramagnetic resonance (EPR) spectroscopy was used to measure the capability of the isocyanide dichloride as a source of chlorine radicals and, secondly, how UV/Vis spectroscopy could be utilised to investigate the extent at which colour was formed under different reaction conditions.



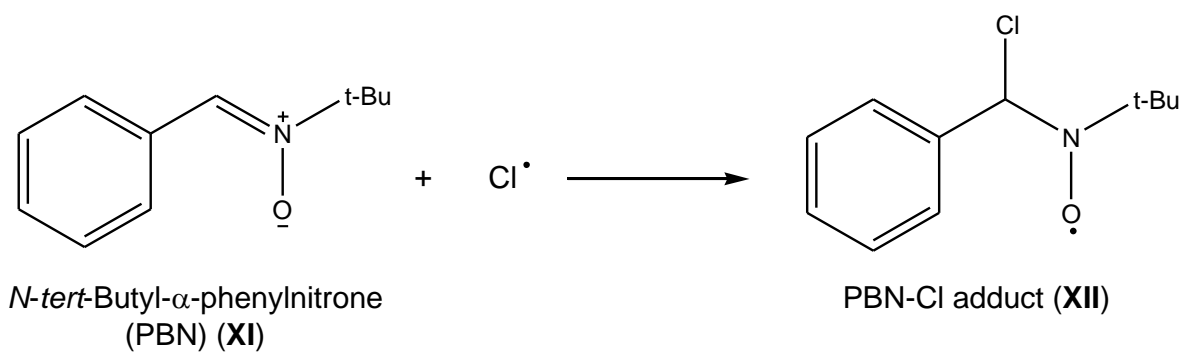
Scheme 17. Modified reaction scheme

Chapter 5

Electron Paramagnetic Resonance (EPR) Study of Isocyanide Dichlorides

5 Electron Paramagnetic Resonance (EPR) Study of Isocyanide Dichlorides

Electron paramagnetic resonance (EPR) studies were carried out on both phenyl isocyanide dichloride (PID) and *p*-tolyl isocyanide dichloride (TID) to discover if chlorine radicals would be produced by irradiation of the compounds. The spin trap *N*-*tert*-butyl- α -phenyl nitron (PBN) (XI) was used in this work in order to trap any chlorine radicals released so they could be recorded by the spectrometer. As discussed in section 1.9.1, chlorine radicals are short-lived and a spin trap is needed in order to record them. Scheme 18 shows the PBN-Cl[•] adduct (XII) that is produced when a chlorine radical is trapped by PBN.



Scheme 18. Addition of chlorine radical to the spin trap, PBN

The spectra produced by the chlorine adduct contains 8 lines with a 1:1:2:2:2:2:1:1 pattern. This stems from three overlapping quartets (Figure 59) as the nitrogen signal will be split into 3 lines as a 1:1:1 triplet due to the hyperfine coupling ($I = 1$). The nitrogen will be coupled to the chlorine, splitting each line into four ($I = 3/2$). Shoulders observed on most of the peaks originate from the chlorine isotope ³⁷Cl. These lines would further split due to the hydrogen but these peaks are weak and not easily discernable. The experimental details of the reactions discussed below are outlined in section 2.15.

It was originally intended to measure the EPR spectrum of the thermal and photo degradation of the isocyanide dichloride compound in the presence of the spin trap. A preliminary thermolysis reaction was carried out on a solution of TID + PBN in *o*-dichlorobenzene in which the solution was heated to 443 K. On following the reaction no signal was recorded by the spectrometer. On further research of the spin trap there are issues regarding its stability on heating. Janzen *et al.* recorded the chlorine adduct of PBN

at temperatures up to 363 K.¹⁴⁶ However Symons *et al.* found it to be thermally unstable over ~270 K.¹⁴⁷ Therefore the photolysis method was forcefully adopted in order to measure the release of chlorine radicals from isocyanide dichlorides.

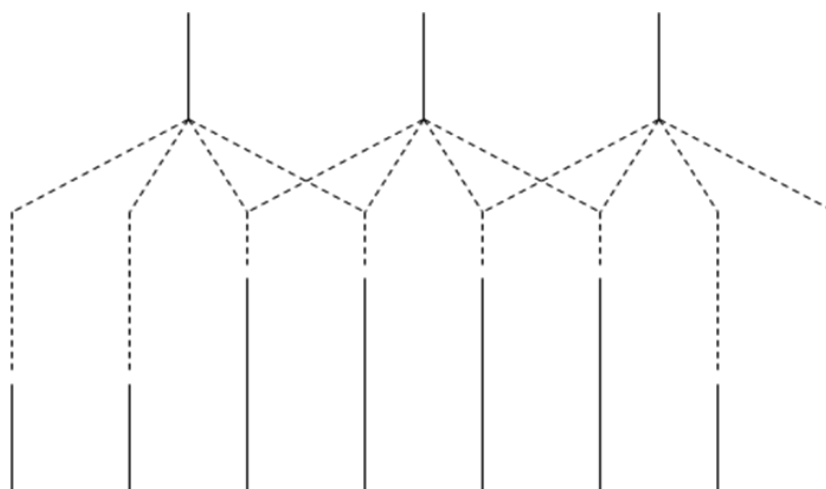


Figure 59. PBN-Cl adduct splitting diagram

5.1 Blank Reactions

It was important first to determine if the isocyanide dichloride compounds or the spin trap, PBN, would form radicals alone in solution. In order to test this a series of blank reactions were run. Solutions of either phenyl isocyanide dichloride (PID), *p*-tolyl isocyanide dichloride (TID) or *N*-*tert*-butyl- α -phenyl nitron (PBN) in benzene were irradiated at $\lambda \geq 310$ nm separately to determine if radicals could be produced. Figure 60 shows the EPR spectra of a solution of PID in benzene which was irradiated constantly for 47 minutes. The spectrum shown was the last one to be recorded and shows no EPR-active radicals are present in the absence of the spin trap. It is still possible radicals are being formed, although are too short-lived to be recorded directly. A solution of TID in benzene also produced the same result. However, when a solution of the spin trap, PBN, in benzene was irradiated constantly, the spectra showed a radical was present (Figure 61). The spectrum shown was recorded after 47 minutes and shows three equal lines with splitting to three smaller lines. This is consistent with a nitrogen radical coupling to a hydrogen atom with the hyperfine constants: $a_N = 14.31$ G, $a_H = 1.96$ G. This radical species was not present when the sample was recorded in the dark and increased as irradiation continued. When the irradiation was stopped, scanning of spectra was continued for a further 47 minutes. In this time no decrease in the signal was noticed. This indicates this radical is a predominately

stable species. The hyperfine couplings indicate this radical to be the hydroxyl adduct of PBN, hydroxybenzyl-*N-tert* butyl nitroxide (XIII) (Figure 62)¹⁴⁸, likely arising from trace water in the solution. Table 18 gives the hyperfine values seen in the literature. The formation of this radical is in small amounts and can be described as negligible; therefore it will not interfere with further experiments (this is explained further in section 5.4).

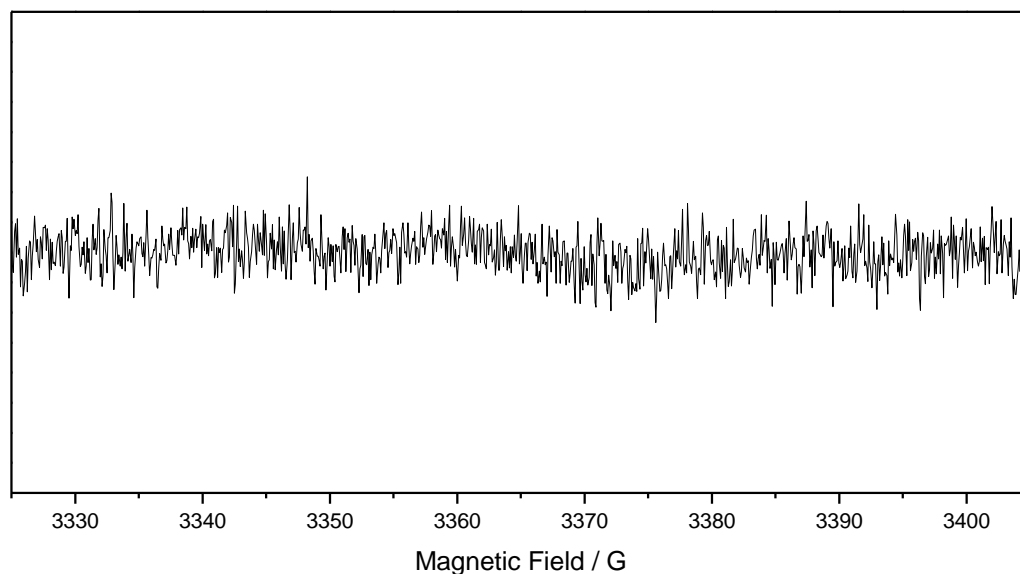


Figure 60. EPR spectrum of phenyl isocyanide dichloride (PID) in benzene after 47 minutes of constant irradiation

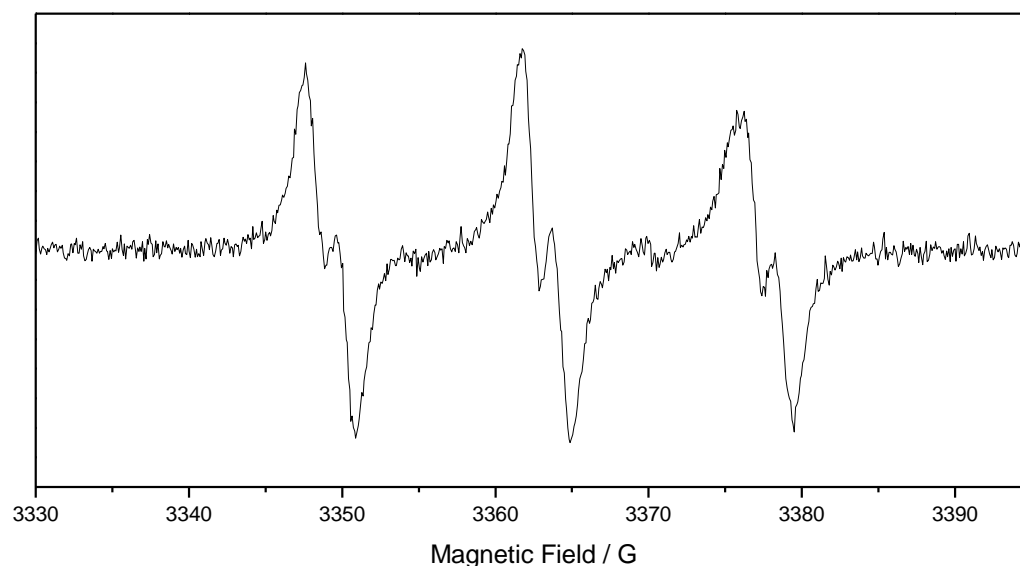


Figure 61. EPR spectrum of *N-tert*-butyl- α -phenylnitron (PBN) in benzene after 47 minutes of constant irradiation

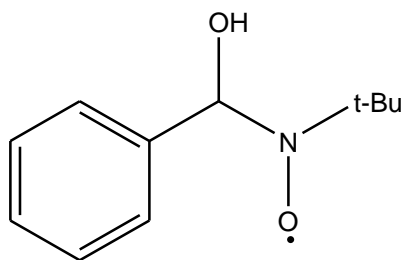


Figure 62. Hydroxybenzyl-*N*-*tert* butyl nitroxide (XIII)

Solvent	<i>a</i> / G		Reference
	¹⁴ N	¹ H	
C ₆ H ₆	14.31	1.96	Present work
H ₂ O	15.46	2.72	⁸⁰
H ₂ O	13.40	2.00	⁷⁹
CCl ₃ F	14.00	2.80	¹⁴⁸

Table 18. Hyperfine coupling constants for hydroxybenzyl-*N*-*tert* butyl nitroxide radical observed together with literature values

5.2 Identification of the EPR Active Species

The next step was to ascertain the spin trap could be used to observe any radicals that were being formed from the isocyanide dichlorides. For this PBN was added to solutions of PID or TID in benzene. Samples were then irradiated for either 30 seconds before scanning commenced or constantly while scanning was in progress. This allowed the monitoring of the formation of the PBN-Cl adduct. Figure 63 shows the spectra recorded when a solution of PID + PBN underwent constant irradiation. The first scan was recorded immediately after irradiation was started and shows an 8 line pattern consistent with the chlorine adduct of PBN. After 25 minutes the spectra is more defined and the coupling to the ³⁵Cl and ¹H are distinguishable. After 50 minutes the spectra shows little change. The hyperfine splitting constants for the chlorine adduct for PID + PBN in benzene are $a_N = 12.32$ G, $a_{Cl-35} = 6.25$ G, $a_{Cl-37} = 5.20$ G and $a_H = 0.80$ G, which is consistent with previous studies (Table 19).^{79, 80, 146, 149}

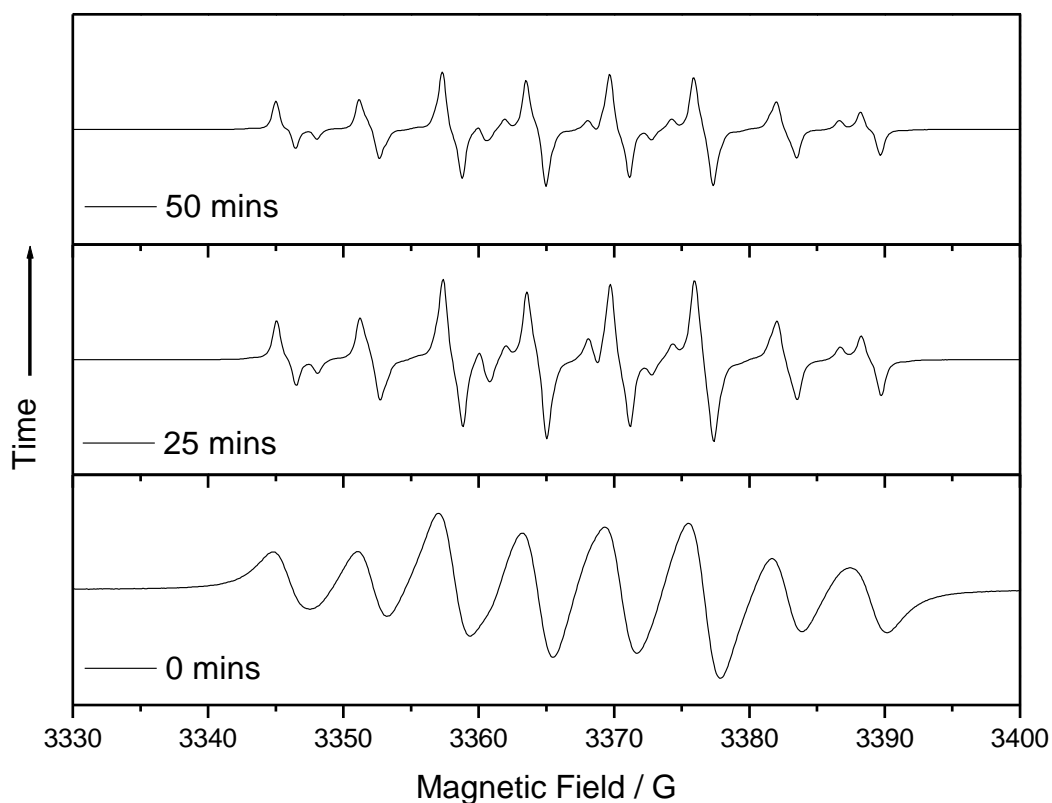


Figure 63. EPR spectra of PID + PBN in benzene with constant irradiation at 0, 25 and 50 minutes

Solvent	<i>a</i> / G				Reference
	¹⁴ N	³⁵ Cl	³⁷ Cl	¹ H	
DMSO	12.56	6.28			present work ^a
C ₆ H ₆	12.32	6.25	5.20	0.80	present work ^b
C ₆ H ₆	12.28	6.18	5.20	0.78	present work ^c
C ₆ H ₆	12.12	6.05	4.88	0.75	146
CCl ₄	12.22	6.08	5.00	0.80	150
CH ₃ CN	12.70	6.20	5.12	0.89	80
CH ₃ CN	12.33	6.20	5.12	0.83	79
C ₆ H ₆	12.31	6.36	5.00	0.75	149

Table 19. Hyperfine coupling constants for PBN-Cl adduct observed together with literature values, a-c derived from: (a) PtCl₆²⁻, (b) C₆H₅N=CCl₂, (c) 4-CH₃C₆H₄N=CCl₂

This result therefore shows that the chlorine adduct of PBN is formed when PID + PBN is irradiated in solution. This evidence points towards chlorine radicals being formed by PID

which can only be seen when a spin trap is used. No evidence of any hydrolysis product is seen in the spectra.

An experiment was then carried out where a solution of PID + PBN in benzene was irradiated for only 30 seconds. Scanning was started immediately after the lamp was switched off and scanning continued for 100 minutes. Initially the signal for the chlorine adduct is replicated, Figure 64 shows selected spectra at 0, 12.5, 25 and 50 mins. This radical decays as the scanning proceeds whereby a three line signal referring to a second radical species is formed. This species has a hyperfine splitting of $a_N = 8.00$ G, indicating a nitrogen based radical without any coupling to other atoms.

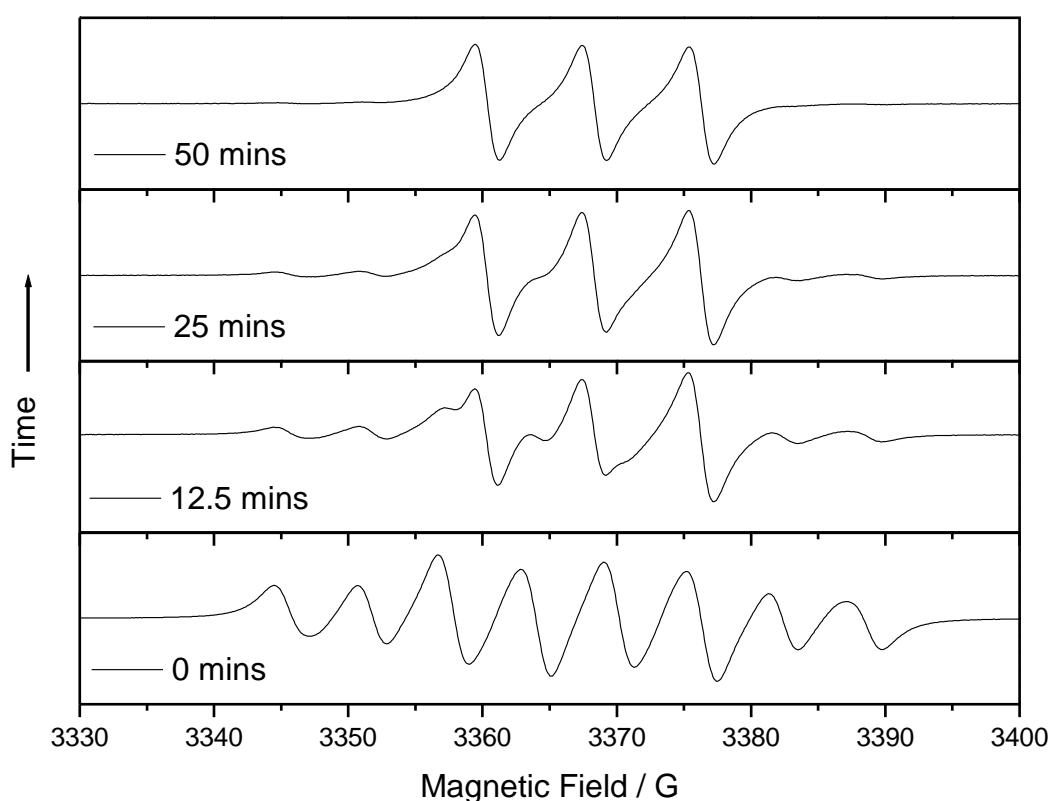


Figure 64. EPR spectra of PID + PBN in benzene after 30 s irradiation

Several different possibilities were considered for the identification of the second radical, these included compounds that could possibly be formed in the irradiation of PID + PBN in solution. The hydrolysis product of PBN, hydroxybenzyl-*N-tert* butyl nitroxide (XIII), which is seen in the blank reactions, can be ruled out as the hyperfine splitting have different values as that seen before and also no splitting to ^1H is seen. The second postulate is that after initial irradiation the residual PID would form a radical (XIV) (Figure 65). If this was the case and it was long-lived enough in order to record the spectrum, it would be

seen in the blank reaction when PID was irradiated without the spin trap. As we see no evidence for this we can again rule this species out. The PBN-PID adduct (XV) (Figure 65). would stem from the addition of residual PID after cleavage of the chlorine to the PBN spin trap forming a second adduct. However the splitting pattern of this radical would be more complicated than the 3 lines due to coupling with nearby hydrogen atoms. The PBN cation radical (XVI) (Figure 65) of PBN has been demonstrated to occur when laser flash photolysis is used at 266nm.¹⁵¹ However no epr spectra have been reported for the cation and it would be expected to occur in the blank reaction when a solution of PBN in benzene was irradiated. Again we can therefore rule this species out as an option. Benzoyl-*N*-*tert*-butyl nitroxide radical (XVII) (Figure 65) has been previously reported to occur in reactions involving PBN with chlorine, benzene or other oxidizing agents.^{149, 152} The spectra and splitting values are also consistent with our results (Table 20) therefore the identity of the unknown species in the spectra can be assigned to benzoyl *N*-*tert*-butyl nitroxide radical (XVII).

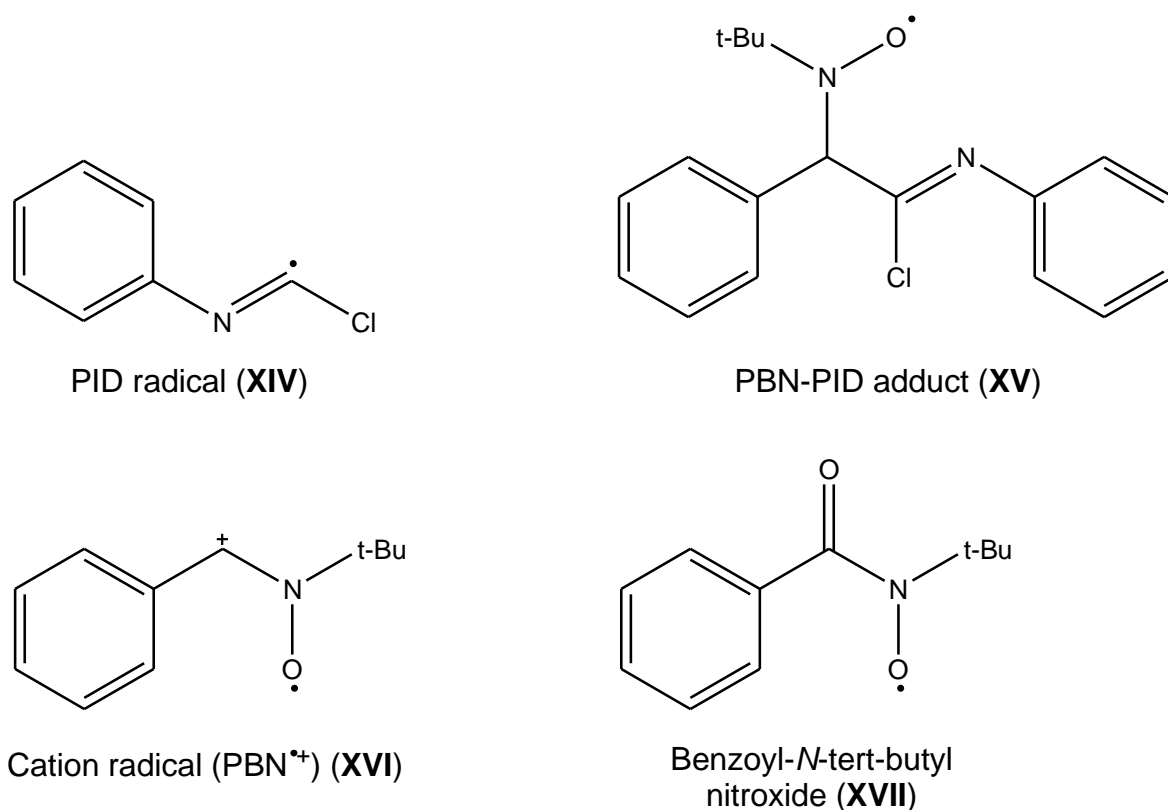


Figure 65. Postulates for identity of second radical species on irradiation of PID + PBN in benzene

Solvent	a / G	Reference
	^{14}N	
C_6H_6	8.00	present work ^a
C_6H_6	8.01	present work ^b
CH_3CN	8.08	79
$\text{CH}_3(\text{CH}_2)_4\text{CH}_3$	7.89	149
C_6H_6	7.67	152

Table 20. Hyperfine coupling constants for benzoyl-*N-tert*-butyl nitroxide radical (XVII) observed together with literature values, a-b derived from: (a) $\text{C}_6\text{H}_5\text{N}=\text{CCl}_2$, (b) $4\text{-CH}_3\text{C}_6\text{H}_4\text{N}=\text{CCl}_2$

Before each experiment that was run a spectrum of the starting solution (PID + PBN in benzene) was recorded to see if any radicals would appear without irradiation. In around 50% of the solutions a small signal was seen indicating radicals were indeed present. Figure 66 shows an example spectrum where 100 scans were performed and the spectra added together, producing a clearer signal to look at. This signal clearly shows a mixture of the PBN-Cl adduct (XII) and the benzoyl *N-tert*-butyl nitroxide radical (XVII). As this signal is small compared to those seen in the irradiated solution, it is possible daylight may be affecting the solutions while they are being prepared. One solution which was kept in the dark showed no signal when scanned by the spectrometer. This was used to test the reaction without irradiation over time, whereby the solution was scanned for 47 minutes at 1 scan every 14 seconds. A weak three line signal (Figure 67) which appeared after 22 minutes and increased over time indicated the formation of the benzoyl *N-tert*-butyl nitroxide radical. This is an interesting result as firstly no hydrolysis product is seen as with PBN in solution without the PID and also no chlorine adduct is formed. This will be discussed further in section 5.6 but it is clear that several different processes are occurring in this reaction.

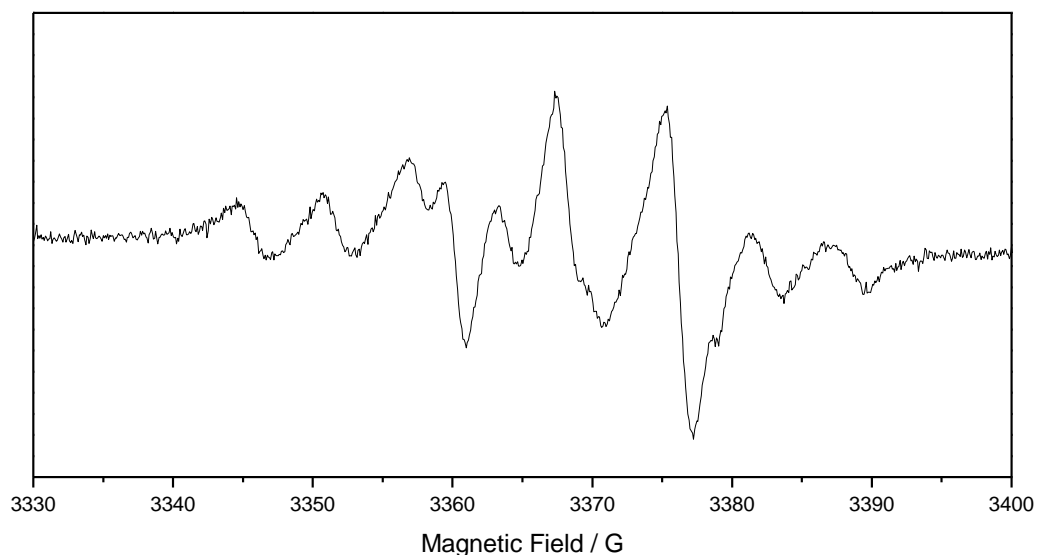


Figure 66. EPR spectrum of PID + PBN in benzene without irradiation

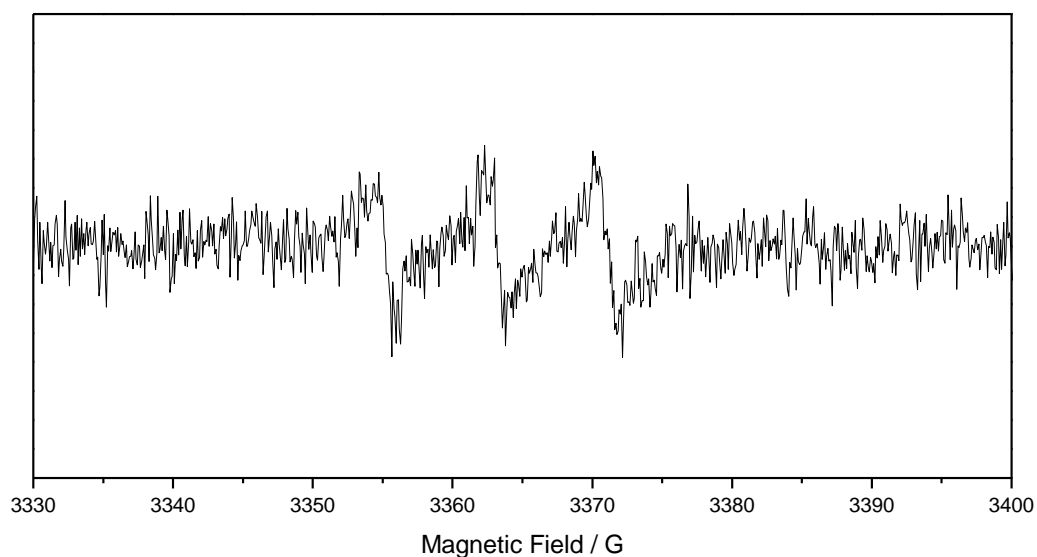


Figure 67. EPR spectrum of PID + PBN in benzene without irradiation (dark) after 47 minutes

5.3 Verification of Benzoyl *N-tert*-butyl Nitroxide Radical

5.3.1 DFT Calculations

In order to confirm the second species as the benzoyl-*N-tert*-butyl nitroxide radical (XVII), DFT calculations were carried out at Manchester on the molecule and also on the PBN-PID adduct (XV). This adduct was also investigated as it was the one candidate which could not

be fully ruled out from the blank experiments carried out. Figure 68 shows the spin densities for both species.

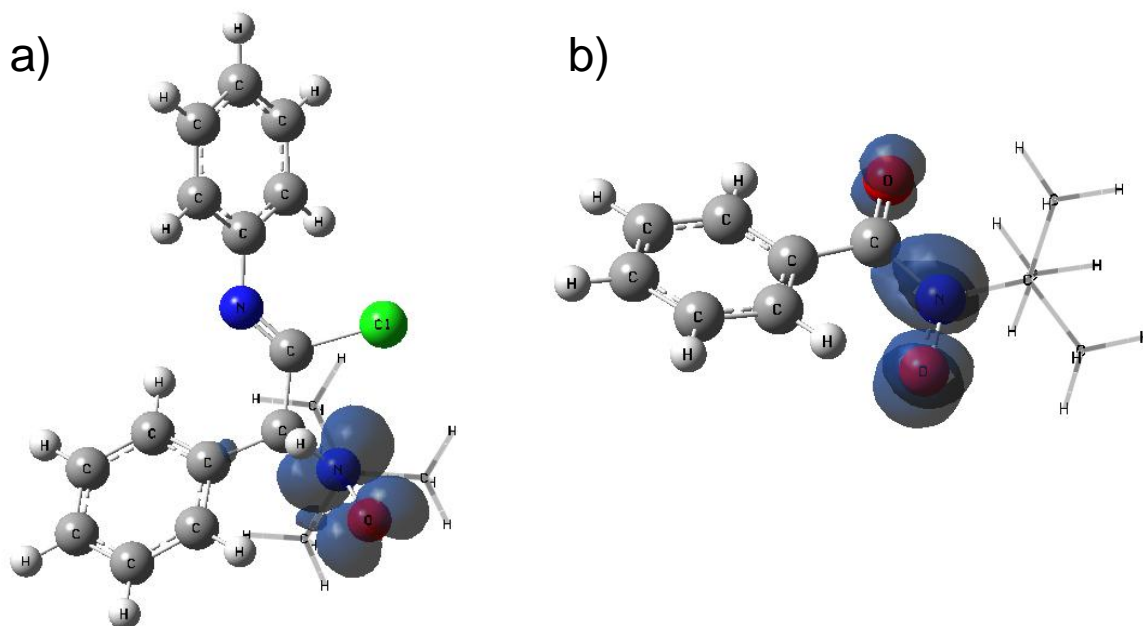


Figure 68. B3LYP/EPR-III (CI: IGLO-III) spin densities (isosurface value 0.004 au, *t*-Bu group shown in wireframe for clarity) for a) benzoyl-*N*-*tert*-butyl nitroxide radical (XVII) and b) PBN-PID adduct (XV)

In the PBN-PID adduct (XV) the Mulliken spin densities on the N–O• unit are 0.45 (N) and 0.51 (O), the Fermi contact couplings are 12.2 G (N) and –14.8 G (O). The protons of the phenyl unit nearer to the radical centre show very small spin densities (range 0.0003 – 0.0023) with the largest Fermi contact coupling being 0.3 G. In the benzoyl-*N*-*tert*-butyl nitroxide radical (XVII) the spin densities on the N–O• unit are 0.27 (N) and 0.58 (O), the O atom of the carbonyl unit carries most of the remaining spin density (0.14). The carbonyl O atom pulls away significant spin density from the N atom, reducing the hyperfine coupling. The corresponding Fermi contact couplings are 5.5 G (N), –14.8 G (O) and –3.5 G on the carbonyl O atom. The spin density and the hyperfine coupling on the O atom are both very similar in (XVII) and (XV), while those for N are significantly different. In (XVII) the phenyl protons again show very small spin densities, with the largest proton hyperfine being less than 0.1 G. Comparisons with experimental values in Table 20, suggest that the second species observed is (XVII) rather than (XV). Fermi contact couplings are typically slightly underestimated in Gaussian orbital calculations¹¹⁸ due to the difficulty of treating the density at the nucleus. For species (XVII) experimental values

in solution are 7.67 – 8.08 G for the N hyperfine. These values are substantially smaller than those calculated for (XV) but are a little larger than those calculated for (XVII). Thus assignment to radical (XVII) is favoured.

5.3.2 Simulations

Simulations on selected spectra were carried out in order to validate the experimental results. Figure 69 show the simulation of the spectra recorded when a solution of PID + PBN underwent constant irradiation. Figure 70 shows the simulation of the 30 s irradiated solution at both 0 and 50 minutes. The results show good correlations for both the PBN-Cl adduct (XII) and the benzoyl-N-tert-butyl nitroxide radical (XVII). This excellent agreement between the simulated and observed spectra reinforces the assignments for the octet and triplet splitting patterns. The reactions carried out on *p*-Tolyl isocyanide dichloride (TID) gave the same results as the PID indicating both compounds behaved in the same way under irradiation with the spin trap.

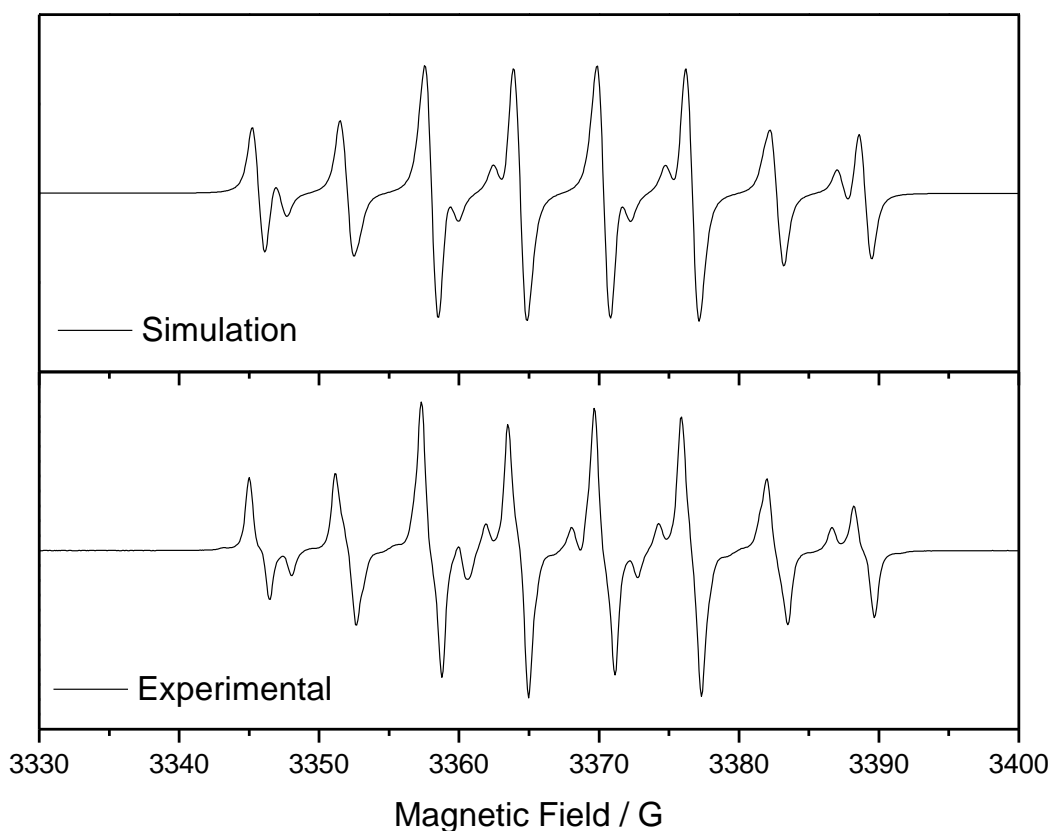


Figure 69. Simulation and experimental spectra of PID + PBN in benzene after 50 mins constant irradiation, parameters from simulation are $a_N = 12.32$ G, $a_{Cl-35} = 6.25$ G, $a_{Cl-37} = 5.20$ G and $a_H = 0.80$ G

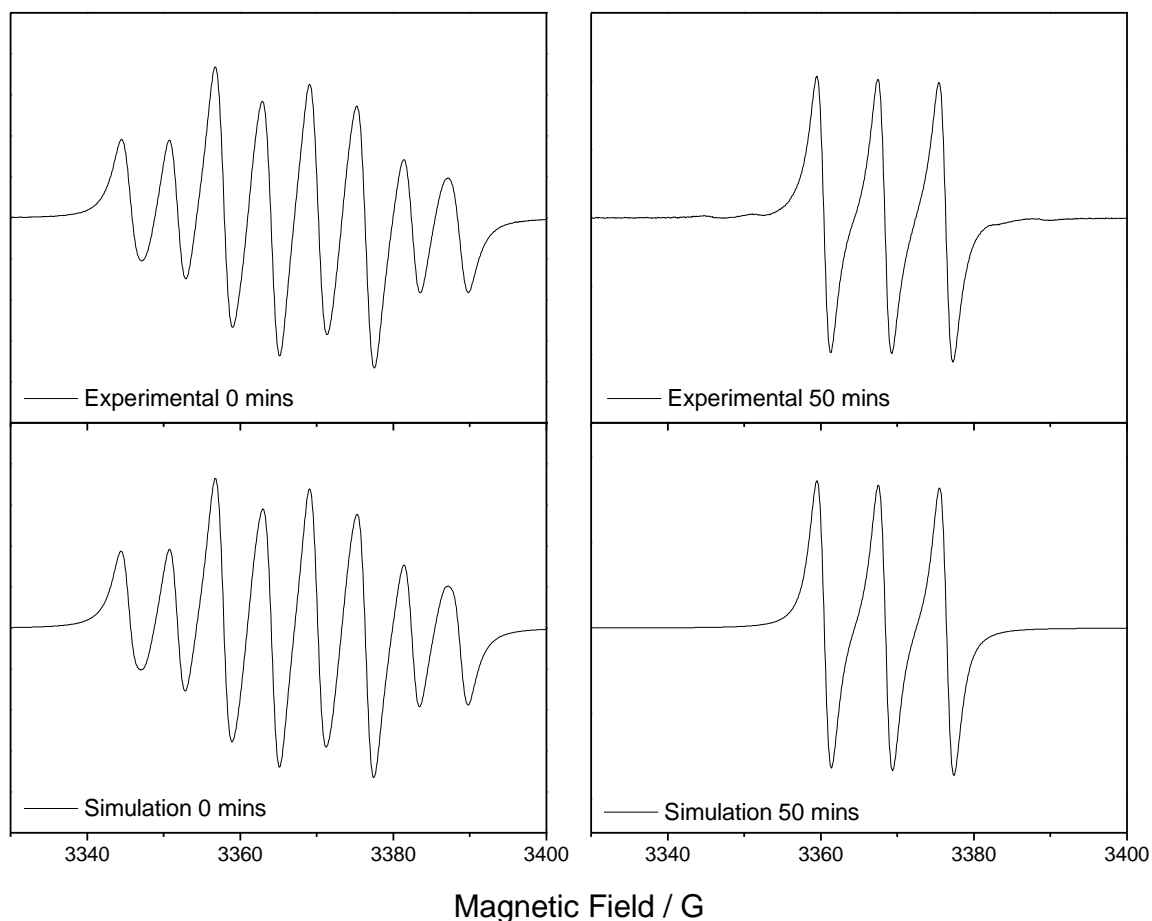


Figure 70. Simulation and experimental spectra of PID + PBN in benzene after 30 s irradiation, parameters from simulation are 0 mins – $a_N = 12.32$ G, $a_{Cl-35} = 6.25$ G, $a_{Cl-37} = 5.20$ G, 50 mins – $a_N = 8.00$ G

5.4 Low Temperature Study

Reactions were carried out at low temperatures to see if there would be any effect on the radicals produced. In theory the lifetime of the radicals should be increased by the cold temperatures but it is also possible the production of the radicals would be slowed down. Solutions of phenyl isocyanide dichloride (PID) + *N-tert*-Butyl- α -phenylnitron (PBN) were made up in toluene in order to access temperatures below 273 K. Five different temperatures were investigated, 193 K, 223 K, 253 K, 283 K, 313 K. For each temperature the sample was irradiated for 30 seconds and stopped. Scanning was started immediately with 1 scan collected every 30 seconds. Figure 71 shows the spectra recorded immediately after irradiation at 0 minutes and 50 minutes later at the different temperatures.

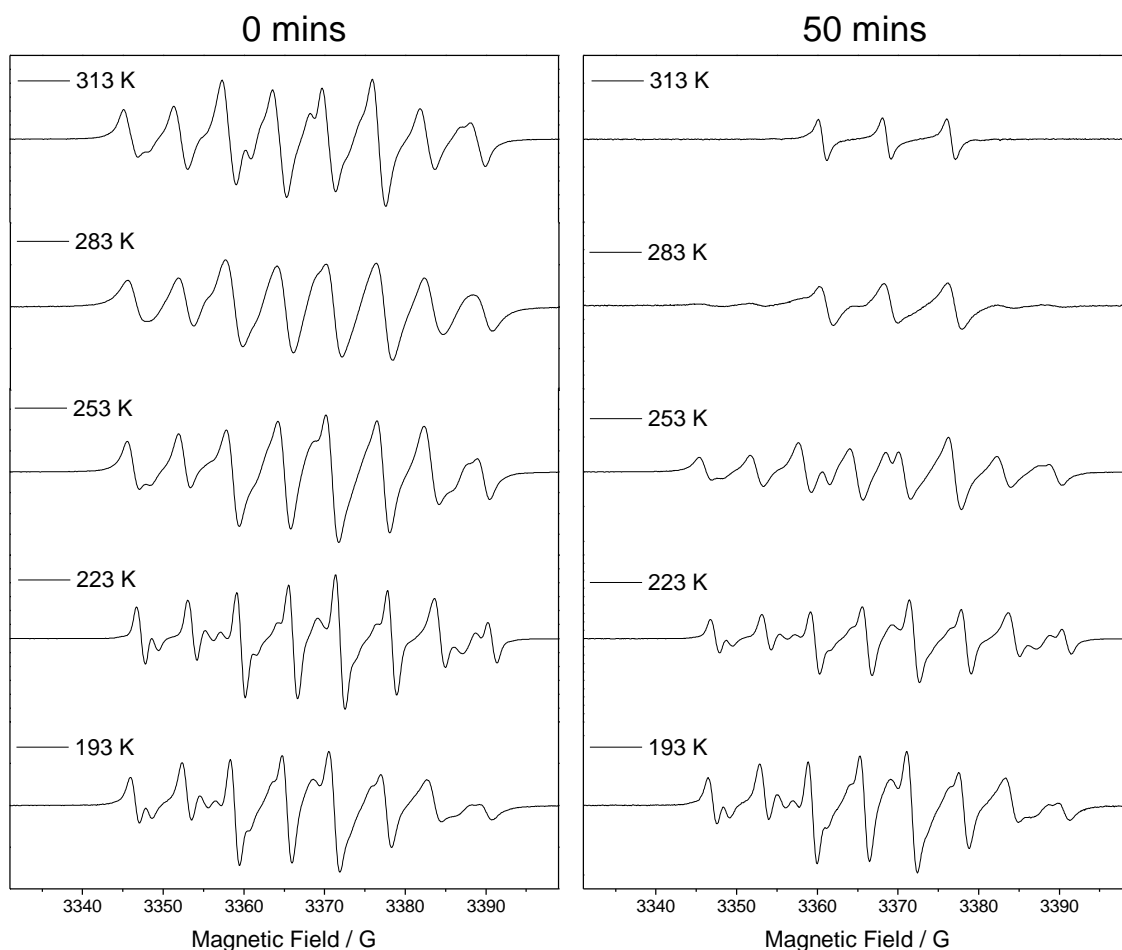


Figure 71. EPR spectra of PID + PBN in toluene after 30 s irradiation at various temperatures

The resultant spectra recorded at 283 K are the closest to room temperature and the spectra we have seen previously (Figure 64). An 8 line signal referring to the PBN-Cl adduct (XII) appears however no splitting to the ^{35}Cl and ^1H are seen. As the temperature is lowered to 253, 223 and 193 K, the spectra become more defined as peaks pertaining to the ^{35}Cl and ^1H splitting begins to develop. This is possibly due to slower spin-lattice relaxation or slower exchange interactions, such as electron transfer. At the higher temperature of 313 K, two small shoulder peaks can be seen. These are from the benzoyl *N-tert*-butyl nitroxide radical (XVII) which is already starting to form.

After 50 minutes, the two lowest temperatures, 193 K and 223 K, show little change in the spectra. No sign of a second species is seen, indicating the reaction has been slowed down or is not occurring at this temperature. The PBN-Cl adduct (XII) only shows slight decay therefore the longevity of the radical increases as temperature decreases. The spectra at 253 K shows a mixture of the two species, indicating the PBN-Cl adduct is decaying and the benzoyl *N-tert*-butyl nitroxide radical is forming. At 283 K the PBN-Cl adduct has almost

fully decayed, with small humps showing signs of the radical. The benzoyl radical is clearly seen therefore the formation of this must increase with increasing temperature. This is backed up by the spectrum recorded at 313 K as all of the PBN-Cl adduct is gone and only the benzoyl radical is seen.

Simulations were carried out on selected spectra at 193 K and 223 K. When these were subtracted from the experimental spectra, the 6 line signal relating to hydroxybenzyl-*N-tert* butyl nitroxide, the hydrolysis product of PBN can be seen. Calculations carried out estimated this radical to make up on average 14.8 % of the total signal. Therefore we can count this as negligible as the signal for the PBN-Cl adduct dominates the spectra recorded.

5.5 PBN Concentration Study

Reactions were also carried out using different concentrations of *N-tert*-Butyl- α -phenylnitron (PBN). In each solution the concentration of phenyl isocyanide dichloride (PID) was kept constant (0.1 M) and the concentration of PBN was changed (0.1 M, 0.05 M and 0.026 M). This parameter was changed in the hope the results may give an insight into the reaction mechanism involved in the formation of the benzoyl *N-tert*-butyl nitroxide radical (XVII). Figure 72 shows the spectra at 0, 12,5 and 25 minutes after the samples had been irradiated for 30 seconds. As before, the PBN-Cl adduct is formed, decays and then the benzoyl radical is formed. The spectra shows that the concentration of PBN has little effect on the reaction, with the higher concentration possibly producing more radicals as the chlorine adduct takes longer to decay. This is consistent since the PID is equal or in excess, the more PBN should produce more of the PBN-Cl adduct.

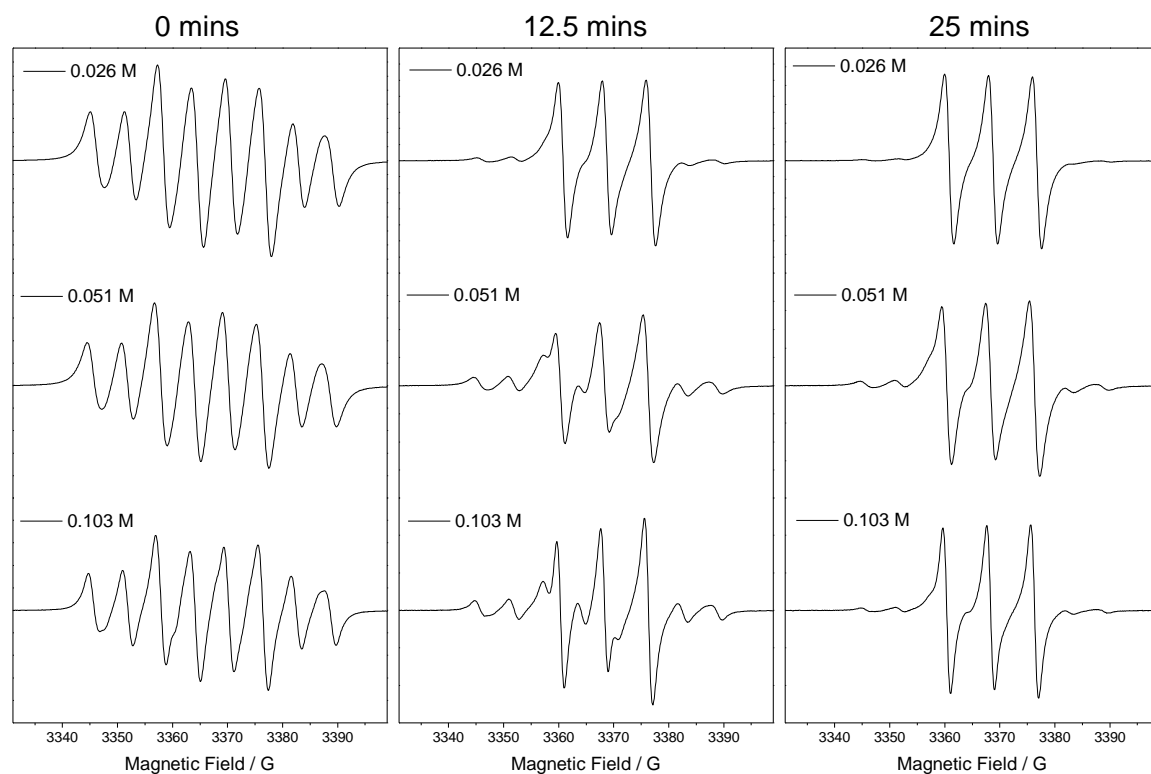


Figure 72. EPR spectra of PID in benzene with different concentrations of PBN after 30 s irradiation

Spectra was also recorded under constant irradiation (Figure 73), again showing similar results to that seen previously whereby the PBN-Cl adduct is formed throughout the process, the spectra becoming more defined as time goes on. As the concentration of the PBN increases, the three line spectrum for the benzoyl radical starts to become more apparent. This helps to confirm the species as the benzoyl radical as it is clear this radical is formed from the spin trap, PBN and not from the PID as the production of it changes with PBN concentration. As more of the benzoyl radical is formed with higher PBN concentration, this could be indicative of a reaction taking place between the PBN-Cl adduct and PBN.

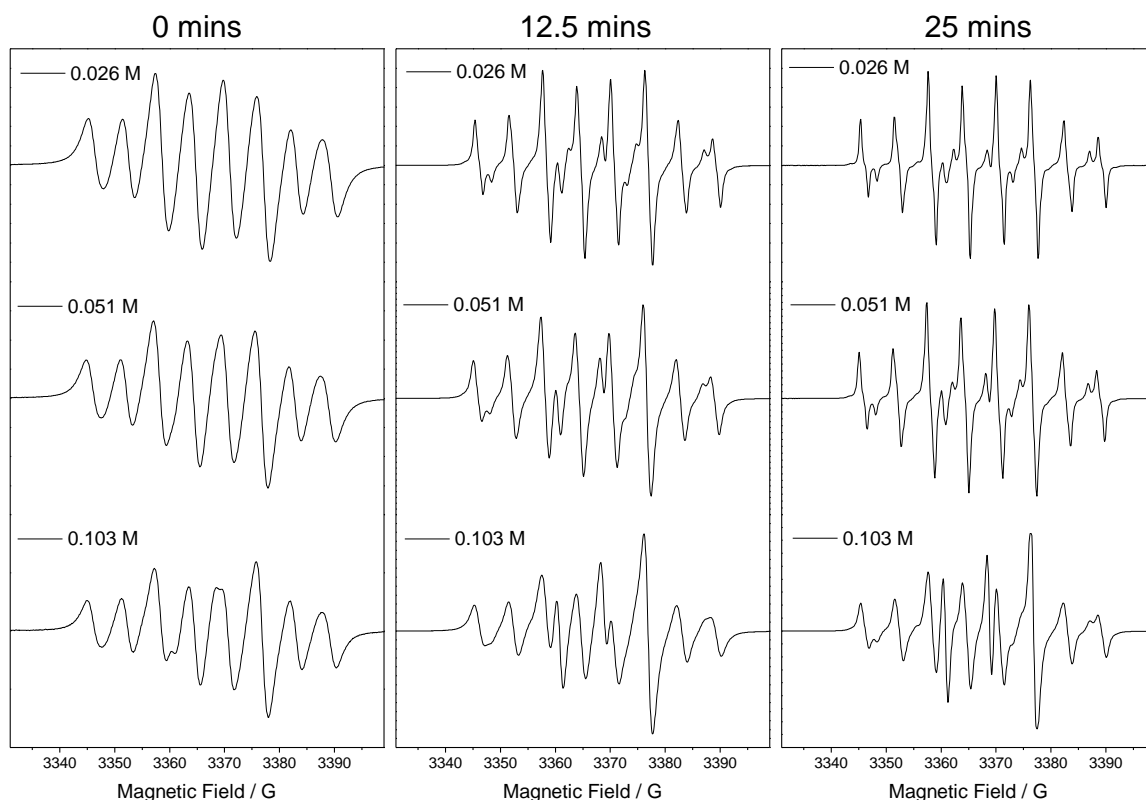


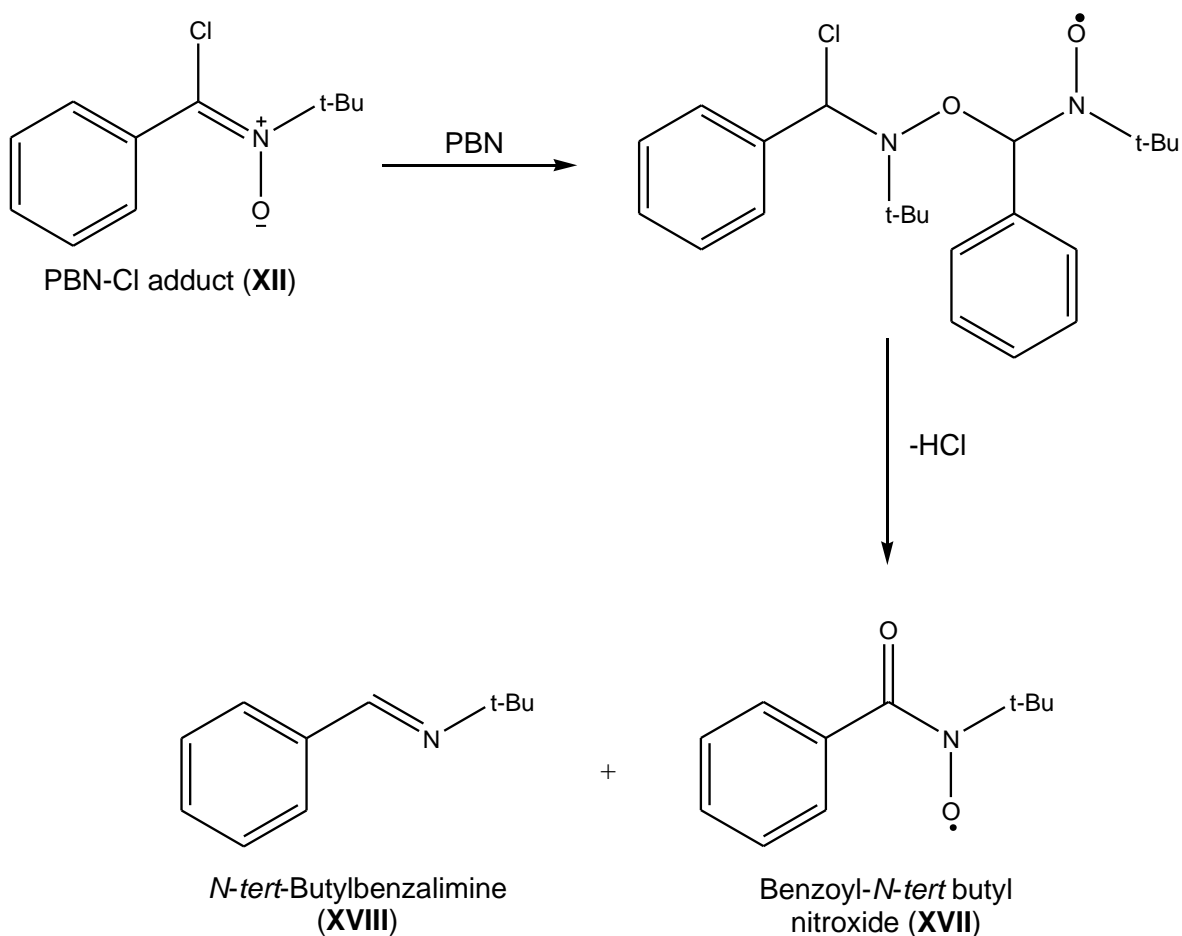
Figure 73. EPR spectra of PID in benzene with different concentrations of PBN with constant irradiation

5.6 Reaction Study and Kinetics

From the EPR spectra presented thus far it is clear the PBN-Cl adduct (XII) is formed from a chlorine atom transfer process between PID and PBN. It has not been established whether the second radical which is formed, benzoyl *N-tert*-butyl nitroxide radical (XVII), is a product of further reaction of the PBN-Cl adduct, or formed directly from the PBN. Benzoyl radicals leading to benzoyl spin adducts can be formed from benzaldehyde, an impurity sometimes found in *N-tert*-Butyl- α -phenylnitron (PBN).⁷² However if this was the case here the blank reactions involving PBN would have showed the formation of the benzoyl radical. Reactions instead show the hydrolysis product, hydroxybenzyl-*N-tert* butyl nitroxide (XIII), is formed.

It is proposed that the benzoyl-*N-tert*-butyl nitroxide radical can be formed from a reaction between the PBN-Cl adduct and additional PBN in a consecutive reaction (Scheme 19).¹⁴⁹ The benzoyl radical should be accompanied by a second product, *N-tert*-butylbenzylimine (XVIII)¹⁵¹. Evidence for the formation of this species is provided by the GC-MS spectrum,

m/z 162 (M^+ , $C_6H_5CH=NC(CH_3)_3$, 9%), 105 ($C_6H_5CH=N$, 41%), 77 (C_6H_5 , 15%), of a sample of PID + PBN, which had been irradiated for 45 min.



Scheme 19. Formation of benzoyl-*N*-tert-butyl nitroxide radical through a consecutive reaction

In an attempt to understand the reaction mechanism in more depth, a series of experiments were carried out to investigate the route of formation of the benzoyl radical and the kinetic processes involved within a generalised reaction scheme. As outlined in the experimental (Section 2.15.6), solutions of PID + PBN in benzene were irradiated at different temperatures over time. The irradiation was then stopped while scanning continued to look at the decay processes of the radicals formed. Figure 74 shows the reaction profile for the intensity of the PBN-Cl adduct with Figure 75 showing the benzoyl radical.

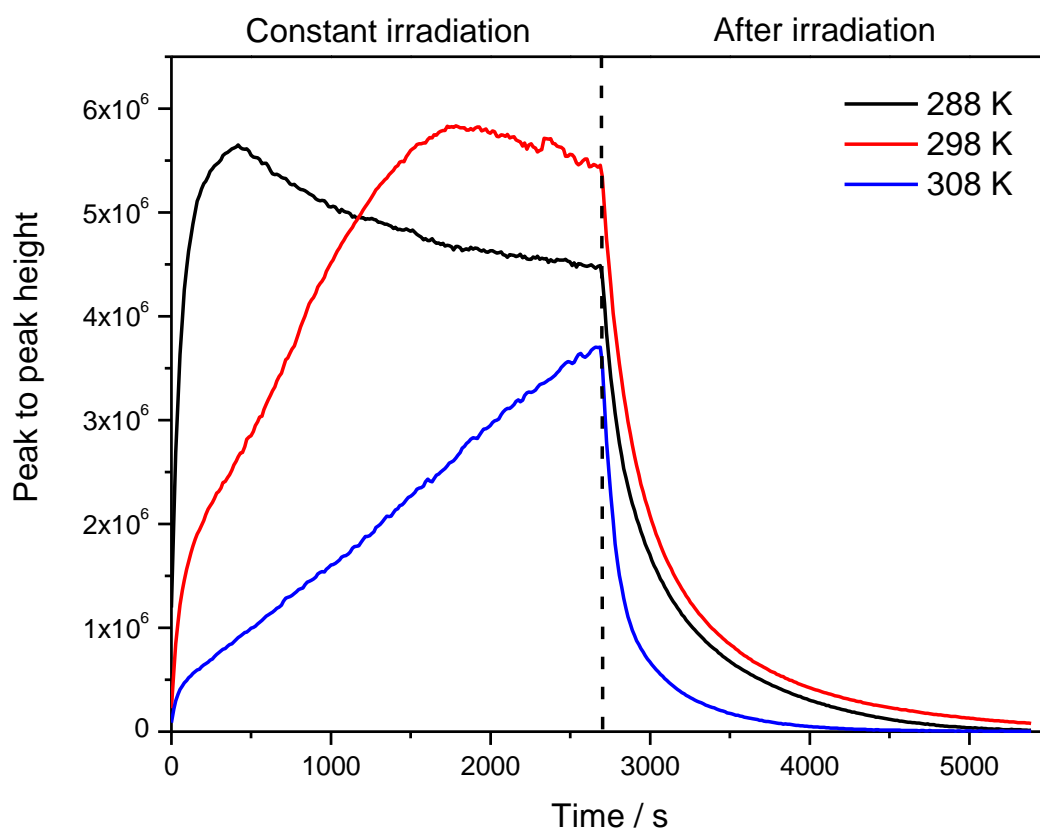


Figure 74. Reaction profile of the PBN-Cl adduct at various temperatures

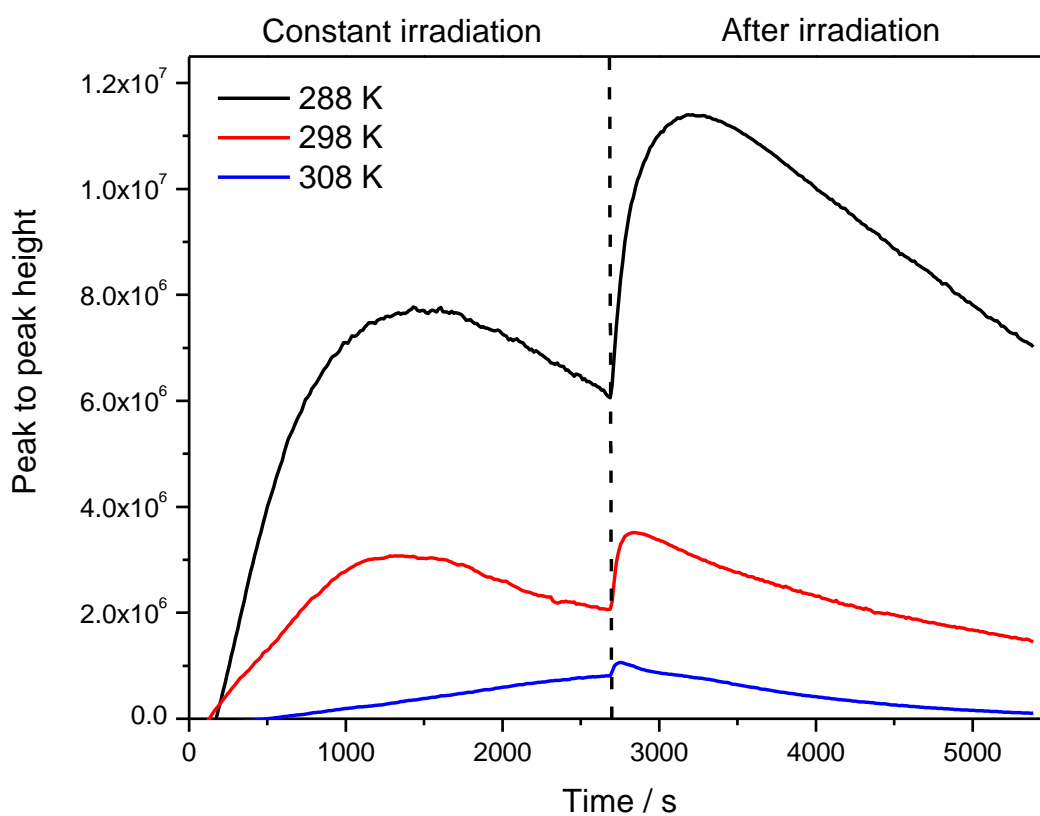


Figure 75. Reaction profile of the benzoyl radical at various temperatures

The formation of the chlorine adduct shows an initial steep increase until a steady rate is reached. At this point radicals are both being formed and are decaying simultaneously. After a period of time the chlorine radicals reach a maximum concentration, possibly at the point where no starting material is left; after this point only the decay process is seen. As the temperature is increased, the rate of radical formation is slower. This is indicative of the higher temperature favouring the back reaction/decay process. After the irradiation is stopped the chlorine radicals rapidly decay, with the highest temperature giving the fastest decay rate. Table 21 shows the half life values for both the radicals at the three different temperatures to confirm this. The decay process for the PBN-Cl adduct (XII) approximates to single exponentials, however they do not adhere to simple first order kinetics over the full duration studied, implying that the decay process is not first order over the full time sequence studied, indicating a degree of complexity in the decay process.

Temperature / K	Half life ($t_{1/2}$) / s	
	PBN-Cl adduct (XII)	Benzoyl radical (XVII)
288	308	2516
298	315	2063
308	207	1161

Table 21. Half life values for radicals produced by PID + PBN in solution

The profile for the benzoyl radical (Figure 75) is very different, which is produced after ~ 3 minutes and at a slower rate. Similar to the chlorine adduct it reaches a maximum concentration then starts to decrease, again due to radical decay. When the irradiation is stopped, the benzoyl radical initially increases in concentration to a second maximum, and then slowly decays as time progresses. This behaviour indicates that the benzoyl radical is not being formed solely from further reaction of the PBN-Cl adduct with PBN (Scheme 19) as indicated by Sang et al.¹⁴⁹ However this does not rule out this mechanism completely, as it may be happening under irradiation. Plots of $[A]_0 - [A]$ versus time for all three temperatures for times > 3500 s show an approximately linear fit (Figure 76), therefore the decay process of the benzoyl radical can be assigned to zero order kinetics. This indicates the decay process to be a simple one compared to the decay of the PBN-Cl adduct. Summarising, stage 1 of the reaction under irradiation approximates to first order kinetics, whereas the second stage after irradiation follows zero order kinetics.

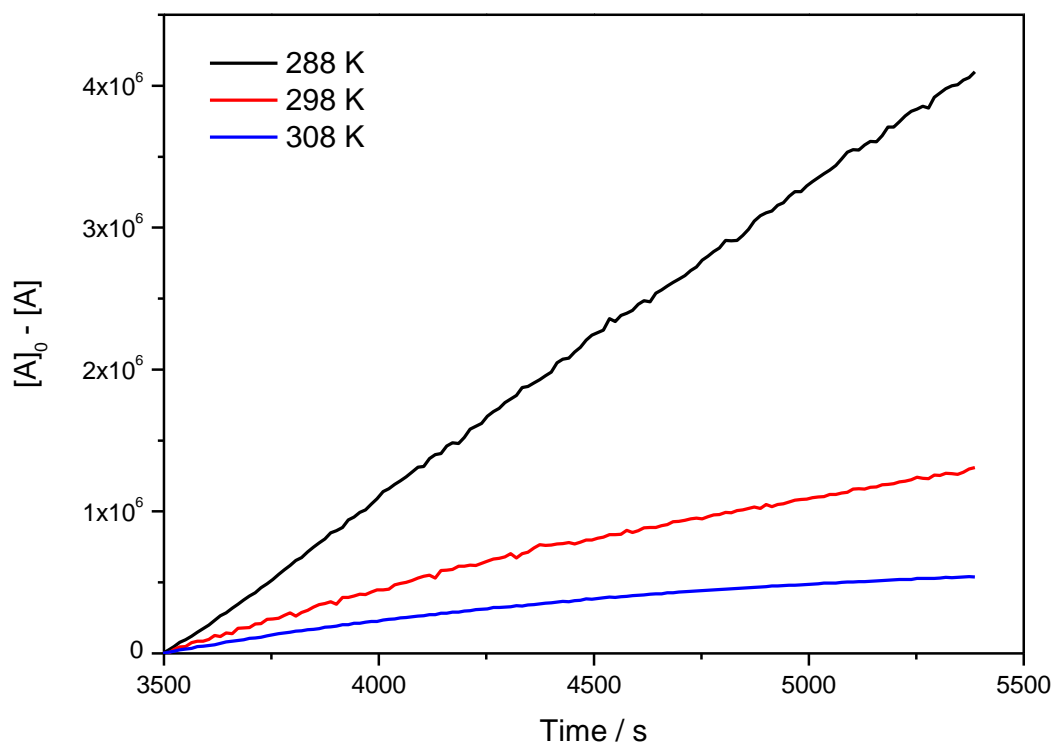


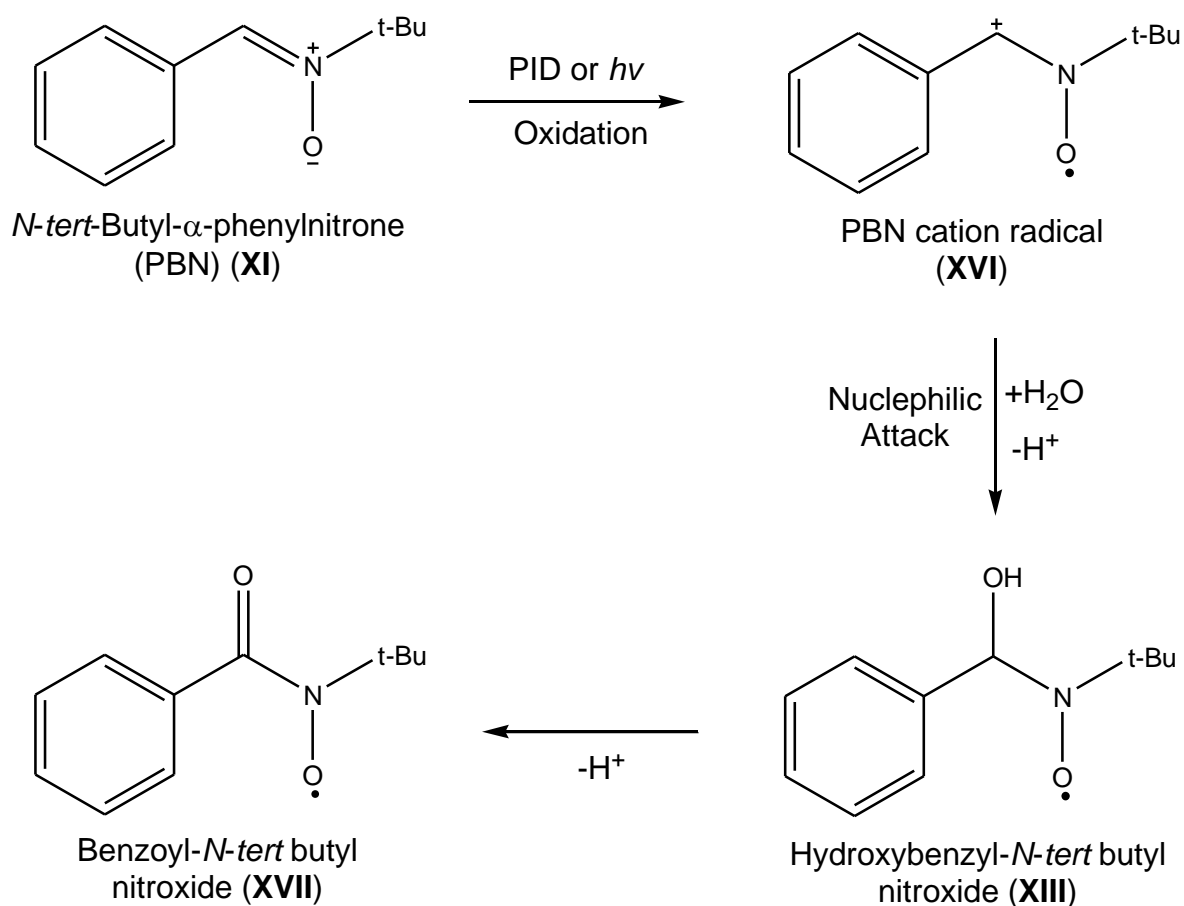
Figure 76. Plot of $[A]_0 - [A]$ versus time for benzoyl-*N*-*tert*-butyl nitroxide (XVII) > 3500 s at various temperatures

These results point towards two separate processes occurring simultaneously to form both radicals. The benzoyl radical is not solely formed from the PBN-Cl adduct in a consecutive reaction, however the presence of the starting material, PID, is required as the benzoyl radical is not formed when PBN is irradiated in solution on its own. As mentioned previously a solution of PID + PBN kept in the dark does show a small amount the benzoyl radical (VII) being formed, demonstrating the possibility of a non-photochemical route.

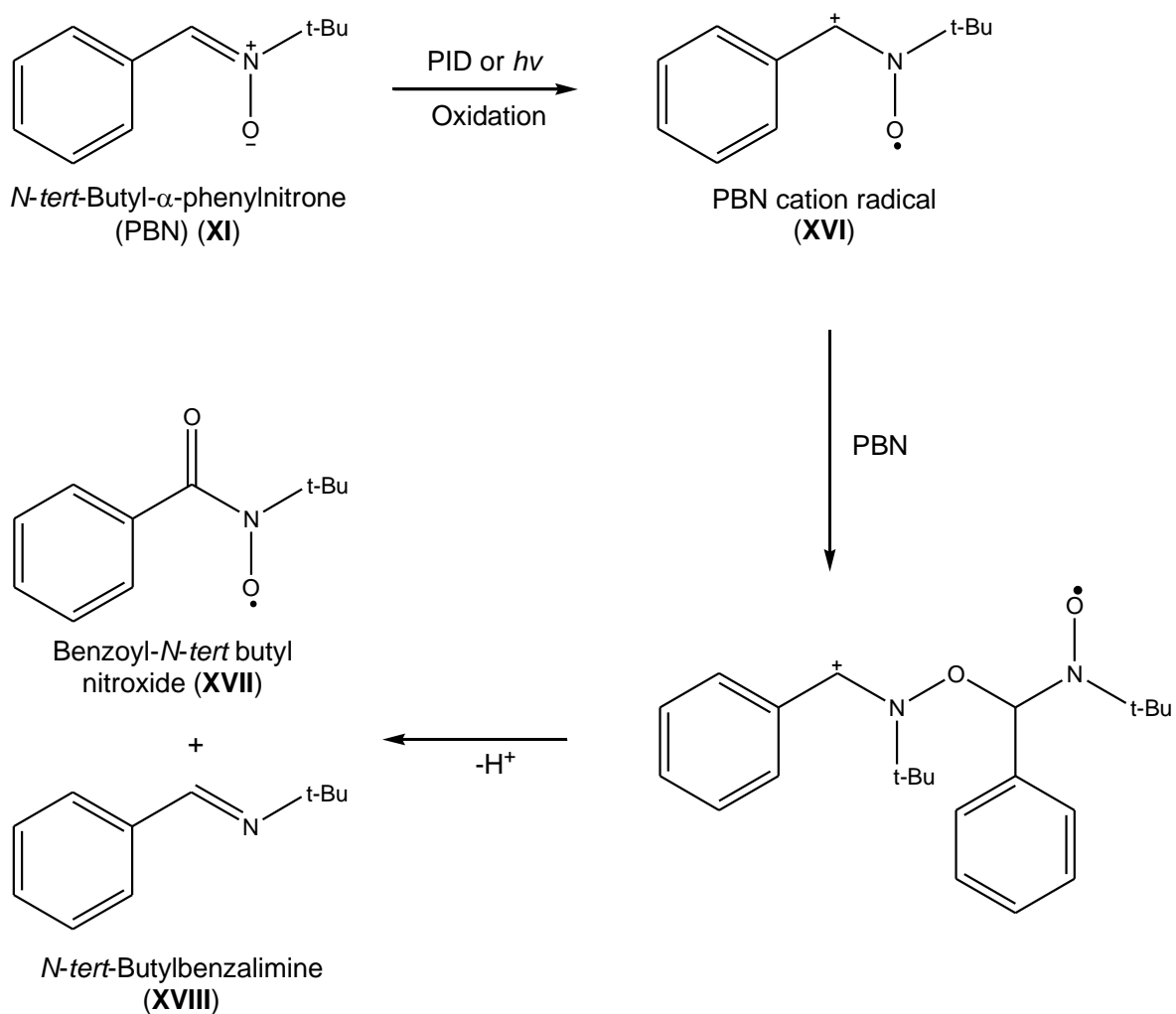
Scheme 20 and Scheme 21 show two postulated pathways for the formation of the benzoyl radical without the involvement of the PBN-Cl adduct (XII). Both schemes involve the formation of the $\text{PBN}^{\bullet+}$ cation radical as described previously in section 5.2. This can be formed by either a photochemical process or by chemical oxidation due to the presence of the PID. Ebersson¹⁵³ has commented on the formation of the cation via oxidation processes, whilst Zuberev¹⁵¹ has reported on the use of photoionisation. A possible chemical oxidising agent would be dichlorine, formed from decomposition of PID. The cation can then either undergo nucleophilic attack from an OH (Scheme 20), presumably from water in the solvent, to form the hydroxy benzyl-*N*-*tert* butyl aminoxyl radical, which will be oxidised to the benzoyl radical. However if this was the case we would expect the hydroxyl

radical to last long enough in order for the spectra to be recorded, especially as it is seen in the blank reaction of PBN in benzene. The second scheme (Scheme 21 shows the cation reacting with a second molecule of PBN to form the benzoyl radical plus a second product *N-tert*-butylbenzylimine (XVIII).¹⁵¹ As mentioned previously this product has been found in the GC-MS of a sample of PID + PBN which had been irradiated for 45 minutes.

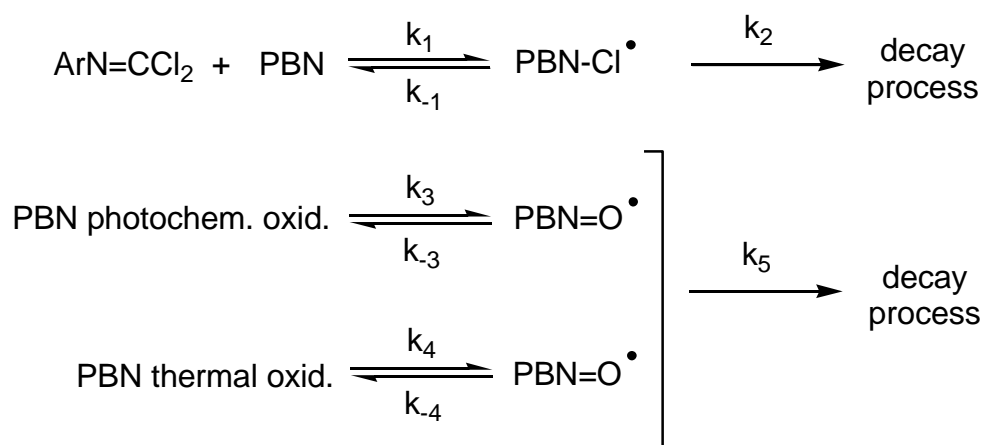
These observations lead to the belief the benzoyl radical is being formed from two different competing pathways. Excess PBN reacts with either the PBN-Cl adduct (XII) or the PBN^{•+} cation radical (XVI). Both mechanisms are promoted by the presence of PID. Scheme 22 shows the proposed overall kinetic scheme outlining the processes taking place in the irradiation of a PID in the presence of the spin trap, PBN.



Scheme 20. Postulated scheme 1 for the formation of benzoyl *N-tert*-butyl nitroxide radical



Scheme 21. Postulated scheme 2 for the formation of benzoyl *N-tert*-butyl nitroxide radical



Scheme 22. Proposed kinetic processes

5.7 Summary

EPR studies have been carried out on both phenyl isocyanide dichloride and *p*-tolyl isocyanide dichloride. The irradiation of both compounds with the addition of the spin trap, PBN, has shown the chlorine adduct, PBN-Cl[•] is formed indicating a Cl-atom transfer reaction is taking place. This reaction also indicates that isocyanide dichlorides can act as a source of chlorine radicals. A secondary radical, benzoyl *N*-*tert*-butyl nitroxide radical is also formed. The kinetic analysis carried out shows the reaction is not a simple one but stems from two competing reactions where excess PBN will react with the PBN-Cl adduct (XII) or the PBN^{•+} cation radical (XVI), a process initiated by photolysis or the isocyanide dichloride.

Importantly with respect to the industrial scenario, these studies confirm aryl isocyanide dichloride compounds to be a source of Cl[•]. Previously this had been assumed but was not proven.

Chapter 6

Isocyanide Dichlorides

6 Isocyanide Dichlorides

From the previous chapters, it has been proven that the urea side reaction from the phosgenation of 4,4'-methylene diphenyl diisocyanate (MDI) can indeed lead to isocyanide dichlorides via formation of a chloroformamidine-*N*-carbonyl chloride (CCC). It was therefore important to understand the role at which these molecules play in the colouration problems seen in the final MDI product. This chapter outlines the investigation into the isocyanide dichloride molecules and the extent of colouration.

6.1 Reaction of Isocyanide Dichlorides with Isocyanates (Preliminary Reactions)

Initially it was unclear as to whether the isocyanide dichloride compounds were stable molecules. As they could not be acquired from any supplier, phenyl isocyanide dichloride (PID) and *p*-tolyl isocyanide dichloride (TID) were produced as described in section 2.10. Both compounds were also characterized by various techniques (section 2.11). It was found that isocyanide dichlorides (IX) are unstable in atmospheric conditions, hydrolysis to carbamoyl chlorides (X) readily occurs on contact with moisture in the air. This led to the initial belief that these compounds could be unstable and break down easily upon heating.

6.1.1 Heat Treatments (Low Temperature Studies)

Preliminary studies were carried out on *p*-tolyl isocyanide dichloride (TID) in solution with various isocyanates at temperatures of 353 K to find out if any colouration takes place. Three different isocyanates were chosen, *p*-tolyl isocyanate (TI), 4-benzylphenyl isocyanate (4-BAI) and 4,4'-methylene diphenyl isocyanate (MDI). Each had a varying degree of complexity, it was hoped the simplest compound in *p*-tolyl isocyanate would give an indication into the reaction mechanism. Reactions were carried out in a round bottom flask attached to a condenser; details are outlined in section 2.14.2. Analysis was carried out by UV/Vis spectroscopy as this provided a useful method in analysing coloured species.

Initial blank reactions were carried out to test the reaction methods and to determine if any colour was formed by the isocyanate or solvent. Acetonitrile was chosen as a solvent as it has a boiling point of 355 K allowing the solutions to be refluxed at the required temperature (~ 353 K). It is also a common solvent for use in UV/Vis spectroscopy as it does not absorb above 190 nm thus will not interfere with the product spectra, allowing measurements in both the UV and visible range to be carried out.⁸³ Solutions were diluted in order to record the UV range spectra.

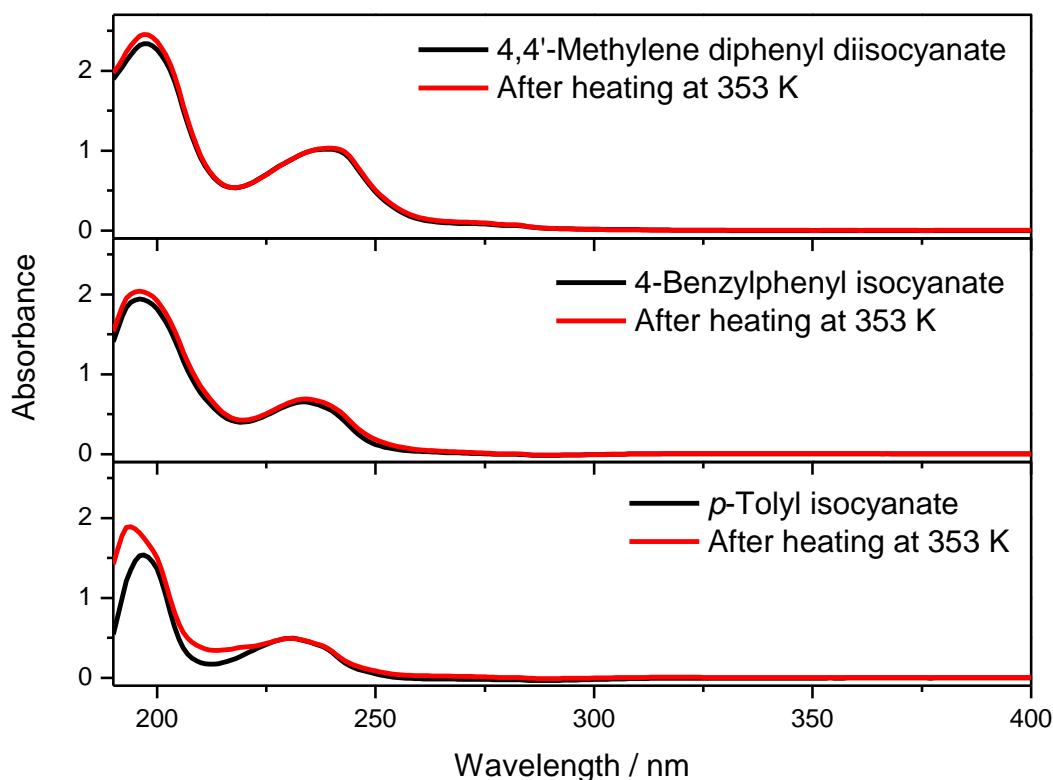


Figure 77. UV spectra before and after thermolysis of selected isocyanates

Figure 77 shows the UV spectra of the isocyanate starting materials before and after heating at 353 K. The spectra for both 4-BAI and MDI show that no changes are observed in the reaction solution indicating the compounds are unchanged. The spectrum for TI does show a slight change after heating below 220 nm however this is very small and no noticeable changes were seen in the solution by the naked eye. The spectra for TID in solution before and after thermolysis are shown in Figure 78 (UV range) and Figure 79 (visible range). Again no major changes are noted in the spectrum; however there is a slight decrease in absorbance below 350 nm. This could be due to decomposition of the *p*-tolyl isocyanide dichloride (TID) to the carbamoyl chloride, therefore decreasing the concentration of the TID in solution. These results indicate that the three isocyanate

compounds are thermally stable up to 353 K. The TID only shows a small change therefore can also be considered relatively stable up to this temperature. This is an unexpected result for the TID as it was initially expected to break down upon heating due to the hydrolysis seen at ambient temperature.

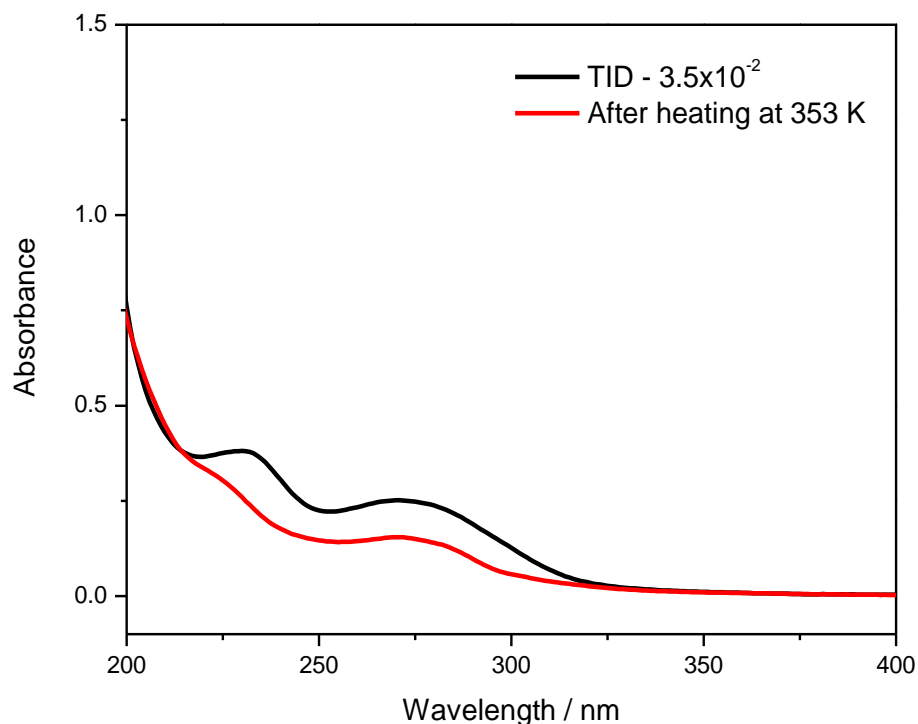


Figure 78. UV spectra before and after thermolysis of TID – UV region

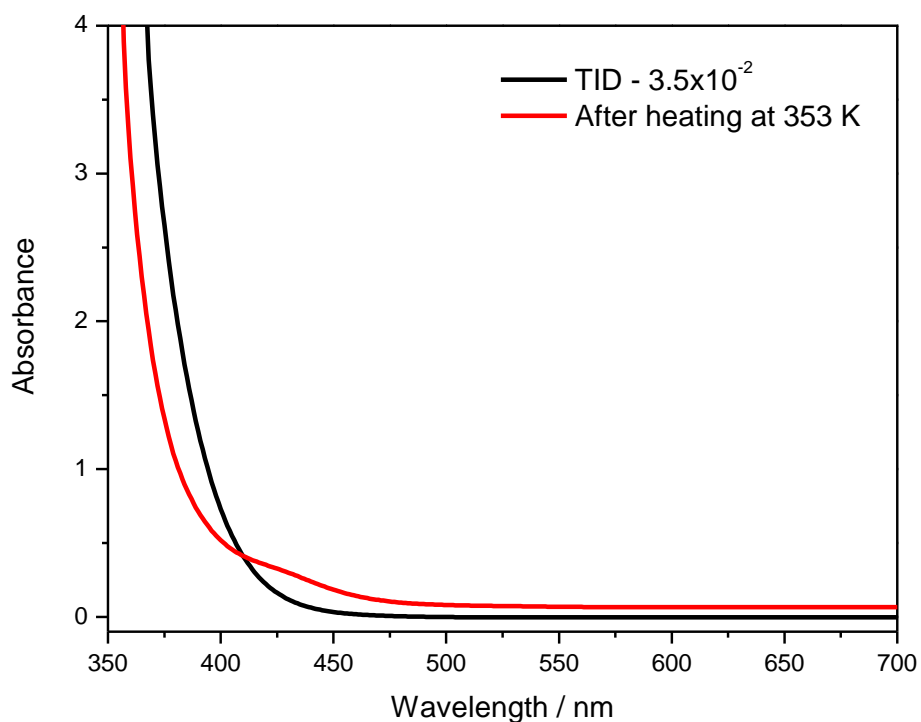


Figure 79. UV spectra before and after thermolysis of TID – visible region

Reactions were then carried out on mixtures of *p*-tolyl isocyanide dichloride (TID) with *p*-tolyl isocyanate (TI) or 4-benzylphenyl isocyanate (4-BAI). The absorbance spectra of TID with TI in the UV range (Figure 80) shows a small increase in absorbance after the reaction was carried out. The visible range spectra (Figure 81) shows a feature ~ 410 nm indicating a reaction between the compounds is taking place. Although the solutions before and after the reactions were light yellow, the visible spectrum indicates colour is increased in intensity. It is likely this change is too small to notice with the naked eye.

When changing the isocyanate to 4-BAI, the spectra in the UV region (Figure 82) shows a peak at ~ 230 nm in the starting solution is shifted to ~ 260 nm after heating at 353 K for 2 hours. It is possible the peak at 260 nm is indicative of a quinonoid type structure of the 4-BAI (Figure 83). Schollenberger and Stewart¹⁵⁴ found that in their investigations of urethane material based on 4,4'-methylene diphenyl diisocyanate (MDI), the absorbance spectra showed a peak at 245 nm decreased on exposure to light, whilst a peak at 275 nm increased. The explanation for this was the loss of aromaticity due to the formation of a quinonoid structure. The solution mixture before and after reaction again looked similar in colour to the naked eye, however small solid particles were noted forming after the reaction was stopped.

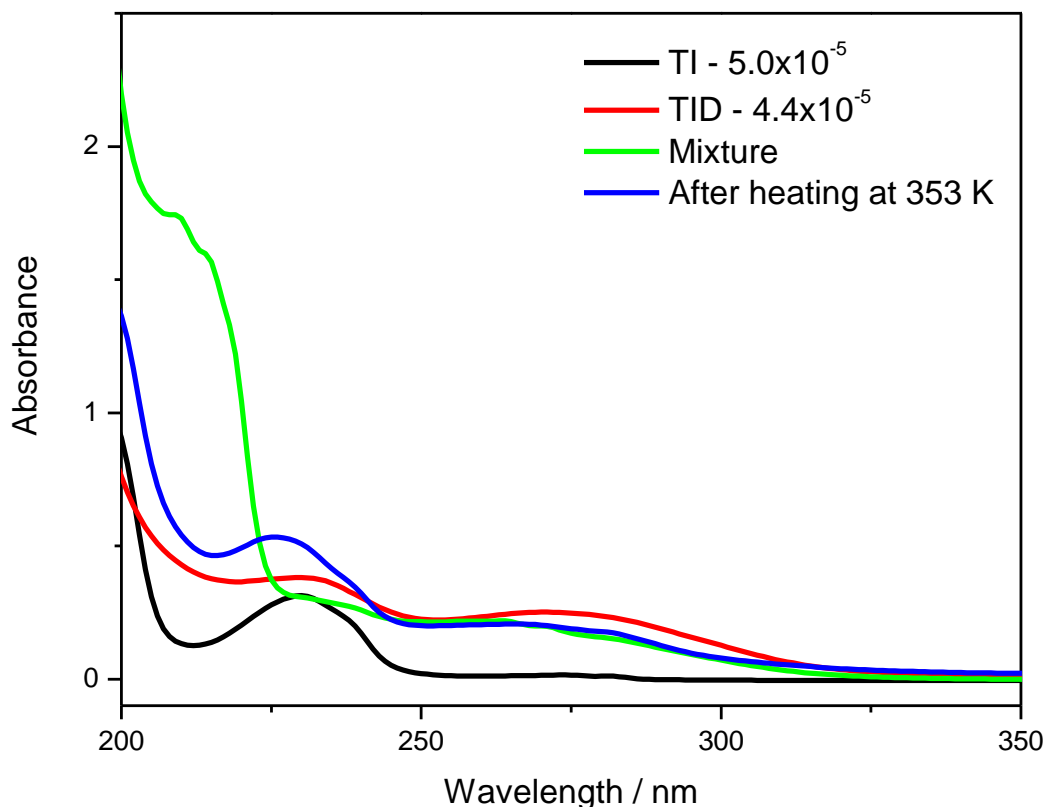


Figure 80. UV spectra of thermolysis of TID + TI in acetonitrile – UV region

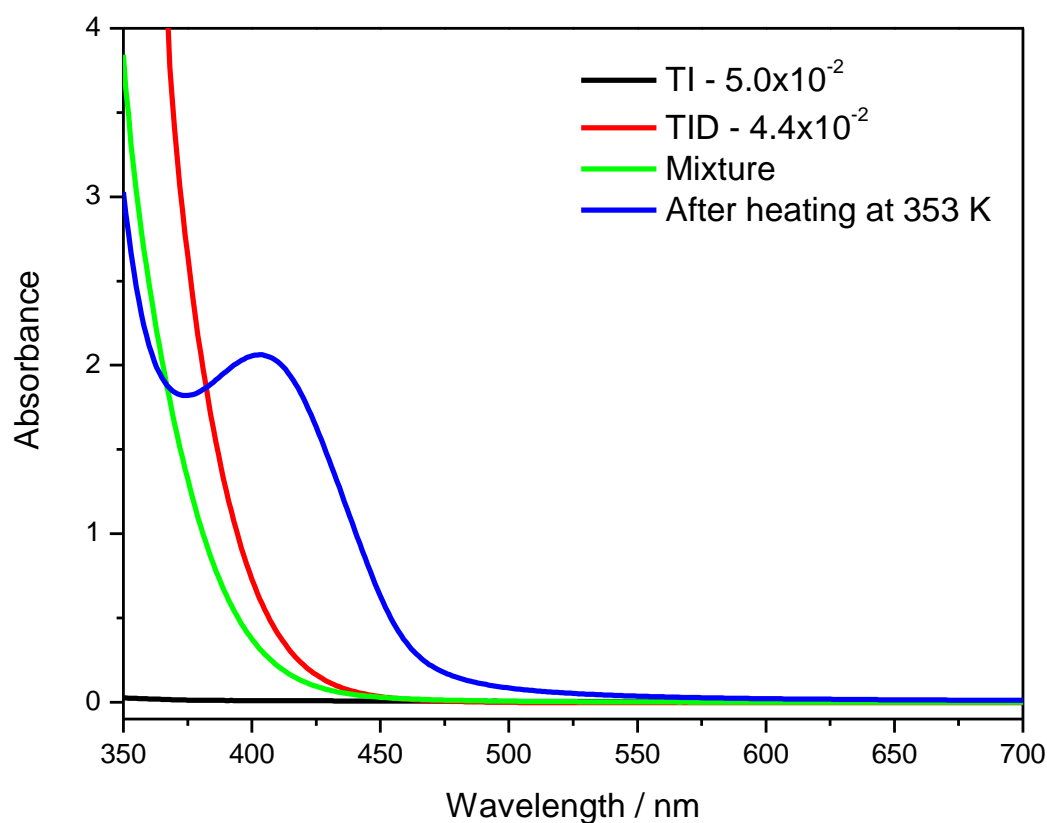


Figure 81. UV spectra of thermolysis of TID + TI in acetonitrile – visible region

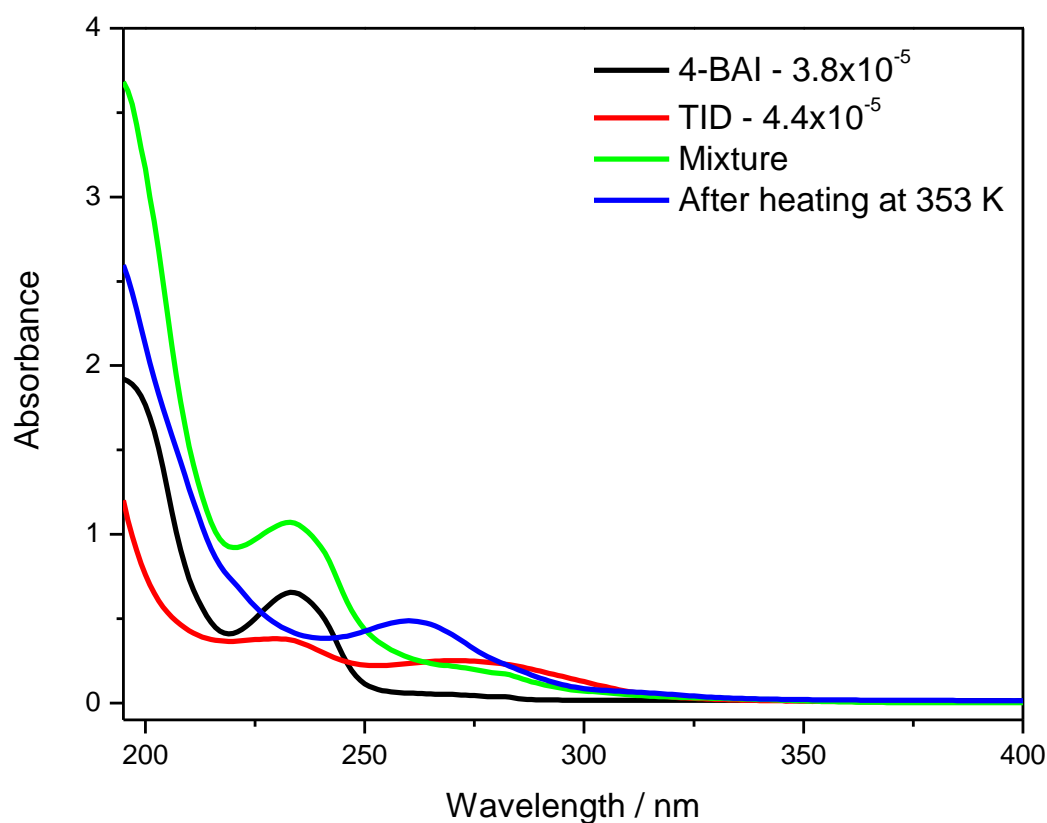


Figure 82. UV spectra of thermolysis of TID + 4-BAI in acetonitrile – UV region

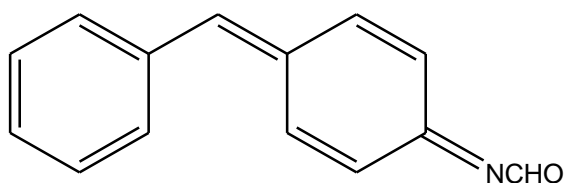


Figure 83. Quinone type structure arising from 4-benzylphenyl isocyanate (4-BAI)

An experiment was then carried out to follow the reaction over time to determine if the feature at 260 nm would increase as the reaction progressed. A solution of TID + 4-BAI in acetonitrile was heated to 313 K and followed by drawing samples periodically for analysis. The reaction was carried out at both high and low concentrations to analyse both the visible and UV regions. The spectra recorded in the UV region is presented in Figure 84 and shows a feature appears at ~270 nm after the first sample is analysed at 30 minutes. Again this could possibly be due to a quinonoid compound. Over time this peak shows slight differences in size, although these are not consistent with respect to time; this is presented in Figure 85, where the absorbance at 273 nm was plotted against time. The feature at 230 nm which refers to the isocyanate, does not change as the reaction proceeds. The spectra in the visible range (Figure 86) also shows no evident changes to the solution.

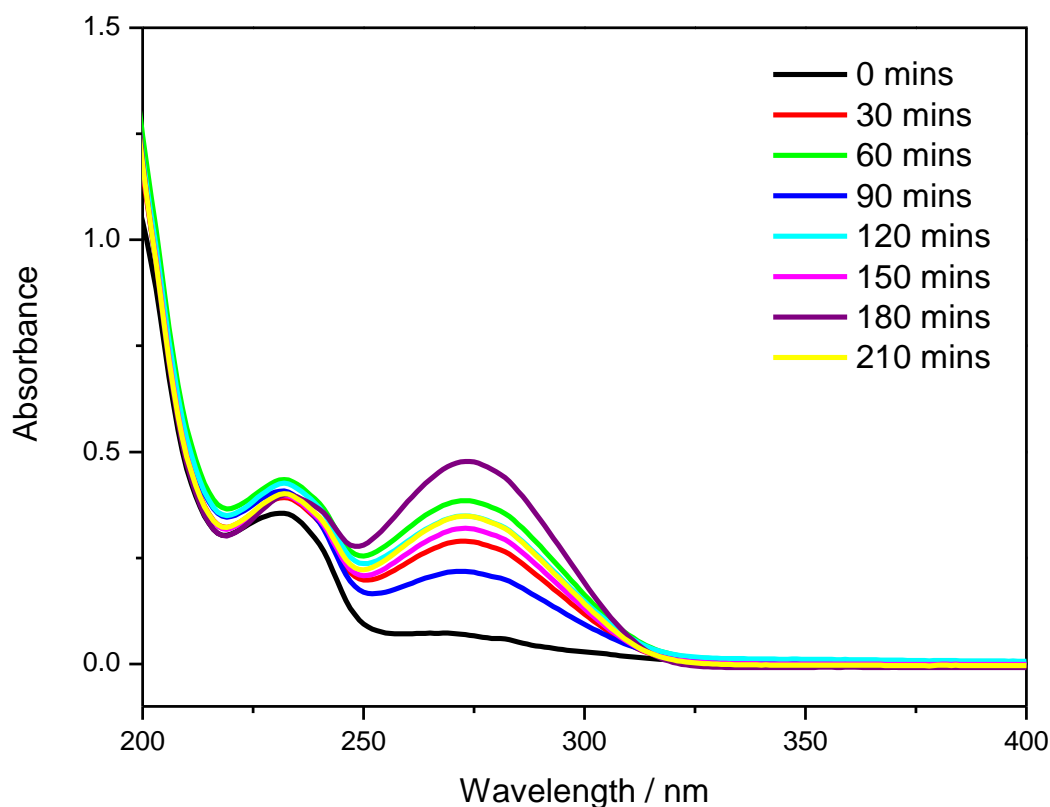


Figure 84. UV spectra of thermolysis of TID + 4-BAI in acetonitrile at 313 K over 3.5 hours – UV region

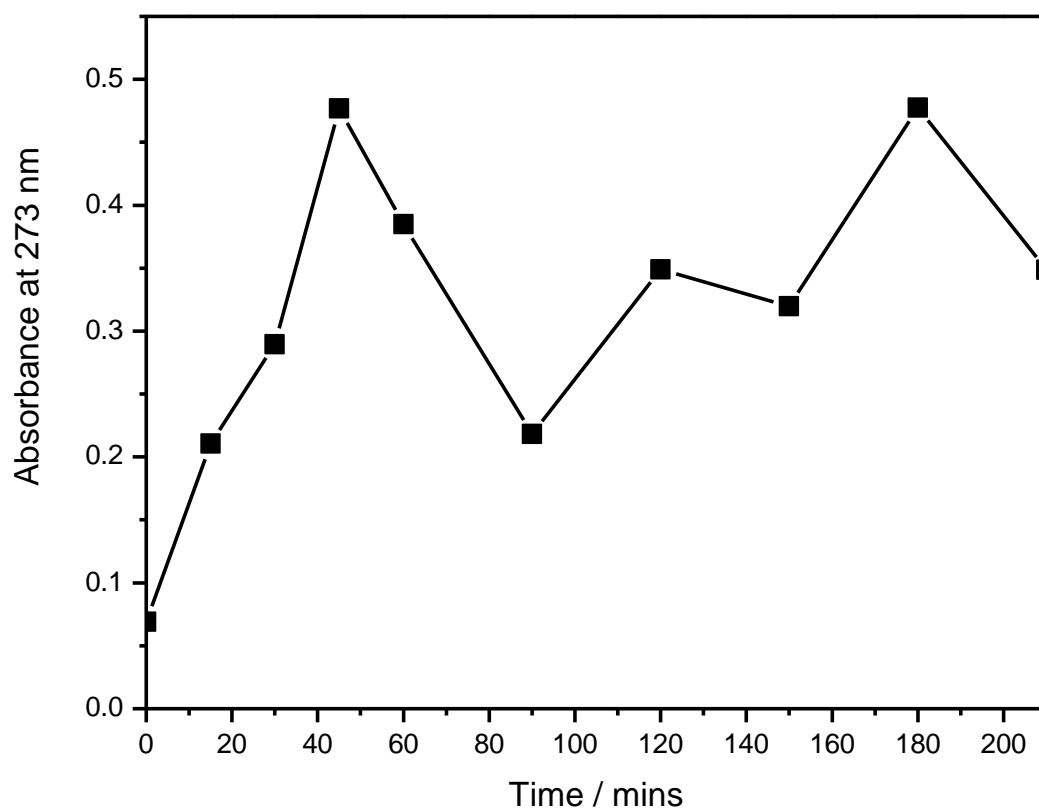


Figure 85. Plot of absorbance at 273 nm vs time for reaction of TID + 4-BAI at 313 K

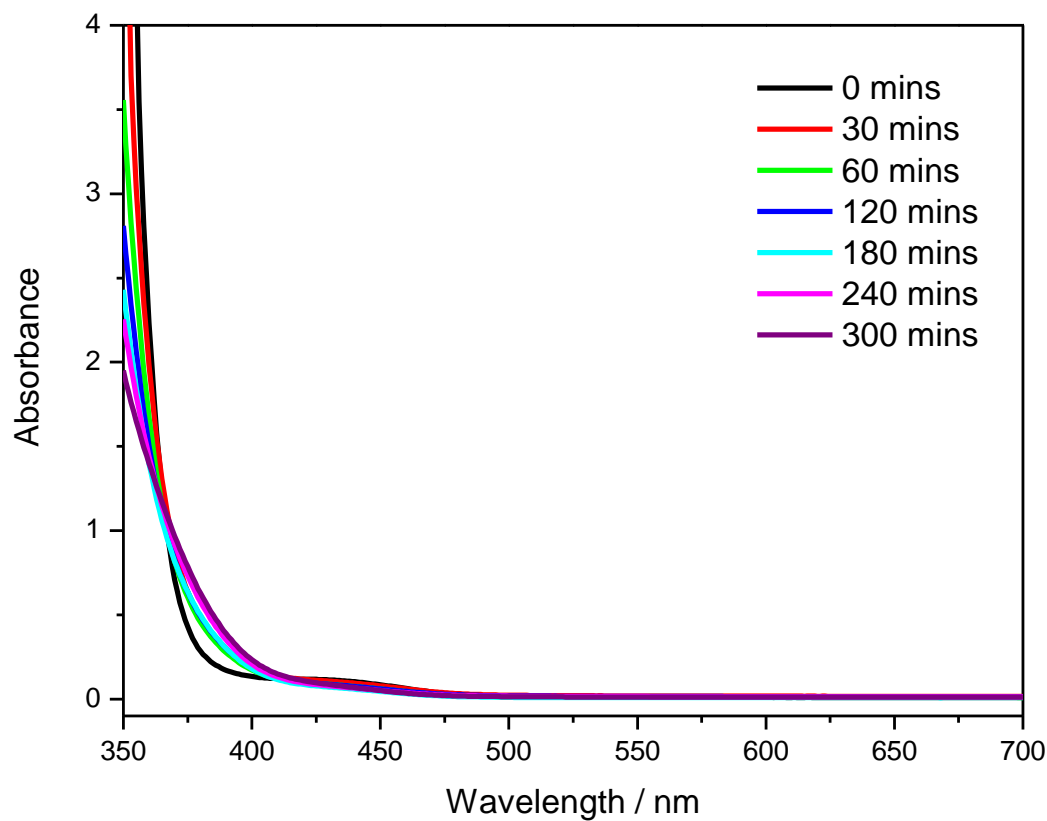


Figure 86. UV spectra of thermolysis of TID + 4-BAI in acetonitrile at 313 K over 5 hours – visible region

A reaction was carried out with the third isocyanate, MDI. Again the solution was heated to 353 K for 1 hour and spectra recorded in both UV and visible regions (Figure 87 and Figure 88). The low concentration spectra show a feature at 275 nm in the mixture before the heating process. However this disappears after the reaction, this is contradictory to what is seen with the other isocyanates. Again, solid particles had formed in the reaction. It is possible that as these particles were not soluble in acetonitrile, this contributed to the unexpected result that no features are seen in the UV spectrum after heating. At the higher concentration, the spectra show a shift in absorbance after heating. The solution mixture from this experiment turned from light yellow to orange, backing up what is seen in the spectra (visible region). This represents the first result for the observation of significant colouration. The reactions carried out up to this point suggest that the TID is reacting with the isocyanate but only to a small extent as little or no colour is observed. The most complex isocyanate, MDI, produces the highest absorbance and is most successful in delivering a positive result. These results are surprising as it was thought that the isocyanide dichlorides would readily react at low temperatures. At this juncture it was recognised that heating the solutions to 353 K was not causing major changes to the colouration of the solutions.

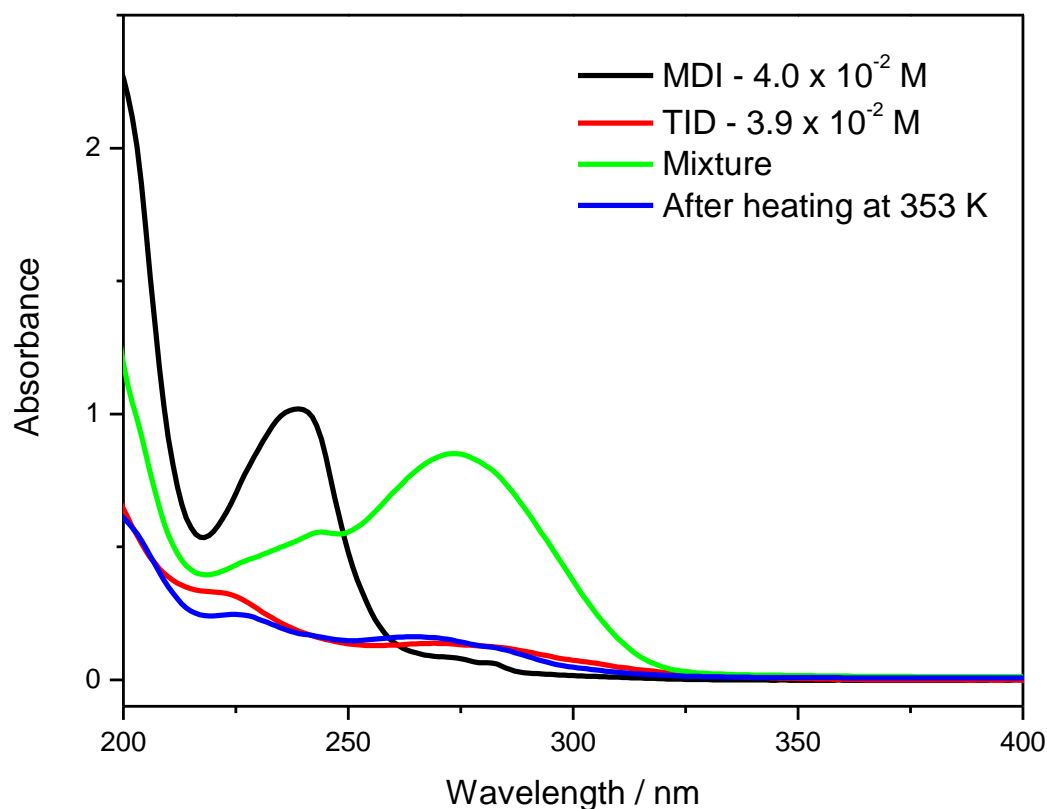


Figure 87. UV spectra of thermolysis of TID + MDI in acetonitrile – UV region

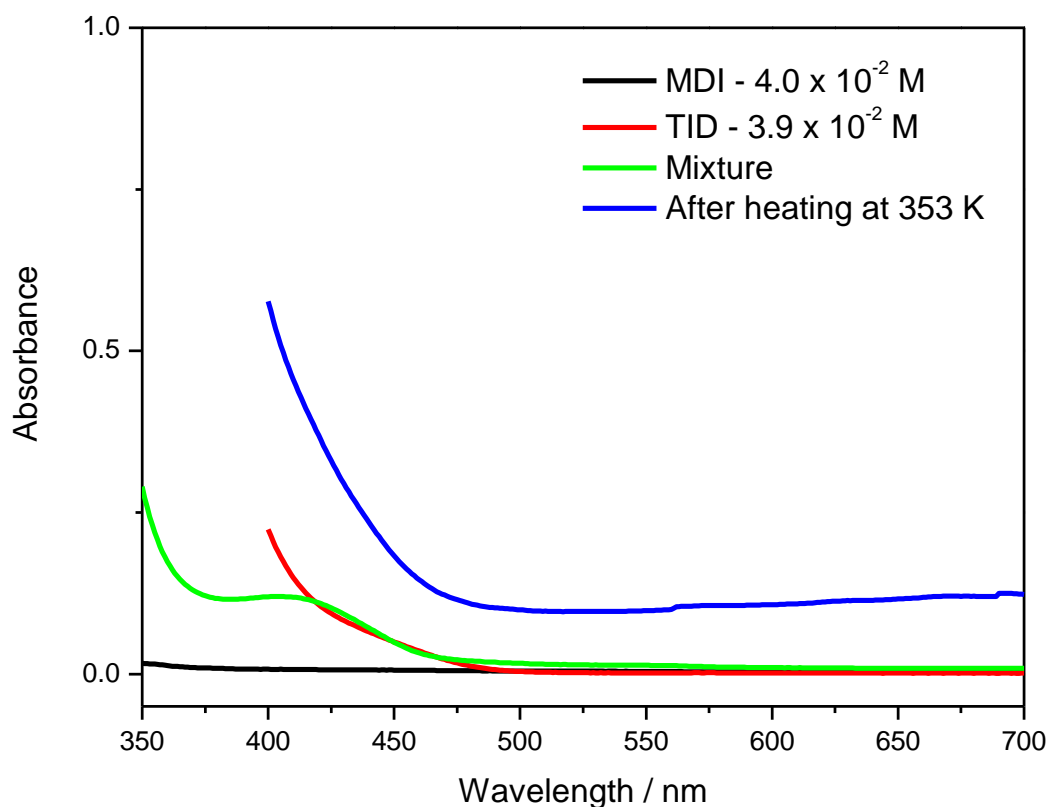


Figure 88. UV spectra of thermolysis of TID + MDI in acetonitrile – visible region

6.1.2 Photolysis Reaction

The use of an irradiation source was used to look at the effect of photolysis on a mixture of *p*-tolyl isocyanide dichloride (TID) + 4-benzylphenyl isocyanate (4-BAI) in order to investigate if this energy would succeed in promoting the reaction. Experiments were carried out at two concentrations to record both the UV and visible spectra. The resultant spectra show differences to the solutions heated at 353 K. The UV region of the spectra recorded (Figure 89) does not show any distinct features, however in the visible region the spectra recorded after irradiation shows the absorbance of the mixture shifts from ~375 nm to ~475 nm (Figure 90). The solution during the reaction changes from colourless to brown as shown in the picture in Figure 90.

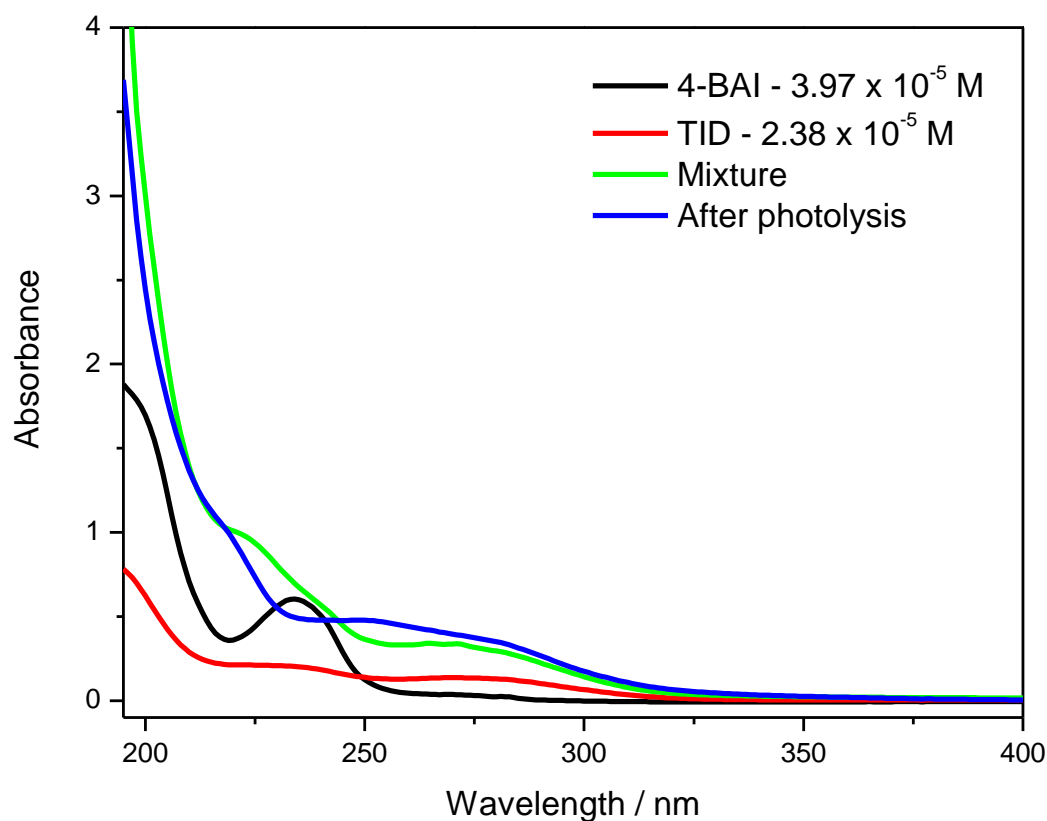


Figure 89. UV spectra of photolysis of TID + 4-BAI in acetonitrile – UV region

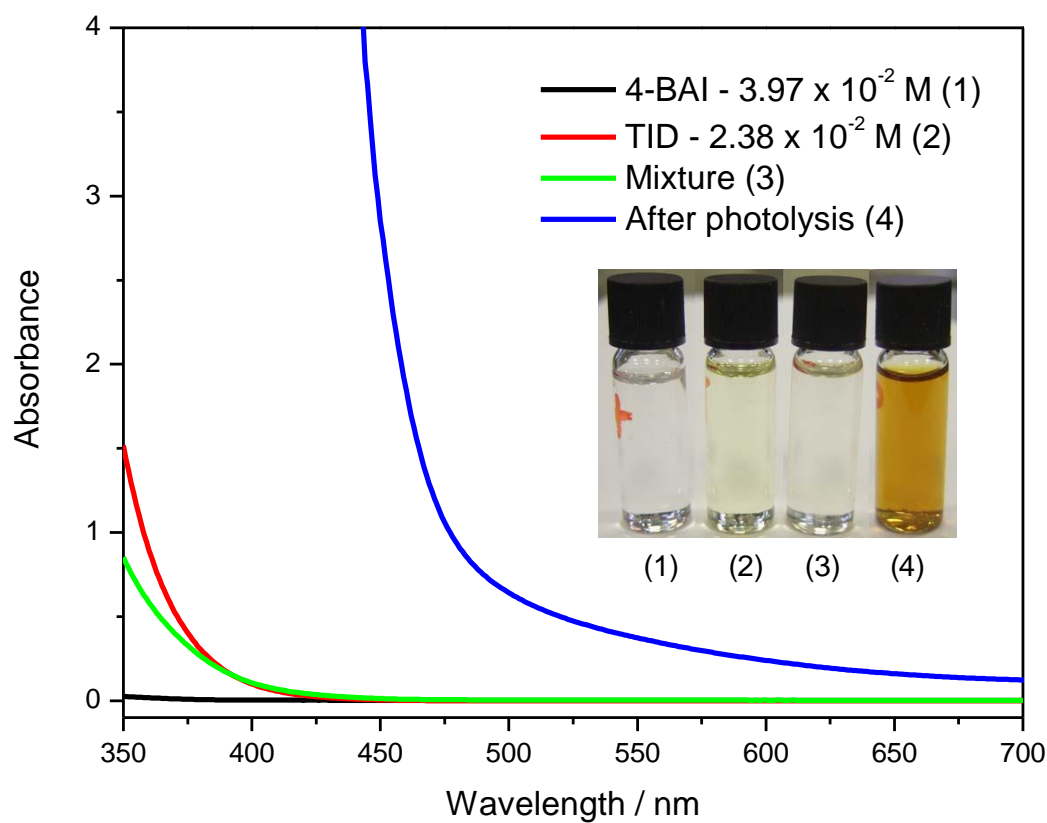


Figure 90. UV spectra of photolysis of TID + 4-BAI in acetonitrile – visible region

6.1.3 Identification of Products Using Spectroscopic Methods

In order to investigate the possible product formed in the reactions above, FTIR and $^1\text{H-NMR}$ analysis were carried out on reactions involving *p*-tolyl isocyanide dichloride (TID) and 4,4'-methylene diphenyl diisocyanate (MDI). For the thermolysis reaction no solvent was used in order to allow the reaction to take place at a higher temperature. Both compounds were added to a round bottom flask connected to a condenser and heated to 373 K for one hour. As the MDI melts at ~ 313 K the application of a solvent was not needed for the reactions to mix. The product formed from the reaction was a dark brown/red oil. For the photolysis reaction a solution of TID + MDI in acetonitrile was irradiated for 3 hours. Afterwards the solvent was evaporated to leave a brown oil. Both products were analysed using ATR-FTIR and $^1\text{H-NMR}$ (chloroform-d used as a solvent). Figure 91 and Figure 92 show the spectra obtained along with the spectra of the starting materials for comparison.

The infrared spectra of the products after both reactions show a considerable amount of the MDI is still present ($\nu(\text{C=O}) = \sim 2260 \text{ cm}^{-1}$), however the band referring to the C=N stretch of the TID (1647 cm^{-1}) has almost disappeared. In the thermolysis case a band at 1750 cm^{-1} indicates possible hydrolysis to the carbamoyl chloride is taking place, however after photolysis an unknown band appears at 1690 cm^{-1} . Bands at $\sim 800 \text{ cm}^{-1}$ and $\sim 1570 \text{ cm}^{-1}$ are possibly due to loss of aromaticity in the MDI compound, however this is limited. A peak at $1700 - 1750 \text{ cm}^{-1}$ indicates a new carbonyl species is being formed. These results are in comparison to the reaction carried out by Schollenberger on a MDI based urethane compound.¹⁵⁴ The $^1\text{H-NMR}$ spectra recorded is ambiguous, however in both cases the peak for the methylene bridge in MDI at 3.75 ppm appears after the reaction, on the other hand the methyl group on the TID (peak at 2.20 ppm) decreases. From these results no distinct product can be identified and only a small amount of the isocyanate has reacted. Hence backing up the conclusions from the UV/Vis spectra that no distinct changes are noted in the compounds that are reacting.

The results so far therefore indicate that the colouration cannot be linked to a new product as the chromophore cannot be identified by spectroscopic techniques. This implies the colouration is due to a low concentration species with a high molar extinction coefficient. The UV spectra of reactions involving 4-BAI and the IR spectra looking at MDI may indicate the loss of aromaticity and the formation of a quinonoid type structure. This would relate to the yellowing seen in aromatic based polyurethanes.⁵

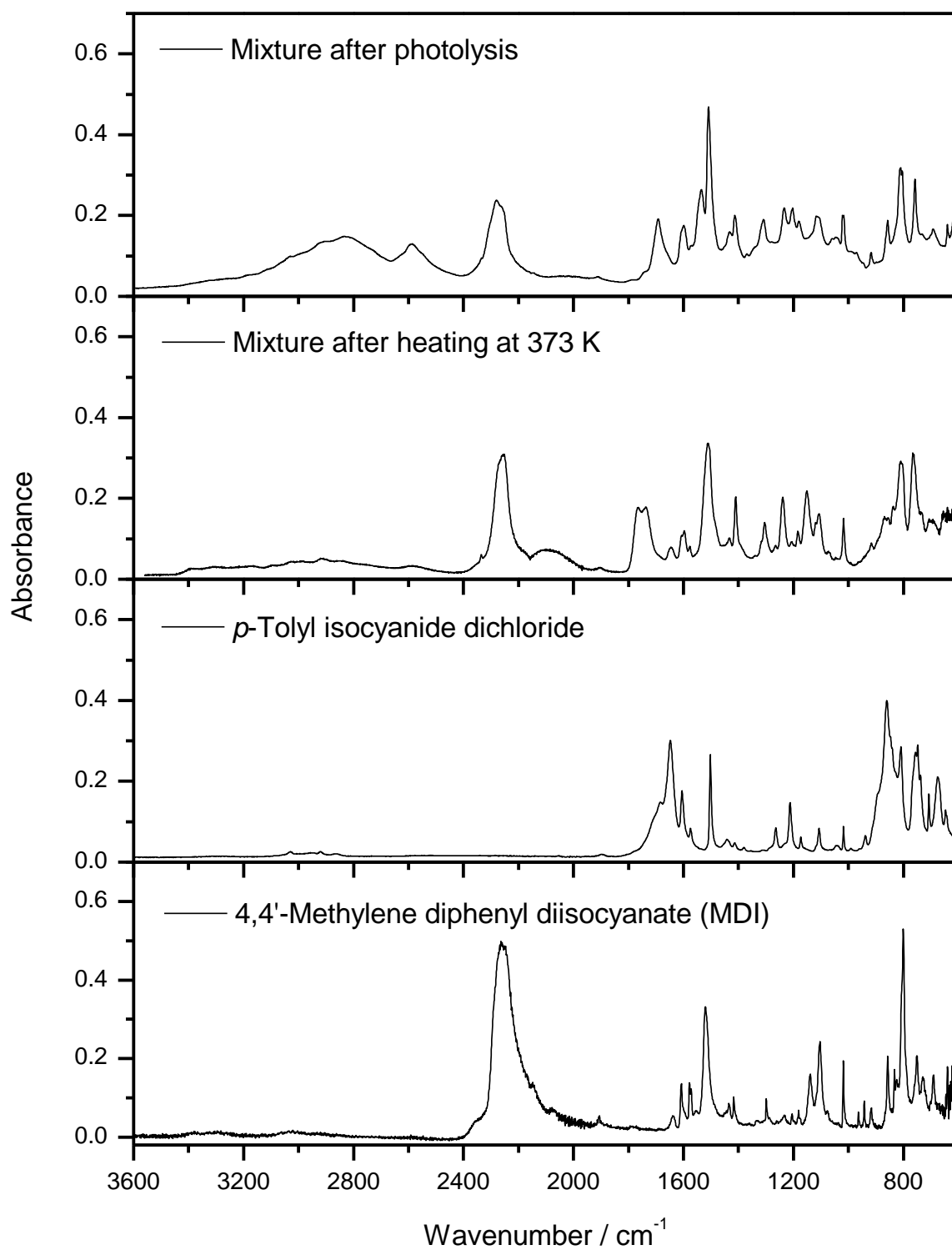


Figure 91. FTIR spectra of MDI, TID and mixtures after heating at 373 K and photolysis

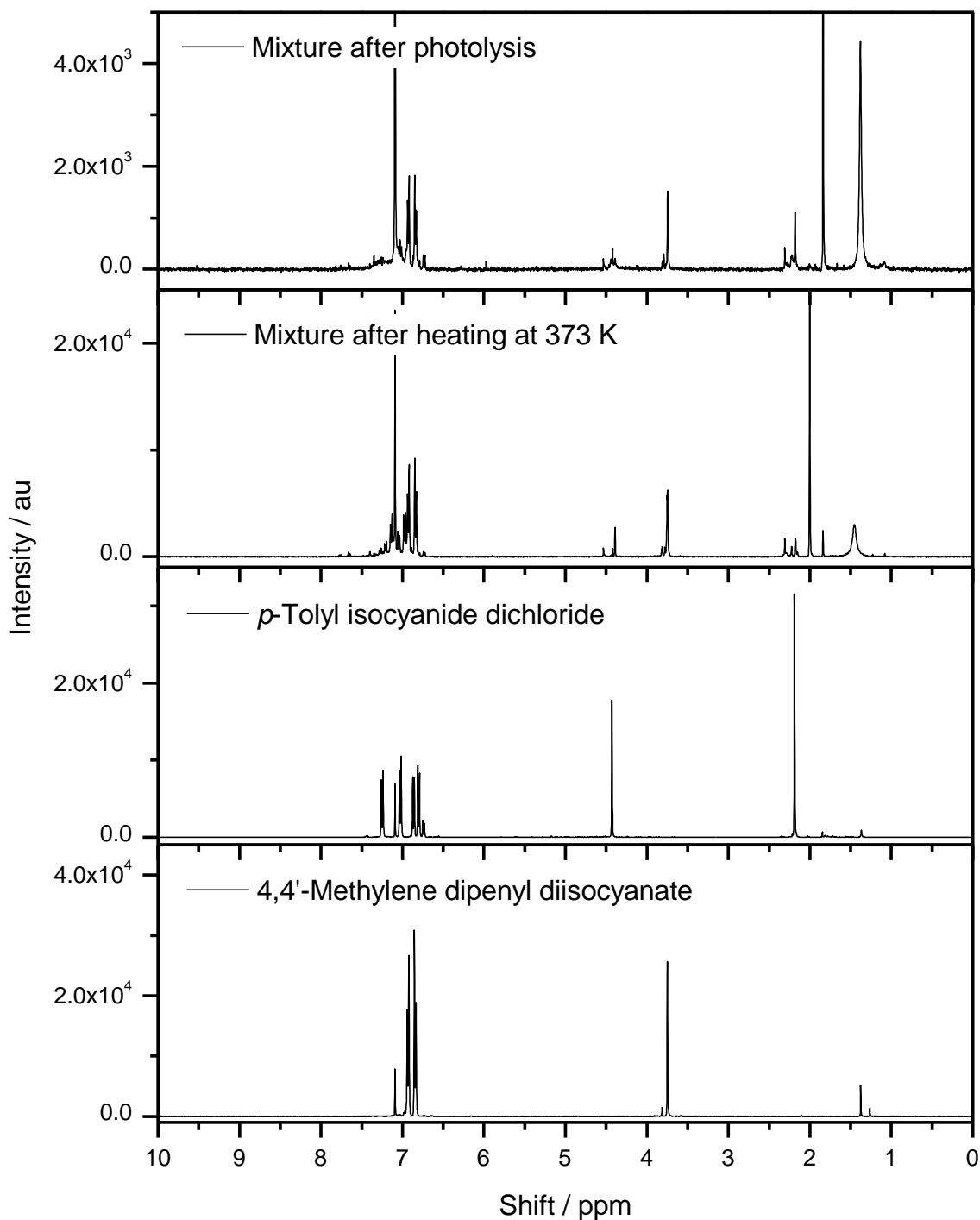


Figure 92. ^1H -NMR spectra of MDI, TID and mixtures after heating at 373 K and photolysis

6.1.4 Analysis and Characterisation of Isocyanide Dichlorides

It is clear from the thermolysis reactions carried out thus far that further characterization of the isocyanide dichlorides was needed. Both phenyl isocyanide dichloride (PID) and *p*-tolyl isocyanide dichloride (TID) were comprehensively analysed by FTIR, ^1H and ^{13}C NMR, GCMS, thermal analysis (TGA and DSC) and by calculation of the available

chlorine. These methods and the results are outlined in section 2.11. The TGA carried out on the compounds shows that they start to decompose at 338 K. However the majority of the mass loss occurs between 393 and 413 K. Hence further thermolysis reactions were carried out at higher temperatures. It is conceded that the early colour studies were perhaps over-cautious but it is noted that molecules with a number of Cl atoms can be prone to thermal decomposition due to steric interactions¹⁵⁵ and a cautious approach was initially favoured.

6.1.5 Heat Treatments (High Temperature Studies)

Mixtures of *p*-tolyl isocyanide dichloride (TID) + 4-benzylphenyl isocyanate (4-BAI) in solution were heated to 403 K and 453 K for 2-3 hours and the analysis carried out by UV/Vis. In order to reflux the solutions at these temperatures a different solvent to acetonitrile had to be used. The process solvent, chlorobenzene (bp = 405 K) and *o*-dichlorobenzene (bp = 453 K) were used, however this restricted the spectra that could be recorded as these solvents interfere in the absorption below 300 nm therefore only the visible range could be studied. Figure 93 and Figure 94 show the resultant spectra. At 403 K the product solution shows a peak at ~ 430 nm indicating the colour change seen in the associated picture of the vial (light yellow). The reason for the spectra absorbing above 550 nm is due to the solid particles in the solutions. These particles likely arise from the hydrolysis of the TID to the insoluble carbamoyl chloride as the absorbance is seen before the reaction in the solution of TID with 4,4'-methylene diphenyl diisocyanate (MDI).

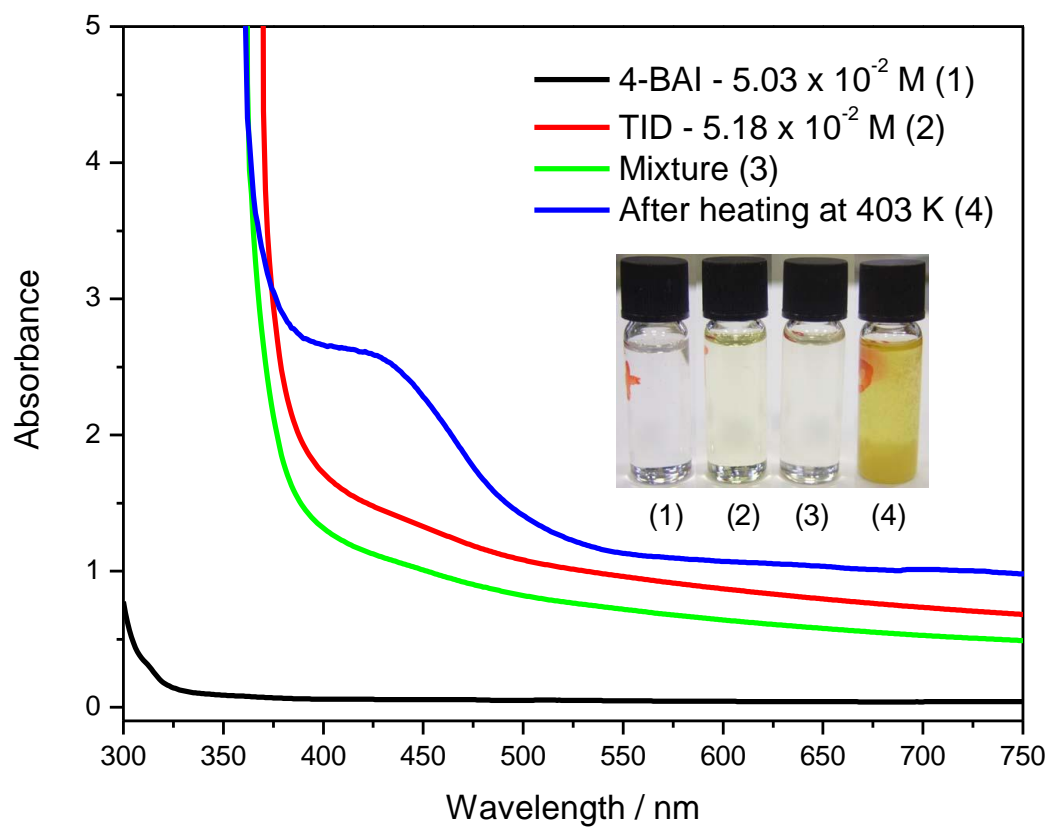


Figure 93. UV spectra of thermolysis of TID + 4-BAI in chlorobenzene at 403 K

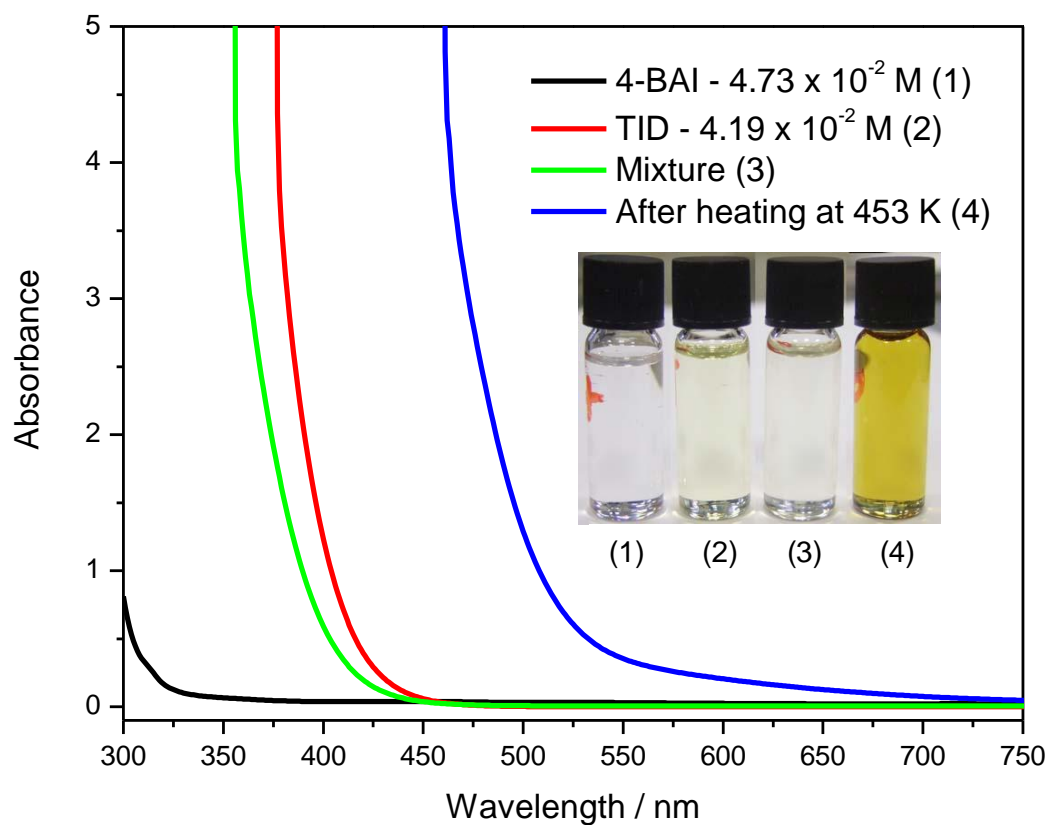


Figure 94. UV spectra of thermolysis of TID + 4-BAI in *o*-dichlorobenzene at 453 K

At the higher temperature of 453 K the absorbance of the solution after heating is increased to ~475 nm, with the absorbance going off the scale at this point. Again this is reflected in the picture, where the solution after heating is dark yellow in colour. These results are consistent with the TGA and DSC analysis proving that a high amount of energy is needed to break down the isocyanide dichloride molecule. In the reactions studied thus far, the use of light (broad band UV-Vis irradiation) and a temperature of 453 K are sufficient to allow decomposition of the dichloride to produce colour formation. However the way in which decomposition occurs and the source of the colouration are not clear at this juncture.

The postulated reaction mechanism involves attack of the methylene bridge in polymeric MDI by chlorine radicals produced from isocyanide dichlorides to form a conjugated compound.⁵¹ Therefore it was important to establish whether a different compound not containing any isocyanate groups would produce a similar result. The compound 1,4-dibenzylbenzene (DBB) was acquired from Sigma-Aldrich. This compound consists of 3 benzene rings attached by methylene linkages with no other functional groups (Figure 95). A solution of DBB + *p*-Tolyl isocyanide dichloride (TID) in *o*-dichlorobenzene (ODCB) was heated at 453 K for 3 hours. The spectrum of the solution after heating (Figure 96) shows an increase in absorption ~400 – 500 nm, with a yellow colour seen with the naked eye. ¹H-NMR spectra were recorded for this reaction, however no distinct changes were seen. This was not the result expected as it was hoped information regarding the attack of chlorine radicals on the methylene bridge would be distinguishable. This again demonstrates that as no clear evidence is seen in the spectroscopy for new products, the chromophore responsible for the colour is produced in small amounts.

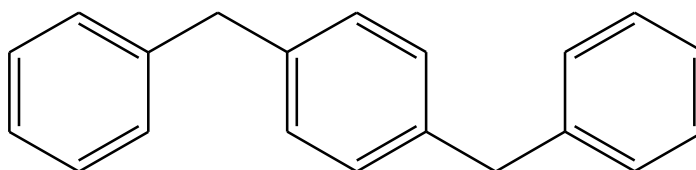


Figure 95. 1,4-Dibenzylbenzene

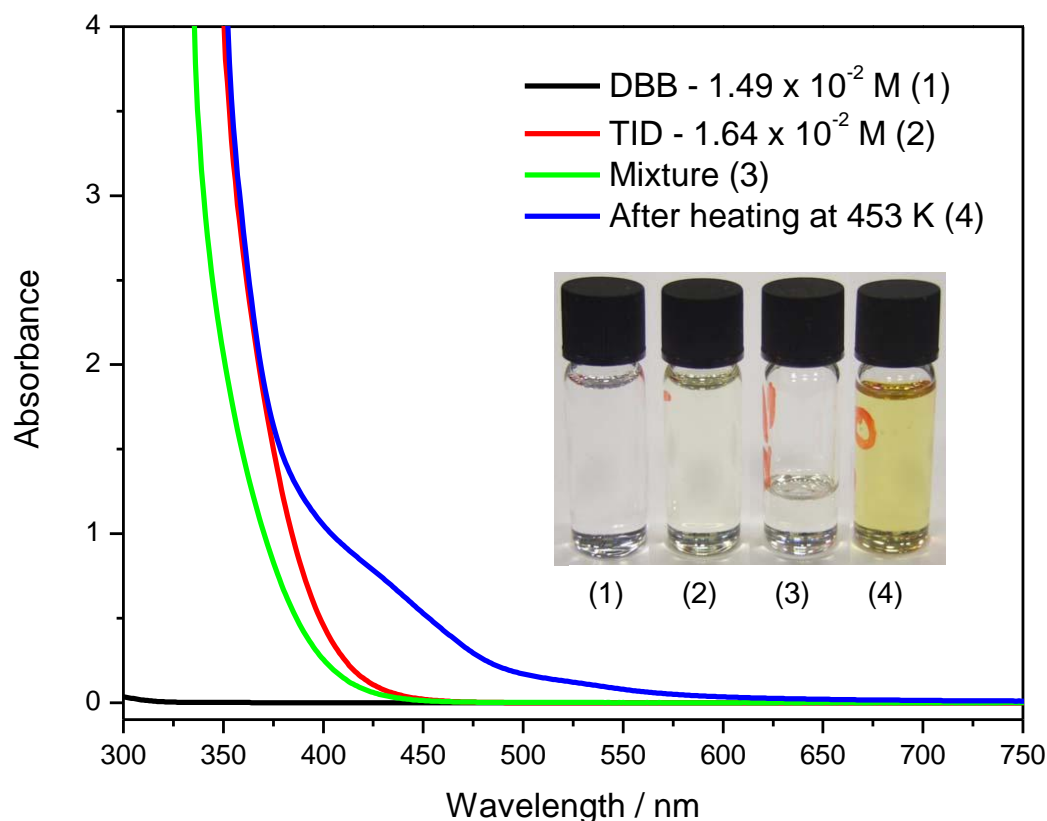


Figure 96. UV spectra of thermolysis of TID + DBB in *o*-dichlorobenzene at 453 K

Blank reactions whereby separate solutions of 4-benzylphenyl isocyanate (4-BAI) and *p*-tolyl isocyanide dichloride (TID) in *o*-dichlorobenzene (ODCB) underwent heating to 453 K were also carried out. The results from these reactions (Figure 97) were surprising as although the 4-BAI solution showed no changes, the TID solution showed a considerable colour change, with higher absorption in the range of 400 – 500 nm. This indicates the isocyanide dichloride molecule is reacting with itself and is acting as the main source of colour. The addition of isocyanate intensifies the colour, suggesting that the colouration arises from two contributions:

- a) Breakdown of *p*-tolyl isocyanide dichloride (TID)
- b) Reaction products via reaction of active phase of *p*-tolyl isocyanide dichloride (TID) and isocyanate

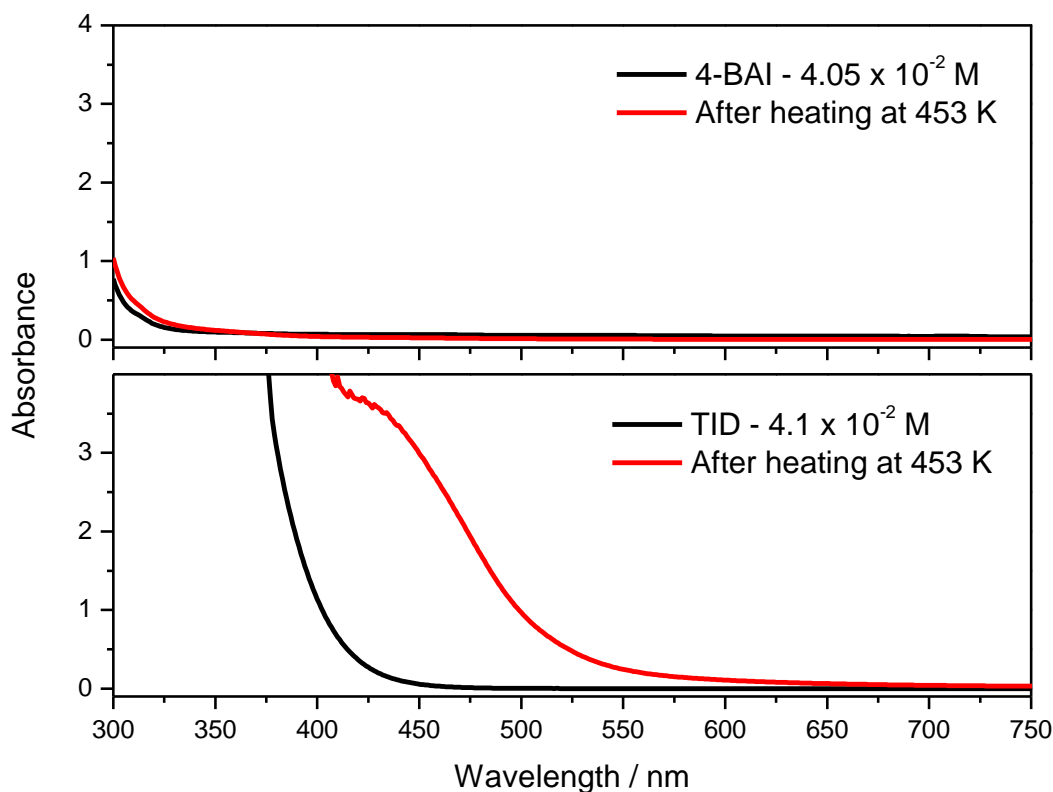


Figure 97. UV spectra of thermolysis of TID and 4-BAI in *o*-dichlorobenzene at 453 K

6.2 Source of Colour Formation

The reactions discussed in section 6.1 indicate TID as the main source of colour with the intensity increasing as a secondary reactant is added. To establish these results, the concentration dependence of the isocyanide dichloride was examined. Reactions that were carried out at Huntsman Polyurethanes Process Research & Development Laboratory in Rozenburg allowed the analysis of solutions using an industrial method.

6.2.1 Yellow Index Analysis (Rozenburg)

Yellow index is a test carried out at the industrial centre to test the quality of the product; it measures the yellow colour using absorbance methods (ASTM D1925).¹⁵⁶ A number of combinations of compounds were tested involving 4-fluoromethylphenyl isocyanide dichloride (4F-PID), 1,3-di-*p*-tolylchloroformamidine-*N*-carbonyl chloride (TCCC), phosgene and 4,4'-methylene diphenyl diisocyanate (MDI). Table 22 shows the solutions used. 4F-PID was used in these reactions as the fluorine would act as a marker in the GCMS analysis to help distinguish any product formed from the isocyanide dichloride

compound. For each experiment the concentration of 4F-PID or TCCC was varied, whilst keeping the concentration of MDI constant. The full reaction details can be found in section 2.13.2. Solutions were heated to 448 K for 2 hours, with analysis for yellow index carried out before and after the reaction.

Figure 98 shows the yellow index measurements of the different solutions with respect to the 4F-PID or TCCC concentration. For all the results the yellow index of the starting solution has been subtracted from the final result, therefore each line on the graph shows the increase in colour. The results show that the 4F-PID mixed with MDI gives the largest colour change, followed by the 4F-PID solution. The TCCC solutions also produce colour although not much change is seen when MDI is added. The TCCC solution in the absence of phosgene does not produce colour, this is due to the TCCC being converted to the carbodiimide as outlined in Section 4.1.1. The black square at 0.05 M indicates a solution of MDI in the absence of 4F-PID or TCCC. This acts as a blank and shows no colour is produced from MDI on its own. The graph also shows that the colour intensity increases with concentration of the 4F-PID or TCCC. In the case of the TCCC solutions the appearance of colour could be down to 2 possibilities:-

1. The 1,3-di-*p*-tolylchloroformamidine-*N*-carbonyl chloride (TCCC) is releasing chlorine to react further
2. The 1,3-di-*p*-tolylchloroformamidine-*N*-carbonyl chloride (TCCC) is first breaking down to the *p*-tolyl isocyanide dichloride which then produces colour

GCMS analysis was carried out on the highest concentrated solutions in each reaction after the experiment had been carried out. For the TCCC solutions in the phosgene atmosphere, the *p*-tolyl isocyanide dichloride (TID) and the *p*-tolyl isocyanate (TI) are seen in the spectrum. Thus it is very likely the isocyanide dichloride is responsible for the colouration rather than the TCCC directly.

Experiment Number	Reactants
1	MDI
2	4F-PID
3	4F-PID + 0.05M MDI
4	CCC + 0.05M MDI
5	CCC with 1% phosgene
6	CCC + 0.05M MDI with 1% phosgene

Table 22. Solutions used to measure yellow index

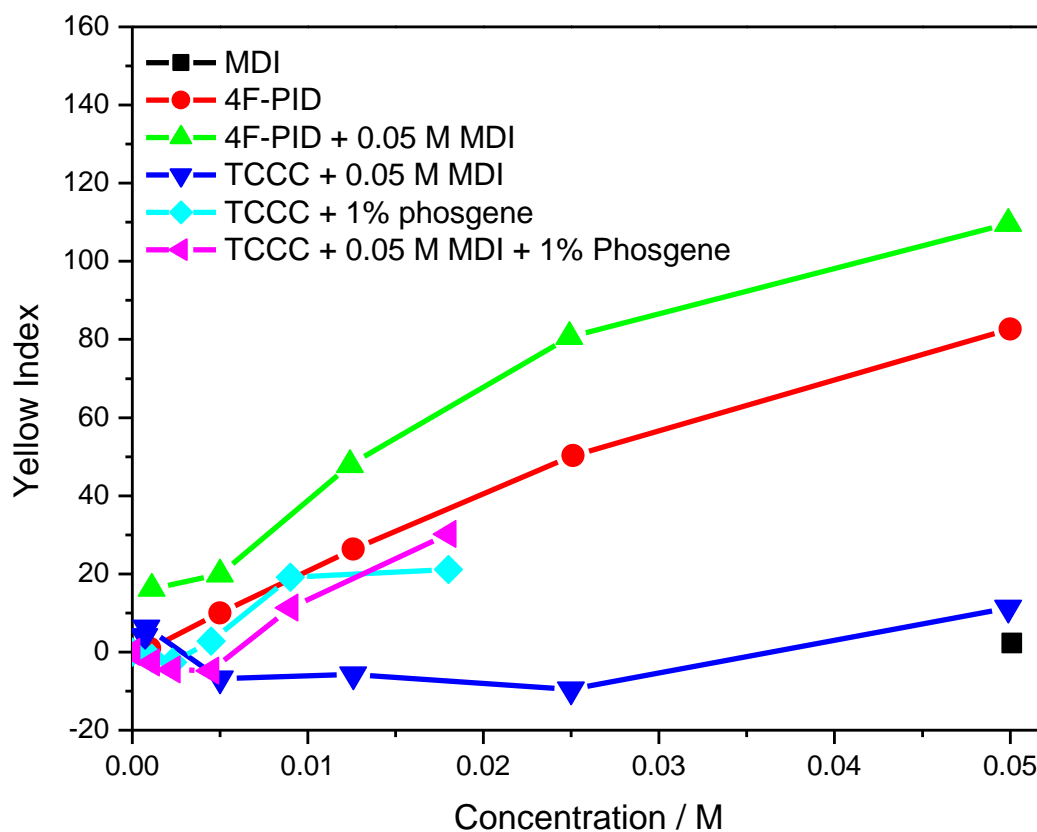


Figure 98. Graph of yellow index vs concentration for solutions heated at 448 K for 2 hours

6.2.2 Thermolysis and Photolysis of Isocyanide Dichlorides – Concentration Dependence

After identifying the isocyanide dichloride moiety as a source of colour, further reactions were carried out in order to understand the reaction mechanisms occurring in both the thermolysis and photolysis of isocyanide dichlorides. For this a series of reactions were carried out involving phenyl isocyanide dichloride (PID), 4,4'-methylene diphenyl diisocyanate (MDI) and polymeric MDI. Three different combinations were looked at, PID in ODCB, PID + MDI in ODCB and PID + polymeric MDI in ODCB. For each combination a number of solutions containing differing PID concentrations were made up, with the isocyanate concentration kept constant throughout. See section 2.14.3 for experimental details. Each solution was heated to 448 K or irradiated in a photoreactor for 2 hours. Reactions involving heat were carried out both with and without a nitrogen purge. UV spectroscopy was used to look at the changes in absorbance of the solutions before and after the reactions.

The UV spectra for the reactions of phenyl isocyanide dichloride (PID) in ODCB can be seen in Figure 99 along with colour pictures of the solutions. The solution with the highest concentration of PID is on the left hand side, decreasing to the right. For the starting solutions an increase in the concentration of PID results in absorption at a higher wavelength. After heating at 448 K, a similar pattern is seen and each solution has also shifted to a higher wavelength. However the photolysis results are different, a shift in the wavelength is still seen in all of the solutions however it is not concentration dependent. When looking at the solutions containing MDI and PMDI, Figure 100 and Figure 101 respectively, similar results are seen. In each case the photolysis of the material produces a higher shift in wavelength, however heating of the solutions is uniform with respect to concentration. The only exception in this case is the highest concentration of PID in the presence of MDI after heating. This is an anomalous result although a repeat of the reaction produced the same outcome. The starting solution with the highest concentration in the PID + PMDI case shows a high absorbance, this is due to solid particles in the mixture.

It is noted at this point that combining PID and polymeric MDI at 448 K leads to highly coloured solutions. In fact the colouration seen in the vials in Figure 101 is similar to that encountered in the industrial operation. Thus it is thought that the trends seen at the industrial complex are being reproduced and the proceeding methodology provides some insight to factors that influence the process of colour formation.

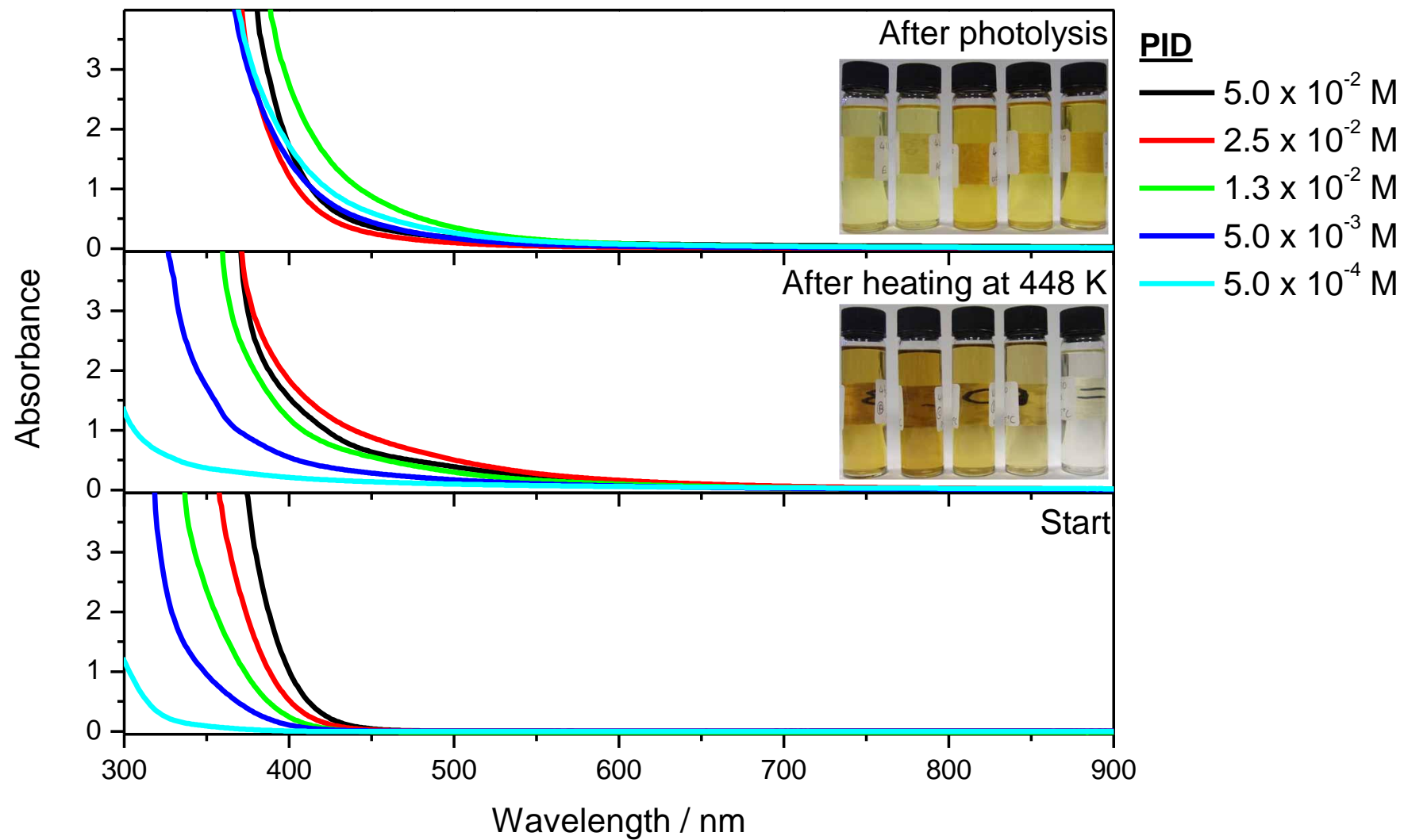


Figure 99. UV spectra of solutions of PID (at different concentrations indicated) before and after heating at 448 K or photolysis for 2 hours

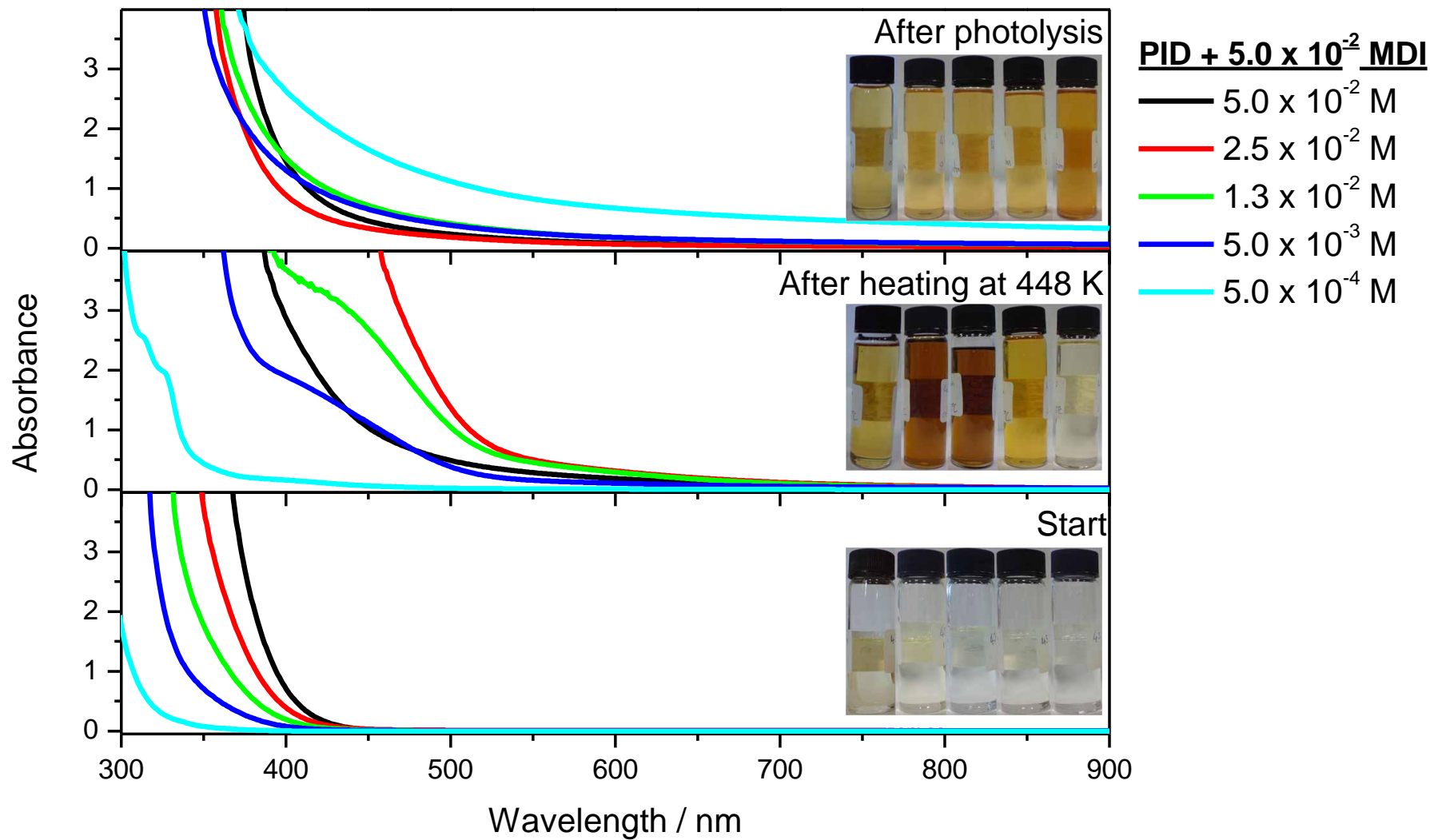


Figure 100. UV spectra of solutions of PID (concentrations shown in legend) + 0.05 M MDI before and after heating at 448 K or photolysis for 2hours

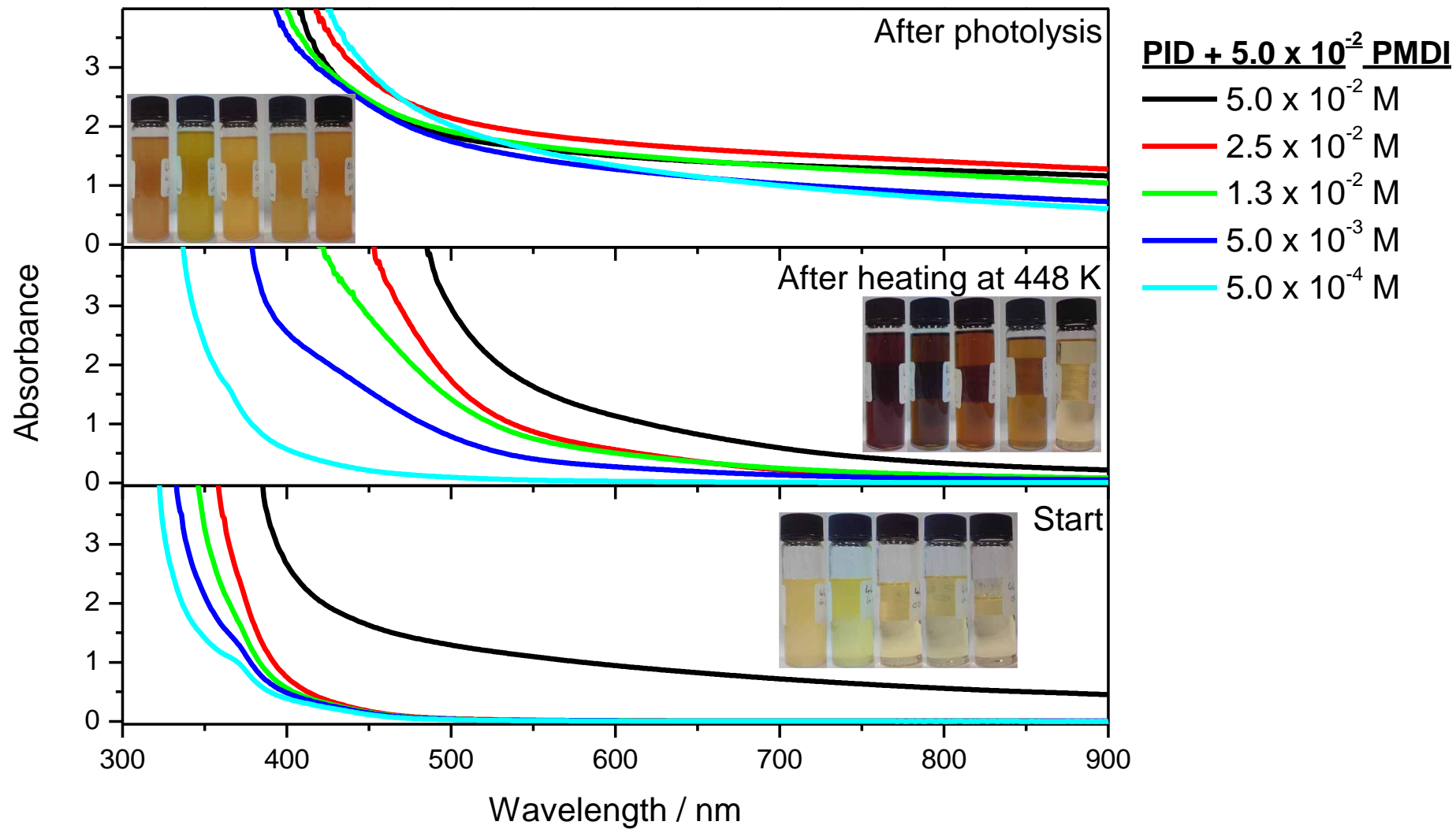


Figure 101. UV spectra of solutions of PID (concentrations shown) + 0.05 M polymeric MDI before and after heating at 448 K or photolysis for 2 hours

6.2.3 Nitrogen Purge Experiments (High Temperature)

The thermolysis reactions involving MDI and PMDI were repeated using a nitrogen purge throughout the reaction. The UV spectra are shown in Figure 102 and Figure 103. These results differ drastically from those seen before (Figure 100 and Figure 101). Again all the solutions are consistent with regards to concentration of PID. However the shift in wavelength after heating is not as dramatic as in the solutions without the N₂ purge. In order to compare all of the reactions, the integrals of the curves between 450 and 500 nm was plotted against concentration (Figure 104). The solutions were also examined visually; Table 23 shows pictures of the solutions after the reaction has taken place. It is clear from the results that with both heating and irradiation, the colour intensity increases with the conjugation of the isocyanate, i.e. PMDI gives the darkest coloured solutions. For the photolysis reactions the concentration of the PID does not seem to affect the colour, whereas it does have an effect on the heated solutions. Generally with the heated reactions the intensity of the colour increases with PID concentration. The reactions with the nitrogen purge produce colour that is less intense than the reactions with no nitrogen.

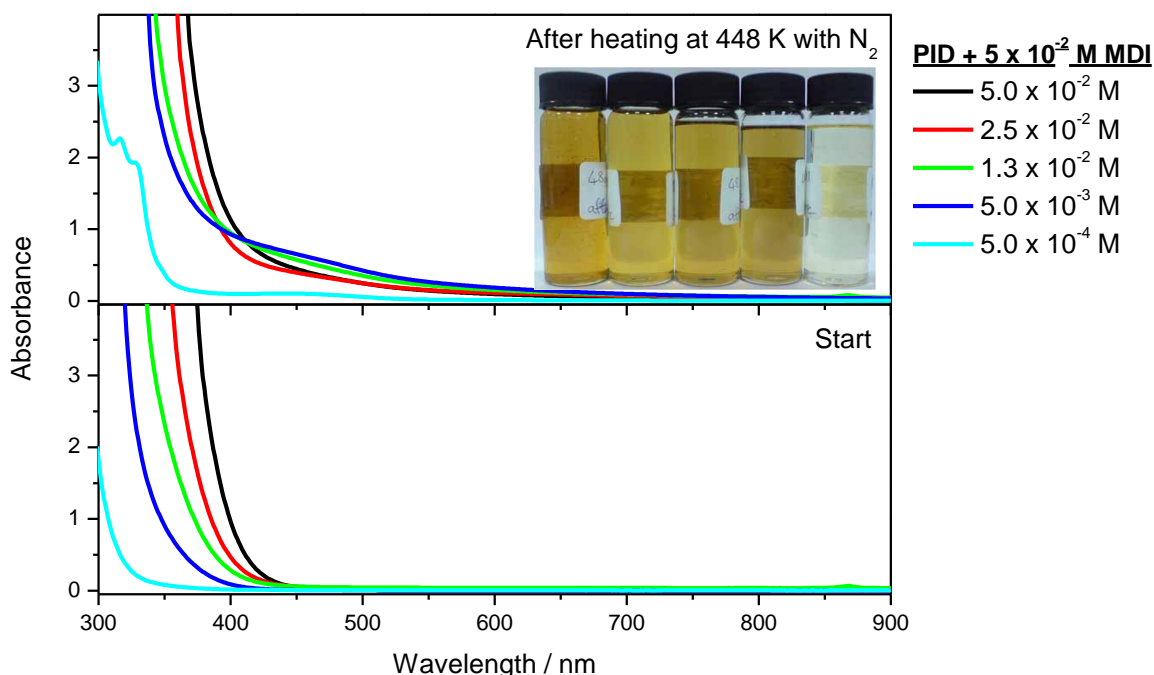


Figure 102. UV spectra of PID + 0.05 M MDI in solution before and after heating at 448 K with a N₂ purge for 2 hours

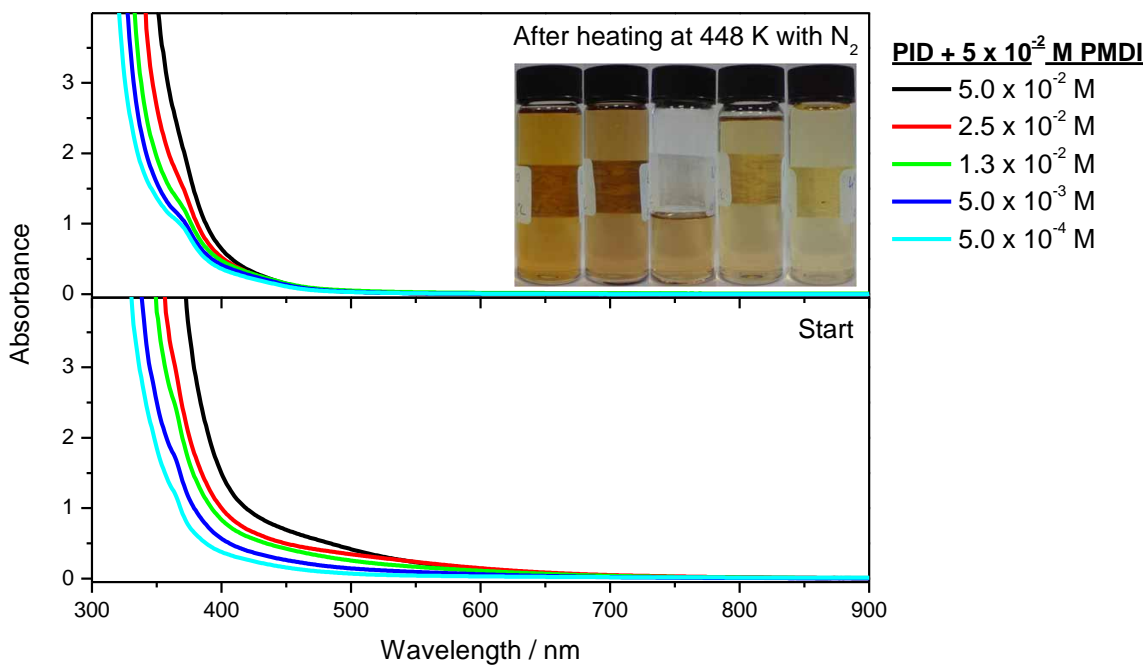


Figure 103. UV spectra of PID + 0.05 M PMDI in solution before and after heating at 448 K with a N_2 purge for 2 hours

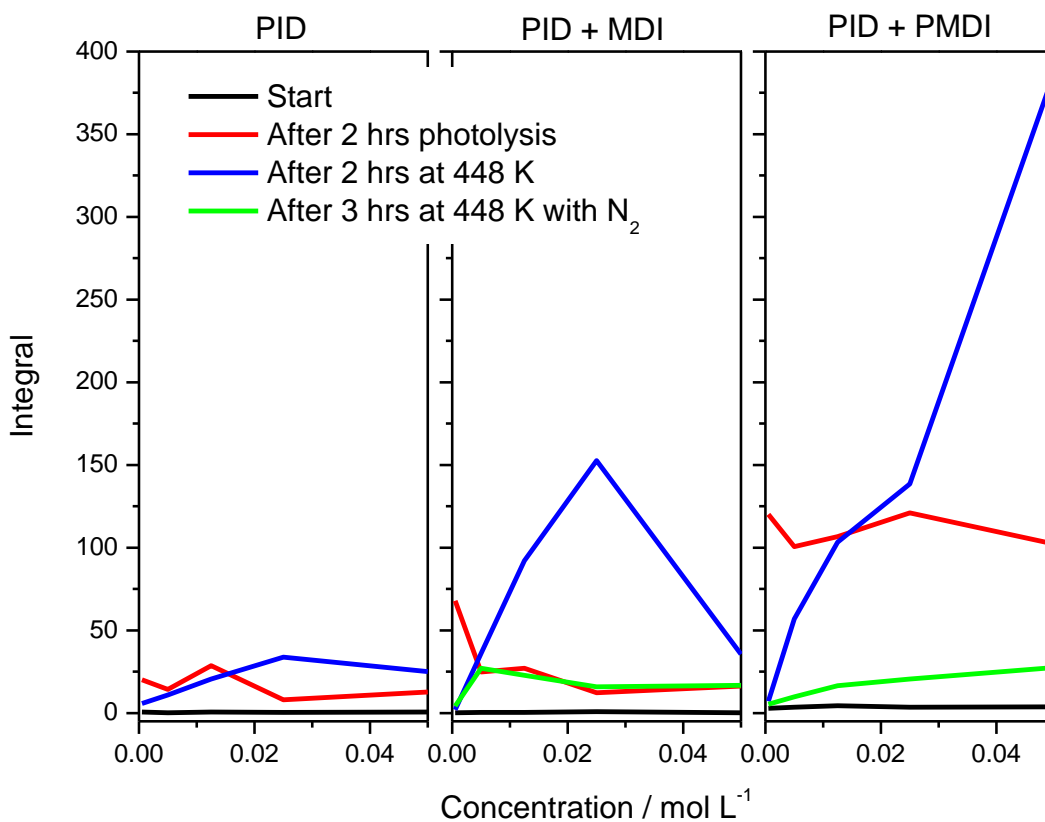


Figure 104. Integrations of the UV spectra from Figure 99 to Figure 101

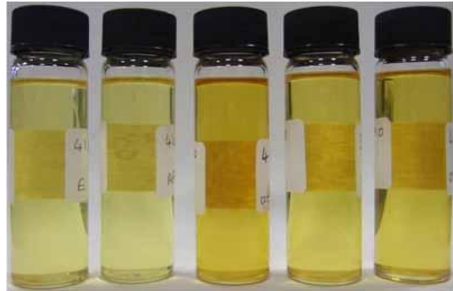

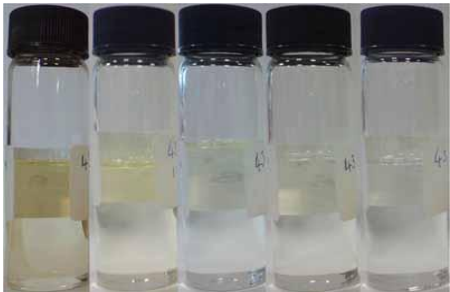
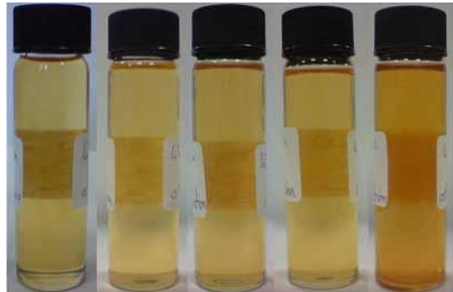


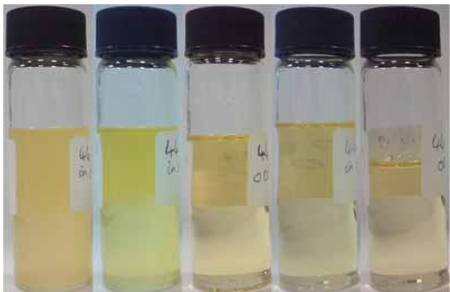



	At start	After photolysis	After heating at 448 K	After heating at 448 K with N ₂ purge
PID	Photograph not available			NA
PID + MDI				
PID + Polymeric MDI				

Table 23. Colour photos of solutions of PID, PID + MDI and PID + PMDI before and after reactions (highest concentration is on the left hand side, decreasing to the right)

Two of the reactions carried out were also studied over time. Both reactions contained PID + polymeric MDI, one with a nitrogen purge and one without (Figure 105). The results from these showed that once the colour is initially formed the reaction slows down, where little if any more colouration is seen. This profile is suggestive of a concentration limited reaction.

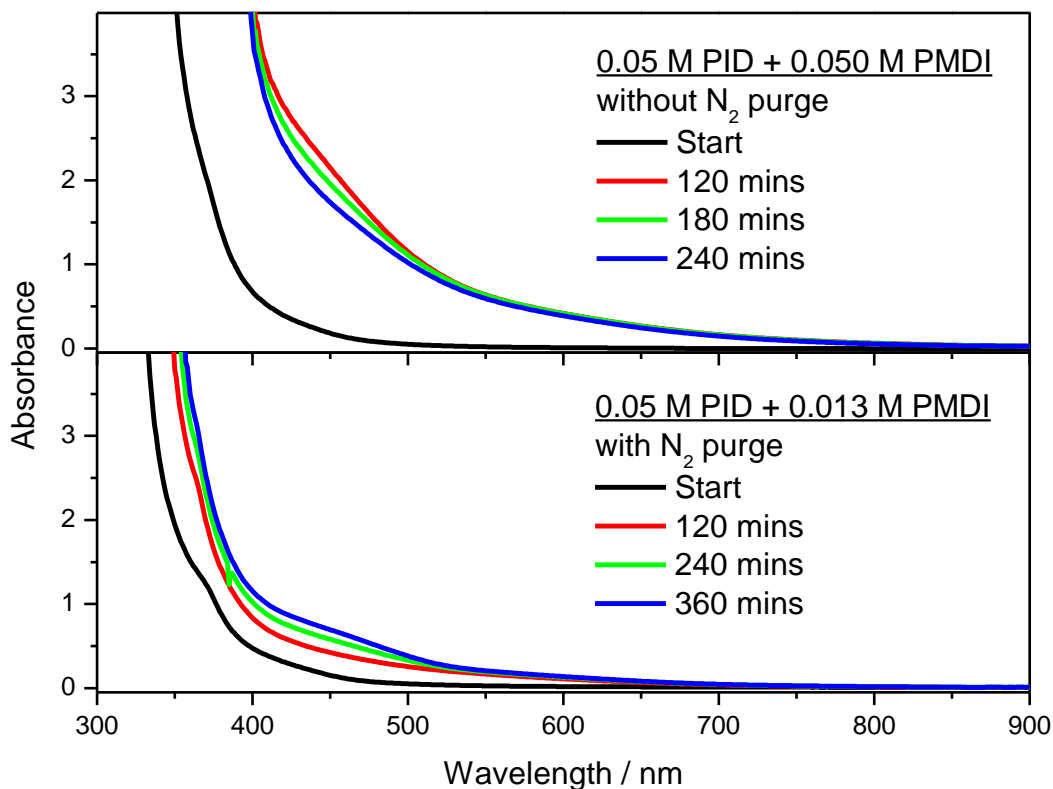


Figure 105. UV spectra of PID + PMDI in solution heated to 448 K over time

In order to back up the results seen, a reaction was carried out whereby a solution of PID + PMDI was heated to 448 K for 2 hours with the N_2 purge. After this time the purge was stopped and samples taken for a further 2 hours. The results, shown in Figure 106, show that an increase in absorbance is seen after the first hour with the N_2 purge. This does not change after the second hour. When the N_2 purge is stopped, the absorbance increases for a second time, then is unchanged after the fourth hour. These results confirm that the use of the inert gas quenches the reaction and that after the initial increase in absorption, no further increase in colouration takes place.

Summarising, these purge experiments establish the processes leading to colour, Cl^{\bullet} formation following thermal decomposition of phenyl isocyanide dichloride (PID), which can then react with MDI, however, the presence of air (O_2) appears to amplify the

colouration process. Temporal studies (Figure 105) suggest the amplification process to be concentration limited with respect to an unspecified reagent.

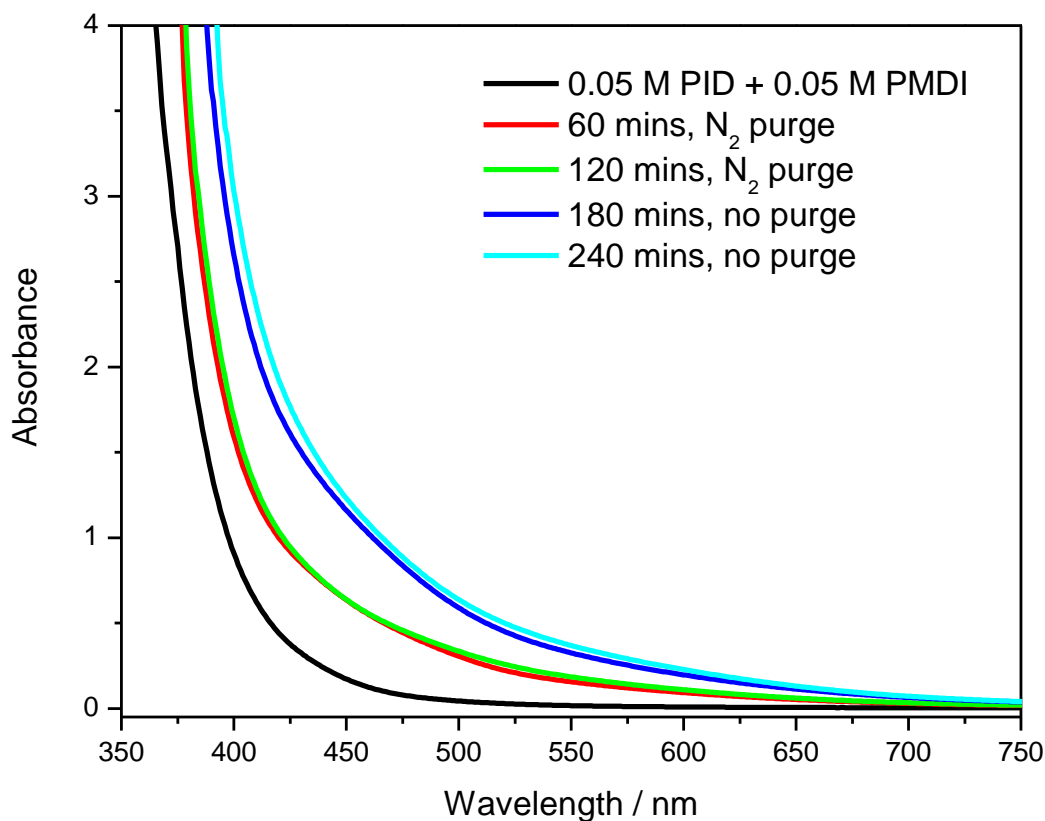


Figure 106. UV spectra of PID + PMDI in solution heated to 448 K with N₂ purge for 120, then purge stopped

6.2.4 Analysis of Product Mixtures by GCMS

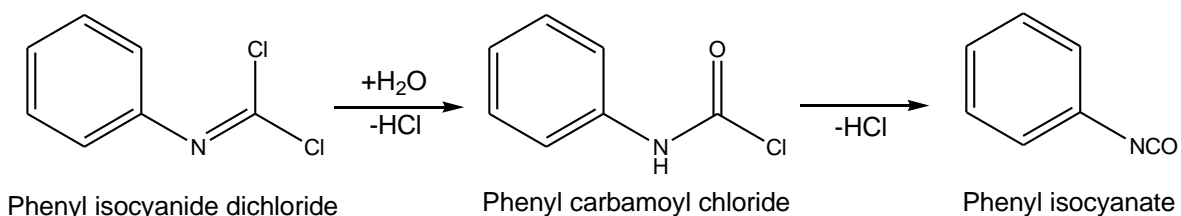
Samples from the thermolysis and photolysis reactions were selected for analysis by GC-MS. The samples chosen were 0.05M PID in ODCB, 0.05M PID + 0.05M MDI in ODCB and 0.05M PID + 0.05M polymeric MDI in ODCB. Table 24 shows the outcome of a semi-quantitative analysis where the compounds found in the analysis are indicated as follows: + low peak height, ++ medium peak height, +++ high peak height. The double lines in the table have been added to separate the reactions where the data can be sensibly compared. The main conclusions drawn from the analysis are outlined below.

Component	PID Start	PID UV	PID heat	MDI + PID start	MDI + PID UV	MDI + PID heat	Poly + PID start	Poly + PID UV	Poly + PID heat
Phenyl isocyanate (PI)	++	+	++	+	+	+++	+	+	++
Phenyl isocyanide dichloride (PID)	+++	+	++	+++	+++	++	+++	+++	+++
Phenyl isothiocyanate (PIT)	++	++	++	++	+	+++	+	+	++
Chlorinated phenyl isothiocyanate (CI-PIT)	+	+	+++	trace	trace	++	trace	trace	+
Dichlorobiphenyl isomers (DCBPh)	trace	+	trace	trace	+	trace	trace	++	trace
Trichlorobiphenyl isomers (TCBPh)	-	++	-	-	+++	-	-	+++	-
MDI	-	-	-	+++	+++	+++	++	++	++
CI-MDI	-	-	-	-	-	trace	-	-	+
Triiso	-	-	-	-	-	-	++	++	++

Table 24. Table of components found in the GCMS analysis, PID = phenyl isocyanide dichloride, MDI = 4,4'-methylene diphenyl diisocyanate, Poly = Polymeric MDI, + = low peak height, ++ = medium peak height, +++ = high peak height

a) Thermolysis

From the heating reactions, the main product is phenyl isocyanate. This may be a product from hydrolysis of the phenyl isocyanide dichloride (PID) involving the loss of HCl (Scheme 23). The results also show that the PID concentration of the sample is decreased by ~50%. However both the isothiocyanate and the chlorinated isothiocyanate concentration have increased. If the isothiocyanate is being chlorinated then the isothiocyanate concentration would be expected to decrease not increase. Small amounts of the chlorinated MDI are also found in the heat treatments of PID + MDI and PMDI (284 m/z). This compound lends evidence to the chlorination of the isocyanates by the isocyanide dichloride.



Scheme 23. Hydrolysis of phenyl isocyanide dichloride (PID) leading to phenyl isocyanate

b) Photolysis

The main products seen from the photolysis reactions are dichlorobiphenyl and trichlorobiphenyl (Figure 107), with several isomers found in each sample. These compounds are not seen in the thermolysis reactions. This indicates a radical based reaction process is taking place, possibly with the generation of a phenyl radical reacting with the *o*-dichlorobenzene solvent. The mechanism for this reaction could possibly involve abstraction of a hydrogen atom from the solvent or substitution of a hydrogen atom induced by the phenyl radical.¹⁵⁷ The GC-MS peak for PID does not show any change to the concentration of PID, indicating the decomposition of the compound is limited and the chromophore produced is a minority species.

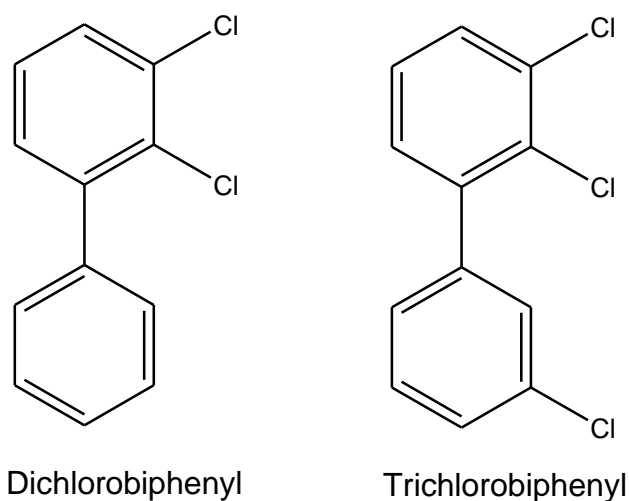
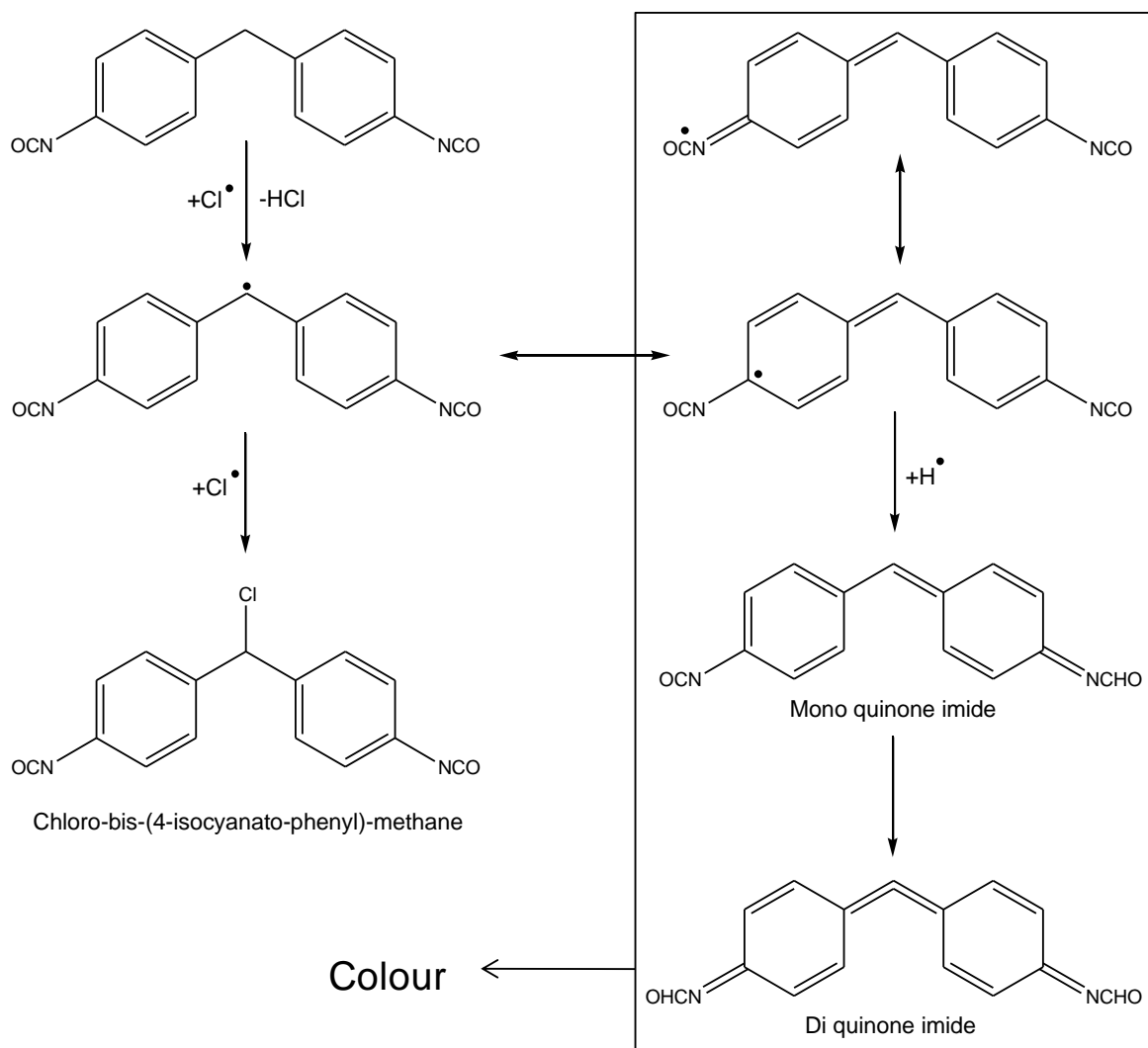


Figure 107. Chlorinated compounds

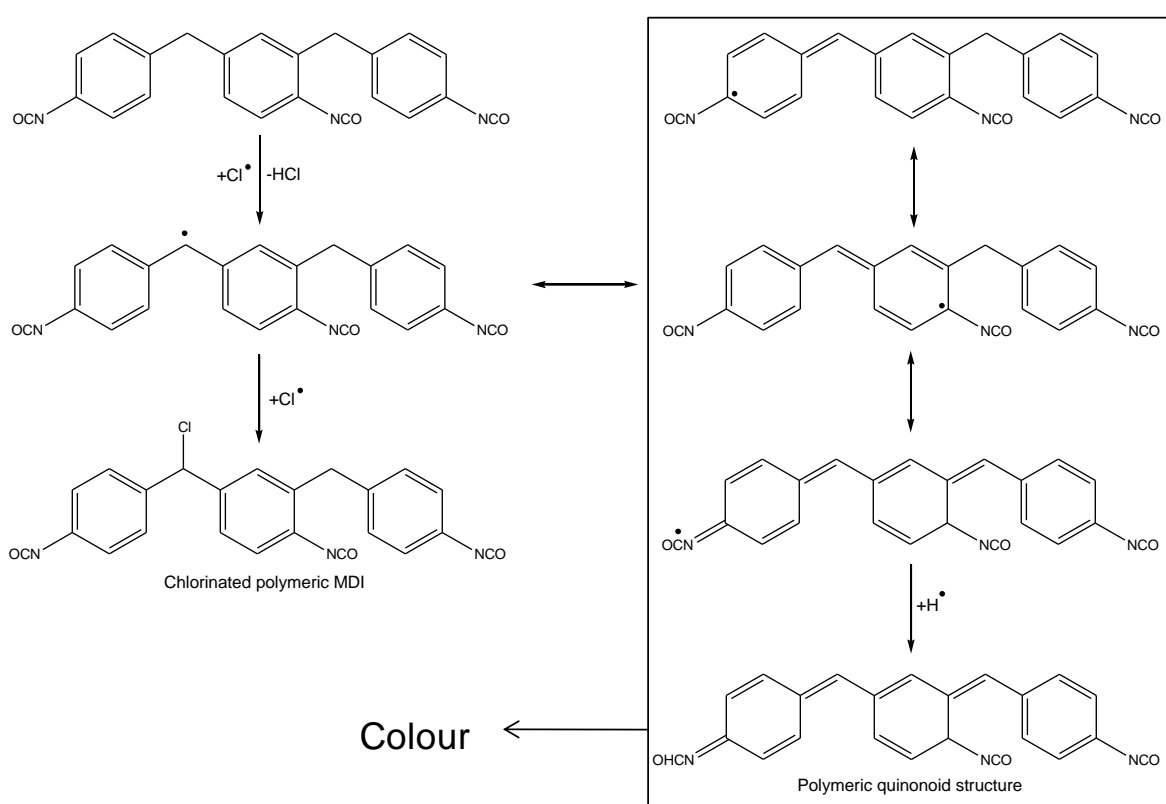
6.3 Summary and Discussion

The results from the heat treatments show that isocyanide dichloride acts as a source of colour when heated to temperatures comparable to those used in the production of MDI (448 K). Isocyanide dichloride produces colour on its own in solution, however, the addition of MDI increases the intensity of the colour, with further increase occurring in solutions with polymeric MDI. A proposed mechanism for the colouration of the final commercial product involves the conjugation of the aromatic isocyanates. The Cl^\bullet radicals produced from the isocyanide dichloride compounds will attack the methylene bridge in the backbone of MDI by abstracting hydrogen and forming a conjugated compound leading to a quinonoid structure (Scheme 24).



Scheme 24. Conjugation of MDI via attack from Cl^\bullet radicals

As polymeric MDI forms long chains this process will produce highly conjugated systems which can cause colouration as they absorb light in the visible region of the electromagnetic spectrum. Scheme 25 shows how a longer chain isocyanate compound would be affected. As the chain increases the maximum absorption increases moving from the UV range to the visible range. This happens as the double bonds in the chain act as auxochromes which are the components responsible for adsorption in the visible range. A well known example of this is β -carotene.⁸³ A product of this reaction would be chlorinated MDI (at the methylene bridge) (chloro-bis-(4-isocyanato-phenyl)-methane), which has been found in the MDI product stream at the industrial complex, although Ulrich¹⁸ has stated this compound arises from the presence of chlorine in phosgene.



Scheme 25. Conjugation of Polymeric MDI via attack from Cl[•] radicals

There are many studies in the literature on the photo and thermal degradation of polyurethanes based on MDI.^{47, 154, 156, 158} Although we are investigating the starting isocyanate material, the findings in the literature are relevant to the observations made here. Several reports have suggested the formation of quinonoid groups and associated conjugation in polyurethanes based on aromatic isocyanates is one of the reasons for the colouration seen in this class of compound.^{47, 159, 160} A study on the irradiation of an MDI

based polyurethane indicated that an accumulation of paramagnetic products was observed, favouring the formation of conjugated bonds. The stability of these paramagnetic species was found to be high at temperatures up to 453 K,¹⁵⁹ indicating they would be stable in the industrial process.

Within the research carried out in this chapter, the UV and infrared studies on mixtures of *p*-tolyl isocyanide dichloride (PID) and 4-BAI or MDI have indicated the loss of aromaticity (Sections 6.1.1 and 6.1.3) which leads to further conjugation and the possible formation of a quinonoid structure. Quinonoid compounds are known chromophores, derivatives of quinomethanes and quinone imines constitute an important group of dyes and pigments such as crystal violet and phenolphthalein as they show strong absorption in the visible range of the spectrum.^{161, 162} GCMS analysis carried out on mixtures of PID with MDI or Polymeric MDI has shown evidence of the chlorination of the methyl bridge within the isocyanate compound. These results lead to the mechanism proposed (Scheme 24) as being favoured in the production of colour seen in this body of work.

6.3.1 Issues Relating to Oxidising Reagents

In the thermal reactions the addition of a nitrogen purge has been proven to quench the reaction and decrease the formation of colour. It is possible that oxygen or water present in the solutions in the absence of the purge may be playing a part in the reaction. Oxygen has previously been found to increase the rate at which yellowing occurs in polyurethane materials. In a study of the thermal degradation of the isocyanate TDI (toluene diisocyanate), the presence of oxygen produced a darker colour to the reaction in nitrogen.⁴⁹ No explanation is given for the colour change in this case. Ultraviolet radiation decreased the time in which the isocyanate took to turn yellow in nitrogen.

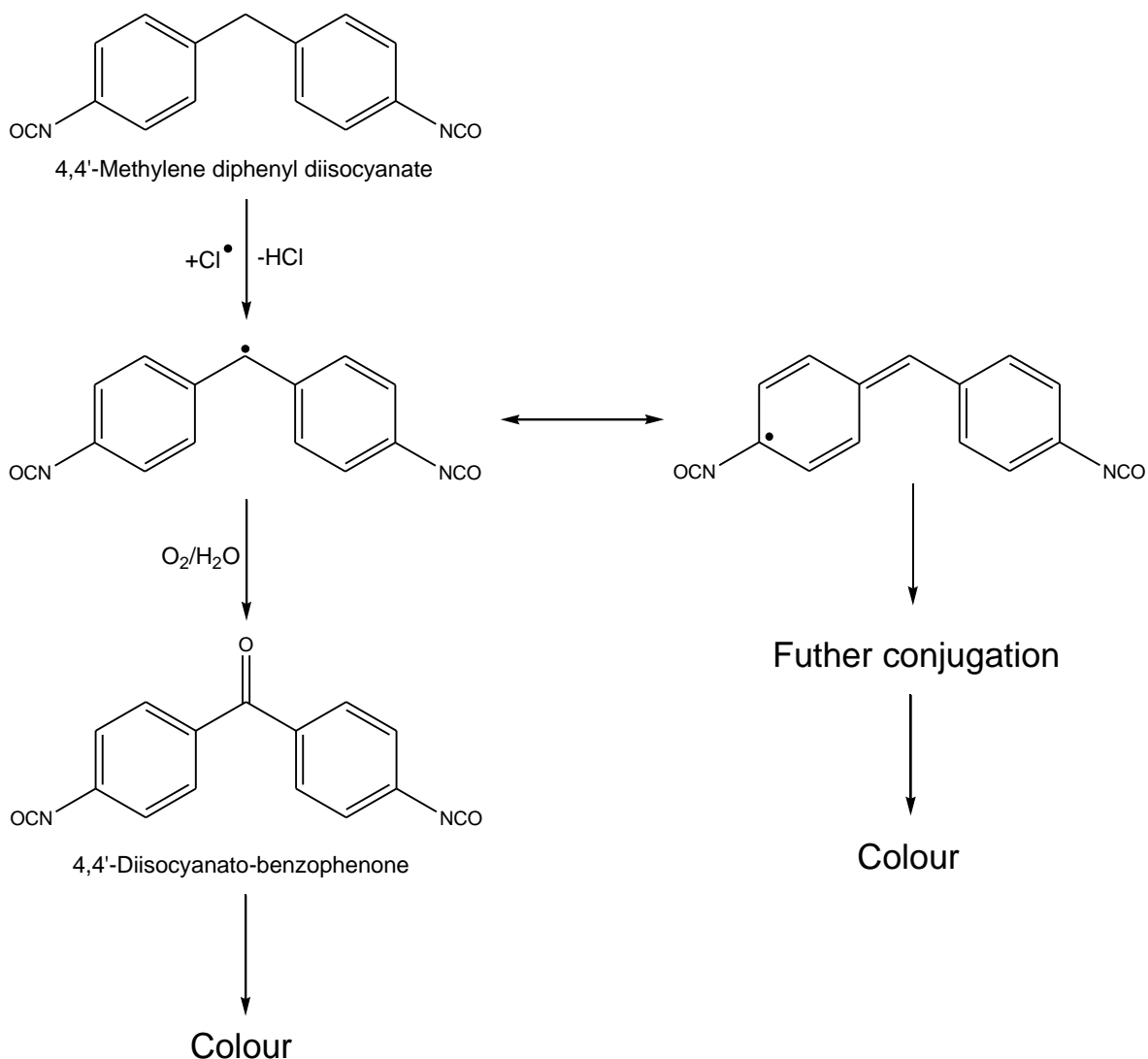
Beachell and Chang⁴⁸ studied the photodegradation of polyurethanes by looking at the photolysis of a model compound (ethyl *N*-phenylcarbamate). They reported that when the reaction was carried out in oxygen, the UV/Vis spectra showed the absorbance was shifted to a higher wavelength than when the reaction was carried out in nitrogen, along with an increase in the rate of the reaction. This is similar to what is seen in the UV/Vis spectroscopy analysis carried out in this project on mixtures of PID and MDI/polymeric MDI. On further study by Beachell and Chang it was found that the addition of

benzophenone increased the rate of oxygen consumption. This was due to a triplet-triplet energy transfer system from the benzophenone (donor) to the urethane.⁴⁸

The role of oxygen can be linked to the formation of quinonoid structures via oxidation of the methylene bridge in MDI based polyurethanes. Schollenberger states that the oxidation will be activated by heat or light to form the quinone-imide structure.¹⁵⁴ From this process a compound with a carbonyl at the methylene bridge position will be formed, similar in structure to benzophenone. It was found that phosphorescence emission from MDI based polyurethanes was similar to that of benzophenone, suggesting that the emission is from the triplet state of an aromatic carbonyl group.⁴⁷ In the infrared studies carried out on a mixture of MDI and TID, it was evident a new carbonyl species was being formed. It is unclear although whether this is from the MDI or the TID. However the formation of carbonyls via oxidation looks to play a part in the colouration process. 4,4'-Diisocyanatobenzophenone is a potential product from oxidation of MDI (Scheme 26). This compound has been found by GCMS analysis in an industrial sample of MDI.¹⁶³

The oxidation of organic molecules to quinonoid structures is well known and has useful applications such as for molecular switching devices.¹⁶⁴⁻¹⁶⁸ A study relevant to the work here has shown that polyethylene terephthalate undergoes thermal and thermo-oxidative degradation to form a conjugated aromatic systems leading to colour. The rate of the reaction was faster in air than in nitrogen and the formation of a quinonoid structure was deemed to be the most important factor contributing to the colouration.¹⁶⁹ It has also been found that radicals can play a part in the mechanism, for example phenoxy radicals can be oxidized to form quinonoid chromophores.¹⁷⁰

Schollenberger also commented on the oxidation of an *m*-phenylene diisocyanate based urethane and aniline to form a quinonoid structure.¹⁵⁴ TID has been proven to readily hydrolyse to the carbamoyl chloride which in turn can form the isocyanate, therefore it is possible that the isocyanide dichloride compounds could undergo reaction processes to form a quinone. This would create a mechanism for the formation of colour seen when PID is heated or irradiated on its own in solution. Further to this the Cl radicals produced by the isocyanide dichlorides will 'activate' the isocyanate species (MDI/polymeric MDI) in order for oxidation and/or conjugation to occur (Scheme 26).



Scheme 26. Activation of MDI by Cl^{\bullet} followed by oxidation and conjugation

6.3.2 Colour Formation

Blank reactions carried out where the isocyanate 4-benzylphenyl isocyanate (4-BAI) underwent a heat treatment at 463 K showed no colour was produced and the UV spectra indicated no changes to the solution. Therefore it can be said that in the absence of the isocyanide dichloride, no visible colour is produced. From the work carried out in this project it is believed that isocyanide dichlorides are formed from the thermolysis of chloroformamidine-*N*-carbonyl chloride (CCC) compounds and that they act as a trigger for colouration.

The absence of oxygen will attenuate the colour intensity, thus colour formation is accentuated to a fixed degree in the presence of oxygen. It is possible that different

chromophores with similar UV/Vis spectra are being formed. The conjugated species and the quinonoid structures responsible for absorbance in the visible region would therefore come from two separate sources. Both pathways would be initiated by the hydrogen abstraction of the methylene bridge in the isocyanate by chlorine radicals produced from the isocyanide dichloride (Scheme 26). Along with the conjugation pathway, oxidation by molecular oxygen would promote formation of carbonyl species similar to benzophenone, leading to an added source of colour.

6.3.3 Thermolysis Vs Photolysis

In the reactions involving heat, the colour generally intensifies as the concentration increases. However this is not always the case and a concentration dependence does not exist in the photolysis reactions. This may suggest two or more absorbing species are formed or there are competing processes.

It can thus be concluded that the irradiation of the solutions provide different results than the heat treatments. This is also seen in the GCMS analysis, where the irradiated mixtures produced multiple chlorinated compounds, presumably occurring from radical based processes. Therefore this is indicative of different reaction pathways occurring. Below are the proposed events occurring in each situation:

a) Thermolysis:



b) Photolysis:



Although different mechanisms are involved in producing colour, it is believed that in both instances the colour is due to conjugated chromophores. In each case the formation of which will be dependent on the means of initiation, i.e. thermal or photolytic. The thermal case corresponds to the industrial scenario.

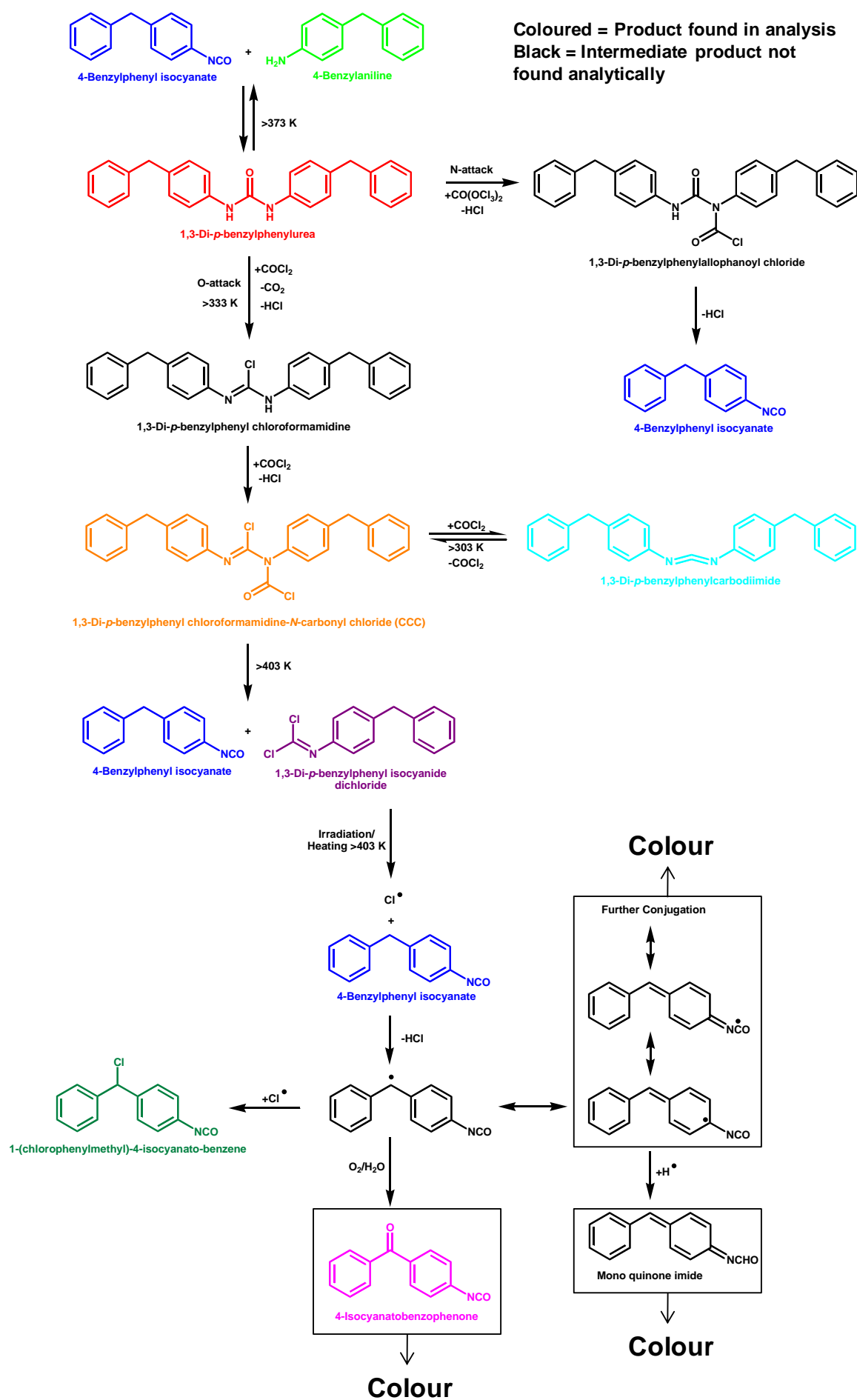
Chapter 7

Conclusions

7 Conclusions

The aim of this project was to investigate a side reaction in the production of MDI and its link to the colouration seen in the final product. The work was based on a postulated reaction scheme⁵⁰ leading to chloroformamidine-*N*-carbonyl chloride (CCC) compounds via the phosgenation of ureas. This compound would then decompose to give an isocyanide dichloride, which would release chlorine radicals resulting in highly conjugated polymeric MDI, providing a high absorbance in the visible range.

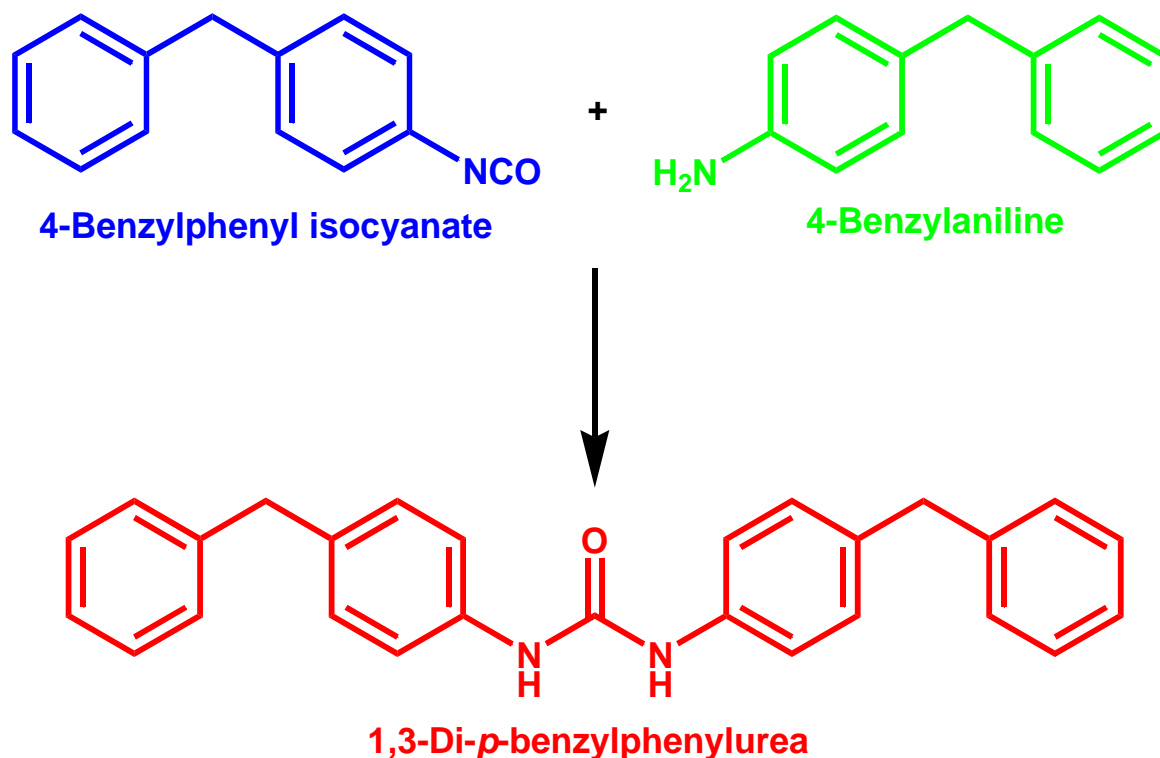
Scheme 27 shows the full reaction scheme starting with 4-benzylphenyl isocyanate (4-BAI). The reaction scheme has been modified from the postulated reaction reported by Twitchett⁵⁰ with the observations noted within this project. It is noted that Twitchett provided little experimental evidence for his postulate and this work is seen as explicitly exploring that chemistry. The next sections go on to explain each part of the scheme in more detail.



Scheme 27. Full reaction scheme

7.1 Side Reaction from Ureas to Isocyanide Dichlorides

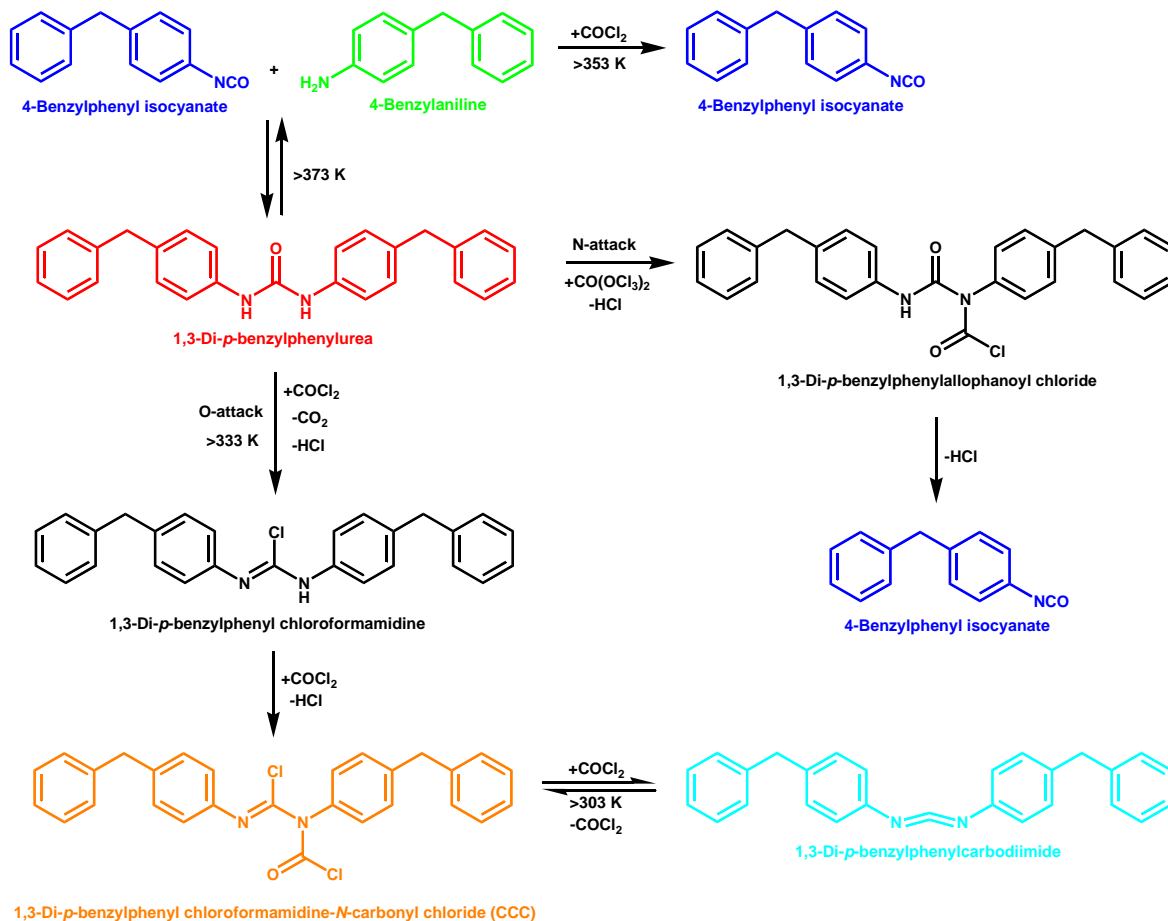
Initial reactions carried out reacting isocyanate materials with amines proved to form solid urea compounds (Scheme 28). Two urea compounds, 1,3-diphenylurea and 1,3-di-*p*-benzylphenylurea were used as model compounds to investigate the reaction of ureas with phosgene.



Scheme 28. Reaction between isocyanate and amine to form urea

Phosgenation reactions were carried out using the solid bis(trichloromethyl) carbonate (triphosgene) as this provided a source of phosgene that was safer to handle in the small quantities used in the laboratory. The compound was either added directly to the reactor or first decomposed producing a stream of phosgene gas into the reactor via an Eckert cartridge. Reactions with both 1,3-diphenylurea and 1,3-di-*p*-benzylphenylurea showed a mixture of products was produced in the reactions, dependent on the conditions used. Several reaction pathways can occur (Scheme 29), with triphosgene and phosgene reacting in different ways. It is proposed that triphosgene will favour N-attack of the urea to form an allophanoyl chloride, breaking down to an isocyanate. Phosgene however will favour O-attack, leading to the chloroformamidine-*N*-carbonyl chloride (CCC) moiety. This compound will decompose to isocyanate and isocyanide dichloride in the presence of a

large excess of phosgene. In the absence of phosgene however, the CCC will decompose to produce the carbodiimide. It is also postulated a third route leading to the isocyanate occurs, via breakdown of the urea to amine and isocyanate, with the amine further phosgenated to the isocyanate.

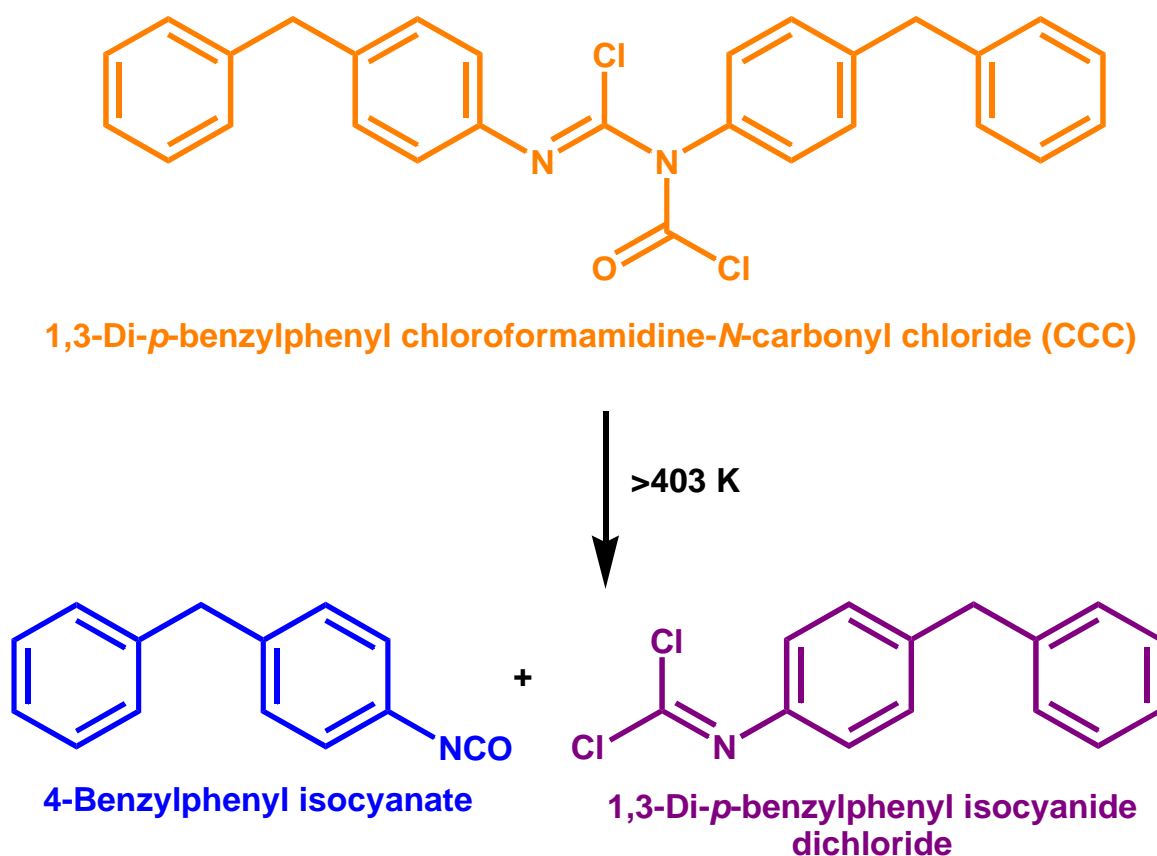


Scheme 29. Phosgenation of phosgene – competing reactions

Crystallographic studies on 1,3-di-*p*-benzylphenyl urea have showed the structure of the compound to be tightly packed with hydrogen bonding between the oxygen of the carbonyl group and the amide hydrogens, with π -stacking between the aromatic rings. This is consistent with studies on other aryl ureas, which show a similar arrangement. $^1\text{H-NMR}$ methods used to investigate the solubility of 1,3-diphenyl urea, 1,3-di-*p*-benzylphenyl urea and oligomeric urea showed that they are relatively insoluble in the process solvent, chlorobenzene (MCB). Infrared studies on the solid ureas also backed up the crystallographic work which indicates the ureas are only found in the amide form in the solid state and do not undergo tautomerization. A mechanism has therefore been proposed

whereby the solvated phosgene will react with the solid urea at the oxygen position to form the CCC.

Heat treatments on the CCC moiety have confirmed isocyanide dichloride as a decomposition product, along with the isocyanate at temperatures above 403 K (Scheme 30). The reaction is hindered by the amount of phosgene present in the solution, the lack of which can lead to the carbodiimide being formed. This reaction occurs at a lower temperature of 313 K, with an increase of carbodiimide formed as the temperature increases. In the industrial process this reaction will occur at the point the polymeric MDI mixture undergoes heat treatments to remove excess phosgene and HCl (the stripper stage shown in Figure 1). The high temperatures coupled with a high concentration of phosgene are ideal conditions for formation of the isocyanide dichloride.



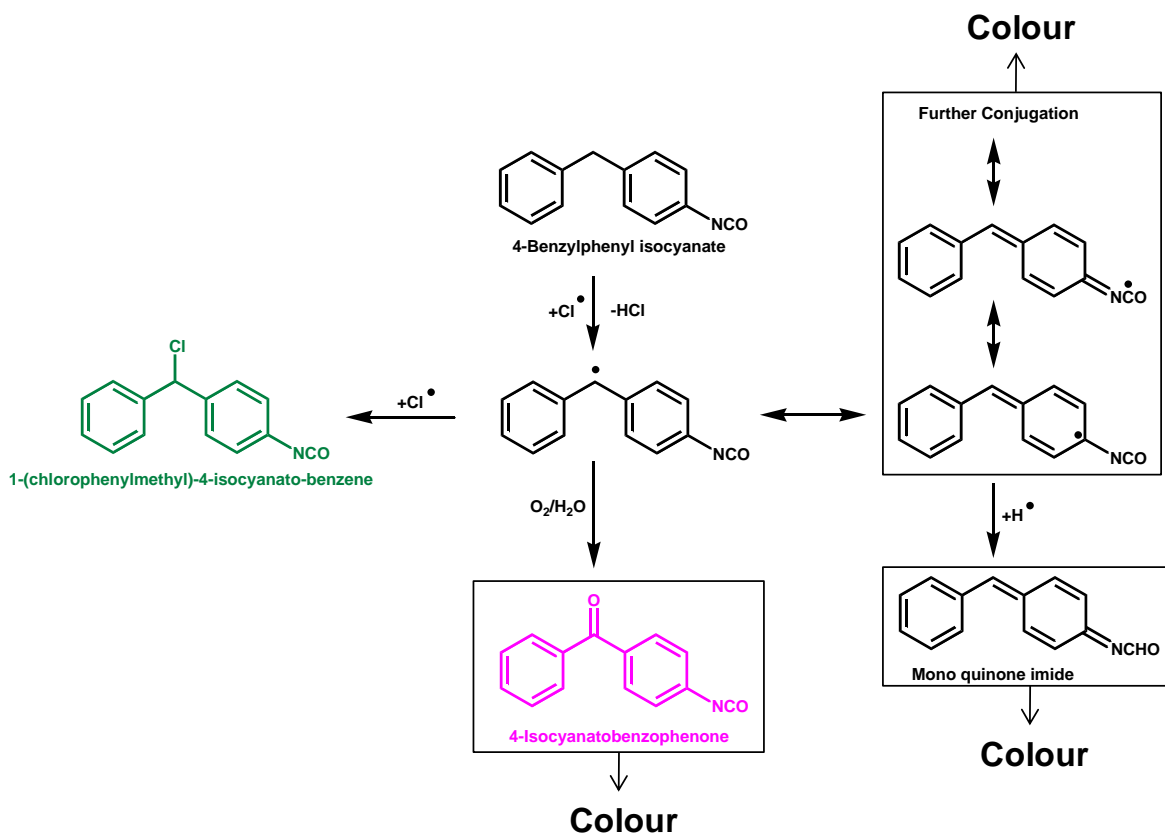
Scheme 30. Decomposition of chloroformamidine-*N*-carbonyl chloride (CCC) to isocyanide dichloride and isocyanate

7.2 Radical Chemistry

Electron paramagnetic resonance (EPR) spectroscopy of photo-irradiated samples provided evidence that isocyanide dichlorides can act as a source of chlorine radicals. PBN was used as a spin trap. The reaction forms an eight line spectrum consistent with the PBN-Cl adduct of the spin trap. A secondary radical produced in the reaction with a three line spectrum was assigned as benzoyl *N-tert*-butyl nitroxide radical, the identification of which is backed up by DFT calculations. The analysis of the growth and decay characteristics of both radicals indicate the species are formed in concurrent reactions. This led to a postulated mechanism for the reaction scheme leading to the benzoyl radical. This involved the oxidation of PBN through irradiation or on reaction with the isocyanide dichloride to form a $\text{PBN}^{\bullet+}$ radical cation. This reacts with excess PBN to form the benzoyl radical. A competing mechanism whereby the benzoyl radical is formed from reaction between excess PBN and the PBN-Cl adduct is also thought to occur.

7.3 Formation of Colour

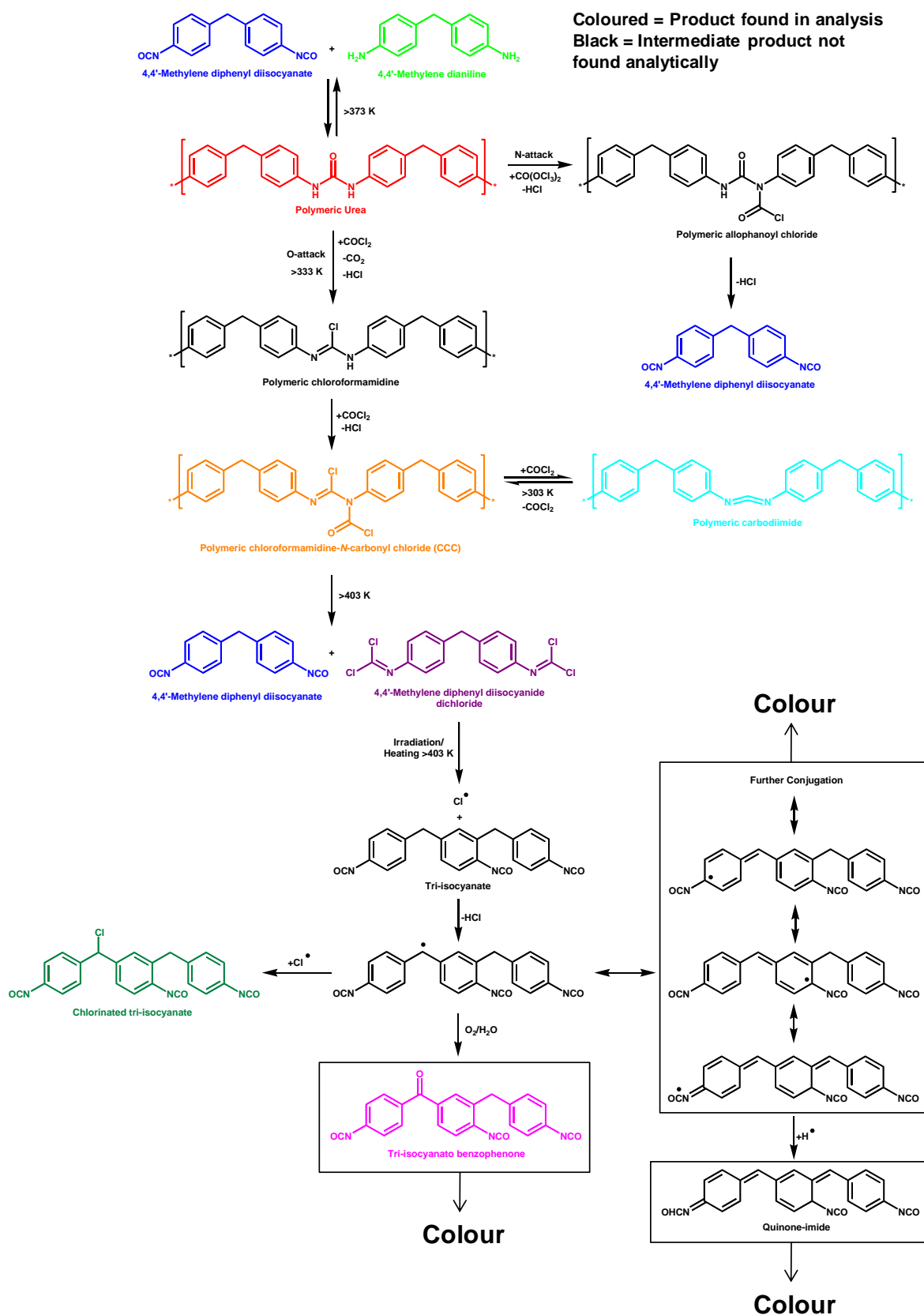
Both phenyl and *p*-tolyl isocyanide dichlorides were synthesized and characterised by a variety of techniques. The compounds were found to be stable up to 403 K in an inert atmosphere. However upon heating above this temperature or by irradiation of the compounds the molecule would decompose and initiate the colouration of the solution. Addition of MDI and Polymeric MDI increased the intensity of the colour, with studies also proving a concentration dependence between the isocyanide dichloride and colour intensity. This confirmed the isocyanide dichloride was responsible for the onset of colour. The removal of oxygen from the system quenches the reaction indicating one mechanism for the colouration process originates from the oxidation of the methylene bridge in the MDI backbone. Cl radicals are proposed to activate this process also leading to conjugation and the formation of quinonoid type structures (Scheme 31). GCMS analysis carried out on the mixtures of PID with MDI or polymeric MDI indicated that the irradiation of the solutions resulted in chlorination and formation of phenyl radicals.



Scheme 31. Reaction of chlorine radicals with 4-BAI to produce colour

7.4 MDI Scheme

Scheme 32 shows the full reaction scheme focusing on MDI and the conjugation of the polymeric MDI. This scheme, based on the experimental work on the model systems, is more relevant to the compounds that will be produced in the industrial process.



Scheme 32. Full reaction scheme based on MDI

7.5 Future Work

With reference to Scheme 27 it is noted that indirectly chloroformamidine-*N*-carbonyl chloride (CCC) is the source of the colour, with this species only existing in the presence of phosgene. In the industrial complex it is the thermal decomposition of this compound which leads to the formation of isocyanide dichlorides. These compounds can act as a source of chlorine radicals which lead to colouration in the final product. One possible route for minimising this process could be to purge the product solution < 400 K, thus favouring the carbodiimide compound which is in equilibrium with the CCC. This method would also reduce any oxygen content in the solution which can amplify the presence of the chromophores responsible for the colour. Further work is necessary to exploit the potential of this suggestion. It is also recommended that additional investigation into the role of oxygen in the process is carried out. Being able to pinpoint the chromophoric species by analytical methods would help to fully understand the oxidation process.

8 References

1. M. B. Smith and J. March, *March's Advanced Organic Chemistry*, 5th edn., John Wiley & Sons, New York, 2001.
2. O. Bayer, *Angew. Chem.*, 1947, **A59**, 257-272.
3. I. G. Farbenindustrie-AG, *Polyurethans and Polyureas*, DE 728981, 1942.
4. W. B. Seymour, *Modern Plastics Technology*, Reston Publishing Company, Reston, 1975.
5. D. Randall and S. Lee, *The Polyurethanes Book*, John Wiley & Sons, 2002.
6. J. H. Saunders and R. J. Slocombe, *Chem. Rev.*, 1948, **43**, 203-218.
7. R. G. Arnold, J. A. Nelson and J. J. Verbanc, *Chem. Rev.*, 1957, **57**, 47-76.
8. A. v. Wurtz, *Annalen der Chemie und Pharmacie*, 1849, **71**, 326-342.
9. J. H. Saunders and K. C. Frisch, *Polyurethanes: Chemistry and Technology*, Interscience Publishers, New York, 1962.
10. W. Hentschel, *Ber. Dtsch. Chem. Ges.*, 1884, **17**, 1284-1289.
11. L. Gattermann, *Justus Liebigs Ann. Chem.*, 1888, **244**, 29-76.
12. G. Wegener, M. Brandt, L. Duda, J. Hofmann, B. Kleszczewski, D. Koch, R.-J. Kumpf, H. Orzesek, H.-G. Pirkl, C. Six, C. Steinlein and M. Weisbeck, *Appl. Catal., A*, 2001, **221**, 303-335.
13. K. Weissemel and H.-J. Arpe, *Industrial Organic Chemistry*, 3rd edn., Wiley-VCH, Weinheim, 2003.
14. A. de Angelis, P. Ingallina and C. Perego, *Ind. Eng. Chem. Res.*, 2004, **43**, 1169-1178.
15. E. K. Gibson, PhD Thesis, University of Glasgow, 2007.
16. E. K. Gibson, J. M. Winfield, K. W. Muir, R. H. Carr, A. Eaglesham, A. Gavezzotti, S. F. Parker and D. Lennon, *Phys. Chem. Chem. Phys.*, 2009, **11**, 288-297.
17. E. K. Gibson, J. M. Winfield, K. W. Muir, R. H. Carr, A. Eaglesham, A. Gavezzotti and D. Lennon, *Phys. Chem. Chem. Phys.*, 2010, **12**, 3824-3833.
18. H. Ulrich, *Chemistry and Technology of Isocyanates*, John Wiley & Sons, New York, 1996.
19. H. C. Beachell and C. P. N. Son, *J. Polym. Sci., Part A: Gen. Pap.*, 1964, **2**, 4773-4785.
20. S. G. Entelis and O. V. Nesterov, *Usp. Khim.*, 1966, **35**, 917-930.
21. R. Carr, *Communication with Huntsman Polyurethanes*, January 2007.
22. L. Dobbin, *Ann. Sci.*, 1945, **5**, 270-287.
23. T. A. Ryan, C. Ryan, E. A. Seddon and K. R. Seddon, *Phosgene and Related Carbonyl Halides*, Elsevier, Amsterdam, 1996.
24. L. Cotarca and H. Eckert, *Phosgenations - A Handbook*, Wiley-VCH, Weinheim, 2003.
25. K. Kurita and Y. Iwakura, *Org. Synth.*, 1979, **59**, 195.
26. V. B. Arce, V. C. O. Della, A. J. Downs, S. Parsons and R. M. Romano, *J. Org. Chem.*, 2006, **71**, 3423-3428.
27. J. L. Hales, J. I. Jones and W. Kynaston, *J. Chem. Soc.*, 1957, 618-625.
28. H. Eckert and B. Forster, *Angew. Chem., Int. Ed.*, 1987, **26**, 894-895.
29. H. P. Hood and H. R. Murdock, *J. Phys. Chem.*, 1919, **23**, 498-512.
30. H. C. Ramsperger and G. Waddington, *J. Am. Chem. Soc.*, 1933, **55**, 214-220.
31. L. Cotarca, P. Delogu, A. Nardelli and V. unji, *Synthesis*, 1996, **1996**, 553-576.
32. L. Pasquato, G. Modena, L. Cotarca, P. Delogu and S. Mantovani, *J. Org. Chem.*, 2000, **65**, 8224-8228.
33. W. H. Daly and D. Poché, *Tetrahedron Lett.*, 1988, **29**, 5859-5862.

34. S. B. Damle, *Chem. Eng. News*, 1993, **71**, 4.
35. R. Trotzki, M. Nuchter and B. Ondruschka, *Green Chem.*, 2003, **5**, 285-290.
36. X. Peng, H. Yu, Y. Hang and J. Wang, *Dyes and Pigments*, 1996, **32**, 193-198.
37. H. Zhang and D. M. Rudkevich, *Chem. Commun.*, 2007, 1238-1239.
38. Y. Zhou, R. Gong and W. Miao, *Synth. Commun.*, 2006, **36**, 2661-2666.
39. Y. C. Charalambides and S. C. Moratti, *Synth. Commun.*, 2007, **37**, 1037-1044.
40. G. Lewandowski and E. Milchert, *J. Hazard. Mater.*, 2005, **119**, 19-24.
41. R. Juárez, P. Concepción, A. Corma, V. Fornés and H. García, *Angew. Chem., Int. Ed.*, 2010, **49**, 1286-1290.
42. P. Uriz, M. Serra, P. Salagre, S. Castillon, C. Claver and E. Fernandez, *Tetrahedron Lett.*, 2002, **43**, 1673-1676.
43. R. Juárez, A. Corma and H. García, *Top. Catal.*, 2009, **52**, 1688-1695.
44. N. Lucas, A. P. Amrute, K. Palraj, G. V. Shanbhag, A. Vinu and S. B. Halligudi, *J. Mol. Catal. A: Chem.*, 2008, **295**, 29-33.
45. R. Carr, *Background Slides on MDI Colour*, Internal Report, 2007.
46. H. C. Beachell and C. P. N. Son, *J. Appl. Polym. Sci.*, 1964, **8**, 1089-1096.
47. N. S. Allen and J. F. McKellar, *J. Appl. Polym. Sci.*, 1976, **20**, 1441-1447.
48. H. C. Beachell and I. L. Chang, *J. Polym. Sci., Part A: Polym. Chem.*, 1972, **10**, 503-520.
49. H. C. Beachell and C. P. N. Son, *J. Appl. Polym. Sci.*, 1963, **7**, 2217-2237.
50. H. J. Twitchett, *Chem. Soc. Rev.*, 1974, **3**, 209-230.
51. R. P. Redman, *Tolylene Diisocyanate: The Chemistry of the Phosgenation of Ureas*, Technical Report, ICI, 1972.
52. K. C. Nicolaou and T. Montagnon, *Molecules that Changed the World*, Wiley-VCH, Weinheim, 2008.
53. K. C. Nicolaou and E. J. Sorensen, *Classics in Total Synthesis: Targets, Strategies, Methods*, Wiley-VCH, Weinheim, 1996.
54. T. P. Vishnyakova, I. A. Golubeva and E. V. Glebova, *Usp. Khim.*, 1985, **54**, 429-449.
55. J. W. Baker and D. N. Bailey, *J. Chem. Soc.*, 1957, 4649-4651.
56. A. W. von Hofmann, *Justus Liebigs Ann. Chem.*, 1849, **70**, 129-149.
57. D. F. Kutepov, *Russ. Chem. Rev.*, 1962, **31**, 633-655.
58. P. Vaughan and J. Donohue, *Acta Crystallogr.*, 1952, **5**, 530-535.
59. S. B. Hendricks, *J. Am. Chem. Soc.*, 1928, **50**, 2455-2464.
60. S. V. Deshapande, C. C. Meredith and R. A. Pasternak, *Acta Crystallogr., Sect. B: Struct. Sci.*, 1968, **24**, 1396-1397.
61. S. George and A. Nangia, *Acta Crystallogr., Sect. E: Struct. Rep. Online*, 2003, **E59**, o901-o902.
62. H. Ulrich, J. N. Tilley and A. A. R. Sayigh, *J. Org. Chem.*, 1964, **29**, 2401-2404.
63. D. P. Fairlie, T. C. Woon, W. A. Wickramasinghe and A. C. Willis, *Inorg. Chem.*, 1994, **33**, 6425-6428.
64. P. E. Allegretti, V. Peroncini, E. A. Castro and J. J. P. Furlong, *Int. J. Chem. Sci.*, 2003, **1**, 1-12.
65. P. Skurski and J. Simons, *J. Chem. Phys.*, 2001, **115**, 8373-8380.
66. Z. Piasek and T. Urbanski, *Tetrahedron Lett.*, 1962, **3**, 723-727.
67. J. A. Weil and J. R. Bolton, *Electron Paramagnetic Resonance: Elementary Theory and Practical Applications*, 2nd edn., John Wiley & Sons, Hoboken, 2007.
68. F. Scheinmann, *An Introduction to Spectroscopic Methods for the Identification of Organic Compounds Vol. 2*, Pergamon Press, Oxford, 1974.
69. M. Symons, *Chemical and Biochemical Aspects of Electron-Spin Resonance Spectroscopy*, Van Nostrand Reinhold, Wokingham, 1978.
70. M. J. Perkins, *Adv. Phys. Org. Chem.*, 1980, **17**, 1-64.

71. E. G. Janzen, *Acc. Chem. Res.*, 1971, **4**, 31-40.
72. E. G. Janzen and D. L. Haire, in *Advances in Free Radical Chemistry: A Research Annual*, ed. D. D. Tanner, JAI Press, Greenwich, 1990, vol. 1.
73. V. E. Zubarev, V. N. Belevskii and L. T. Bugaenko, *Usp. Khim.*, 1979, **48**, 1361-1392.
74. D. J. Reed, in *Kirk-Othmer Encyclopedia of Chemical Technology*, ed. M. Howe-Grant, 2000, vol. 5, pp. 1017-1072.
75. D. H. R. Barton, *J. Chem. Soc.*, 1949, 148-155.
76. D. H. R. Barton and K. E. Howlett, *J. Chem. Soc.*, 1951, 2033-2038.
77. N. N. Greenwood and A. Earnshaw, *Chemistry of the Elements*, 2nd edn., Butterworth Heinemann, Oxford, 1997.
78. N. Vanderkooi, Jr. and J. S. MacKenzie, in *Free Radicals in Inorganic Chemistry*, American Chemical Society, 1962, vol. 36, pp. 98-101.
79. D. Rehorek, E. G. Janzen and Y. Kotake, *Can. J. Chem.*, 1991, **69**, 1131-1133.
80. D. Rehorek, C. M. Dubose and E. G. Janzen, *Inorg. Chim. Acta*, 1984, **83**, L7-L8.
81. R. K. Freidlina, I. I. Kandror and R. G. Gasanov, *Usp. Khim.*, 1978, **47**, 508-536.
82. F. Rouessac and A. Rouessac, *Chemical Analysis: Modern Instrumentation Methods and Techniques*, 2nd edn., John Wiley & Sons, Chichester, 2007.
83. D. H. Williams and I. Fleming, *Spectroscopic Methods in Organic Chemistry*, 5th edn., McGraw-Hill, London, 1995.
84. F. Scheinmann, *An Introduction to Spectroscopic Methods for the Identification of Organic Compounds Vol. 1*, Pergamon Press, Oxford, 1970.
85. P. R. Griffiths, *Chemical Infrared Fourier Transform Spectroscopy*, John Wiley & Sons, London, 1975.
86. B. C. Smith, *Fundamentals of Fourier Transform Infrared Spectroscopy*, CRC Press, Boca Raton, 1996.
87. N. B. Colthup, L. H. Daly and S. E. Wiberly, *Introduction to Infrared and Raman Spectroscopy*, 2nd edn., Academic Press, New York, 1975.
88. P. R. Griffiths and J. A. d. Haseth, *Fourier Transform Infrared Spectrometry*, 2nd edn., John Wiley & Sons, Hoboken, 2007.
89. H. Eckert and B. Gruber, *Method and device for safe preparation of laboratory gases in sealed storage container and reactor*, DE 19860496, 1999.
90. Aldrich, *Chemfiles*, 2002, **2**, 7.
91. C. M. Hill, M. B. Towns and G. Senter, *J. Am. Chem. Soc.*, 1949, **71**, 257-258.
92. G. Piccardi and R. Udusti, *Microchim. Acta*, 1983, **79**, 109-114.
93. S. W. Kubala, D. C. Tilotta, M. A. Busch and K. W. Busch, *Anal. Chem.*, 1989, **61**, 2785-2791.
94. L. Yoder, *J. Ind. Eng. Chem.*, 1919, **11**, 755-755.
95. A. T. Stuart, *J. Am. Chem. Soc.*, 1911, **33**, 1344-1349.
96. M. A. Rosanoff and A. E. Hill, *J. Am. Chem. Soc.*, 1907, **29**, 269-275.
97. D. Lin-Vien, N. B. Colthup, W. G. Fateley and J. G. Grasselli, *The Handbook of Infrared and Raman Characteristic Frequencies of Organic Molecules*, Academic Press, 1991.
98. F. Betzler, MSci Research Project, University of Glasgow, 2008.
99. L. J. Farrugia, *J. Appl. Crystallogr.*, 1999, **32**, 837-838.
100. G. Sheldrick, *Acta Crystallogr., Sect. A: Found. Crystallogr.*, 2008, **64**, 112-122.
101. A. L. Spek, *J. Appl. Crystallogr.*, 2003, **36**, 7-13.
102. H. Ulrich and A. A. R. Sayigh, *J. Org. Chem.*, 1963, **28**, 1427-1429.
103. C. J. Wilkerson and F. D. Greene, *J. Org. Chem.*, 1975, **40**, 3112-3118.
104. R. S. Bly, G. A. Perkins and W. L. Lewis, *J. Am. Chem. Soc.*, 1922, **44**, 2896-2903.
105. D. B. Murphy, *J. Org. Chem.*, 1964, **29**, 1613-1615.
106. E. Kühle, B. Anders and G. Zumach, *Angew. Chem., Int. Ed.*, 1967, **6**, 649-665.

107. J. Katzhendler and A. Goldblum, *J. Chem. Soc., Perkin Trans. 2*, 1988, 1653-1660.
108. *The Aldrich library of FT-IR spectra*, 1997, **2** (2), 3106:B.
109. C. V. Stephenson, W. C. Coburn Jr and W. S. Wilcox, *Spectrochim. Acta*, 1961, **17**, 933-946.
110. R. Bacaloglu and C. A. Bunton, *Tetrahedron*, 1973, **29**, 2721-2723.
111. C. J. Pouchert, *The Aldrich library of NMR Spectra*, 1983, **2** (1), 1124:B.
112. J. A. Pople, W. G. Schneider and H. J. Bernstein, *High-resolution Nuclear Magnetic Resonance*, McGraw-Hill Book Company, New York, 1959.
113. M. J. Frisch, G. W. Trucks, H. B. Schlegel, G. E. Scuseria, M. A. Robb, J. R. Cheeseman, J. Montgomery, J. A. T. Vreven, K. N. Kudin, J. C. Burant, J. M. Millam, S. S. Iyengar, J. Tomasi, V. Barone, B. Mennucci, M. Cossi, G. Scalmani, N. Rega, G. A. Petersson, H. Nakatsuji, M. Hada, M. Ehara, K. Toyota, R. Fukuda, J. Hasegawa, M. Ishida, T. Nakajima, Y. Honda, O. Kitao, H. Nakai, M. Klene, X. Li, J. E. Knox, H. P. Hratchian, J. B. Cross, V. Bakken, C. Adamo, J. Jaramillo, R. Gomperts, R. E. Stratmann, O. Yazyev, A. J. Austin, R. Cammi, C. Pomelli, J. W. Ochterski, P. Y. Ayala, K. Morokuma, G. A. Voth, P. Salvador, J. J. Dannenberg, V. G. Zakrzewski, S. Dapprich, A. D. Daniels, M. C. Strain, O. Farkas, D. K. Malick, A. D. Rabuck, K. Raghavachari, J. B. Foresman, J. V. Ortiz, Q. Cui, A. G. Baboul, S. Clifford, J. Cioslowski, B. B. Stefanov, G. Liu, A. Liashenko, P. Piskorz, I. Komaromi, R. L. Martin, D. J. Fox, T. Keith, M. A. Al-Laham, C. Y. Peng, A. Nanayakkara, M. Challacombe, P. M. W. Gill, B. Johnson, W. Chen, M. W. Wong, C. Gonzalez and J. A. Pople, *Gaussian 03, Revision E.01*, Gaussian Inc, Wallingford CT, 2004.
114. A. D. Becke, *J. Chem. Phys.*, 1993, **98**, 5648-5652.
115. R. Krishnan, J. S. Binkley, R. Seeger and J. A. Pople, *J. Chem. Phys.*, 1980, **72**, 650-654.
116. A. D. McLean and G. S. Chandler, *J. Chem. Phys.*, 1980, **72**, 5639-5648.
117. T. Clark, J. Chandrasekhar, G. W. Spitznagel and P. V. R. Schleyer, *J. Comput. Chem.*, 1983, **4**, 294-301.
118. V. Barone, in *Recent Advances in Density Functional Methods (Part 1)*, ed. D. P. Chong, World Scientific Publishing Co., Singapore, 1995, vol. 1.
119. W. Kutzelnigg, U. Fleischer and M. Schindler, in *NMR Basic Principles and Progress*, eds. P. Diehl, E. Fluck, H. Günther, R. Kosfeld and J. Seelig, Springer-Verlag, Berlin, 1991, vol. 23.
120. C. L. Kwan and T. F. Yen, *Anal. Chem.*, 1979, **51**, 1225-1229.
121. D. Lin-Vien, N. R. Colthup, W. G. Fateley and J. G. Grasselli, *The Handbook of Infrared and Raman Characteristic Frequencies of Organic Molecules*, Academic Press, London, 1991.
122. D. K. White and F. D. Greene, *J. Org. Chem.*, 1978, **43**, 4530-4532.
123. B. Cardillo, R. Galeazzi, G. Mobbili, M. Orena and M. Rossetti, *Tetrahedron: Asymmetry*, 1994, **5**, 1535-1540.
124. T. D. J. D'Silva, A. Lopes, R. L. Jones, S. Singhawangcha and J. K. Chan, *J. Org. Chem.*, 1986, **51**, 3781-3788.
125. H. Ulrich and A. A. R. Sayigh, *Angew. Chem., Int. Ed.*, 1966, **5**, 704-712.
126. H. Divisova, H. Havlisova, P. Borek and P. Pazdera, *Molecules*, 2000, **5**, 1166-1174.
127. A. R. Ali, H. Ghosh and B. K. Patel, *Tetrahedron Lett.*, 2010, **51**, 1019-1021.
128. A. A. R. Sayigh, J. N. Tilley and H. Ulrich, *J. Org. Chem.*, 1964, **29**, 3344-3347.
129. W. B. Bennet, J. H. Saunders and E. E. Hardy, *J. Am. Chem. Soc.*, 1953, **75**, 2101-2103.
130. R. Richter, B. Tucker and H. Ulrich, *J. Org. Chem.*, 1981, **46**, 5226-5228.
131. R. J. Knopf, *J. Chem. Eng. Data*, 1968, **13**, 582-585.

132. H. Ulrich, *Chemistry and Technology of Carbodiimides*, John Wiley & Sons, Chichester, 2007.
133. J. C. Sheehan and P. A. Cruickshank, *Org. Synth.*, 1968, **48**, 83.
134. N. M. Weinshenker, C. M. Shen and J. Y. Wong, *Org. Synth.*, 1977, **56**, 95.
135. F. Kurzer and K. Douraghi-Zadeh, *Chem. Rev.*, 1967, **67**, 107-152.
136. A. Wells, *Synth. Commun.*, 1994, **24**, 1715 - 1719.
137. J. C. Sheehan, P. A. Cruickshank and G. L. Boshart, *J. Org. Chem.*, 1961, **26**, 2525-2528.
138. Y. Marcus, *The Properties of Solvents*, John Wiley & Sons, Chichester, 1998.
139. R. S. Drago and K.F.Purcell, *Non-Aqueous Solvent Systems*, Academic Press, London, 1965.
140. C. Reichardt, *Solvents and Solvent Effects in Organic Chemistry*, 2nd edn., Wiley-VCH, Weinheim, 1988.
141. C. I. Jose, *Spectrochim. Acta, Part A*, 1969, **25**, 111-118.
142. J. Hocker, *J. Appl. Polym. Sci.*, 1980, **25**, 2879-2889.
143. S.-K. Wang and C. S. P. Sung, *Macromolecules*, 2002, **35**, 877-882.
144. A. L. Daniel-da-Silva, J. C. M. Bordado and J. M. Martín-Martínez, *J. Polym. Sci., Part B: Polym. Phys.*, 2007, **45**, 3034-3045.
145. A. Farrell, MSci Undergraduate Research Project, University of Glasgow, 2009.
146. E. G. Janzen, B. R. Knauer, L. T. Williams and W. B. Harrison, *J. Phys. Chem.*, 1970, **74**, 3025-3027.
147. M. C. R. Symons, E. Albano, T. F. Slater and A. Tomasi, *J. Chem. Soc., Faraday Trans. 1*, 1982, **78**, 2205-2214.
148. S. Bhattacharjee, M. N. Khan, H. Chandra and M. C. R. Symons, *J. Chem. Soc., Perkin Trans. 2*, 1996, 2631-2634.
149. H. Sang, E. G. Janzen, C. M. DuBose, E. J. Geelsb and J. Lee Poyer, *J. Chem. Soc., Perkin Trans. 2*, 1996, 1985-1991.
150. E. G. Janzen, H. J. Stronks, D. E. Nutter, Jr., E. R. Davis, H. N. Blount, J. L. Poyer and P. B. McCay, *Can. J. Chem.*, 1980, **58**, 1596-1598.
151. V. Zubarev and O. Brede, *J. Chem. Soc., Perkin Trans. 2*, 1994, 1821-1828.
152. E. G. Janzen and B. J. Blackburn, *J. Am. Chem. Soc.*, 1969, **91**, 4481-4490.
153. L. Ebersson, *J. Chem. Soc., Perkin Trans. 2*, 1992, 1807-1813.
154. C. S. Schollenberger and F. D. Stewart, *J. Elastom. Plast.*, 1972, **4**, 294-331.
155. I. W. Sutherland, PhD Thesis, University of Glasgow, 2006.
156. R. P. Singh, N. S. Tomer and S. V. Bhadraiah, *Polym. Degrad. Stab.*, 2001, **73**, 443-446.
157. M. Nakada, C. Miura, H. Nishiyama, F. Higashi, T. Mori, M. Hirota and T. Ishii, *Bull. Chem. Soc. Jpn.*, 1989, **62**, 3122-3126.
158. K. Umemura, H. Yamauchi, T. Ito, M. Shibata and S. Kawai, *J. Wood Sci.*, 2008, **54**, 289-293.
159. O. G. Tarakanov, L. V. Nevskji and V. K. Beljakov, *J. Polym. Sci., Part C: Pol. Sym.*, 1968, **23**, 193-199.
160. T. E. Cauffman, *The Influence of Urethane Acrylate Molecular Weight and Structure on Accelerated Weathering*, RadTech Int. North Am., Sartomer, 1994.
161. A. Skancke and P. N. Skancke, in *The Chemistry of the Quinonoid Compounds, Part 1*, ed. S. Patai, John Wiley & Sons, Chichester, 1988, vol. 2, pp. 1-28.
162. G. Ferguson, D. R. Pollard, J. M. Robertson, D. M. Hawley, G. O. P. Doherty, N. B. Haynes, D. W. Mathieson, W. B. Whalley and T. H. Simpson, *Chem. Commun.*, 1965, 640-642.
163. R. Carr, *Communication with Huntsman Polyurethanes*, 2009.
164. K. Yoshida, N. Oga, M. Kadota, Y. Ogasahara and Y. Kubo, *J. Chem. Soc., Chem. Commun.*, 1992, 1114-1115.

165. S. H. Kawai, S. L. Gilat, R. Ponsinet and J.-M. Lehn, *Chem.-Eur. J.*, 1995, **1**, 285-293.
166. A. Q. Zhang, C. Q. Cui, Y. Z. Chen and J. Y. Lee, *J. Electroanal. Chem.*, 1994, **373**, 115-121.
167. S. Béarnais-Barbry, R. Bonneau and A. Castellan, *J. Phys. Chem. A*, 1999, **103**, 11136-11144.
168. S. Béarnais-Barbry, R. Bonneau and A. Castellan, *Photochem. Photobiol.*, 2001, **74**, 542-548.
169. J. Yang, Z. Xia, F. Kong and X. Ma, *Polym. Degrad. Stab.*, 2010, **95**, 53-58.
170. H.-T. Chang, Y.-C. Su and S.-T. Chang, *Polym. Degrad. Stab.*, 2006, **91**, 816-822.